Università Politecnica delle Marche
Corso di Dottorato di Ricerca in Ingegneria Civile, Ambientale, Edile e Architettura
Curriculum in Ingegneria Civile, Ambientale, Edile e Architettura
XXXIII ciclo

---

# Advanced experimental characterization of bituminous binders extended with renewable materials in asphalt pavements

PhD Dissertation of:
**Lorenzo Paolo Ingrassia**

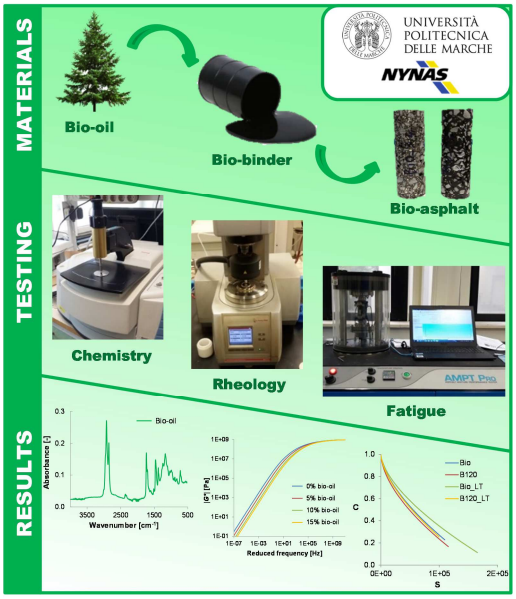


Advisor: **Prof. Francesco Canestrari**

Co-Advisor: **Dr. Xiaohu Lu**

Co-Advisor: **Dr. Gilda Ferrotti**

Curriculum Supervisor: **Prof. Francesco Fatone**

Università Politecnica delle Marche
Corso di Dottorato di Ricerca in Ingegneria Civile, Ambientale, Edile e Architettura
Curriculum in Ingegneria Civile, Ambientale, Edile e Architettura
XXXIII ciclo

---

# Advanced experimental characterization of bituminous binders extended with renewable materials in asphalt pavements

PhD Dissertation of:

**Lorenzo Paolo Ingrassia**

Advisor: **Prof. Francesco Canestrari**

Co-Advisor: **Dr. Xiaohu Lu**

Co-Advisor: **Dr. Gilda Ferrotti**

Curriculum Supervisor: **Prof. Francesco Fatone**

Università Politecnica delle Marche
*Dipartimento di Ingegneria Civile, Edile e Architettura*
Via Brecce Bianche — 60131 - Ancona, Italy

*“Leave this world a little better than you found it”*
*(Robert Baden-Powell)*

# Acknowledgements

First of all I would like to thank my Advisor, Prof. Francesco Canestrari, who saw something special in me four years ago, and from that moment on gave me the chance to live unimaginable experiences, which made me grow immensely from a human and professional point of view.
A heartfelt thanks to my Co-Advisor, Dr. Xiaohu Lu, who has been a great inspiration for me as a researcher.
Thanks to my Co-Advisor, Gilda, for her invaluable support at the beginning of this experience, when I really needed it.
Thanks to Fabrizio, for putting me at ease from the very first moment.
Thanks to all the research group of the DICEA – Infrastructure Area: PhD students, professors, researchers and technicians.
Thanks to Prof. Y. Richard Kim, for the extraordinary opportunity to be part, albeit for a short time, of his incredible research group.
Thanks also to Prof. Mihai Marasteanu for his great kindness and for having contributed to make one of my dreams come true: the first time in the USA.
Thanks to all the people I met abroad, who enriched me and helped me overcome the distance from home and loved ones.
Thanks to all the inspiring people I met in the various national and international events that I attended.
Thanks to Alessia for the unconditional love that she gives me every day.
Thanks to my sister Alessandra, who taught me how extraordinary it is to walk in two instead of alone.
Thanks to my Parents, for everything.
Thanks to my Friends, who have shown me that it is possible to choose some people "forever".

Ancona, 17th December 2020
*Lorenzo*

# Ringraziamenti

In primis ci tengo a ringraziare il mio Tutor, il Prof. Francesco Canestrari, che quattro anni fa vide qualcosa di speciale in me, e da quel momento mi ha permesso di fare esperienze inimmaginabili, che mi hanno fatto crescere molto dal punto di vista umano e professionale.
Un sentito grazie al mio Co-Tutor, il Dr. Xiaohu Lu, che è stato per me una grande ispirazione come ricercatore.
Grazie alla mia Co-Tutor, Gilda, per il suo prezioso supporto all'inizio di questo percorso, quando ne avevo davvero bisogno.
Grazie a Fabrizio, per avermi messo a mio agio sin dal primo momento.
Grazie a tutto il gruppo di ricerca dell'Area Strade: dottorandi, professori, ricercatori e tecnici.
Grazie al Prof. Y. Richard Kim, per la straordinaria possibilità concessami di far parte, seppur per poco tempo, del suo incredibile gruppo di ricerca.
Grazie anche al Prof. Mihai Marasteanu per la sua grande gentilezza e per aver contribuito alla realizzazione di un mio sogno: la prima volta negli USA.
Grazie a tutte le persone che ho conosciuto all'estero, che mi hanno arricchito ed aiutato a superare la distanza da casa e dai cari.
Grazie a tutte le stimolanti persone che ho incontrato nei vari eventi nazionali ed internazionali a cui ho partecipato.
Grazie ad Alessia per l'amore incondizionato che mi dona ogni giorno.
Grazie a mia sorella Alessandra, che mi ha insegnato quanto è straordinario camminare in due invece che da soli.
Grazie ai miei Genitori, per tutto.
Grazie ai miei Amici, che mi hanno dimostrato che è possibile scegliersi "per sempre".

Ancona, 17 dicembre 2020
*Lorenzo*

# Abstract

Human activities are progressively leading to the depletion of the (limited) resources of our planet and to the irreversible alteration of ecosystems, putting the quality of life of future generations at risk. For this reason, putting into practice the principles of *sustainability* and *circular economy*, aimed – among the other things – at minimizing resources and energy consumption, wastes and emissions, has become a crucial issue in today's world. Consequently, the construction sector is looking for solutions that can promote sustainability and circular economy without penalizing the performance and durability of construction materials and infrastructures, including the adoption of innovative "green" materials. In this regard, the new challenge in road materials engineering is the development and use of so-called "bio-binders", i.e. binders in which petroleum-based bitumen is partially replaced with bio-materials (especially bio-oils) deriving from residues or by-products from renewable sources (e.g. waste wood, non-edible vegetable biomass, animal manure, etc.). However, even though the use of bio-binders in road pavements would result in significant environmental benefits, the knowledge of these materials is still limited, especially in terms of performance and durability. Within this context, this PhD project (co-funded by the Swedish petrochemical company Nynas AB) focused on the systematic laboratory characterization of bio-binders obtained by partially replacing a conventional bitumen with a wood-based bio-oil that is a residue generated in the processing of a by-product from wood pulp and paper industries. Performance and durability were assessed by investigating several bio-binders properties, including chemistry, morphology, rheology, aging susceptibility, adhesion with aggregates, moisture susceptibility and recycling aspects. A performance-based characterization of the resulting bio-asphalt mixtures was also included in the project. The results obtained are very promising and suggest that the bio-binders can be considered a valid alternative to the traditional bituminous binders with potential benefits also in terms of performance and durability.

# Sommario

Le attività umane stanno progressivamente portando all'esaurimento delle risorse (limitate) del nostro pianeta e all'alterazione irreversibile degli ecosistemi, mettendo a rischio la qualità della vita delle generazioni future. Per questo motivo, mettere in pratica i principi della *sostenibilità* e dell'*economia circolare*, finalizzati – tra le altre cose – a minimizzare il consumo di risorse ed energia, i rifiuti e le emissioni, è diventato un tema cruciale nel mondo di oggi. Di conseguenza, il settore delle costruzioni è alla ricerca di soluzioni in grado di promuovere la sostenibilità e l'economia circolare senza penalizzare le prestazioni e la durabilità dei materiali da costruzione e delle infrastrutture, compresa l'adozione di materiali innovativi con ridotto impatto ambientale. A tal proposito, la nuova sfida nell'ingegneria dei materiali stradali è lo sviluppo e l'utilizzo dei cosiddetti "bio-leganti", ovvero leganti in cui il bitume (che si ottiene dal petrolio) viene parzialmente sostituito con bio-materiali (soprattutto bio-oli) derivanti da residui o sottoprodotti da fonti rinnovabili (es. scarti del legno, biomasse vegetali non commestibili, letame animale, ecc.). Tuttavia, sebbene l'uso di bio-leganti nelle pavimentazioni stradali possa comportare significativi benefici ambientali, la conoscenza di questi materiali è ancora limitata, soprattutto in termini di prestazioni e durabilità. In questo contesto, questo progetto di dottorato (co-finanziato dall'azienda petrolchimica svedese Nynas AB) si è incentrato sulla caratterizzazione sistematica di laboratorio di bio-leganti ottenuti sostituendo parzialmente un bitume convenzionale con un bio-olio che è un residuo generato nella lavorazione di un sottoprodotto delle industrie della pasta di legno e della carta. Le prestazioni e la durabilità sono state valutate investigando diverse proprietà dei bio-leganti, tra cui la chimica, la morfologia, la reologia, la suscettività all'invecchiamento, l'adesione con aggregati lapidei, la suscettività all'acqua ed aspetti legati al riciclaggio. Nel progetto è stata inclusa anche la caratterizzazione delle prestazioni delle risultanti bio-miscele. I risultati ottenuti sono molto promettenti e suggeriscono che i bio-leganti possono essere considerati una valida alternativa ai tradizionali leganti bituminosi con potenziali benefici anche in termini di prestazioni e durabilità.

# Contents

# List of figures

# List of tables

# 1. Introduction

Nowadays, *sustainability* and *circular economy* are two key principles to be pursued in all industry sectors. In fact, the human activities are progressively leading to the depletion of the limited resources of our planet and to the irreversible alteration of ecosystems, putting the quality of life of future generations at risk. In this regard, a sustainable production based on the circular economy concepts would allow to satisfy the needs of the present generation without compromising the possibility of future generations to meet their own needs, through the minimization of resources and energy consumption, wastes and emissions.

This is particularly true especially for the construction sector, which is responsible for the consumption of natural resources (mostly non-renewable) as well as for the production of emissions and wastes, which represent a significant impact on the environment. Therefore, it is truly necessary for the sector to undergo important changes in a relatively short time, including the adoption of new construction technologies and innovative materials, with the goal of promoting sustainability and circular economy without penalizing the performance of construction materials and infrastructures.

Within this general context, the new challenge in road materials engineering is the development and use of so-called "bio-binders", i.e. binders in which the bitumen (which is a petroleum-based product) is partially replaced with renewable bio-materials (especially bio-oils), typically deriving from residues or by-products like waste wood, non-edible vegetable biomass, waste cooking oil, animal manure, etc. In fact, the use of bio-binders in road pavements would result in significant environmental benefits, including the reduction of carbon footprint, the reduced need of petroleum-based products, the recycling of industrial by-products and residues and the decrease of materials to be disposed in landfills. Nevertheless, the knowledge of these materials is still limited in terms of performance and durability, but also in terms of possible impacts on health, safety, environment and life cycle assessment.

In this regard, this PhD project focused on the investigation of bio-binders obtained by partially replacing a conventional bitumen with a wood-based bio-oil that is a residue generated in the processing of a by-product from wood pulp and paper industries, largely available in Northern Europe (especially in Scandinavia) as well as in Northern America. The project was co-funded by the Swedish petrochemical company Nynas AB, that had an interest in exploring the potential and possible drawbacks of these materials.

The research project mainly focused on the laboratory characterization of the bio-binders performance and durability. The structure and contents of the thesis are summarized in Figure 1.1. As can be seen from the figure, several bio-binders properties were investigated, including chemistry, morphology, rheology, aging susceptibility, adhesion with aggregates, moisture susceptibility and recycling aspects. In addition, the last part of the project focused on the performance-based characterization of bio-asphalt mixtures, i.e. asphalt mixtures produced with the studied bio-binders.

Most of the experimental activities described in this thesis were carried out in the Department of Civil and Building Engineering and Architecture (DICEA) at Università Politecnica delle Marche. Part of the activities were carried out at Nynas laboratories (Nynashamn, Sweden) during a research period abroad. A small part of the activities was

also carried out in the laboratories of the Department of Materials, Environmental Science and Urban Planning (SIMAU) at Università Politecnica delle Marche. Finally, a training period spent in the Department of Civil, Construction, and Environmental Engineering at North Carolina State University (Raleigh, USA) was of fundamental importance for the completion of the activities concerning the mixtures characterization. All the activities (laboratory tests, analysis of the results, writing of the related scientific papers) were carried out by the PhD candidate.

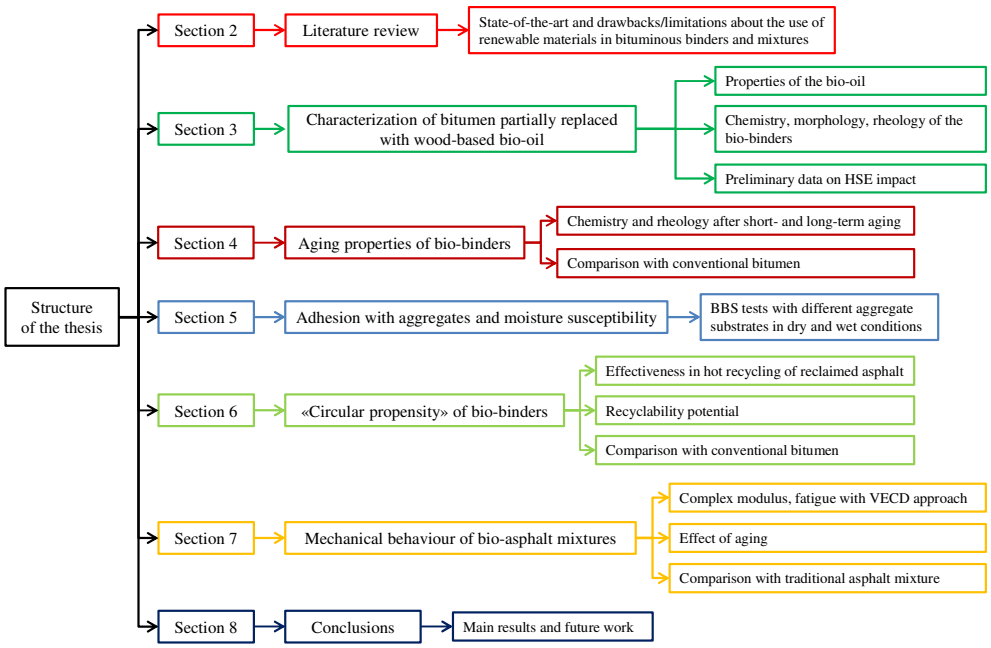


**Figure 1.1** Structure and contents of the thesis

# 2. Renewable materials in bituminous binders and mixtures: literature review

## 2.1 Background

In recent years, the growing environmental concerns have raised the interest of institutions, industry and the whole community towards two crucial concepts: sustainability and circular economy. According to a commonly accepted definition (Brundtland, 1987), sustainability indicates the development that meets the needs of the present without compromising the ability of future generations to meet their own needs. Circular economy, instead, can be defined as a regenerative system in which resource input and waste, emission and energy leakage are minimized by slowing, closing and narrowing energy and material loops through long-lasting design, maintenance, repair, reuse, remanufacturing, refurbishing and recycling, in contrast with a linear economy based on a "make-use-dispose" model of resources' consumption (Geissdoerfer et al., 2017).

Generally speaking, the construction sector is responsible for significant environmental impact, as it implies the consumption of natural resources (mostly non-renewable), causes emissions and produces wastes (Ghisellini et al., 2018; Hendrickson and Horvath, 2000; Kucukvar and Tatari, 2013). Therefore, it is truly necessary for the sector to undergo important changes in a relatively short time, such as the adoption of new construction technologies and innovative materials, aimed at promoting sustainability and circular economy without penalizing the performance and the durability.

Within this context, the road industry is progressively moving towards "green" and more sustainable solutions, aimed at minimizing the environmental impact of the sector while maximizing the use of recycled materials, industrial by-products and wastes in bituminous mixtures (Balaguera et al., 2018; Farina et al., 2017; Giani et al., 2015; Poulikakos et al., 2017; Santos et al., 2017; Thives and Ghisi, 2017).

In this regard, the use of reclaimed asphalt (RA), deriving from the milling of end-of-life pavements, is nowadays a consolidated practice in the production of bituminous mixtures, through the use of hot (Grilli et al., 2016; Stimilli et al., 2016), warm (Frigio and Canestrari, 2018; Stimilli et al., 2017) and cold (Godenzoni et al., 2018; Stimilli et al., 2013) recycling techniques.

However, the new challenge in road materials engineering is to partially replace bitumen with renewable materials obtained as by-products/residues during different industrial processes, as wastes in the everyday life or easily available in nature. Bitumen is the most employed binder in road pavements and derives from petroleum, which is a non-renewable resource that is progressively depleting. On the contrary, these renewable materials are bio-materials (often referred to as "bio-oils" when they are liquid at room temperature) not subjected to depletion.

One of the main purposes of using the so-called "bio-binders" (i.e. binders obtained by replacing part of bitumen with bio-materials) is indeed to reduce the amount of bitumen needed, with the long-term goal of making the road industry less dependent on non-

renewable resources. Moreover, the use of bio-materials in place of bitumen is eco-friendly, as it promotes the reduction of carbon footprint (an increasingly important issue in today's industry) and energy consumption, thus improving the sustainability of road pavements.
Furthermore, it should be pointed out that many bio-materials potentially employable for bituminous application should be otherwise disposed in specific landfills, which represent another relevant impact on the environment. In this perspective, their use in bituminous mixtures contributes to encourage the recycling of wastes generated by other production sectors, while simultaneously reducing the burdens for landfills and the need for new raw materials, according to the principles of circular economy.
In addition to the energy savings, another economic benefit is achieved by considering the entire life cycle of the waste materials employed. In fact, instead of being disposed in landfills at high prices, they are re-used, thus reducing the costs that companies have to face, with an overall economic benefit for the entire production system. Moreover, due to the progressive depletion of petroleum resources, the price of petroleum (and therefore of bitumen) has increased in recent years, leading to a general increase in the costs of road construction and maintenance. However, it cannot be excluded that some bio-materials may cost even more than bitumen, depending also on their production process or necessary pre-treatments (see Section 2.2.2).
Nevertheless, despite the above-mentioned environmental and economic benefits and the current trends that strongly encourage the use of bio-materials, it is essential to adopt a systematic and objective scientific approach in order to evaluate the actual validity of these solutions.
Therefore, from a scientific and technical point of view, it is crucial to understand whether such renewable materials represent a reliable and viable solution to effectively reduce the environmental (and economic) impact of road construction and maintenance without compromising pavement performance or, instead, only a mere speculative pretext for research in a field that is very attractive today, far from being an effective application.
In this regard, this section presents an overview of the renewable materials reported in literature, their effects on performance, health, safety and environment. Finally, the main critical issues/drawbacks concerning the use of renewable materials in bituminous materials are highlighted, with the aim of identifying the aspects that require further studies and research.
The key findings from the literature review are published in Ingrassia et al. (2019a).

## 2.2 Renewable materials used in bituminous binders and mixtures

### *2.2.1 Requirements for the selection of a renewable material*

In order to be considered suitable for application in bituminous binders and mixtures, renewable materials must possess some requirements.
Firstly, they must not imply additional risks for the health and safety of the workers as well as for the environment (Seidel and Haddock, 2012) (see Section 2.4). Specifically, given

their organic nature, they might have a low flash point, which could be a concern considering the typical production and laying temperatures of bituminous mixtures.
The bio-material must be compatible with bitumen. Some information about their compatibility can be obtained through chemical analyses by comparing the composition of the renewable material with that of bitumen in terms of chemical functional groups, elemental composition or SARA (saturates-aromatics-resins-asphaltenes) fractions (Fini et al., 2011).
Another fundamental aspect is that the bituminous mixture containing the renewable material must be recyclable at the end of its life-time in new road pavements. This has to be considered a real "must", since for a very long time the road sector has been promoting materials' recycling and minimizing the use of new raw materials.
Moreover, since money for road construction and maintenance is usually quite limited, to be an economically viable solution, renewable materials should offer some performance benefits with no increase or only a slight increase in the costs of the final mixture (Kluttz, 2012). Otherwise, in case they slightly reduce performance, they should be at least competitive with traditional solutions in terms of costs (Kluttz, 2012). In general, for the production of bio-binders as an alternative to fossil-based binders, certain investment should be expected, especially for refinery or manufacturer, meaning that bio-based products probably might be more expensive than traditional ones. However, it must be emphasized that a higher cost of such materials may be completely offset by their beneficial impact on sustainability.
To be a viable solution also from a commercial point of view, a renewable material should be readily available in large quantities in case of necessity and the final mixture should be transportable without additional efforts as compared to the conventional ones (Kluttz, 2012; Seidel and Haddock, 2012). Therefore, the renewable material should be selected considering also the local production and industrial activities and the by-products consequently available on the local market. This also reduces the economic and environmental costs of transport.
In general, the fewer are the changes necessary to the traditional storage, mixing, transport, paving and compaction conditions, the greater is the possibility of using a certain renewable material in bituminous binders and mixtures. Specifically, a bio-binder containing a renewable material should not suffer phase separation and/or chemical changes during normal storage (Kluttz, 2012), as well as significant degradation during the mixing process. The large-scale production at the asphalt plant should be feasible with none or minor changes to the plant. During transport, segregation should be avoided, whereas, during compaction, the mixture containing the renewable material should be compactable using the common rollers and compaction techniques (Kluttz, 2012). Moreover, the presence of the renewable material in the pavement should not cause exceptional inconvenience to traffic during in-service life or negative consequences from the possible interaction with fuels and oils (Kluttz, 2012) that can be accidentally spilled on the pavement.
Finally, another characteristic sometimes underlined as fundamental is that the renewable material should be a viscous and sticky fluid with binding properties, able to ensure adhesion with the aggregates (Cooper III et al., 2013). This requirement acquires great importance when the goal is to obtain a very high percentage of bitumen replacement, whereas it is not essential in the other cases.

### *2.2.2 Types of renewable materials*

Many different renewable materials have been proposed and studied so far by incorporating them both into unmodified bitumen (Ball et al., 1993; Gondim et al., 2016; Gong et al., 2017; Kowalski et al., 2017; Kowalski et al., 2016; Krol et al., 2016; Oldham et al., 2015; Peralta et al., 2013; Seidel and Haddock, 2012; Somé et al., 2016; Sun et al., 2016; Wen et al., 2012; Xi et al., 2015; Yang et al., 2017; Yang et al., 2015; Yang et al., 2014; Zhu et al., 2017; Zofka and Yut, 2012) and polymer-modified bitumen (Cooper III et al., 2013; Gong et al., 2016; Podolsky et al., 2016; Zhang et al., 2017; Zhu et al., 2017). An overview of the renewable materials investigated up to now is provided in Tables 2.1-2.4 and Table 2.5, which refer to bio-oils and solid bio-materials respectively.

**Table 2.1** Overview of some bio-oils studied so far in literature: wood bio-oils

| Reference | Raw bio-material | Bio-oil function | Bio-oil [%] [a] |
|---|---|---|---|
| Peralta et al., 2012a | Red oak residues | Direct alternative binder | 100 [b] |
| Peralta et al., 2013 | Red oak residues | Reduced environmental impact | 20 [b] |
| Peralta et al., 2014 | Red oak residues | Reduced environmental impact | 20 [b] |
| Grilli et al., 2016 | Pinewood | Rejuvenator | 6 |
| Raouf and Williams, 2010a | Oakwood | Direct alternative binder | 100 [c] |
| Cooper III et al., 2013 | Tall oil from pine | Bitumen extender | 20÷50 |
| Ball et al., 1993 | Tall oil from pine | Bitumen extender | ≤31.5 |
| Bearsley and Haverkamp, 2007a | Tall oil from pine | Bitumen extender | ≤25 |
| Bearsley and Haverkamp, 2007b | Tall oil from pine | Bitumen extender | ≤25 |
| Jimenez del Barco-Carrion et al., 2017a | Pine resin | Rejuvenator | 64 [d] |
| Jimenez del Barco-Carrion et al., 2017b | Pine resin | Rejuvenator | 64 [d] |
| Jimenez del Barco-Carrion et al., 2017c | Pine resin | Rejuvenator | 64 [d] |
| Gondim et al., 2016 | Plant sap from "Petroleum Plant" | Fluxing agent | 3; 5; 10 |
| Yang et al., 2014 | Waste wood resources | Bitumen modifier | 5; 10 |
| Yang et al., 2015 | Waste wood feedstock | Bitumen extender | 30; 70 |
| Yang et al., 2017 | Wood chips, sawdust and shavings | Bitumen modifier | 2, 5, 10 |
| Lei et al., 2017 | Wood plant liquid | Rejuvenator | ≤10 |
| Pouget and Loup, 2013 | Wood plant liquid | Direct alternative binder | 100 [e] |

[a] percentage by weight of the binder; [b] the bio-oil contains 10-15% by weight of ground tire rubber (GTR); [c] the bio-oil contains 0-4% by weight of polymers; [d] the bio-oil is composed of 80% pine resin and 20% linseed oil; [e] the bio-oil contains about 10% by weight of polymers

**Table 2.2** Overview of some bio-oils studied so far in literature: waste cooking oil

| Reference | Raw bio-material | Bio-oil function | Bio-oil [%] |
|---|---|---|---|
| Wen et al., 2012 | - | Bitumen extender | 10; 30; 60 |
| Gong et al., 2016 | - | Rejuvenator | ≤3 |
| Su et al., 2015 | - | Rejuvenator | 2÷10 |
| Zargar et al., 2012 | - | Rejuvenator | 1÷5 |
| Sun et al., 2016 | - | Bitumen modifier | 2; 4; 6; 8 |
| Singh-Ackbarali et al., 2017 | - | Bitumen modifier | 2÷10 |

**Table 2.3** Overview of some bio-oils studied so far in literature: vegetable bio-oils

| Reference | Raw bio-material | Bio-oil function | Bio-oil [%] |
|---|---|---|---|
| Seidel and Haddock, 2012 | Soy | Fluxing agent | 1; 3 |
| Xi et al., 2015 | Soy | Bitumen extender | 25 [a] |
| Jimenez del Barco-Carrion et al., 2017a | Linseed | Rejuvenator | 64 [b] |
| Jimenez del Barco-Carrion et al., 2017b | Linseed | Rejuvenator | 64 [b] |
| Jimenez del Barco-Carrion et al., 2017c | Linseed | Rejuvenator | 64 [b] |
| Kowalski et al., 2016 | Rapeseed | Fluxing agent | 10 |
| Krol et al., 2016 | Rapeseed | Fluxing agent | ≤5 |
| Somé et al., 2016 | Rapeseed | Fluxing agent | 18 |
| Kowalski et al., 2017 | Rapeseed | Rejuvenator | 2.5 |
| Gong et al., 2017 | Bean | Bitumen modifier | 1; 2; 3 |
| Xi et al., 2015 | Cottonseed | Bitumen extender | 25 [a] |
| Zhu et al., 2017 | Cottonseed | Rejuvenator | 5; 10 |
| Garcia et al., 2016 | Sunflower | Rejuvenator | 5 [c] |
| Somé et al., 2016 | Sunflower | Fluxing agent | 18 |
| Ahmad et al., 2018 | Jatropha curcas | Rejuvenator | 1÷5 |
| Podolsky et al., 2016 | Corn | Fluxing agent | 0.5 |
| Raouf and Williams, 2010b | Switchgrass | Direct alternative binder | 100 [d] |
| Chailleux et al., 2012 | Microalgae | Direct alternative binder | 100 |

[a] the bio-oil is a blend of soybean oil and cottonseed oil; [b] the bio-oil is composed of 80% pine resin and 20% linseed oil; [c] percentage by weight of the mixture (capsules containing bio-oil); [d] the bio-oil contains 0-4% by weight of polymers

**Table 2.4** Overview of some bio-oils studied so far in literature: bio-oils of animal origin

| Reference | Raw bio-material | Bio-oil function | Bio-oil [%] |
|---|---|---|---|
| Oldham et al., 2015 | Swine manure | Rejuvenator | 10 |
| Fini et al., 2011 | Swine manure | Fluxing agent | 2; 5; 10 |
| Fini et al., 2012 | Swine manure | Fluxing agent | 2; 5; 10 |
| Samieadel et al., 2018a | Swine manure | Bitumen modifier | 10 |

**Table 2.5** Overview of some solid bio-materials studied so far in literature

| Solid bio-material | Raw bio-material | Bio-material function | Bio-material [%] | Reference |
|---|---|---|---|---|
| Lignin | Wood | Bitumen modifier | Partial replacement of SBS | Kowalski et al., 2016 |
| | Wood | Bitumen modifier | 3; 6; 9 [a] | McCready and Williams, 2008 |
| | Wood | Bitumen modifier | 23 [a] | Pan, 2012 |
| | Wood | Bitumen modifier | 5; 10 [a] | Xu et al., 2017 |
| | Wood | Bitumen modifier | 1; 4; 6 [a] | Batista et al., 2018 |
| | Wood | Bitumen modifier | 5÷20 [a] | Xie et al., 2017 |
| Waste coffee grounds | - | Bitumen modifier | 4; 8 [a] | Zofka and Yut, 2012 |
| Natural fibres | Hemp | Mixture modifier | 0.15÷0.55 [b] | Shanbara et al., 2018 |
| | Jute | Mixture modifier | 0.15÷0.55 [b] | Shanbara et al., 2018 |
| | Coconut residues | Mixture modifier | 0.15÷0.55 [b] | Shanbara et al., 2018 |
| | Coconut residues | Mixture modifier | 0.3÷0.5 [b] | Oda et al., 2012 |
| | Sisal leaves | Mixture modifier | 0.3÷0.5 [b] | Oda et al., 2012 |
| | Sisal leaves | Mixture modifier | 0.05÷0.3 [b] | Ramalingam et al., 2017 |

[a] percentage by weight of the binder, [b] percentage by weight of the aggregates

Most of the proposed renewable materials are of vegetable origin, and many of them derive from wood residues such as lignin, tall oil pitch, wood resins and plant sap, which come from wood processing in pulp and paper industries. It must be pointed out that a type of plant or wood can be specific of a certain area, in which therefore the bio-material is readily available, whereas it could be hard to suppose its use in different or distant areas. Despite such drawback, similarities between different plant species might emerge in terms of effects provided to the bituminous material, thus leading to common general recommendations for renewable materials of wood origin.

Another widely used renewable material of vegetable origin is waste cooking oil, which is available in large quantities all over the world (Su et al., 2015; Sun et al., 2016; Wen et al., 2012). Its disposal is often problematic, since it typically causes problems to the sewerage and purification systems, generating serious water pollution if not properly treated (Azahar et al., 2016; Singh-Ackbarali et al., 2017). Therefore, its use in bituminous materials could help with these drawbacks.

Further examples are bio-oils obtained from vegetable oils and biomass, such as soy, linseed, rapeseed, etc. (Table 2.3). Vegetable solid bio-materials such as natural fibres have also been studied (Table 2.5).

Some materials of animal origin are also used, such as swine manure (Fini et al., 2012; Fini et al., 2011; Oldham et al., 2015; Samieadel et al., 2018a), which has the significant advantage of non-competition with food and raw materials destined for human consumption, as happens for instance even for algae (Chailleux et al., 2012), wood residues (Cooper III et al., 2013; Jimenez del Barco-Carrion et al., 2017b; Jimenez del Barco-Carrion et al., 2017c; Peralta et al., 2012a) or jatropha curcas oil (Ahmad et al., 2018). Moreover, swine manure can cause significant emissions in terms of greenhouse gases (GHGs) when it is stored in lagoons or used as a fertilizer (Fini et al., 2011; Samieadel et al., 2018a). Nevertheless, at the moment it seems rather ambitious to use swine manure for actual large-scale applications.

Other materials like waste motor oil (Fernandes et al., 2017; Lei et al., 2017) and urban plastic waste (Angelone et al., 2016) have often been compared with bio-materials.

However, even if their introduction in bituminous mixtures avoids serious disposal problems, waste motor oil, plastic waste and similar materials cannot be included among renewable materials, since they are petroleum-based products as well. Therefore, there are still concerns about their use, as they might cause harmful emissions during the production and laying of the bituminous mixture and soil and groundwater pollution during the pavement service life, especially if employed without any pre-treatment.
Another aspect to be taken into account is the complexity of the treatment before the employment of the renewable material. Indeed, in most cases, the bio-materials used for bituminous applications are obtained from raw materials through thermal and/or chemical treatments such as:

- pyrolysis (Zhang et al., 2017) and fast pyrolysis, which are typically used to treat wood and plant residues (Cooper III et al., 2013; Peralta et al., 2014; Peralta et al., 2013; Peralta et al., 2012a; Raouf and Williams, 2010a; Raouf and Williams, 2010b; Yang et al., 2017; Yang et al., 2015; Yang et al., 2014);
- esterification, often used for vegetable oils (Gong et al., 2017) and waste cooking oil (Gong et al., 2016; Sun et al., 2016);
- hydrothermal liquefaction, employed for instance for swine manure (Fini et al., 2012; Fini et al., 2011; Samieadel et al., 2018a).

In other cases, the bio-materials are incorporated in bituminous mixtures without any kind of pre-treatment (Singh-Ackbarali et al., 2017; Zofka and Yut, 2012).
Therefore, it is important to evaluate whether the necessary pre-treatment is included in the normal production process of the renewable material or it is additional. Indeed, in the latter case it might imply additional efforts from a technological and economic point of view. On the contrary, when there is no treatment, it is necessary to carefully consider the possible consequences (e.g. on the environment and/or on the workers' health, see Section 2.4) related to the use of the material.
In conclusion, many types of renewable materials can be used and each one may imply specific benefits and drawbacks that must be appropriately evaluated case by case.
Some examples of bio-oils and solid bio-materials are shown in Figures 2.1 and 2.2, respectively.


**(a)** **(b)** **(c)** **(d)**

**Figure 2.1** Examples of bio-oils: (a) bean oil (Gong et al., 2017), (b) oil from pyrolysis of biomass (Zhang et al., 2017), (c) waste sunflower oil and (d) waste rapeseed oil (Somé et al., 2016)

**(a)** **(b)**

**Figure 2.2** Examples of solid bio-materials: (a) coconut fibres, (b) sisal fibres (Oda et al., 2012)

### *2.2.3 Functions of the renewable materials*

According to literature (Jimenez del Barco-Carrion et al., 2017b; Jimenez del Barco-Carrion et al., 2017c; Peralta et al., 2012b; Raouf and Williams, 2010a; Raouf and Williams, 2010b), a bio-material can be broadly used as bitumen modifier (< 10% bitumen replacement), bitumen extender (25% to 75% bitumen replacement) or direct alternative binder (100% replacement).
However, a more detailed function-based classification of the bio-materials has been provided in Tables 2.1-2.5. In fact, despite the great variety of renewable materials used (see Section 2.2.2), their possible functions into bituminous binders and mixtures can be, in general, summarized as follows:

a) if the bio-material shows a behaviour similar to bitumen, it can be used as a bitumen extender, i.e. in partial replacement of bitumen at a dosage higher than 10-15% by weight of the binder (Tables 2.1-2.4). Some authors have investigated even the possibility of a total replacement of bitumen with bio-materials (Tables 2.1-2.4) or non-petroleum based synthetic binders (Airey et al., 2016). However, it is worth underlining that, even though a total replacement of bitumen might be possible from a hypothetical point of view, the technical community as well as the market are unlikely to be ready for this solution in the short or medium term;
b) when the bio-material is characterized by low viscosity (which is a typical characteristic of the bio-oils), it can be used to reduce the consistency of the binder, namely as a fluxing/ softening agent or as a rejuvenator for aged bitumen (Tables 2.1-2.4). The adopted dosage is usually lower than 10% by weight of the binder, but in some cases higher dosages are considered (Jimenez del Barco-Carrion et al., 2017a; Jimenez del Barco-Carrion et al., 2017b; Jimenez del Barco-Carrion et al., 2017c), in order to completely avoid the use of virgin bitumen by combining aged bitumen and bio-oil according to appropriate proportions;
c) when the bio-material is solid (Table 2.5), it can be employed at limited dosages, typically lower than 5% by weight of the binder, as a bitumen/mixture modifier, with the aim of improving one specific property, such as the aging susceptibility (Pan, 2012; Xu et al., 2017; Zofka and Yut, 2012) or the tensile strength (Abiola et

al., 2014; Ramalingam et al., 2017; Shanbara et al., 2018). As for the natural fibres, small quantities, up to 0.5% by weight of the aggregates (Abiola et al., 2014; Oda et al., 2012; Shanbara et al., 2018), are typically added to the bituminous mixture through a dry method that consists of blending the fibres with the hot aggregates before adding the bituminous binder (Abiola et al., 2014; Oda et al., 2012; Ramalingam et al., 2017). Therefore, in the case of solid bio-materials, the environmental benefits deriving from the replacement of bitumen are not fully achieved;

d) if the bio-material causes an undesired worsening of the mechanical properties of the binder (such as reduced permanent deformation resistance or increased aging tendency, which might compromise performance and/or durability), it can still be used by modifying the binder with polymers (Fernandes et al., 2017; Zhang et al., 2017), bio-polymers (Peralta et al., 2012b), crumb rubber (Peralta et al., 2014; Peralta et al., 2013; Peralta et al., 2012a), etc., which are added to minimize the negative effect of the bio-material (see also Section 2.3.1). In this case, since no performance improvement is obtained, the main function of the bio-material is to produce a final binder characterized by reduced environmental impact (Tables 2.1-2.4). It is worth pointing out that the use of renewable bio-polymers instead of traditional polymers, which are petroleum-based products, is preferable for further reducing the environmental impact (Peralta et al., 2012b). Crumb rubber instead cannot be classified as a renewable material, even though it is a critical waste to be disposed of.

Finally, a separate mention should be made for some attempts that have recently been carried out to produce capsules containing bio-oils and incorporate them in the bituminous mixture, with the aim of promoting self-healing when cracking occurs (Garcia et al., 2016) or rejuvenating the aged bitumen in situ (Su et al., 2015) (i.e. the bio-oil is used with the function described in point b)). This kind of application, that seems to be interesting but rather complex, requires a series of additional considerations that are beyond the scope of this thesis.

## 2.3 Performance evaluation

In the following sections the analysis of the available literature concerning the performance of bituminous binders, mixtures and pavements containing renewable materials is presented. Several aspects that should be appropriately taken into consideration and evaluated are also highlighted.

### *2.3.1 Binders*

Much literature exists on the study of the performance of bituminous binders containing bio-materials, since this aspect represents the first necessary step of every experimental investigation in this field.

Firstly, the blending conditions (temperature, time, speed) between the bitumen and the bio-material should be carefully selected (Xi et al., 2015), particularly for solid bio-materials. In fact, as the blending temperature and time increase, the bio-binder becomes more homogeneous, but problems related to aging can arise (Xi et al., 2015). As for the blending speed, it has been observed that high speeds should be preferred (Xi et al., 2015). This blending is normally only a physical process for unmodified bitumen, as it does not lead to the formation of new chemical compounds (Gong et al., 2016; Sun et al., 2016; Yang et al., 2017; Yang et al., 2015), whereas some chemical reaction may occur for polymer-modified bitumen (Gong et al., 2016).

As for the binder performance, in most cases the bio-oils cause a reduction of both viscosity (Figure 2.3) (Fini et al., 2012; Gondim et al., 2016; Gong et al., 2016; Oldham et al., 2015; Seidel and Haddock, 2012; Sun et al., 2016; Yang et al., 2015; Zargar et al., 2012; Zhang et al., 2017) and complex modulus $|G^*|$ (Fini et al., 2012; Gondim et al., 2016; Jimenez del Barco-Carrion et al., 2017b; Jimenez del Barco-Carrion et al., 2017c; Kowalski et al., 2017; Seidel and Haddock, 2012; Singh-Ackbarali et al., 2017; Sun et al., 2016; Yang et al., 2015; Zargar et al., 2012; Zhu et al., 2017) and an increase in the phase angle $\delta$ of the bio-binder (Figure 2.4) (Jimenez del Barco-Carrion et al., 2017a; Jimenez del Barco-Carrion et al., 2017b; Jimenez del Barco-Carrion et al., 2017c; Sun et al., 2016; Zargar et al., 2012; Zhang et al., 2017; Zhu et al., 2017), regardless of the bio-oil type. These effects are due to the viscosity of the bio-oils, which is low when compared to the typical values exhibited by hard or medium-grade bitumens (Table 2.6). Moreover, bio-oils tend to exhibit, even at ambient temperature, a liquid-like behaviour rather than a solid-like behaviour (such as bitumen), which means that their stiffness and elasticity are generally lower with respect to those of bitumen.

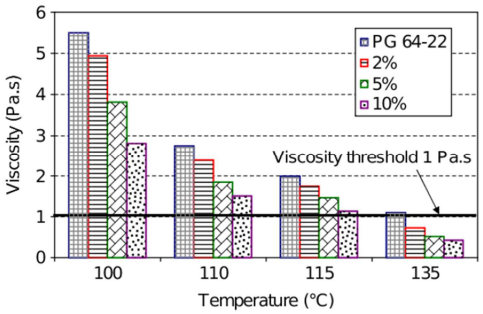


**Figure 2.3** Effect of the bio-oil from swine manure on the viscosity at various dosages and temperatures (Fini et al., 2012)

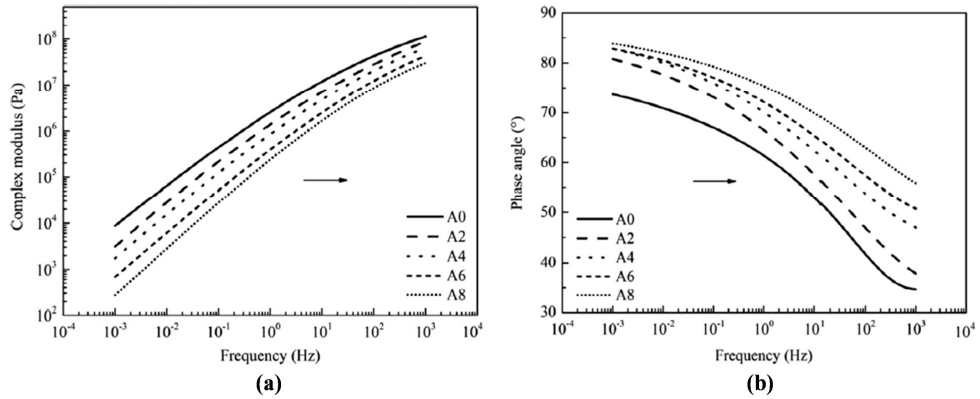


**Figure 2.4** Master curves of (a) complex modulus and (b) phase angle obtained with generalized CAM model at 20°C for different waste cooking oil dosages (0%, 2%, 4%, 6%, 8% by weight) (Sun et al., 2016)

**Table 2.6** Viscosity of some bio-oils, compared with conventional bitumen

| Material | Temperature [°C] | Viscosity [Pa·s] |
|---|---|---|
| Conventional 50/70 bitumen | 135 | 0.51 |
| Bio-oil from wood residues (Yang et al., 2014) | 135 | 0.10 |
| Cottonseed oil (Zhu et al., 2017) | 60 | 0.14 |
| Tall oil pitch (Ball et al., 1993) | 35 | 80.00 |

In terms of conventional properties, an increase in the penetration value (Ball et al., 1993; Gong et al., 2016; Somé et al., 2016; Sun et al., 2016; Zargar et al., 2012) and a decrease of the softening point (Gong et al., 2016; Krol et al., 2016; Sun et al., 2016; Zargar et al., 2012) are simultaneously observed. On the one hand, this softening effect usually results in an improvement of fatigue (Lei et al., 2017; Singh-Ackbarali et al., 2017; Zhu et al., 2017) and low-temperature (Fini et al., 2012; Gong et al., 2016; Lei et al., 2017; Oldham et al., 2015; Podolsky et al., 2016; Sun et al., 2016; Zhu et al., 2017) behaviour as compared to the base bitumen. On the other hand, given the reduced complex modulus and increased phase angle of the final bio-binder with respect to the base bitumen, the rutting resistance is negatively affected (Fini et al., 2012; Lei et al., 2017; Singh-Ackbarali et al., 2017; Sun et al., 2016; Wen et al., 2012; Zhang et al., 2017; Zhu et al., 2017). Consequently, in terms of Performance Grade (PG), there is a reduction in both the lower and the upper performance grade, indicating an improvement of the performance at low temperatures but also a worsening at high temperatures (Lei et al., 2017; Wen et al., 2012) (Table 2.7). In this regard, Lei et al. (2017) have found a linear relationship between the content of different oils and the true (i.e. continuous) high temperature and low temperature performance grade, as shown in Figures 2.5 and 2.6. In these figures, PP-1, PP-2 and PR-3 are petroleum-based oils, BO-1 and BO-2 are bio-oils from wood residues, RW is waste motor oil.

**Table 2.7** Effect of bio-oils on Performance Grade (PG)

| Reference | Bitumen PG | Type of bio-oil | Bio-oil dosage [%] | Bio-binder PG |
|---|---|---|---|---|
| Wen et al., 2012 | PG58-28 | Waste cooking oil | 30 | PG52-34 |
| | | | 60 | PG46-40 |
| | PG82-16 | | 10 | PG76-24 |
| | | | 30 | PG70-28 |
| | PG76-22 | | 10 | PG76-22 |
| | | | 30 | PG70-34 |
| Lei et al., 2017 | PG64-22 | Bio-oil from wood residues | 6 | PG58-28 |
| | | | 7 | PG58-28 |

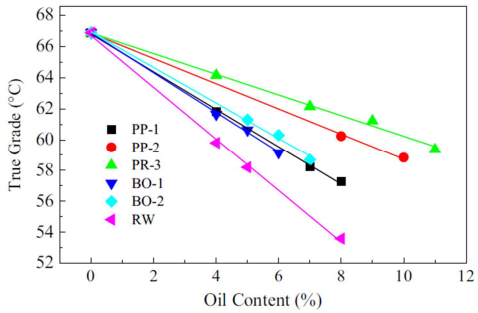


**Figure 2.5** Relationship between oil content and true high temperature performance grade (Lei et al., 2017)

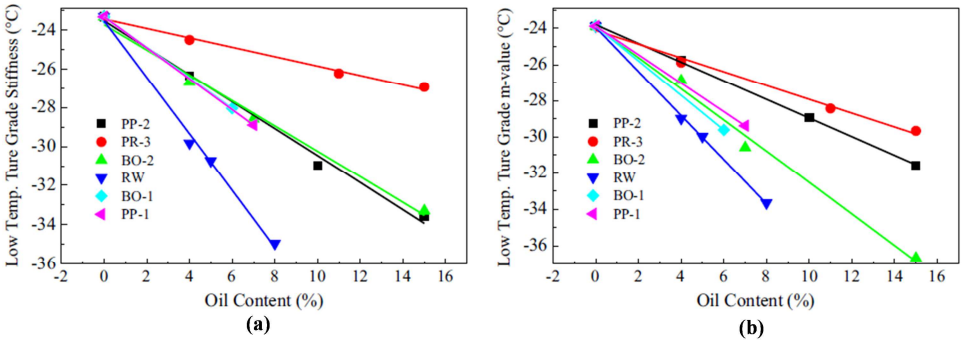


**Figure 2.6** Relationship between oil content and true low temperature performance grade based (a) on stiffness, (b) on m-value (Lei et al., 2017)

From a structural and chemical point of view, this softening effect of the bio-oil on the binder typically emerges as a reduction of the asphaltenes (Gong et al., 2016; Zargar et al., 2012; Zhu et al., 2017), which are considered to be responsible for the consistency and the viscosity of bituminous binders (Eberhardsteiner et al., 2015; Zhu et al., 2017), and of the

carbonyl and sulfoxide functional groups indices (Zhu et al., 2017), which are linked with the degree of oxidation and aging of the binder (Gong et al., 2016; Marsac et al., 2014; Xu et al., 2017; Yang et al., 2017; Yang et al., 2015; Zhu et al., 2017). However, the high oxygen content of some bio-oils may imply an increase in the carbonyl and sulfoxide indices (Gong et al., 2016; Yang et al., 2017; Yang et al., 2015) and hence some doubts have been raised about the use of such indices to evaluate the effect of bio-oils on oxidation and aging (Gong et al., 2016). In this regard, Table 2.8 presents the chemical elemental composition of some bio-oils that have been proposed for bituminous applications, together with the composition of conventional bitumens. From the table, it can be observed that bio-oils tend to exhibit significantly higher content of oxygen and lower content of carbon as compared to bitumen. Moreover, the sulphur content is typically very close to zero for bio-oils, unlike bitumens. Such observations can be considered valid, in general, for different types of biomass, but the chemical composition may substantially differ from case to case (Vassilev et al., 2010).
The effects previously discussed, which seem reasonable given the general characteristics of bio-oils, are typically more pronounced as the dosage of the bio-oil increases, as shown in Figures 2.3, 2.4, 2.5, 2.6 and Table 2.7.

**Table 2.8** Chemical elemental composition of some bio-oils, compared with conventional bitumens

| Material | Carbon [%] | Oxygen [%] | Hydrogen [%] | Nitrogen [%] | Sulphur [%] |
|---|---|---|---|---|---|
| Bitumen 1 (Fini et al., 2011) | 81.60 | 0.90 | 10.80 | 0.77 | - |
| Bitumen 2 (Michalica et al., 2008) | 83.17 | 1.33 | 10.28 | 0.45 | 4.77 |
| Bitumen 3 (Michalica et al., 2008) | 85.20 | 1.25 | 10.30 | 0.58 | 2.67 |
| Bio-oil from wood waste (Yang et al., 2017) | 58.80 | 34.31 | 6.62 | 0.27 | - |
| Bio-oil from swine manure (Fini et al., 2011) | 72.58 | 13.19 | 9.76 | 4.47 | - |
| Bio-oil from pyrolysis of biomass (Zhang et al., 2017) | 54÷56 | 35÷45 | 5.5÷7.2 | 0÷0.2 | - |

In order to compensate the negative impact of the bio-oil on the high-temperature performance, different solutions have been proposed. The most obvious solution is to adopt a harder base bitumen. Instead the addition of polymers such as Styrene-Butadiene-Styrene (SBS) (Zhang et al., 2017) or polyethylene (PE) (Raouf and Williams, 2010a; Raouf and Williams, 2010b) can be considered for widening the range of temperatures in which the bio-binder exhibits good performance. Moreover, it has been found that lignin, which is a bio-polymer, provides a stiffening effect on the binder, ensuring the improvement of the high-temperature performance and the rutting resistance (Batista et al., 2018; McCready and Williams, 2008; Xie et al., 2017; Xu et al., 2017), as demonstrated by the increase in the rutting parameter $G/\sin\delta$ in Figure 2.7. These results have led to the idea that lignin can be effectively used instead of SBS or other traditional polymers (Kowalski et al., 2016). A similar stiffening effect can also be obtained through the addition of polyphosphoric acid (PPA), which allows to improve the elastic behaviour of the binder (Fini et al., 2012). Another way to minimize the effect of the bio-oil is to modify the binder with ground (or crumb) rubber from used tires (GTR) (Peralta et al., 2014; Peralta et al., 2013; Peralta et al., 2012a), which is able to enhance the elasticity of the binder and, thus, its rutting resistance. Instead Kowalski et al. (2017; 2016) and Krol et al. (2016) have proposed a bio-agent from

rapeseed that acts as a bi-functional material. After being added to the bitumen, the bio-agent fluidizes the bitumen by lowering its viscosity. Afterwards, also thanks to the presence of a catalyst, a slow polymerization process (that lasts for about one month) starts in the bio-agent, allowing to partially recover the initial bitumen viscosity. In this way, the workability of the mixture is enhanced during compaction, but the rutting resistance is not negatively affected during the in-service life of the pavement.

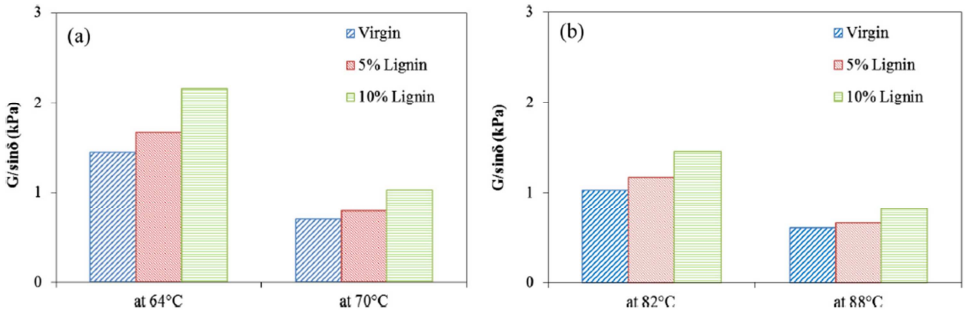


**Figure 2.7** Effect of lignin on the rutting parameter $G/\sin\delta$ for (a) unmodified PG64-22 and (b) SBS-modified PG76-22 (Xu et al., 2017)

When the above-mentioned typical effects of the bio-oil are not found or the effects observed are not consistent with each other (Wen et al., 2012; Yang and You, 2015), the cause may be the accelerated aging of the bio-material. Indeed, greater susceptibility to aging is sometimes observed due to the presence of the bio-material (Bearsley and Haverkamp, 2007a; Yang et al., 2017; Yang et al., 2015; Zhang et al., 2017) as well as significant mass loss (Peralta et al., 2014; Yang et al., 2015) during short-term aging with Rolling Thin Film Oven Test (RTFOT) (EN 12607-1, 2015). In this regard, Zhang et al. (2017) have found that the phase angle increases as the dosage of the bio-oil is increased in unaged conditions, whereas this trend is completely inverted after RTFOT aging (Figure 2.8), which means that the mixture might show unexpected brittleness during its in-service life. In Figure 2.8, "50#" indicates a 50 penetration grade bitumen, "S100" indicates a SBS modified bitumen, "S105", "S110", "S115" and "S120" indicate bio-binders obtained by replacing part of S100 with 5, 10, 15 and 20 % of bio-oil from wood residues, respectively. These results have even led some authors (Kluttz, 2012; Peralta et al., 2012b; Yang et al., 2015) to hypothesize that the common aging procedures and conditions with RTFOT and Pressure Aging Vessel (PAV) (EN 14769, 2013), which are designed to simulate respectively the short-term and long-term aging of traditional binders, might be too severe for binders containing bio-materials, causing the over-aging of the bio-binder. A possible reason is that, due to the organic nature of the bio-material, the bio-binder might suffer significant volatilization of light weight compounds, dehydrogenation (i.e. formation of bigger molecular sized compounds) and oxidation (Yang et al., 2015). The great mass loss can be also caused by water loss (Peralta et al., 2014), as biomass is generally characterized by high moisture content (Vassilev et al., 2010). In this sense, it is evident that the aging susceptibility strongly depends on the chemical composition of the bio-material in question. However, although many studies have focused on the effect of short-term aging on bio-

binders, long-term aging has been less investigated so far (Batista et al., 2018; McCready and Williams, 2008; Xu et al., 2017; Yang et al., 2017; Zofka and Yut, 2012) and therefore further research is needed.

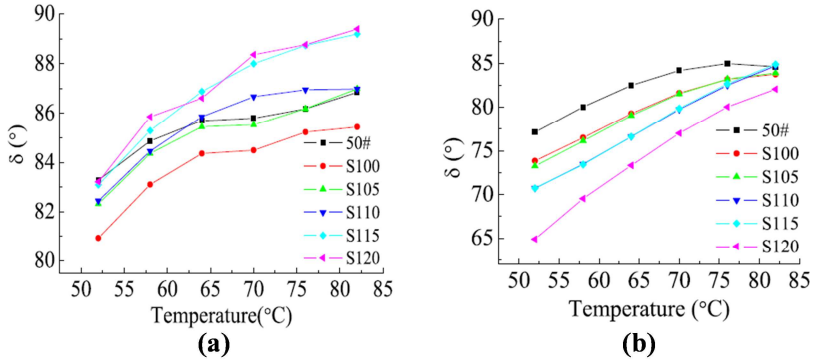


**Figure 2.8** Effect of short-term aging on the bio-binder: relationship between phase angle and temperature (a) before RTFOT and (b) after RTFOT (Zhang et al., 2017)

Conversely, some specific bio-materials added as bitumen modifiers, such as coffee grounds (Zofka and Yut, 2012) and lignin (Batista et al., 2018; McCready and Williams, 2008; Pan, 2012; Xie et al., 2017; Xu et al., 2017), have shown their potential to provide anti-oxidant effect or to reduce hardening susceptibility, thus improving the overall aging resistance. This is due to the fact that such bio-materials are characterized by marked anti-oxidant properties (Pan, 2012; Xu et al., 2017, Zofka and Yut, 2012). However, as regards the use of lignin, it is worth pointing out that the production temperature of the mixture must be kept as low as possible, in order to prevent lignin oxidation that would lead to a significant reduction of the anti-oxidant effect provided to the binder (Pan, 2012). Figure 2.9 shows the anti-oxidant effect of lignin on RTFOT-aged and PAV-aged binders, resulting in a reduction of the carbonyl index $I_{C=O}$.

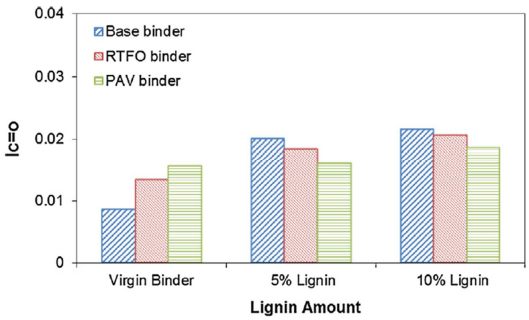


**Figure 2.9** Anti-oxidant effect provided by lignin in terms of reduced carbonyl index $I_{C=O}$ (Xu et al., 2017)

As for the rheological properties of the bio-binders, a thermo-rheologically simple behaviour is usually found (Jimenez del Barco-Carrion et al., 2017a; Jimenez del Barco-Carrion et al., 2017b; Somé et al., 2016), which means that the time-temperature superposition principle (TTSP) is valid (Yusoff et al., 2011), as for conventional bitumens. However, as the dosage of the bio-material increases (and thus the bitumen percentage decreases), the TTSP might no longer be valid (Chailleux et al., 2012; Kluttz, 2012) and, moreover, the usual rheological characterization of the binder and the common SHRP (Strategic Highway Research Program) criteria (Kennedy et al., 1994) could not be applicable. It has been found for example that, for the study of high-temperature performance, oscillatory tests lead to results that are not completely consistent with the results of multiple stress creep recovery (MSCR) tests (Kluttz, 2012; Yang and You, 2015). Instead for non-petroleum based synthetic binders it has been observed that the TTSP is valid, but the rheological behaviour is very different from that of bitumen, probably due to their amorphous or partially crystalline polymeric structure (Airey et al., 2016).
In terms of tendency to separation between bitumen and bio-oil, promising results have been obtained for bio-oil dosages up to 15% (Ball et al., 1993; Sun et al., 2016), as the bio-binders' structure is normally homogeneous, at least in the case of unmodified bitumens. Zhang et al. (2018a) studied the storage stability of bio-binders containing different percentages of bio-oil from waste wood (10, 15, 20, 25, and 30 %) at different storage temperatures (120, 140, 160 and 180 °C). Based on their findings, they recommended to keep the bio-oil content below 25% and the storage temperature below 160°C. Conversely, the introduction of modifying agents such as crumb rubber may cause relevant problems for the storage stability (Peralta et al., 2014; Peralta et al., 2013). However, when studying the compatibility between bitumen and bio-oil deriving from wood residues in terms of solubility, in some cases it has been observed that the flocculation of the asphaltenes might cause undesirable phase separation even for low dosages of the bio-oil (Yang et al., 2017).

### *2.3.2 Mixtures*

As compared to the large number of publications on binders with renewable materials, less literature is available on the mixture performance evaluation.
In general, the presence of bio-oils shows similar effects as those on the binder, causing an improvement of the fatigue (Kowalski et al., 2017; Yang et al., 2014) and low-temperature cracking (Kowalski et al., 2017; Wen et al., 2012) performance and a simultaneous worsening of the rutting resistance (Wen et al., 2012) as compared to the mixture with the base bitumen. In this regard, Figure 2.10 shows the longer fatigue life obtained with four-point beam fatigue tests at 21°C and different strain levels for bituminous mixtures containing bio-binders (in the figure, "OB" indicates the original bio-oil from wood residues, "DWB" indicates the dewatered bio-oil, "PMB" indicates the polymer modified bio-oil, 5% and 10% are the dosages of the bio-oil in the bio-binder). However, at the mixture level, there is greater uncertainty in the performance evaluation, since in some cases there is an unchanged (Yang et al., 2014) or even improved (Cooper III et al., 2013; Somé et al., 2016) behaviour in terms of rutting and a decreased resistance to fatigue cracking (Cooper III et al., 2013; Wen et al., 2012), in contrast with the results obtained for

the corresponding binders. The concern is that these results may be determined by the over-aging of the bio-binder that occurs during the production of the mixture (Jimenez del Barco-Carrion et al., 2017a; Jimenez del Barco-Carrion et al., 2017c; Yang et al., 2014). Moreover, from the investigation of the thermal aging of the mixture, Pouget and Loup (2013) have observed a significant increase in stiffness over time.

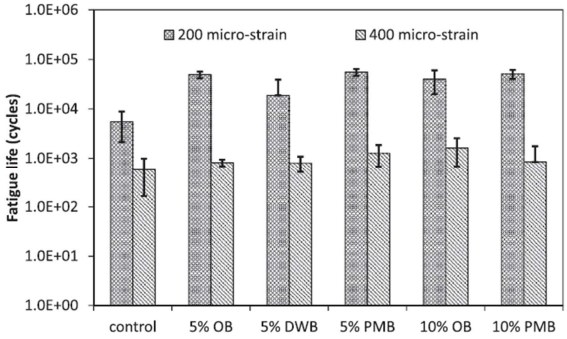


**Figure 2.10** Fatigue life obtained with four-point beam fatigue tests at 21°C and different strain levels for bituminous mixtures containing bio-binders (Yang et al., 2014)

In terms of workability and compactability of the mixture, the general trend observed is an improvement due to the presence of the bio-binder, that allows a decrease in the production and compaction temperatures of the mixture with respect to the base bitumen (which is reasonable, considering the softening effect provided by bio-oils). However, in some cases, reductions of the working temperatures up to 20-30 °C are also observed as compared to control traditional mixtures (produced with a bitumen having penetration grade and/or PG similar to that of the bio-binder) (Cooper III et al., 2013; Kowalski et al., 2017; Podolsky et al., 2016). Nevertheless, it is worth noting that, as the dosage of the bio-oil in the bio-binder increases, the mixture might not respond the same as traditional bituminous mixtures under the shear conditions of the common compaction methods (Kluttz, 2012).

A reduction of the tensile strength of the mixture may emerge as a consequence of the addition of the bio-oil (Cooper III et al., 2013; Grilli et al., 2016; Yang et al., 2014). It has been hypothesized that the lower tensile strength could be due to the generation of biochars that may occur at the typical mixing and compaction temperatures of hot mix asphalt (HMA), resulting in the reduction of the adhesive strength between aggregate and bio-binder (Yang et al., 2014). Bearsley and Haverkamp (2007b), however, have found that the presence of tall oil pitch may enhance the tensile strength.

As for the adhesion between bio-binders and aggregate, it has been found that, when considering the same aggregate, an improvement or a worsening with respect to the adhesion provided by the base bitumen can be achieved, depending on the chemical composition of the base bitumen (Gong et al., 2017). Analogously, the study of the adhesive forces with the aggregate in wet conditions has shown that the susceptibility to moisture damage strongly depends on the characteristics of the base bitumen (Gong et al., 2016). It is likely that the adhesion depends also on the type of aggregate, i.e. the bio-binder could show different performance for different aggregates, but very limited results are

currently available. Jimenez del Barco Carrion et al. (2019) have found that bio-rejuvenated asphalt binders present adhesive and cohesive properties comparable to those of a conventional bitumen with similar penetration grade and superior performance with respect to the reclaimed asphalt binder. Unlike what was observed for the adhesion between aggregate and bio-binders, no problem of moisture susceptibility due to the presence of the bio-material has emerged for the mixtures when testing dry and wet specimens in terms of tensile strength (Bearsley and Haverkamp, 2007b; Cooper III et al., 2013; Grilli et al., 2016; Peralta et al., 2014; Peralta et al., 2013) or compression resistance (Somé et al., 2016). Bearsley and Haverkamp (2007b) have even found a notable improvement of the moisture resistance of the mixture in the case of tall oil pitch. In general, biomass and bio-oils are rich in oxygen-containing chemical functional groups (Vassilev et al., 2010), which are considered the main responsible for the adhesion between bituminous binders and aggregates (Plancher et al., 1977). In this sense, it can be assumed that the resulting high polarity of the bio-binders may lead to improved adhesive properties with respect to traditional bitumen.

As far as the natural fibres are concerned, their effect on the mixture performance strongly depends on the fibres content and length, as well as their arrangement and orientation (Abiola et al., 2014). Moreover, most of the existing literature is focused on discontinuous mixtures, such as stone matrix asphalt (SMA), characterized by a gap-graded solid skeleton (Abiola et al., 2014), whereas dense-graded mixtures have begun to be studied only recently (Ramalingam et al., 2017). In general, natural fibres have the potential to effectively replace artificial and synthetic fibres (Abiola et al., 2014; Shanbara et al., 2018), as significant improvements can be obtained in terms of preventing the drain-down in discontinuous mixtures (Abiola et al., 2014; Oda et al., 2012), extending the fatigue life (Abiola et al., 2014; Ramalingam et al., 2017) and inhibiting the propagation of cracks (Abiola et al., 2014; Shanbara et al., 2018), besides additional tensile strength (Oda et al., 2012). However, the moisture absorption of natural fibres and their compatibility with the matrix still present some uncertainties (Abiola et al., 2014).

Finally, no study concerning the recycling of bituminous mixtures containing renewable materials in future new mixtures has been carried out so far. Since this aspect is crucial for the development of new road materials, it must be thoroughly investigated.

### *2.3.3 Pavement*

As for the field performance, very few data can be found in the scientific literature, which mainly refer to applications where small dosages of bio-material are used (e.g. as rejuvenator).

Through the analysis of the cores extracted from a trial section, Grilli et al. (2016) have shown that the addition of 6% bio-based rejuvenator in the binder allows to increase the RA content of the mixture from 15% to 40%, without altering the volumetric and mechanical characteristics (i.e. indirect tensile strength and indirect tensile stiffness modulus) of the mixture.

Zhou et al. (2018) reported the construction of two test sections in Texas in 2017 to assess the performance of two bio-rejuvenators. The test sections consisted in a 50 mm overlay

over a cracked asphalt pavement. The overlay mixes were designed with 30% RA and 3% rejuvenator (by total binder weight). After three months from the construction, neither cracking or rutting was observed, but it was too early to evaluate the actual field performance of the test sections.
Three test sections with bio-recycled asphalt mixtures were constructed in France at IFSTTAR accelerated pavement test (APT) facility (Blanc et al., 2019a; Blanc et al., 2019b). All the mixtures contained 50% RAP. Two of them were produced with bio-additivated bitumens, whereas the other one was produced with a bio-binder in total replacement of fresh bitumen. The bio-recycled asphalt mixes were compared to a high performance asphalt mix for base layers. The four test sections were characterized by the same pavement structure, consisting of a 9 cm asphalt layer and a 76 cm unbound granular layer over the subgrade. In the first experimental phase, carried out in the summer period, the rutting performance of the test sections was assessed by applying 200˙000 cycles with 65 kN dual wheel loads (corresponding to about 20 years of traffic, 150 truck per day). In the second experimental phase, carried out in the autumn-winter period, the fatigue performance was assessed by applying 1 million load cycles with 65 kN load, followed by 400˙000 cycles with 75 kN load. The bio-recycled asphalt mixtures presented better fatigue performance than the control asphalt mixture and their performance was satisfactory also in terms of rutting (Blanc et al., 2019a).
Given the limited data concerning the field performance against the main distresses that road pavements have to face due to the combined effect of traffic loadings and weathering (e.g. rutting, fatigue and thermal cracking, etc.), further research is needed in order to understand the actual potential and limits related to the use of renewable materials in road pavements. The attention should be focused also on other aspects, such as the compatibility between bio-asphalt mixtures and standard tack coats and the compatibility between bio-asphalt mixtures and contiguous traditional mixtures within the pavement (Kluttz, 2012).

### *2.3.4 Discussion*

The literature review carried out indicates that the introduction of bio-materials in bituminous binders and mixtures is very promising. Indeed, the fluxing effect provided by the bio-oils allows to obtain softer binders with improved performance at low and intermediate temperatures as compared to the base bitumen, which can be used especially in cold climates (Podolsky et al., 2016; Sun et al., 2016). In some cases, the fluxing effect could also be exploited to reduce the production and compaction temperatures of the mixture without compromising the workability (Cooper III et al., 2013; Fini et al., 2012; Fini et al., 2011; Gondim et al., 2016; Podolsky et al., 2016; Seidel and Haddock, 2012; Zhang et al., 2017), which means that the bio-oil may act similarly to warm mix asphalt (WMA) technologies (Rubio et al., 2012), thus leading to significant environmental and economic benefits in terms of reduced emissions and energy consumption (see also Section 2.4). Moreover, the bio-oils show their potential as rejuvenators in mixtures containing RAP (reclaimed asphalt pavement) or RAS (reclaimed asphalt shingles) (Fini et al., 2012; Jimenez del Barco-Carrion et al., 2017a; Krol et al., 2016; Lei et al., 2017), being able to mitigate the increase in stiffness due to the inclusion of aged RAP or RAS. Indeed, the

initial (unaged) properties of short-term aged (Gong et al., 2016) and long-term aged (Zhu et al., 2017) binders can be restored to a notable extent thanks to the addition of the bio-oil.
The high-temperature performance can be effectively enhanced with the addition of polymers, bio-polymers and crumb rubber among others, minimizing the negative impact of the bio-oil and thus allowing the use of bio-binders in a wider range of temperatures (Fini et al., 2012; McCready and Williams, 2008; Peralta et al., 2014; Xie et al., 2017). In fact, the combined use of these materials and bio-oils could potentially improve the binder performance at all temperatures, but further investigation is necessary.
The bio-materials that are solid at room temperature and have anti-oxidant properties, such as lignin and coffee grounds, can be used as bitumen modifiers, in order to improve the aging resistance of the binder (Batista et al., 2018; Xie et al., 2017). Natural fibres instead can be employed to provide additional tensile strength to the bituminous mixture, which may result in improved fatigue and cracking resistance (Ramalingam et al., 2017; Shanbara et al., 2018), or to prevent drain-down in gap-graded mixtures (Oda et al., 2012).
In terms of performance, further research is needed to evaluate the aging process of bio-binders, deepening the study of long-term aging. Moreover, very little information is available concerning the field performance and the recycling of bituminous mixtures containing bio-materials. Further work in this field should be aimed at filling these gaps.
Finally, in order to understand if bio-based products can truly be alternative to the traditional ones, the bio-binder and bio-asphalt mixture properties/performance should be always compared with the properties/performance of the corresponding bitumen (i.e. with similar penetration grade and/or PG) and asphalt mixture.

## 2.4 Health, safety and environment

When introducing a new construction material, its safety issues and possible environment and health impacts (or HSE aspects) must be evaluated (Purinton and Manning, 1996).
As for the health, the main concerns regard the road pavers, who are constantly subjected to asphalt fumes during road construction, rehabilitation and maintenance (Bal et al., 2018; Binet et al., 2002; Boffetta et al., 1997; Çelik et al., 2013; Chauhan et al., 2010; Heikkilä et al., 2003; Lindberg et al., 2008; Väänänen et al., 2006; Väänänen et al., 2005; Väänänen et al., 2003). Several studies indicate genotoxic, mutagenic and carcinogenic risks (Bal et al., 2018; Binet et al., 2002; Boffetta et al., 1997; Çelik et al., 2013), mainly due to the effect of the polycyclic aromatic hydrocarbons (PAH) contained in asphalt materials (Binet et al., 2002). Moreover, it has been shown that the presence of RA aggravates the risks for the workers (Heikkilä et al., 2003; Väänänen et al., 2005), whereas the use of recycled inorganic materials such as coal fly ash as filler in bituminous mixtures does not show any negative consequence (Heikkilä et al., 2003; Väänänen et al., 2005; Väänänen et al., 2003).
However, to date there is little literature concerning the effects of the introduction of renewable (organic) materials in bituminous mixtures on human health. Slight genotoxic effects emerged when waste plastic and tall oil pitch were used, but the effect depended also on the type of bituminous mixture (Lindberg et al., 2008). In the presence of waste plastic and tall oil pitch, the workers also experienced pungent odour, eye and skin irritation, itching and sore throat (Väänänen et al., 2006). These effects might be due to the

waste plastic (non-renewable) rather than to the tall oil pitch (renewable), even though similar symptoms (sharp smell and irritated eyes) were also experienced when a bio-oil from wood residues was used (You et al., 2012).
Gas chromatography-mass spectrometry (GC-MS) together with the mass loss were proposed as a useful means for estimating the emissions and thus the impact on workers' health, without the necessity of a direct measurement (Yang et al., 2017; Yang et al., 2015). Bio-oils from wood residues were found to contain many compounds with boiling point comparable with the mixing and compaction temperatures of traditional HMA, suggesting their preferable use at lower temperatures (Yang et al., 2017). However, it is worth noting that the bio-oil itself was analysed, but more significant information can be obtained by analysing the final bio-binder. Conversely, Batista et al. (2018) have found that lignin does not increase the volatility of the binder, thus not presenting negative impact on human health. Nevertheless, these available data are insufficient to draw any firm conclusion about the effects of renewable materials on human health and further investigation is needed to deepen such a crucial issue.
As far as the impact on environment is concerned, it is well-known that road construction and maintenance imply emissions in the atmosphere (Balaguera et al., 2018; Jullien et al., 2006), whereas during the in-service life of the road, also due to traffic, pollution concerns may arise around the soil, the surface water and the groundwater near the road (Van Bohemen et al., 2003). Excluding emissions due to traffic, which depend on the characteristics of the vehicles in circulation, the emissions attributable to the road materials employed are basically caused by the heating of the bituminous mixture during production and laying (Jullien et al., 2006).
Some studies have shown that the introduction of bio-oils deriving from swine manure (Samieadel et al., 2018a) and jatropha curcas (Ahmad et al., 2018) in the bituminous mixture may reduce the energy consumption and the emission of GHGs, thus indicating promising results in terms of carbon footprint. Indeed Tables 2.9 and 2.10, extracted from Samieadel et al. (2018a) and Ahmad et al. (2018) respectively, show that the use of bio-materials allows the reduction of the emissions of carbon dioxide ($CO_2$), methane ($CH_4$) and nitrous oxide ($N_2O$), which are some of the main GHGs. Analogously, the life cycle assessment (LCA) of biochar modified bio-binders derived from waste pine wood and pig manure highlighted that the "cradle-to-grave" energy consumption for mixtures prepared with these materials is about 25% of the energy consumption for traditional asphalt mixtures (Zhou et al., 2020a). The LCA also indicated that biochar modified bio-binders cause limited GHG emissions thanks to the biochar ability to adsorb volatile organic compounds (VOCs), which should also reduce the risks for human health (Zhou et al., 2020b). Different biochar sources were considered (i.e. pig manure, wood waste and straw biomasses) and it was found that the adsorption performance strongly depended on the biochar type, being the biochar from waste wood the one with the best adsorption ability (Zhou et al., 2020b). Lu et al. (2019a) studied porous asphalt mixtures produced with recycled ceramic aggregates and a bio-based polyurethane binder. Since this type of binder is workable at ambient temperature, they estimated that the energy consumption and GHG emissions for the mixture production and the pavement construction are less than 10% of the energy consumption and emissions in the case of the corresponding porous asphalt mixture. Finally, it must be also emphasized that the reduction of the production and compaction temperatures obtainable in some cases by using bio-oils (similarly to WMA

technologies, see Section 2.3.4) may lead to a reduction in the air emissions as compared to the traditional HMA (Thives and Ghisi, 2017).

**Table 2.9** Emissions calculated to produce 50 kg of binder

| Binder | Dosage of the bio-oil [% by weight of the binder] | $CO_2$ [kg] | $CH_4$ [kg] | $N_2O$ [kg] |
|---|---|---|---|---|
| Conventional asphalt binder | - | 20.05900 | 0.23600 | 0.00014 |
| Bio-binder | 10 | 18.44000 | 0.22000 | 0.00013 |

**Table 2.10** Emissions calculated to produce 1 ton of mixture

| Mixture | Dosage of the bio-oil [% by weight of the binder] | $CO_2$ [kg] | $CH_4$ [kg $CO_2$ equivalent] | $N_2O$ [kg $CO_2$ equivalent] |
|---|---|---|---|---|
| 30% RA | - | 24.3000 | 0.0138 | 0.2686 |
| 40% RA | - | 24.3000 | 0.0138 | 0.2686 |
| 30% RA + bio-oil | < 5 | 19.8100 | 0.0113 | 0.2190 |
| 40% RA + bio-oil | < 5 | 19.8100 | 0.0113 | 0.2190 |

Soil and water contamination are mainly due to the leaching (Andersson-Sköld et al., 2007; Kocher et al., 2005; Vahčič et al., 2008) and transport (Lygren et al., 1984) of the pollutants that are present on the pavement and inside it, which can cause significant pollution of the natural resources (Gjessing et al., 1984). The analysis of the chemical compounds through GC-MS has shown that bio-oils may suffer water solubility (Gong et al., 2016; Yang et al., 2017), which could cause some problems in terms of leaching. Nevertheless, it seems reasonable to assume that the blend formed by bitumen and small quantities of bio-material will exhibit a much lower solubility. However, no literature concerning specifically the impact of renewable materials on soil and water is available to date.
In general, the major environmental concerns are related to the use of waste materials that have not undergone any treatment (see Section 2.2.2) and hence might have negative effects on air, soil and water.
Finally, great attention has to be paid to the safety conditions that must be observed when handling a renewable material, since some specific precautions might be necessary, depending on its nature.
Within this context, more efforts are definitely needed to understand the consequences of the use of renewable materials in road pavements on health, safety and environment. In addition, it must be pointed out that the bio-materials used or proposed for bituminous applications may differ considerably in chemical composition. Thus, since the impact on health, safety and environment is closely related to the chemical composition, HSE assessment should be made case by case.

## 2.5 Summary of the findings from the literature review

The previous sections presented an overview on the use of renewable materials (i.e. bio-materials not subjected to depletion) in partial replacement of bitumen for road pavements.
From the literature review, it is evident that the use of renewable materials in bituminous binders and mixtures leads to significant environmental and economic benefits, such as the reduction of carbon footprint, the reduction of petroleum-based products, the recycling of industrial by-products and residues, the decrease of materials to be disposed in landfills, which are all in line with the key principles of sustainability and circular economy.
However, to be a viable solution from both a practical and a technical point of view, the renewable material should possess a series of fundamental requirements in terms of compatibility with bitumen, availability, handling, logistics and performance. Evaluations related to the possible effects on workers' health and on the environment (emissions in atmosphere, soil and groundwater contamination, etc.) as well as on safety issues are also crucial.
The literature review shows that the use of renewable materials is very promising. The main outcomes in terms of performance can be summarized as follows:

- the bio-oils, regardless of their origin, typically provide a fluxing/softening effect, which improves the performance of the binder at low and intermediate temperatures but negatively affects the high-temperature performance as compared to the base bitumen;
- this fluxing effect can be exploited for the application in cold climates or for rejuvenating aged bitumen. In some cases, the bio-oil may act similarly to warm mix asphalt technologies, reducing production and compaction temperatures of the mixture at equal workability;
- the possible negative impact of the bio-oil on the high-temperature performance can be minimized through the addition of polymers, crumb rubber or bio-polymers, which should be preferred because of their renewable nature;
- the bio-materials that are solid at room temperature can be used as bitumen/mixture modifiers, for instance to improve the aging resistance of the binder if they have anti-oxidant properties or to enhance the tensile strength of the bituminous mixture, as in the case of natural fibres.

However, bio-materials have not been widely used so far in asphalt pavements mainly for the following reasons/drawbacks:

- the long-term performance and durability of bituminous binders and mixtures containing renewable materials have not been enough demonstrated and reported up to now;
- the recyclability of bituminous mixtures containing bio-materials has been little considered so far, although it is extremely important that they are 100% recyclable exactly like traditional mixtures;
- the bio-binders may suffer over-aging as compared to traditional bituminous binders;
- the HSE (health-safety-environmental) aspects of bio-binders and bio-asphalt mixtures have not been enough documented so far. However, the assessment of these aspects is crucial for the industry to accept the use of such materials;

- currently there is limited documentation on the cost-effectiveness and/or life cycle assessment (LCA) of bituminous binders and mixtures containing bio-materials.

In this regard, this research project aimed at filling some of the above-mentioned gaps existing in the scientific literature, especially in terms of performance and durability. It is desirable that the aspects related to HSE and LCA will also be investigated in depth in the future.

# 3. Characterization of bitumen partially replaced with wood-based bio-oil

## 3.1 Background and objectives

The literature analysis (Section 2) highlighted that many types of renewable materials can be used in asphalt pavements, provided that they possess a series of requirements in terms of compatibility with bitumen, availability, handling and logistics as well as none or limited impact on environment and workers' health.
In general, a broad distinction can be made between solid and liquid bio-materials (bio-oils), as their addition to bituminous binders and mixtures provides different effects in terms of performance (Section 2.3). Examples of solid bio-materials are natural fibres and lignin (Table 2.5), whereas the liquid ones can be basically divided into four main groups (Tables 2.1-2.4): wood bio-oils from the paper and pulp industry, bio-oils from agricultural residues and vegetable biomass, waste cooking oil and bio-oils obtained from animal manure. Before the use of such bio-materials in bituminous binders and mixtures, however, a thermal and/or chemical pre-treatment is usually necessary, such as fast pyrolysis, esterification or hydrothermal liquefaction (Section 2.2.2).
The feasibility of very different bitumen replacement percentages has been investigated so far (Section 2.2.3), using renewable materials as modifiers (<10%), extenders (25÷75%) or even direct alternative binders (100%), depending on their characteristics. Nevertheless, the most recent research studies have mainly focused on partial replacement of bitumen, approximately at percentages lower than 15%, and on the characterization of the resulting bio-binders. In fact, the current limited scientific knowledge on the properties of the bio-binders and the unpreparedness of the sector market make higher replacement percentages unlikely in the short or medium term.
Therefore, in order to make the use of bio-materials truly viable in asphalt pavements, a systematic and comprehensive characterization of the resulting bio-binders is needed.
In this regard, this section presents the results of an extensive investigation on the chemical, morphological and rheological properties of bio-binders obtained by partially replacing bitumen with a bio-oil deriving from wood residues. Specifically, the chemical and morphological analyses carried out aimed at highlighting the basic chemical and structural modifications due to the bio-oil addition, whereas the objective of the rheological testing and modelling was to provide a performance-related characterization, useful to predict the actual mechanical behaviour of the bio-binders studied. In addition, the experimental investigation was completed by conventional and viscosity tests. The properties of the pure bio-oil were also studied. Section 3.2 provides also preliminary data on the health, safety and environmental (HSE) impact of the bio-binders, which is one of the main deficiencies emerged from the literature review (Section 2.4).
Most of the data presented and discussed in the following sections are published in Ingrassia et al. (2020a).

## 3.2 Materials

In this research project, a conventional 50/70 penetration grade bitumen was chosen as base bitumen. The main characteristics of the wood-based bio-oil selected are summarized in Table 3.1. This bio-oil is a residue generated in the processing of a by-product from wood pulp and paper industries, and it is available in large quantities in Northern Europe (especially in Scandinavia), but also in Northern America. Specifically, it is produced (refined) from crude tall oil (CTO) and is a complex mixture of numerous chemicals, including rosin acids, fatty acids and neutral compounds. The bio-oil contains similar levels of carbon and hydrogen as compared to traditional bitumen, but also much higher oxygen content (Table 3.1), mostly in the form of acids and esters.
The bio-oil was used in partial replacement of 50/70 bitumen according to different percentages by weight, with the aim of identifying possible trends related to the bio-oil content in the characterization tests. Considering drastic replacement percentages of bitumen currently unrealistic (as anticipated in Section 3.1), 15% was chosen as a maximum feasible bio-oil percentage. Consequently, four binders were studied, as indicated in Table 3.2. The binders containing the bio-oil were prepared through a laboratory mixer, setting the blending speed at 500 rpm and the temperature at 150°C for about 10 minutes.

**Table 3.1** Characteristics of the bio-oil investigated

| Characteristic | | Value |
|---|---|---|
| Kinematic viscosity (EN 12595, 2015) | at 60°C | 712 $mm^2/s$ |
| | at 135°C | 26 $mm^2/s$ |
| Elemental composition | Carbon | 81% |
| | Hydrogen | 11% |
| | Oxygen | 7.5% |

**Table 3.2** Binders studied

| Binder code | 50/70 bitumen [% by weight] | Bio-oil [% by weight] |
|---|---|---|
| 50/70 | 100 | 0 |
| 50/70+A5 | 95 | 5 |
| 50/70+A10 | 90 | 10 |
| 50/70+A15 | 85 | 15 |

In order to make a preliminary assessment of the HSE impact of such bio-binders and to evaluate the feasibility of plant production and paving, two field trials with bituminous binders extended with the studied bio-oil were constructed in October 2016 and September 2018 in Sweden (Lu et al., 2020). Prior to the construction of the field trials, fumes from the bio-oil and from bitumen extended with the bio-oil were generated in the laboratory at elevated temperatures, and their composition was analysed. No compounds were detected at any level that triggered concerns of increased health risk for asphalt workers (Lu et al.,

2020). During asphalt production and paving operation, a different smell was noticed, but the asphalt workers involved commented that the smell was still acceptable (not annoying or irritating) (Lu et al., 2020). The whole process of mixing and paving went smoothly, without any operative difference with respect to traditional mixtures, and the visual inspections indicated a good condition of the trial sections over time (Lu et al., 2020).
In terms of carbon footprint, Lu et al. (2020) estimated a cradle-to-gate carbon footprint of 740 g $CO_2$eq/kg for the bio-oil examined, including raw material production, transport and refining, based on the $CO_2$ emission data published by Cashman et al. (2015). The carbon footprint of bitumen (without infrastructure) was considered equal to 189 g $CO_2$eq/kg, according to Eurobitume (2012). In the analysis, for the bio-oil, a biogenic $CO_2$eq content of -3000 g per kg of bio-oil was assumed. This estimate was made by taking into account that forest products are able to absorb $CO_2$ from the atmosphere and bound it, and by considering that the molecular weight ratio between $CO_2$ and carbon is 3.7 and the bio-oil consists of about 80% carbon (Table 3.1) (Lu et al., 2020). Based on these assumptions, a bio-binder containing 10% bio-oil would have a carbon footprint equal to -55.9 g $CO_2$/kg bio-binder, meaning that $CO_2$ is actually stored using the bio-oil in partial replacement of bitumen. Therefore, a carbon neutral bio-binder would be obtained with 7.5% bio-oil dosage (Lu et al., 2020). The estimation was based also on EN 15804 (2012) and CEN TR 16970 (2016) and the bio-oil was assumed to be manufactured from sustainably managed forests. Obviously, this estimate strongly depends on the assumptions and boundary conditions considered (e.g. the type of fuel used for manufacturing and transport, etc.).
The construction of the field trials and the estimate of the carbon footprint were carried out by the company Nynas AB, which co-funded the PhD project.

## 3.3 Methods

### *3.3.1 Fourier transform infrared spectroscopy*

In a material, the different types of molecular bonds are characterised by specific vibration and rotation modes. The energy associated to these modes is quantified and a higher level can be reached only if an amount of energy exactly equal to the difference between two energy levels is transmitted to the molecule. Since the energy of a photon is equal to the product of the frequency of the radiation and the Planck's constant, a certain type of bond can reach a higher activation level only by absorbing a quantum corresponding exactly to a specific infrared frequency. This means that each type of bond can be identified by characteristic bands in the absorption spectrum of the transmitted infrared radiation and its concentration in the material can be deduced from the intensity of the absorption in these bands according to the Beer–Lambert law:

$$A(\nu) = \log\left(\frac{I_0}{I}\right) = \varepsilon_i(\nu) \cdot l \cdot C_i \tag{3.1}$$

where $A(\nu)$ is the absorbance for the wavenumber $\nu$, $I_0$ is the intensity of the incident light, $I$ is the intensity of the transmitted light, $\varepsilon_i(\nu)$ is the molar absorption coefficient for the

wavenumber $v$, $l$ is the optical path length, $C_i$ is the studied species concentration (Marsac et al., 2014).

Two Fourier transform infrared (FTIR) measurement principles are commonly used for bitumen characterization: transmission and reflection mode. In transmission mode the infrared beam passes through the sample. Therefore, this method requires the preparation of very thin bitumen films and/or the use of a solvent. The bitumen sample can be prepared at least in three different ways: by spreading a hot binder droplet on an infrared transparent plate with a spatula; by spreading a solution of bitumen on the plate followed by the solvent evaporation to obtain a thin film of bitumen; by analysing a sample of bitumen solution. This method was the first used to characterize bitumen and most of the data available in literature were obtained in transmission mode. However, the preparation of the sample is time-consuming and may differ from laboratory to laboratory. Instead, in reflection mode with the attenuated total reflectance (ATR) technique, the infrared beam enters a crystal with high refractive index held in contact with the sample. The beam reflects at the crystal/sample interface and penetrates for just a few μm into the sample. After one or more reflections, the radiation is attenuated for the specific wavelengths absorbed by the material. In the case of bitumen, the material must be heated to place a droplet on a base plate. It should be also pointed out that, for the same mode (transmission/reflection), the FTIR measurements can also differ in terms of number of individual scans averaged, wavenumber range analysed and wavenumber resolution (Marsac et al., 2014).

In this part of the research project, FTIR analysis was carried out to investigate the chemical composition of the pure bio-oil as well as the binders in terms of functional groups. The analysis was performed in reflection mode with the ATR technique (Figure 3.1), by placing a drop of the material on the diamond crystal base plate of the spectrometer and measuring the absorbance at ambient temperature in a range of wavenumbers between 500 and 4000 $cm^{-1}$, with a resolution of 4 $cm^{-1}$. For each specimen, the spectrum resulting from the average of 32 scans was considered, and overall three specimens were tested for each material. The tests were performed at Nynas laboratory during a research period spent in Nynashamn (Sweden).

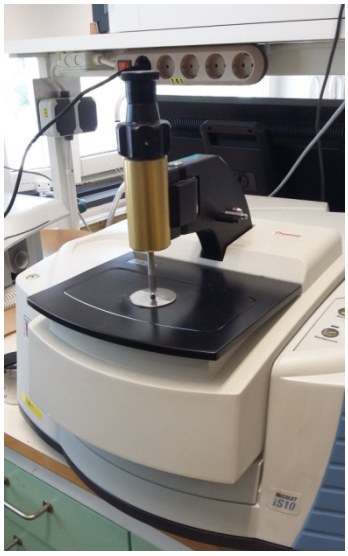

**Figure 3.1** FTIR analysis in reflection mode

### *3.3.2 Thin layer chromatography with flame ionization detection*

Thin layer chromatography with flame ionization detection (TLC-FID), commonly named Iatroscan analysis, was performed according to IP 469 (2006) in order to determine saturates, aromatics, resins and asphaltenes (SARA) fractions of the pure bio-oil and the binders.

Bitumen typically consists of about 85% carbon, 10% hydrogen, and heteroatoms such as sulphur (0–9%), oxygen (0–2%) and nitrogen (0–2%), as well as traces of metals such as vanadium, nickel and iron. These elements combine to form a great variety of organic compounds that are significantly different in terms of molecular structure, molecular size and polarity. Due to the difficulty of performing an exact chemical analysis on individual chemical species, it is very common to use separation techniques to obtain better defined material classes. Saturates, aromatics, resins and asphaltenes are the generic fractions obtained from the separation of bitumen. In general, saturates lack polar functional groups and comprise straight and branched aliphatic hydrocarbons, together with alkyl-naphthenes and some alkyl-aromatics. Aromatics comprise low molecular weight naphthenic compounds with paraffinic chains, and substituted monocyclic and polycyclic aromatic hydrocarbons. Resins are soluble in a defined hydrocarbon (e.g. n-heptane) and have a composition close to that of asphaltenes but with a lower molecular weight and a somewhat higher H/C ratio. Asphaltenes are a class of hydrocarbon components which are typically defined to be the n-heptane or n-pentane insoluble and toluene soluble components of petroleum materials (Lu et al., 2017).

TLC-FID is one of the methods that can be used for the SARA analysis. It consists in the separation of mixtures on thin bonded layers of adsorbent (stationary phase) with a solvent

(mobile phase), combined with the combustion of organic components in a hydrogen/air flame to produce ions and electrons which are collected by a charged electrode to produce a small current that is amplified to produce a signal.
For the analysis, about 0.1 g of material was dissolved in dichloromethane to obtain a 2% solution, from which a small portion was applied to adsorption quartz rods filled with active silica (1 µl for each rod). Immediately prior to the test portion application, the quartz rods were scanned to clean and activate the silica adsorbent. Heptane, toluene-heptane (80:20) and dichloromethane-methanol (95:5) were then used in sequence on the rods to separate saturates, aromatics and resins respectively, leaving the asphaltenes not eluted. Specifically, the rods were left in the developing tanks with heptane, toluene-heptane and dichloromethane-methanol until the solvent travelled respectively about 100 mm, 50 mm and 20 mm from the application point up the quartz rods. All the phases were followed by the drying of the rods for about 10 min in a drying chamber. The rods (five for each material) were then positioned in the Iatroscan equipment and analysed (Figure 3.2). The tests were performed at Nynas laboratory during a research period spent in Nynashamn (Sweden).


**Figure 3.2** Iatroscan analysis: (a) equipment overview, (b) analysis of the rods

### *3.3.3 Microscopic analysis*

In the microscopic analysis, a white light source was used to investigate the morphology of the binders in transmitted mode. When there is phase separation into the binder, this technique allows to clearly identify the phases, as in the case of polymer-modified bitumen (Ferrotti et al., 2017).
For the analysis, thin specimens were prepared by pouring a tiny drop of hot binder (heated at about 160°C) on a glass plate, covered by a cover-glass, and then analysed at ambient temperature, considering a magnification between 100x and 400x. The analysis was carried out at Nynas laboratory during a research period spent in Nynashamn (Sweden).

### *3.3.4 Conventional tests*

The conventional tests allow to measure penetration and softening point of bituminous binders, which are usually referred to as "conventional properties" because they are empirical properties, not directly related to the mechanical behaviour of the binder. Historically, penetration and softening point have long been used to assess the binder consistency at intermediate and high service temperatures. In Europe, they are still widely used to classify bituminous binders.

The penetration tests were performed according to EN 1426 (2015). Since the expected penetration was lower than 160 · 0.1 mm, the bitumen was poured into a metal container with internal depth of 35 mm and internal diameter of 55 mm. The amount of poured bitumen was such as to ensure a sample depth at least 10 mm greater than the expected penetration. The sample was cooled at ambient temperature for at least 1 hour and then conditioned in a water bath at 25°C for at least 1 hour. Afterwards, the sample was removed from the water bath and immediately subjected to the test. The test consisted in the penetration of a standard needle for 5 s into the bitumen sample. The applied load, given by the needle weight plus the needle holder weight plus a 50 g mass, was equal to 100 g. At least three determinations were carried out on the sample, by ensuring the contact between the needle tip and the sample surface and considering points not less than 10 mm from the sides of the container and not less than 10 mm apart from each other (Figure 3.3).

The softening point tests were carried out according to the ring and ball method (EN 1427, 2015). The bitumen was poured into two brass rings with standard dimensions and then cooled at ambient temperature for at least 1 hour. Any excess bitumen was cut away and the sample rings were assembled with the ring holder and the ball centering guides. The assembly was then immersed in the water bath. The two balls, having a diameter of 9.5 mm and a mass of 3.5 g, were also immersed in the bath. The water temperature was lowered to 5°C using some ice and maintained constant for a minimum of 15 min. The balls were positioned in the centering guides and the test was carried out by imposing a temperature increase rate of 5°C/min. The softening point was determined as the temperature at which the two discs softened enough to allow the balls, enveloped in bitumen, to fall a distance of 25.4 mm (Figure 3.4)


**Figure 3.3** Penetration test

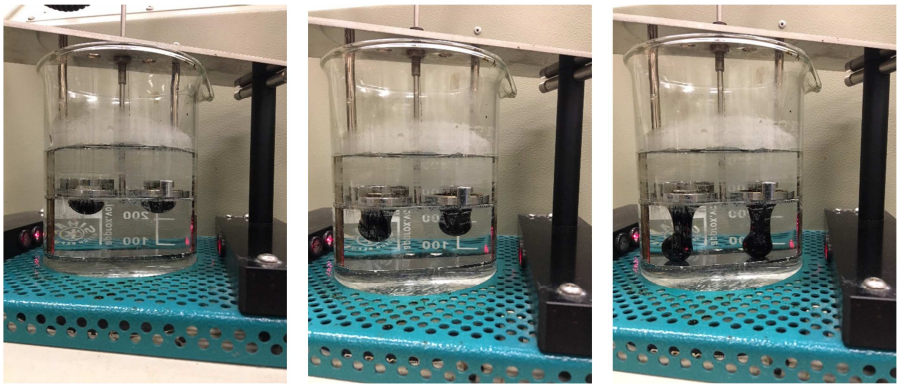

**Figure 3.4** Softening point test

### *3.3.5 Viscosity tests*

The dynamic viscosity of the binders was determined using a Brookfield rotational viscometer (coaxial viscometer) according to ASTM D4402 (2015). The dynamic viscosity represents the resistance to flow of a liquid and is the ratio between the applied shear stress and the shear rate.
10.5 g of binder were poured into the sample container, which was then positioned into the heater, whose temperature was set through a temperature controller (Figure 3.5). Based on the expected viscosity, the most appropriate spindle was selected among spindle S21 (the

biggest one), spindle S27 and spindle S28 (the smallest one). Specifically, smaller spindles were used for higher viscosities.
Six temperatures were investigated, 80, 90, 105, 120, 135 and 150 °C, starting from the lowest one. For the first temperature (80°C) a conditioning time of 1 h was considered, whereas for the following temperatures the conditioning time was reduced to 15 min. In order to evaluate the shear rate dependency of the binders, at each temperature five measurements were performed by considering different working rates of the viscometer (10, 30, 50, 70 and 90 %), corresponding to different shear rates. The viscosity readings were taken after the measurement became stable. For each binder, at least two specimens were tested.


**Figure 3.5** Brookfield rotational viscometer and related temperature controller

### *3.3.6 Frequency sweep tests*

The rheological properties of bituminous binders (i.e. complex shear modulus and phase angle) are usually determined through oscillatory shear tests, by imposing a certain sinusoidal shear strain (or stress) and measuring the resulting shear stress (or strain). The complex shear modulus is defined as in Equation (3.2):

$$G^* = |G^*| \cdot e^{i\delta} = G_1 + iG_2 \tag{3.2}$$

where $|G^*|$ is the norm of the complex shear modulus, defined as the ratio between the stress amplitude and the strain amplitude; $\delta$ is the phase angle, i.e. the phase difference between stress and strain; $i$ is the imaginary unit; $G_1$ and $G_2$ are the storage modulus and the

loss modulus respectively, i.e. the real part and the imaginary part of the complex modulus, defined as follows:

$$G_1 = |G^*| \cdot \cos \delta \tag{3.3}$$

$$G_2 = |G^*| \cdot \sin \delta \tag{3.4}$$

In this experimental investigation, the rheological properties of the binders were investigated through frequency sweep tests, carried out with a dynamic shear rheometer (DSR) in plate-plate configuration (Figure 3.6), according to EN 14770 (2012). Nine temperatures were investigated, ranging from 0 to 80 °C with a step of 10°C. At each testing temperature, the frequency was increased in logarithmic steps from 1 to 100 rad/s (i.e. from 0.159 to 15.9 Hz).

8 mm diameter parallel plates with 2 mm gap were used to test the binders at 40, 30, 20, 10 and 0 °C, starting from 40°C to avoid any damage in the specimen due to the brittleness at low temperatures. The adoption of the 8 mm geometry at low temperatures aims at limiting the torque value to be applied with the DSR. 25 mm diameter parallel plates with 1 mm gap were used instead to test the binders at 30, 40, 50, 60, 70 and 80 °C, starting from 30°C to avoid any permanent deformation in the specimen. The adoption of the 25 mm geometry at high temperatures allows more accurate measurements when the binder is softer. 30 and 40 °C were tested with both geometries because the typical complex modulus values of bituminous binders require to move from one geometry to the other in this range of temperatures.

The specimens were prepared by pouring the binder (slightly in excess) into silicone molds. To perform the test, the specimen was placed onto the lower DSR plate and then the upper plate was lowered until a gap slightly higher than the testing gap. In this configuration, the binder in excess was trimmed. After trimming, the gap was reduced to the testing value, allowing a slight bulging of the specimen. After a conditioning period of 15 min, the test was started. For the following temperatures, the conditioning period was reduced to 7.5 min.

All the tests were conducted at a low shear strain equal to 0.05%, which allowed all the specimens to be tested within the linear viscoelastic (LVE) domain. At least two specimens were tested for each binder.

**Figure 3.6** Dynamic shear rheometer

### *3.3.7 1S2P1D model*

For thermo-rheologically simple materials such as conventional bitumens, the time-temperature superposition principle (TTSP) is valid and therefore the rheological results obtained in the LVE range for a limited interval of testing frequencies at different temperatures can be shifted in the frequency domain at a selected reference temperature. The modelling of the shifted experimental data allows to develop the master curves of the rheological properties, which are useful to predict the material behaviour in a significantly wider range of frequencies (and thus of temperatures) (Anderson et al., 1994).
In this part of the project, a generalized version of the Huet-Sayegh rheological model (Sayegh, 1967), known as 2S2P1D (Olard and Di Benedetto, 2003), was considered for the modelling of the rheological results. The model consists in the combination of two springs, two parabolic elements and one dashpot, and was selected because of its general good adaptability to rheological experimental data. When it is applied to bituminous binders, one spring can be removed (Olard and Di Benedetto, 2003; Yusoff et al., 2013). In this case, the model is usually named as 1S2P1D and its expression is the following:

$$G^*(\omega) = \frac{G_g}{1 + \alpha(i\omega\tau)^{-k} + (i\omega\tau)^{-h} + (i\omega\beta\tau)^{-1}} \tag{3.5}$$

where $G_g$, $k$, $h$, $\alpha$, $\beta$ and $\tau$ are the six parameters that fully describe the rheological behaviour of the binder for a given temperature in the frequency domain (Olard and Di Benedetto, 2003; Perez-Martinez et al., 2016; Yusoff et al., 2013):

- $G_g$ is the glassy modulus, i.e. the value of the complex modulus $G^*$ when $\omega \rightarrow \infty$, and describes the behaviour of the spring;
- $k$ and $h$ are dimensionless parameters describing the behaviour of the parabolic elements and defined so that $0 < k < h < 1$;
- $\alpha$ is a dimensionless parameter that represents the balance between the two parabolic elements;
- $\beta$ is a dimensionless parameter related to the Newtonian viscosity $\eta$ of the dashpot and defined according to the following equation:

$$\eta = G_g \cdot \beta \cdot \tau \tag{3.6}$$

- $\tau$ is the characteristic time, which depends on temperature and is defined as follows:

$$\tau = a_T(T) \cdot \tau_0 \tag{3.7}$$

where $\tau_0$ is the value of $\tau$ at the selected reference temperature $T_{ref}$ and $a_T(T)$ is the shift factor at temperature $T$, which can be expressed with the Williams-Landel-Ferry (WLF) law (Williams et al., 1955), as in Equation (3.8):

$$\log(a_T) = -\frac{C_1(T - T_{ref})}{C_2 + (T - T_{ref})} \tag{3.8}$$

in which $C_1$ and $C_2$ are empirical constants.
Therefore, including also $C_1$ and $C_2$, eight parameters have to be determined in the modelling process. The same parameters can be used to obtain also the master curve of the phase angle $\delta$ (Yusoff et al., 2013).
For the modelling, $G_g$ was fixed equal to $10^9$ Pa as suggested in literature (Anderson et al., 1994), whereas $h$ was fixed equal to 0.56 and $k$ varied in a narrow range between 0.22 and 0.25, in line with previous findings (Olard and Di Benedetto, 2003; Yusoff et al., 2013). Instead $\alpha$, $\beta$, $\tau_0$, $C_1$ and $C_2$ were varied without any restriction. A temperature of 20°C was selected as reference temperature for the master curves and, at this temperature, the parameters were determined by minimizing the error between model and experimental data, in order to obtain the best fitting.

## 3.4 Results and analyses

### *3.4.1 FTIR*

The absorbance spectra obtained for one specimen of 50/70, 50/70+A15 and pure bio-oil are presented in Figure 3.7, from which it can be observed that the shape of the spectra is very similar from 2000 to 4000 $cm^{-1}$ (Figure 3.7 (a)). Instead, in the range of wavenumbers between 500 and 2000 $cm^{-1}$ (Figure 3.7 (b)), the spectra of the base bitumen and the pure

bio-oil have different shape but both exhibit peaks at 1700, 1600, 1460, 1376 and 1030 $cm^{-1}$. These peaks correspond respectively to the C=O stretch of the carbonyl functional group, the C=C stretch of the aromatic group, the $CH_2$ and $CH_3$ bend of the aliphatic group and the S=O stretch of the sulfoxide group. The peaks in common are due to the fact that bitumen and bio-oil are both composed of hydrocarbons (fossil hydrocarbons in the case of bitumen, non-fossil hydrocarbons in the case of the bio-oil) and suggest the good compatibility between the two materials.

Despite these similarities, the bio-oil shows some additional peaks with respect to 50/70 bitumen. Specifically, a sharp peak at 1735 $cm^{-1}$ and another peak around 1242 $cm^{-1}$, which are completely absent in the 50/70 bitumen spectrum, can be noted. These peaks are due, respectively, to the C=O and C-O stretch of the esters and appear, to a lower extent, in the 50/70+A15 spectrum as well, as a result of the blending between bitumen and bio-oil. Therefore, these two peaks can be reasonably considered as a useful means for quantifying the content of the bio-oil investigated. The fact that no additional peaks are observed in the bio-binder spectrum suggests that a mere physical blending occurs between bitumen and bio-oil, without any chemical reaction.

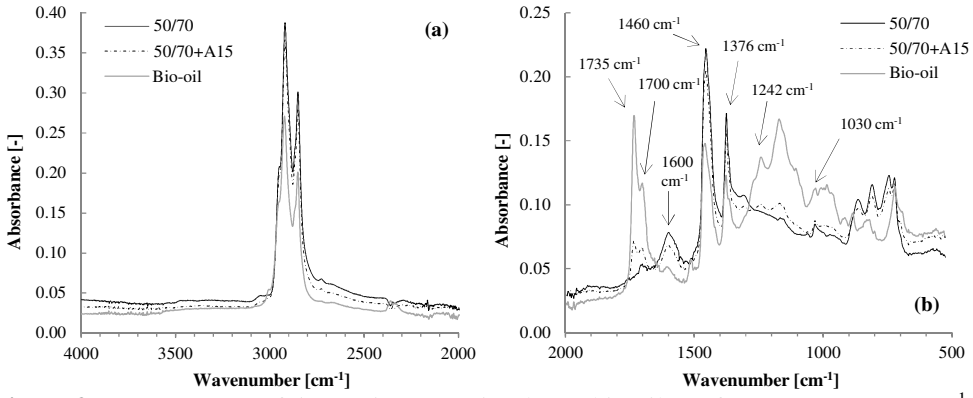


**Figure 3.7** FTIR spectra of 50/70, 50/70+A15 and pure bio-oil: (a) from 2000 to 4000 $cm^{-1}$, (b) from 500 to 2000 $cm^{-1}$

In order to compare the materials tested in detail, the spectral analysis was carried out through an integration method consisting in determining the area below the absorbance spectrum around the abovementioned peaks. Specifically, a tangential approach was considered, namely a relative base line tangential to the spectrum was chosen for each peak (Hofko et al., 2018; Hofko et al., 2017). Consequently, seven areas were determined for each specimen and then the average and standard deviation were calculated for each material, as summarized in Table 3.3.

The results clearly confirm that the ester areas $A_{1735}$ and $A_{1242}$ can be effectively considered to detect the presence of the bio-oil studied in bituminous binders. Indeed their values, that are equal to zero for 50/70 bitumen, progressively increase along with the amount of the bio-material. The aliphatic absorbance of the binder seems to be slightly reduced by the addition of the bio-oil, probably because the latter is characterized by lower $A_{1460}$ and $A_{1376}$ as compared to the base bitumen. A similar observation can be made for the sulfoxide area,

even though it should be highlighted that the addition of the bio-material alters the shape of the spectrum for wavenumbers approximately between 920 and 1050 $cm^{-1}$, making the peak at 1030 $cm^{-1}$ less distinct (Figure 3.7 (b)). Therefore, the sulfoxide index alone might not be suitable for studying the aging of such bio-binders. Moreover, an evident reduction, which is greater with increasing content of bio-oil, occurs for $A_{1600}$, as the aromatic peak at 1600 $cm^{-1}$ is much less prominent in the bio-oil spectrum compared to 50/70 one (Figure 3.7 (b)). On the contrary, the carbonyl area at 1700 $cm^{-1}$ has a general trend to increase with the amount of bio-oil, but in this case the differences between the binders have the same order of magnitude as the standard deviation, thus not allowing a firm conclusion to be drawn. However, this increment seems reasonable considering that the pure bio-material is characterized by a greater value of $A_{1700}$ with respect to the base bitumen.

**Table 3.3** FTIR peak areas

| Peak area | Abs. mode | 50/70 | 50/70+A5 | 50/70+A10 | 50/70+A15 | Bio-oil |
|---|---|---|---|---|---|---|
| $A_{1700}$ | C=O stretch | 0.126±0.003 | 0.122±0.024 | 0.138±0.009 | 0.143±0.013 | 0.371±0.020 |
| $A_{1600}$ | C=C stretch | 1.512±0.003 | 1.380±0.039 | 1.197±0.041 | 0.989±0.033 | 0.180±0.003 |
| $A_{1460}$ | $CH_2$ bend | 5.709±0.003 | 5.535±0.062 | 5.414±0.111 | 5.059±0.066 | 3.553±0.037 |
| $A_{1376}$ | $CH_3$ bend | 1.551±0.008 | 1.561±0.012 | 1.545±0.018 | 1.467±0.004 | 1.328±0.021 |
| $A_{1030}$ | S=O stretch | 0.256±0.013 | 0.202±0.017 | 0.132±0.004 | 0.118±0.007 | 0.136±0.012 |
| $A_{1735}$ | C=O stretch | 0.000±0.000 | 0.111±0.002 | 0.240±0.023 | 0.334±0.008 | 1.723±0.045 |
| $A_{1242}$ | C-O stretch | 0.000±0.000 | 0.049±0.004 | 0.100±0.008 | 0.164±0.007 | 0.858±0.009 |

### *3.4.2 SARA fractions*

A qualitative comparison of the chromatograms obtained for one rod of the base bitumen and one rod of the pure bio-oil is shown in Figure 3.8 (a). The difference between the chromatograms is very evident, as 50/70 presents – as expected – four peaks corresponding to saturates, aromatics, resins and asphaltenes, whereas the bio-material exhibits only the peaks of (by definition) aromatics and resins plus a very small one for asphaltenes, while saturates are completely absent. Moreover, it should be noted that, for the bio-oil, the retention times of aromatics and resins are rather different from those of the base bitumen. The higher retention times observed could be due to a stronger affinity with the stationary phase, determined by the high polarity of the bio-oil. For the bio-binders, this difference in the retention resulted in an additional peak between aromatics and resins (Figure 3.8 (b)), which was included in the aromatics in the quantitative analysis performed later. On the contrary, no additional peak emerged between resins and asphaltenes (Figure 3.8 (b)), but in some cases an imperfect separation between such peaks was observed. For this reason, the sum of these two fractions was also considered.

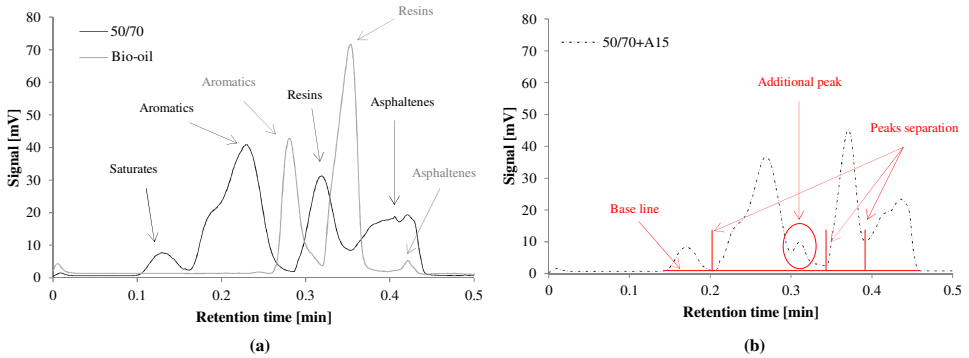


**Figure 3.8** Chromatograms of (a) 50/70 and pure bio-oil, (b) 50/70+A15

In order to quantify the SARA fractions, the chromatogram related to each rod was integrated by considering a common base line for all peaks and separating the fractions as shown in Figure 3.8 (b), thus determining the area of every peak. Afterwards, for every single rod, the relative percentage of each fraction was calculated by dividing the corresponding peak area by the total area. The values presented in Table 3.4 were then obtained by averaging the results of the rods analysed for each material. Furthermore, based on the results achieved for 50/70 and the pure bio-oil and assuming no chemical reaction between them after blending, the values of SARA fractions for the bio-binders were also estimated through a simple mathematical calculation and shown in Table 3.4 in brackets and italics, for comparison with the experimental values. The estimation was made considering the following formula, given for the resins for simplicity but valid for all fractions:

$$est.resins_{\ 50/70+Ax} = \left(\frac{100-x}{100}\right) exp.resins_{50/70} + \left(\frac{x}{100}\right) exp.resins_{\ bio-oil} \qquad (3.9)$$

where $x$ is the bio-oil amount (5, 10 or 15 %), "*est.*" and "*exp.*" indicate the estimated and experimental value, respectively.

**Table 3.4** SARA fractions: experimental and estimated (in brackets and italics) values

| Material | Saturates [%] | Aromatics [%] | Resins [%] | Asphaltenes [%] | Res+Asph [%] | Colloidal Index |
|---|---|---|---|---|---|---|
| 50/70 | 5.7 | 47.3 | 21.8 | 25.2 | 47.0 | 0.45 |
| 50/70+A5 | 5.4 *(5.4)* | 46.5 *(46.6)* | 24.4 *(23.9)* | 23.9 *(24.1)* | 48.2 *(48.0)* | 0.41 *(0.42)* |
| 50/70+A10 | 4.9 *(5.1)* | 45.5 *(45.9)* | 24.6 *(26.1)* | 25.0 *(22.9)* | 49.6 *(49.0)* | 0.43 *(0.39)* |
| 50/70+A15 | 4.9 *(4.8)* | 44.8 *(45.2)* | 27.2 *(28.2)* | 23.1 *(21.8)* | 50.3 *(50.0)* | 0.39 *(0.36)* |
| Bio-oil | 0.0 | 33.2 | 64.3 | 2.5 | 66.8 | 0.03 |

From the experimental results summarized in Table 3.4, it can be noted that a trend linked with the bio-oil content exists for all fractions. Specifically, as the amount of bio-oil increases, saturates, aromatics and asphaltenes are progressively reduced, whereas resins are markedly increased. The only exception is represented by 50/70+A10, for which the resins' content seems slightly underestimated while the asphaltenes' amount slightly

overestimated due to a poor separation between the two fractions (their sum is in fact in line with the other results). In general, the small differences observed from the comparison between experimental and estimated values (Table 3.4) confirm that only a physical blending occurs between bitumen and bio-oil, without any chemical reaction.
Moreover, from the experimental data, the colloidal index (*CI*) was easily calculated according to Equation (3.10), in order to predict the effect provided by the bio-oil addition in terms of conventional properties (Mangiafico et al., 2016).

$$CI = \frac{asphaltenes + saturates}{aromatics + resins} \tag{3.10}$$

Based on literature (Mangiafico et al., 2016), it is expected that the reduction of asphaltenes and *CI* caused by the bio-oil (Table 3.4) leads to an increase of penetration and a decrease of the softening point. It is worth pointing out that, for 50/70+A10, the value of *CI* is affected by the partial overlapping of resins and asphaltenes.
In addition, it can be assumed that the reduced aromaticity, detected also from FTIR analysis (Table 3.3), might affect the viscoelastic properties of the binders (Soenen and Redelius, 2014).

### *3.4.3 Morphology*

Figure 3.9 shows the images obtained from the microscopic analysis of the base bitumen 50/70 and the bio-binder with the maximum amount of bio-oil considered, i.e. 15%, with a magnification equal to 200x. It is evident that both images are monochromatic, meaning that 50/70+A15 presents a perfectly homogeneous structure, without any phase separation, exactly like the base bitumen. The images referring to lower bio-oil contents (5 and 10%) and different magnifications are not shown here, as they look very similar to the ones provided.
This outcome confirms that little energy is required for blending bitumen and the selected bio-material and also suggests that no problems in terms of storage stability should emerge for the binders investigated.

**(a)** **(b)**

**Figure 3.9** Images obtained for (a) 50/70 and (b) 50/70+A15, with 200x magnification

### *3.4.4 Conventional properties*

The results of the conventional tests are summarized in Table 3.5, which shows that the bio-material provides a consistency reduction that results in increased penetration and decreased softening point, and the effect is higher as its dosage increases, in accordance with the outcomes of SARA analysis.
The results of the tests were also used to calculate the Penetration Index (*PI*) in order to estimate the temperature susceptibility of the binders at intermediate temperatures (Hunter et al., 2015):

$$PI = \frac{1952 - 500\log(Pen_{25}) - 20 \cdot SP}{50\log(Pen_{25}) - SP - 120} \tag{3.11}$$

where $Pen_{25}$ is the penetration at 25°C (0.1 mm) and *SP* is the softening point (°C). Specifically, the temperature susceptibility is higher when *PI* is lower. The results obtained suggest that the addition of the bio-oil has a small influence on the temperature susceptibility, since the variation of *PI* is limited (Table 3.5).
Moreover, based on penetration, softening point and *PI*, the potential penetration grade class of the bio-binders was predicted according to the specifications provided by EN 12591 (2009). As can be seen from Table 3.5, each increase of 5% bio-oil leads to a softer grade class. However, it is worth pointing out that, for a thorough classification of the bio-binders according to EN 12591 (2009), the effect of aging should also be taken into account.

**Table 3.5** Penetration, softening point and Penetration Index values with consequent potential penetration grade class

| Binder | Penetration [0.1 mm] | Softening point [°C] | Penetration Index [-] | Potential penetration grade class |
|---|---|---|---|---|
| 50/70 | 51.5 | 49.7 | -1.21 | - |
| 50/70+A5 | 71.3 | 47.0 | -1.16 | 70/100 |
| 50/70+A10 | 114.4 | 43.5 | -0.87 | 100/150 |
| 50/70+A15 | 153.5 | 39.8 | -1.25 | 160/220 |

### *3.4.5 Viscosity*

The results of the viscosity tests are shown in Figure 3.10. Six series of points are plotted for each binder, corresponding to the temperatures investigated. Specifically, for each binder, the highest viscosity value corresponds to the lowest testing temperature (80°C), whereas the lowest viscosity value corresponds to the highest testing temperature (150°C). In general, lower shear rates were imposed at lower temperatures, because the higher viscosity of the binder implies a higher working rate of the viscometer and thus smaller shear rates have to be considered.
From the results obtained, a Newtonian behaviour can be assumed for all binders at all testing temperatures, as the viscosity is independent of the shear rate. Note that at the highest temperature (150°C) some experimental points are missing, since shear rates higher

than 200 $s^{-1}$ cannot be investigated with the equipment employed. Moreover, it should be pointed out that two different spindles were used, namely S28 for viscosities higher than 1800 mPa·s and S21 for viscosities lower than 1800 mPa·s.

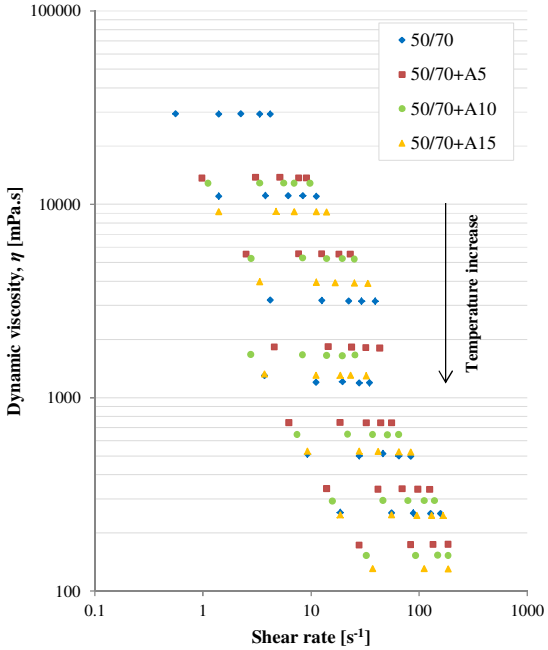


**Figure 3.10** Dynamic viscosity as a function of shear rate

Since the assumption of Newtonian behaviour is valid, the viscosity value measured at a working rate of the viscometer equal to 50% was considered in order to further compare the binders (Figure 3.11 (a)). A progressive viscosity reduction is obtained as the dosage of bio-oil increases, being the base bitumen the most viscous binder and 50/70+A15 the least viscous binder at all testing temperatures. However, a significant decrease in viscosity is observed after the addition of 5% bio-oil, whereas the decrease is less evident when the bio-oil amount is further increased, as can be seen from the values of Δ, which represents the viscosity percentage reduction with respect to 50/70 bitumen, calculated according to Equation (3.12) and provided in Figure 3.11 (b).

$$\Delta_i(\%) = \frac{\eta_{50/70} - \eta_i}{\eta_{50/70}} \cdot 100 \tag{3.12}$$

where $i$ = 50/70+A5, 50/70+A10, 50/70+A15.
Based on these results, the bio-oil examined, which is able to considerably reduce bitumen viscosity even in small quantities, might be also employed to promote the self-healing of bituminous mixtures. Indeed, according to a technique recently developed (Garcia et al.,

2010; Norambuena-Contreras et al., 2018), low-viscosity oils can be encapsulated and incorporated in the mixture. Then, the formation of cracks will break the capsule shell, allowing the oil to be released. In this way, the oil will reduce the viscosity of bitumen, which will be able to flow into the cracks, providing self-healing.
Considering the reference Superpave viscosity values for mixing and compacting bituminous mixtures (0.17 Pa·s and 0.28 Pa·s, respectively) (Kennedy et al., 1994), the potential mixing and compaction temperatures for the binders were determined through the regression of the experimental data on the log(log$\eta$)-temperature diagram. From Table 3.6, it can be observed that the working temperatures can be reduced up to 10°C with respect to 50/70 bitumen when the dosage of the bio-material is equal or lower than 10%, whereas a potential reduction of about 15°C can be achieved with 15% dosage. This reduction was somehow expected because of the softening effect provided by the bio-oil and such working temperatures should be compared to those of conventional bitumens having analogous penetration.

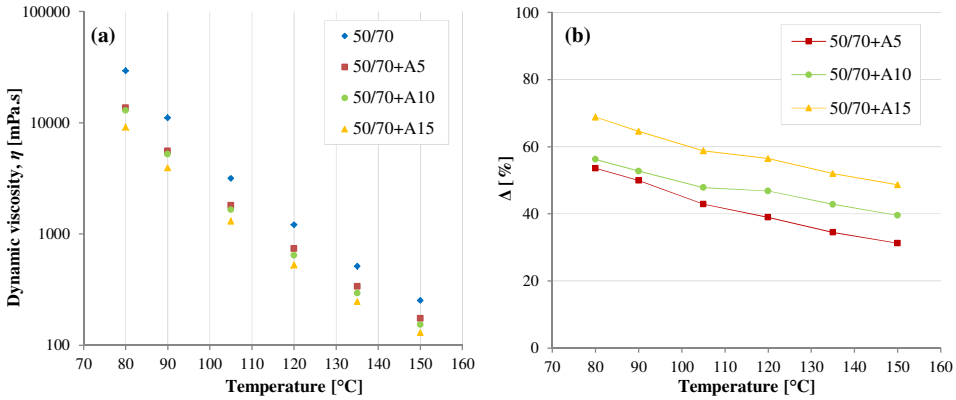


**Figure 3.11** Analysis of viscosity data: (a) dynamic viscosity as a function of temperature, (b) viscosity percentage reduction with respect to 50/70 bitumen

**Table 3.6** Superpave mixing and compaction temperatures for the binders tested

| Binder | Mixing temperature [°C] | Compaction temperature [°C] |
|---|---|---|
| 50/70 | 159 | 148 |
| 50/70+A5 | 149 | 138 |
| 50/70+A10 | 147 | 137 |
| 50/70+A15 | 143 | 133 |

In order to assess the temperature susceptibility of the binders even at high temperatures, the regression of the viscosity-temperature relationship was considered, according to the following equation (ASTM D2493, 2016; Cardone et al., 2014):

$$\log\log\eta = RI + VTS \cdot \log T \tag{3.13}$$

where $\eta$ is the viscosity (mPa·s), *RI* is the regression intercept, *VTS* is the regression slope that represents the viscosity-temperature susceptibility parameter, $T$ is the temperature (°R). The results of the regression are given in Table 3.7, together with the coefficient of determination $R^2$, whose values (very close to 1) demonstrate that Equation (3.13) characterizes the viscosity-temperature relationship very well for the bio-binders studied. In general, a lower absolute value of *VTS* indicates a less pronounced temperature susceptibility. The results show that there is not a clear correlation between *VTS* value and bio-oil dosage, confirming what has been previously observed in terms of Penetration Index (Section 3.4.4) and thus allowing to conclude that the bio-material studied does not significantly affect the temperature susceptibility of bituminous binders.

**Table 3.7** Regression parameters of the viscosity-temperature relationship shown in Equation (3.13)

| Binder | *RI* | *VTS* | $R^2$ |
|---|---|---|---|
| 50/70 | 10.239 | -3.4214 | 0.9998 |
| 50/70+A5 | 10.073 | -3.3741 | 0.9999 |
| 50/70+A10 | 10.412 | -3.4960 | 0.9999 |
| 50/70+A15 | 10.336 | -3.4743 | 1.0000 |

### *3.4.6 Rheology*

The raw rheological results obtained from the frequency sweep tests are plotted in Figure 3.12 (a) and Figure 3.12 (b), which show respectively the Black diagram, i.e. the representation of the norm of the complex modulus $|G^*|$ as a function of the phase angle $\delta$, and the Cole-Cole diagram, i.e. the representation of the loss modulus $G_2$ as a function of the storage modulus $G_1$.

From Figure 3.12 (a), it can be observed that all binders tested exhibit a thermo-rheologically simple behaviour, as the experimental data obtained at different temperatures and frequencies align along the same curve, thus allowing the master curves of the rheological properties to be obtained (Airey, 2002). The binders begin to lose their thermo-rheological simplicity at high temperatures, i.e. when the phase angle approaches 90°. This is true particularly for 50/70+A15, as some experimental points are evidently not aligned with the others, suggesting that bio-binders with bio-oil dosages higher than 15% might have only a partial thermo-rheologically simple behaviour.

As for the comparison between the binders, the increasing amount of bio-oil causes a progressive shift of the experimental data towards right and down in the Black diagram, i.e. higher values of phase angle $\delta$ and lower values of complex modulus $|G^*|$ (Figure 3.12 (a)), and towards left and down in the Cole-Cole diagram, i.e. lower storage $G_1$ and loss $G_2$ moduli (Figure 3.12 (b)).

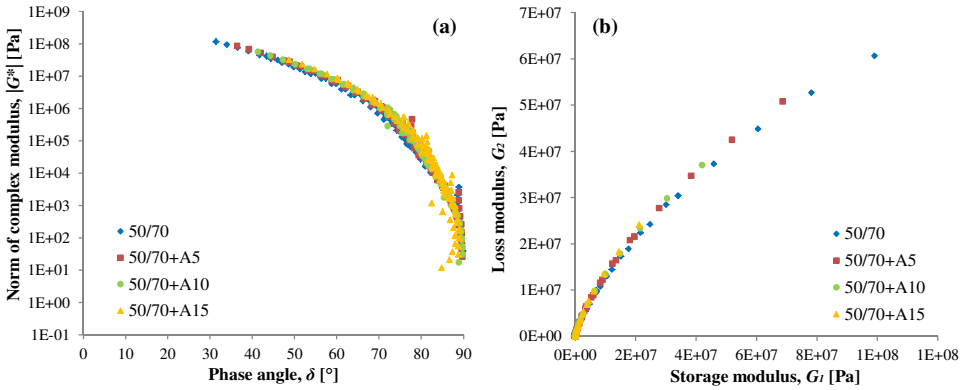


**Figure 3.12** Raw rheological results: (a) Black diagram and (b) Cole-Cole diagram

A further comparison between the binders in terms of rheological behaviour is provided in Figure 3.13, which shows the master curves of complex modulus and phase angle at 20°C, as well as in Figure 3.14, presenting the master curves of storage modulus and loss modulus at 20°C. The 1S2P1D and WLF parameters deriving from the modelling are summarized in Table 3.8.

Firstly, it should be noted the 1S2P1D model fits quite well the experimental data in terms of complex modulus as well as storage and loss moduli, for all binders. Some imprecision can be observed only at low reduced frequency (i.e. high temperatures). Moreover, the effect of the reduced thermo-rheological simplicity previously highlighted mainly emerges in the storage modulus master curve at low frequencies for high dosages of bio-oil (≥10%), as the experimental data are not perfectly aligned (Figure 3.14 (a)). In terms of phase angle, instead, the model fitting is less accurate (especially at intermediate frequencies), but the ranking of the different binders is respected (Figure 3.13 (b)). The slight inaccuracy in the modelling of the phase angle has been already highlighted in literature (Olard and Di Benedetto, 2003; Yusoff et al., 2013).

Figure 3.13 confirms what previously observed from the Black diagram, namely the bio-material produces a reduction of $|G^*|$ and an increase of $\delta$, which are more pronounced for higher dosages. These effects emerge in a wide range of reduced frequencies, indicating that an improvement of the low-temperature performance of the binder might be achieved thanks to the decreased stiffness and elasticity provided by the addition of the bio-oil, whereas, on the other hand, the high-temperature behaviour might be negatively affected. Moreover, Figure 3.14 suggests that the reduction of $|G^*|$ is predominant with respect to the increase of $\delta$, since both $G_1$ and $G_2$ are progressively reduced with increasing bio-oil content.

In terms of 1S2P1D parameters (Table 3.8), $\beta$ seems to remain about constant, regardless of the bio-material dosage. Conversely, a significant reduction of $\alpha$ and $\tau_0$ is observed as the bio-oil amount increases, due to its softening effect. This result is in agreement with literature, as softer binders are typically characterized by lower values of $\alpha$, $\beta$ and/or $\tau_0$ (Olard and Di Benedetto, 2003; Perez-Martinez et al., 2016; Yusoff et al., 2013). Moreover, at very high temperatures (or analogously very low frequencies), the rheological model is

equivalent to a linear dashpot (Olard and Di Benedetto, 2003) whose behaviour is governed by Equation (3.6). Being in this case $G_g$ and $\beta$ constant, the reduction of $\tau$ generates a decrease of the Newtonian viscosity of the model $\eta$ (Equation (3.6)) that seems consistent with the viscosity reduction observed from the experiments at high temperatures (Figure 3.11).

As for the WLF parameters (Table 3.8), $C_1$ and $C_2$ seem to decrease as the bio-oil dosage increases, even though 50/70+A15 does not follow this trend. The reduction of $C_1$ and $C_2$ might also be a consequence of the softening effect provided by the bio-material.

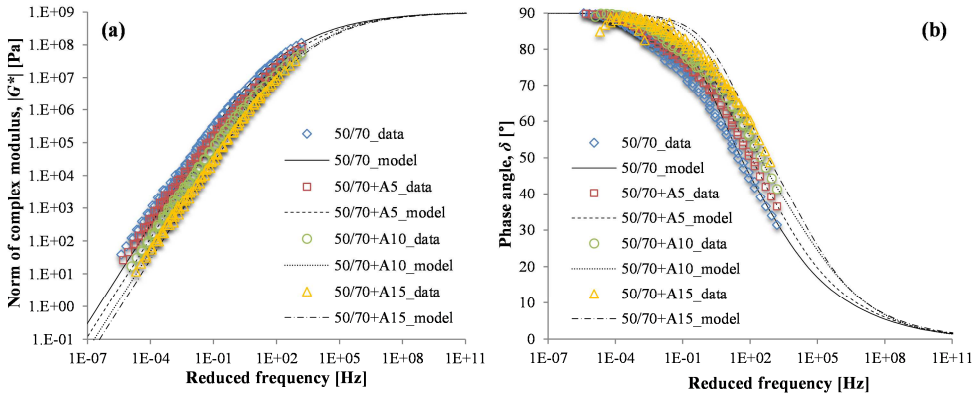


**Figure 3.13** Master curves of (a) complex modulus and (b) phase angle, at a reference temperature of 20°C

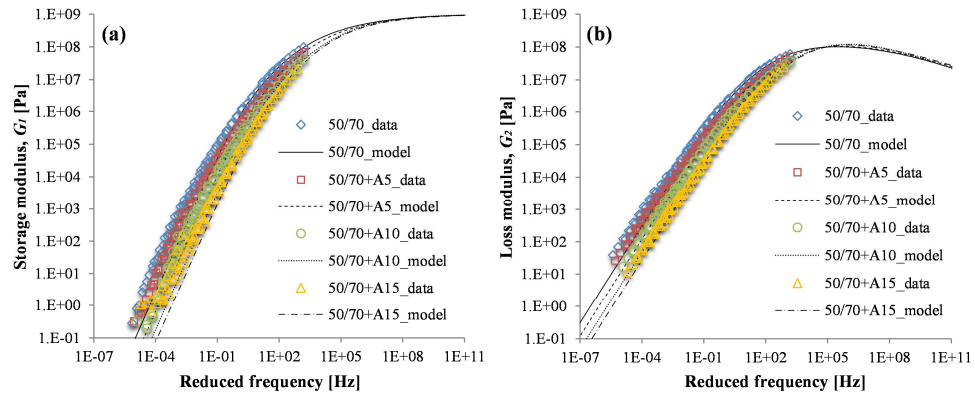


**Figure 3.14** Master curves of (a) storage modulus and (b) loss modulus, at a reference temperature of 20°C

**Table 3.8** 1S2P1D and WLF parameters

| Binder | $G_g$ [Pa] | $k$ | $h$ | $\alpha$ | log $\beta$ | log $\tau_0$ | $C_1$ | $C_2$ |
|---|---|---|---|---|---|---|---|---|
| 50/70 | 1.00E+09 | 0.22 | 0.56 | 2.4 | 1.74 | -5.05 | 25 | 262 |
| 50/70+A5 | 1.00E+09 | 0.22 | 0.56 | 2.2 | 1.73 | -5.44 | 23 | 248 |
| 50/70+A10 | 1.00E+09 | 0.25 | 0.56 | 2.0 | 1.74 | -5.85 | 17 | 188 |
| 50/70+A15 | 1.00E+09 | 0.22 | 0.56 | 1.7 | 1.73 | -6.10 | 23 | 286 |

### *3.4.7 Rutting and fatigue tendency*

In order to provide a more effective performance-based characterization, an indication of the rutting and fatigue tendency of the binders studied was obtained by calculating the Superpave parameters introduced by the Strategic Highway Research Program (SHRP) (Kennedy et al., 1994) from the rheological data available. Rutting and fatigue cracking are the two main load-related distresses affecting asphalt pavements. Rutting occurs at high service temperatures (when the mixture is softer) and consists in the formation of channelled longitudinal depressions in the wheelpath area due to the accumulation of permanent deformations. Fatigue cracking is the predominant distress at intermediate service temperatures and is due to the progressive degradation of the asphalt mixture properties due to the cyclic stresses/strains caused by traffic loadings. Cracking can initiate on the pavement surface and propagate downwards ("top-down cracking") or it can initiate at the bottom of the asphalt layers and propagate upwards ("bottom-up cracking").
The calculated Superpave parameters are shown in Figure 3.15, where the small error bars represent the standard deviation. It should be pointed out that, according to the microscopic analyses performed, the bio-binders tested are characterized by a completely homogeneous structure, as the introduction of the bio-oil into the bitumen (up to 15% by weight) does not determine any phase separation (Section 3.4.3). Therefore, the Superpave parameters for rutting and fatigue (originally proposed for traditional bitumens) can be considered reliable to characterize the behaviour of such binders at high and intermediate service temperatures, respectively.
The rutting parameter $|G^*|/\sin\delta$ was determined at 10 rad/s (i.e. 1.59 Hz) at four temperatures: 50, 60, 70, 80 °C (Figure 3.15 (a)). The higher is the value of $|G^*|/\sin\delta$, the higher is the resistance of the binder to permanent deformation, and thus the lower the rutting tendency of the resulting mixture should be (Kennedy et al., 1994). A value of 1 kPa is assumed as a reference in unaged condition, which is the situation in which the binder is usually more deformable. As can be seen from Figure 3.15 (a), the increasing addition of bio-oil causes a progressive reduction of $|G^*|/\sin\delta$ and therefore a worsening of the resistance to permanent deformation and rutting at high service temperatures. Specifically, for 50/70+A15, $|G^*|/\sin\delta$ is lower than 1 kPa already at 60°C, whereas, for 50/70+A5 and 50/70+A10, the requirement is no longer met at 70°C. On the contrary, the base bitumen still shows a value greater than 1 kPa at 70°C. The results indicate that the upper Performance Grade (PG) limit, which is the temperature at which no problems in terms of rutting occur, might be between 50 and 60 °C for 50/70+A15, between 60 and 70 °C for 50/70+A5 and 50/70+A10, and between 70 and 80 °C for the base bitumen.

Nevertheless, it should be pointed out that the bio-binders differ from the base bitumen in terms of penetration grade. A more reasonable comparison should be made by considering bitumens with similar penetrations to those of the bio-binders. Moreover, as anticipated in Section 2.3.1, this softening effect has been already observed in previous research concerning bio-oils (Lei et al., 2017; Sun et al., 2016). Therefore, several solutions have been proposed in literature to improve the high-temperature performance of bio-binders, such as the addition of crumb rubber (Peralta et al., 2012a), polymers (Zhang et al., 2017) and bio-polymers (e.g. lignin) (Kowalski et al., 2016; Xu et al., 2017), which have the potential to extend the range of applicability temperatures of the binder.
The fatigue parameter $|G^*|\sin\delta$ instead was calculated at 10 rad/s (1.59 Hz) at three intermediate service temperatures: 10, 20, 30 °C (Figure 3.15 (b)). In this case, lower values of the parameter indicate a better resistance of the binder to fatigue cracking (Kennedy et al., 1994). The evaluation of $|G^*|\sin\delta$ is normally required after long-term aging, as the binder is stiffer and thus more prone to cracking. Therefore, the results presented here, which refer to unaged binders, only give an indication of the possible effect of the bio-oil on the fatigue resistance. Figure 3.15 (b) shows that the bio-material provides a reduction of $|G^*|\sin\delta$ and this effect is more apparent as its dosage increases, suggesting that an improvement of the fatigue resistance might be achieved. Also in this case, the observed fatigue behaviour of the bio-binders should be compared to that of bitumens with equal penetration.

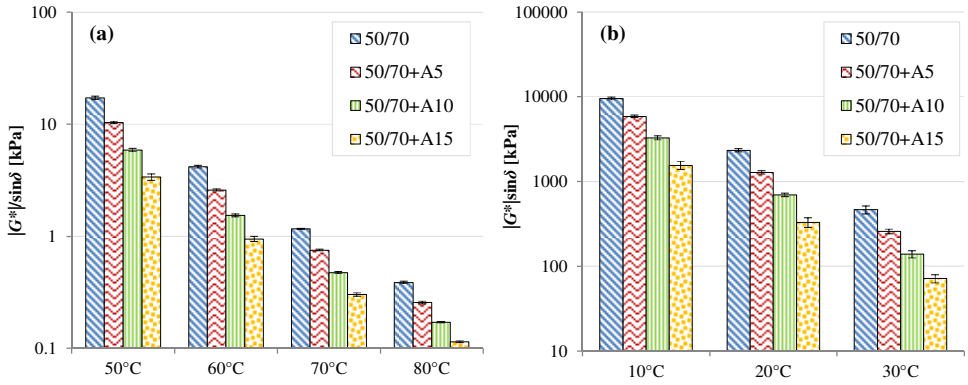


**Figure 3.15** Superpave parameters: (a) rutting and (b) fatigue

## 3.5 Summary of the findings

The objective of this part of the research project was to provide an extensive characterization of the properties of bio-binders obtained by partially replacing a conventional 50/70 bitumen with a wood-based bio-oil at four different percentages: 0, 5, 10 and 15 %. Various tests were performed, including chemical, morphological and rheological as well as conventional and viscosity tests. Rheological modelling was also carried out.

Based on the results and analyses presented, the following conclusions can be drawn:

- in terms of functional groups, the main effects provided by the addition of the bio-oil to bitumen are the development of new peaks related to esters and a significant reduction of aromatics;
- in terms of SARA fractions, the bio-binders present reduced saturates, aromatics and asphaltenes along with increased resins as compared to the base bitumen;
- when mixed together, the bitumen and the wood-based bio-oil undergo only a physical blending, without any chemical reaction;
- the microscopic investigation demonstrates that the bio-binders are completely homogeneous, and therefore no concerns in terms of blending energy and storage stability are expected;
- the bio-material provides a consistency reduction, namely penetration increases while softening point decreases, producing binders with softer grades;
- a Newtonian behaviour can be assumed for all the binders tested and, as the dosage of the bio-material increases, a progressive viscosity reduction is observed;
- temperature susceptibility does not seem to be significantly affected by the bio-material;
- a thermo-rheologically simple behaviour is observed up to 15% of the bio-material. The bio-oil causes an increase in the phase angle and a reduction of the complex modulus, which seems to be predominant, in a wide range of frequencies;
- overall, a good fitting of the rheological data can be achieved with 1S2P1D model, especially in terms of complex modulus. Moreover, the decrease of the parameter $\tau_0$, which is more evident as the bio-oil dosage increases, seems to be reasonably consistent with the viscosity reduction observed.

These findings indicate that the wood bio-oil examined is suitable to be used in partial replacement of bitumen for road pavements and its addition to the base bitumen leads to softer binders, which could be used, for instance, in cold climates or as fresh binders in the recycling of reclaimed asphalt. Another potential application might be to produce capsules containing the bio-oil and incorporate them in the bituminous mixture, with the aim of promoting self-healing when cracking occurs.

In addition, parallel activities (not directly included in this PhD project) demonstrated that full-scale field trials with this type of bio-binders are satisfactory from the operative point of view and in terms of HSE impact and exhibit good condition over time. A preliminary cradle-to-gate carbon footprint analysis showed that bituminous binders extended with 7.5% of the bio-oil in question can be carbon neutral.

# 4. Aging properties of bio-binders

## 4.1 Background and objectives

Despite the significant environmental and economic benefits deriving from the use of bio-binders, great uncertainty on the durability and long-term performance of such materials still exists, as emerged from the literature review (Section 2.5).

In fact, the properties of bituminous binders change over time due to aging, which is a complex process that involves irreversible and reversible mechanisms. The irreversible ones, which are predominant, include chemical changes due to oxidation, volatilization of light components and exudation, whereas the reversible mechanism is usually referred to as physical hardening and can be attributed to the reorganization of bitumen molecules (e.g. wax crystallization) to meet an optimum thermodynamic state. As a consequence of such chemical, physical and morphological changes, the binders undergo a noticeable hardening and their mechanical behaviour can be considerably altered, leading to possible distresses in road pavements. Aging occurs both during production, transportation, laying and compaction of bituminous mixtures and during the in-service life of asphalt pavements. The first stage, known as short-term aging, is mainly due to the high working temperatures adopted to ensure the workability of the mixture, whereas the second stage, typically referred to as long-term aging, is caused by the exposure of the pavement to oxygen, atmospheric agents and ultraviolet radiation (Lu and Isacsson, 2002; Lu and Isacsson, 2000; Zhang et al., 2012).

As anticipated in Section 2.3.1, previous studies have shown that certain bio-binders may exhibit greater aging susceptibility with respect to conventional bitumens (Bearsley and Haverkamp, 2007a; Yang et al., 2017; Yang et al., 2015; Zhang et al., 2017) as well as significant mass loss during aging (Peralta et al., 2014; Yang et al., 2015), indicating the presence of large amounts of volatile components in the bio-materials employed. In some cases, the effect induced by the bio-oil on the mechanical properties of the binder in unaged conditions was completely inverted after aging (Yang et al., 2015; Zhang et al., 2017), denoting the over-aging of the bio-material and a possible unexpected behaviour during in-service life. Moreover, as already highlighted in the literature review (Section 2.3.1), the long-term aging of bio-binders has been little investigated so far. Therefore, further research is needed to predict the actual behaviour of bio-binders in the field.

In this regard, this part of the project focused on the investigation of the short-term and long-term aging properties of the same bio-binders studied in Section 3, with the aim of filling some gaps in the scientific literature. The experimental investigation carried out included conventional tests, chemical analyses as well as rheological testing and modelling. The tests and analyses were also performed on one conventional bitumen for comparison purposes. Possible correlations between chemical and rheological changes induced by aging were also sought, in order to identify reliable parameters to be used as aging indicators for the bio-binders studied.

The results presented in the following sections are published in Ingrassia et al. (2019b).

## 4.2 Materials and methods

### *4.2.1 Materials*

This part of the project focused on the characterization of the aging properties of the same binders previously investigated in unaged conditions (Section 3), i.e. 50/70, 50/70+A5, 50/70+A10 and 50/70+A15, plus one conventional bitumen, coded as "B1" and characterized by penetration similar to that of the bio-binder containing 10% bio-oil (see Section 4.3.1).

### *4.2.2 Aging procedures and conventional tests*

Short-term and long-term aging were simulated in the laboratory through Rolling Thin Film Oven Test (RTFOT) and Pressure Aging Vessel (PAV), respectively.
The RTFOT procedure, standardized by EN 12607-1 (2015), simulates the bitumen aging occurring during production, transportation and laying of the bituminous mixture. Short-term aging is simulated by heating a moving film of bitumen in a specific oven to a specified temperature (163°C) for a given period of time (75 min) with a constant supply of air (4 l/min). The RTFOT oven is equipped with a vertical circular carriage with eight openings and spring clips for firmly holding glass containers with standard dimensions in a horizontal position. The bitumen is poured into the glass containers, each one filled with 35 g of bitumen. The containers are then positioned in the carriage, filling any unused spaces in the carriage with empty containers (Figure 4.1). The combination of carriage rotation (15 r/min), temperature and air allows the formation of a thin film of aged bitumen, which is recovered at the end of the 75 min.
The PAV procedure, standardized by EN 14769 (2013), should simulate the bitumen aging occurring during about 10-15 years of pavement in-service life. The long-term aging protocol consists in heating a static film of RTFOT-aged bitumen to a specified temperature under a certain air pressure for a given period of time. In this research project, a temperature of 100°C, a pressure of 2.1 MPa and a duration of 20 h were considered. The bitumen is poured into metal containers with 140 mm diameter. A maximum of 10 metal containers, each one containing 50 g of bitumen, are placed in the pan holder, which is then placed into the pressure vessel to be aged (Figure 4.2). After the 20 h of aging, the pan holder with the filled metal containers is removed from the pressure vessel and placed in an oven at 170°C for 30 min to remove any air bubbles formed in the binder during the aging procedure (the air bubbles are removed by stirring the binder in each container). Then the long-term aged bitumen is recovered for testing.
Prior to the chemical and rheological tests, all the binders were subjected to conventional tests, i.e. determination of penetration (EN 1426, 2015) and softening point (EN 1427, 2015).

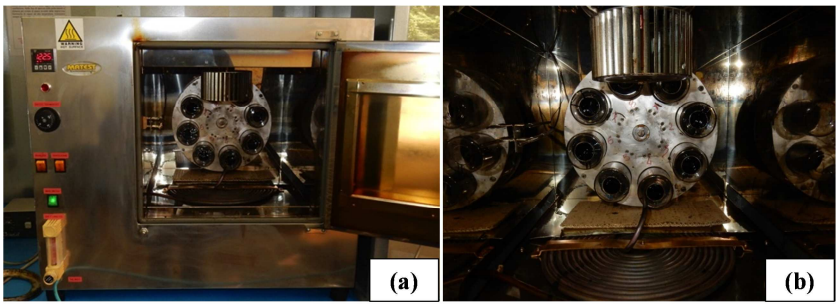


**Figure 4.1** RTFOT equipment: (a) overview, (b) detail of the glass containers positioned in the carriage


**Figure 4.2** PAV equipment: (a) overview, (b) pan holder with metal containers

### *4.2.3 Chemical analyses*

Fourier transform infrared spectroscopy (FTIR) was carried out in reflection mode with the attenuated total reflectance (ATR) in order to determine the effect of aging on the binder functional groups. The absorbance was measured at ambient temperature on a small drop of binder placed on the diamond crystal base plate of the spectrometer in a range of wavenumbers between 500 and 4000 $cm^{-1}$, with a resolution of 4 $cm^{-1}$. Each spectrum was obtained as the average of 32 consecutive scans on the specimen and analysed through an integration method consisting in the determination of the area under the most significant peaks by means of a tangential approach (Hofko et al., 2018; Hofko et al., 2017) (the same testing procedure and analysis method considered for the unaged binders, Section 3). Overall, three specimens for each binder were tested.

The compositional changes due to aging were also evaluated through thin layer chromatography with flame ionization detection (TLC-FID, commonly known as Iatroscan analysis) according to IP 469 (2006). The samples were prepared by dissolving about 0.1 g of binder in dichloromethane to obtain a 2% solution, which was spotted onto adsorption quartz rods filled with active silica (five rods were analysed for every binder, each one was spotted with 1 µl of solution). On the rods, saturates, aromatics and resins were separated by using n-heptane, toluene-heptane (80:20) and dichloromethane-methanol (95:5), respectively, while asphaltenes remained not eluted. The chromatograms obtained were

integrated in order to determine the relative percentages (by weight) of saturates, aromatics, resins and asphaltenes (SARA) fractions. In the integration, a common base line for all peaks was considered, and the separation of the peaks was identified at the minima of the chromatogram (analogously to the procedure considered to analyse the unaged binders, Section 3).
All the chemical analyses were carried out at Nynas laboratory during a research period spent in Nynashamn (Sweden).

### *4.2.4 Rheological testing and modelling*

The influence of aging on the rheological properties of the binders was investigated by performing frequency sweep tests with a dynamic shear rheometer (DSR) in plate-plate configuration, according to EN 14770 (2012). The testing conditions were the same adopted in the investigation of the unaged binders (Section 3). Specifically, nine temperatures were considered in the experiments, ranging from 0 to 80 °C with a step of 10°C, and at each temperature the frequency was increased from 1 to 100 rad/s (i.e. from 0.159 to 15.9 Hz) with a fixed logarithmic step. A shear strain equal to 0.05% was imposed in all tests, allowing all the rheological measurements within the linear viscoelastic (LVE) domain. At least two specimens were tested for each binder.
The modelling of the experimental data was carried out through 1S2P1D rheological model, i.e. 2S2P1D model applied to the case of bituminous binders (Olard and Di Benedetto, 2003; Yusoff et al., 2013). Analogously to the modelling of the unaged binders (Section 3), $G_g$ was fixed equal to $10^9$ Pa as suggested in literature (Anderson et al., 1994), whereas $h$ was imposed equal to 0.56 and $k$ varied in a narrow range between 0.22 and 0.25, since it has been demonstrated that these two parameters are about constant, regardless of binder type and aging level (Yusoff et al., 2013). 20°C was selected as the reference temperature for the master curves and, at this temperature, the model parameters were determined by minimizing the error between model and experimental data.

## 4.3 Results and analyses

### *4.3.1 Conventional properties*

From the previous experiments carried out on unaged binders, it was found that the bio-oil provides a consistency reduction that results in progressively increased penetration and decreased softening point as its amount is increased (Section 3.4.4). Figure 4.3 shows that this is generally true not only in unaged conditions, but also after short- and long-term aging. As for the comparison between 50/70+A10 and B1, their conventional properties are similar, even though B1 seems to be slightly harder in terms of penetration at all aging conditions. As expected, aging causes a decrease in the penetration and an increment of the softening point, without altering the overall ranking of the binders emerged in unaged conditions.

In addition, the mass loss during RTFOT aging was evaluated according to EN 12607-1 (2015). All the binders exhibited a mass loss lower than 1%, which is generally considered a maximum acceptable value for binders destined to paving applications (Kennedy et al., 1994). However, a specific trend related to the bio-oil content was not observed.

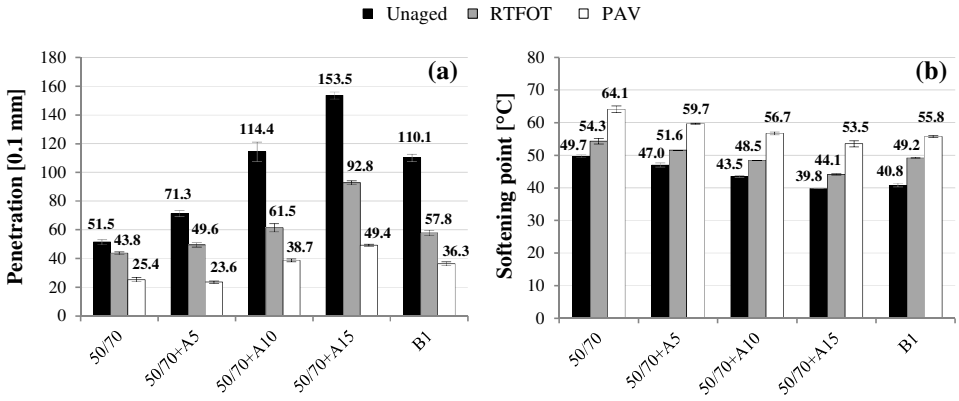


**Figure 4.3** Conventional properties: (a) penetration, (b) softening point

## *4.3.2 FTIR*

As an example of the results, the absorbance spectra obtained before and after aging for one specimen of B1 and 50/70+A10 are shown in Figure 4.4 (a) and Figure 4.4 (b), respectively. Only wavenumbers between 500 and 2000 $cm^{-1}$ are presented, as the most significant peaks related to bio-oil modification and aging are all in this part of the spectrum. As already observed from the analysis of the unaged binders (Section 3.4.1), the main differences between the bio-binders studied and the conventional bitumens are the peaks at 1735 $cm^{-1}$ and 1242 $cm^{-1}$, completely absent in the bitumen spectrum, which are due to the bio-oil and appear also after aging.

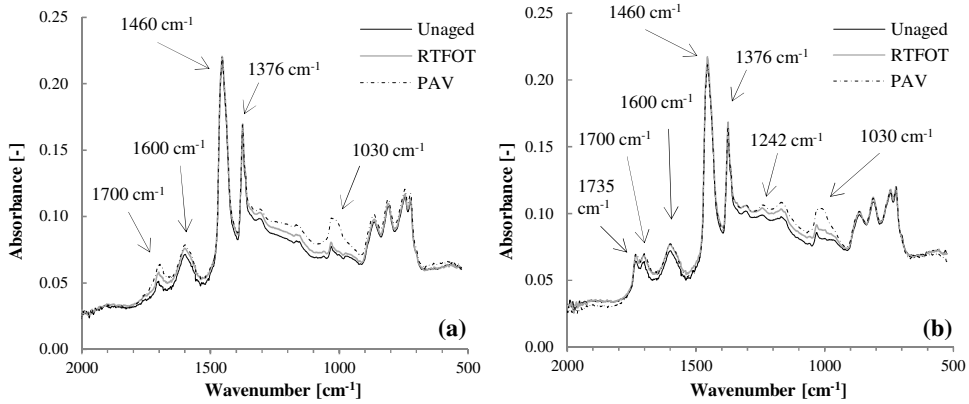


**Figure 4.4** Absorbance spectra of (a) B1 and (b) 50/70+A10, for wavenumbers between 500 and 2000 $cm^{-1}$

In order to quantitatively compare the binders, five indices were determined from the spectral analysis, as in Equations (4.1)-(4.5):

$$I_{1700} = \frac{A_{1700}}{A_{1460} + A_{1376}} \tag{4.1}$$

$$I_{1600} = \frac{A_{1600}}{A_{1460} + A_{1376}} \tag{4.2}$$

$$I_{1030} = \frac{A_{1030}}{A_{1460} + A_{1376}} \tag{4.3}$$

$$I_{1735} = \frac{A_{1735}}{A_{1460} + A_{1376}} \tag{4.4}$$

$$I_{1242} = \frac{A_{1242}}{A_{1460} + A_{1376}} \tag{4.5}$$

where $A_{1700}$, $A_{1600}$, $A_{1030}$, $A_{1735}$ and $A_{1242}$ are the absorbance areas around the peaks corresponding respectively to the C=O stretch of the carboxylic acids at 1700 $cm^{-1}$ (usually named as carbonyl functional group), the C=C stretch of the aromatics at 1600 $cm^{-1}$, the S=O stretch of the sulfoxides at 1030 $cm^{-1}$, the C=O and C-O stretch of the esters at 1735 $cm^{-1}$ and 1242 $cm^{-1}$. $A_{1460}$ and $A_{1376}$ instead are the areas related to the $CH_2$ and $CH_3$ bend of the alkanes (commonly indicated as aliphatic groups) around the peaks at 1460 $cm^{-1}$ and 1376 $cm^{-1}$, which are usually not affected by aging (Lamontagne et al., 2001) and thus appear in the denominator in Equations (4.1)-(4.5).

The investigation of the oxidative aging of conventional bitumens is normally performed through $I_{1700}$ and $I_{1030}$, as also confirmed by Figure 4.4, where an increment of $A_{1700}$ and

$A_{1030}$ after aging is observed for both B1 and 50/70+A10. In fact, it is well-known that bitumen oxidation mainly leads to the formation of carbonyl groups characterized by C=O bonds and sulfoxides, which are the main responsible for the physical and rheological changes undergone by bitumen during aging (Petersen and Glaser, 2011; Petersen, 2009). However, other possible meaningful indices for the study of the oxidative aging of the bio-binders are shown in Figure 4.5, where each graph presents a different scale on the y-axis, as the values of the various indices differ significantly from each other.

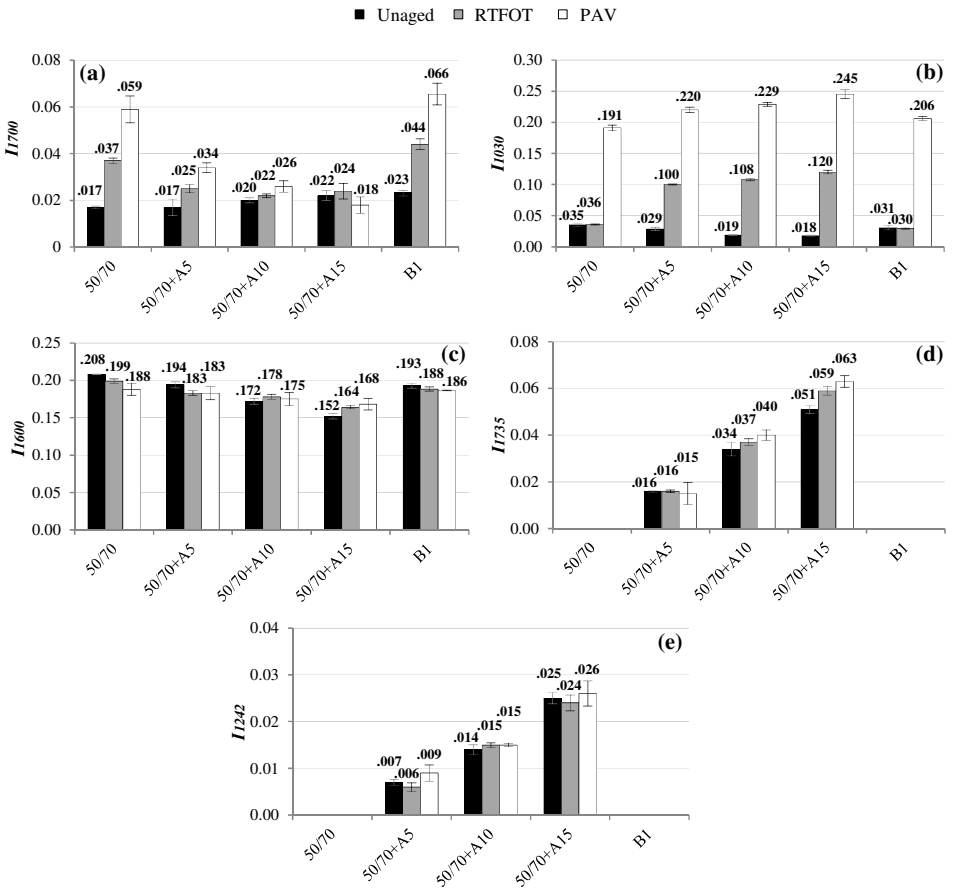


**Figure 4.5** FTIR indices: (a) $I_{1700}$, (b) $I_{1030}$, (c) $I_{1600}$, (d) $I_{1735}$, (e) $I_{1242}$

In terms of $I_{1700}$, as the bio-oil amount is increased, a slight increment is observed in unaged conditions, whereas this trend is inverted after aging, leading to significant lower values of $I_{1700}$ for the bio-binders as compared to the conventional bitumens (Figure 4.5 (a)). This suggests that the bio-oil may somehow inhibit the formation of carbonyl compounds, usually associated with the oxidation process. On the contrary, as compared to 50/70, the bio-oil addition causes a slight reduction of $I_{1030}$ before aging (Figure 4.5 (b)), but a

remarkable increase after short- and long-term aging, determining higher values of $I_{1030}$ for the bio-binders with respect to the conventional bitumens. However, the addition of the bio-oil seems to alter the shape of the spectrum around 1030 $cm^{-1}$ making the sulfoxide peak less distinct because certain C-O bonds from the bio-oil show absorbance in a similar range of wavenumbers, and this effect appears to be even more evident after aging (Figure 4.4 (b)). This means that, for the bio-binders, functional groups other than sulfoxides might be also included when determining $A_{1030}$. As shown in Figure 4.5 (c), the aromatic index $I_{1600}$ is progressively reduced with increasing bio-oil contents before and after aging, which indicates lower aromaticity in the bio-binders with respect to the conventional bitumens.
As already observed from the analysis of the unaged binders (Section 3.4.1), $I_{1735}$ and $I_{1242}$ (zero for 50/70 and B1) can be effectively used as indicators to identify and quantify the bio-material studied within bituminous binders, as their values increase along with the bio-oil amount, both in unaged and aged conditions (Figures 4.5 (d) and 4.5 (e)).
As far as the aging effect is concerned, Figure 4.5 shows that there are no clear trends between $I_{1600}$ and aging, and this is also the case for $I_{1242.}$ On the other hand, for the sulfoxide index $I_{1030}$, a significant increase is observed after both RTFOT and PAV for the bio-binders while only after PAV for the conventional bitumens. In addition, $I_{1700}$ generally increases with aging for all binders as well as $I_{1735}$ for the bio-binders.
In summary, the presence of the bio-oil seems to significantly reduce the formation of carbonyl compounds at 1700 $cm^{-1}$ during aging, but, on the other hand, additional oxidized compounds related to esters are observed at 1735 $cm^{-1}$. Since the absorbance area at 1030 $cm^{-1}$ remarkably increases with aging, the contribution of the sulfoxides should also be taken into account for the bio-binders, even though the alteration of the spectrum caused by the bio-oil addition might imply a certain overestimation of the sulfoxide area.

### *4.3.3 SARA fractions*

Typical chromatograms obtained for B1 and 50/70+A10 are presented in Figure 4.6 (a) and Figure 4.6 (b), respectively. As for the bio-binders, the additional peak between aromatics and resins due to bio-oil's aromatics, already found in unaged conditions (Section 3.4.2), can be noticed also after long-term aging (Figure 4.6 (b)). Moreover, in general, as the aging level increases, an evident reduction of the aromatics' peak and a clear increase of the resins' peak can be observed, together with a worsening of the separation between resins and asphaltenes (Figures 4.6 (a) and 4.6 (b)).

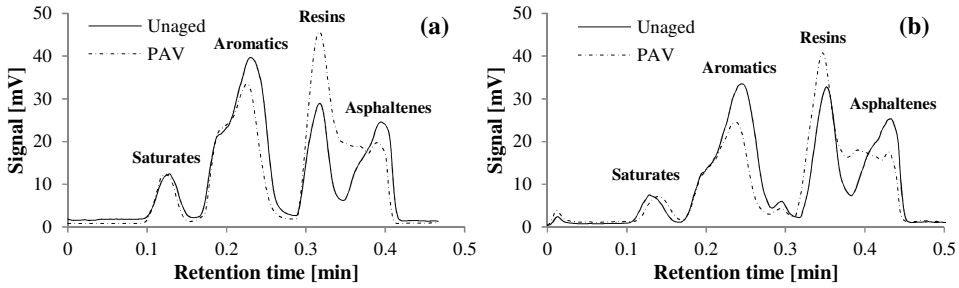


**Figure 4.6** Chromatograms of (a) B1 and (b) 50/70+A10

The results of the quantitative analysis carried out for all binders are shown in Figure 4.7. Note that, in the figure, different scales are used on the y-axis, in order to make the comparison between the various binders clearer.

As far as the effect of the bio-oil is concerned, it was already shown in Section 3.4.2 that, in unaged conditions, saturates, aromatics and asphaltenes are generally decreased, whereas resins as well as the sum of resins and asphaltenes are increased. The same trends can be observed also after short-term and long-term aging, except for asphaltenes, for which the values obtained might be affected by slightly imprecise integrations of the chromatograms (Figure 4.7). For the conventional bitumens (50/70 and B1), the effect of a softer grade broadly emerges as an increment of saturates and aromatics and a clear decrease of the sum of resins and asphaltenes, as can be seen from Figure 4.7.

Furthermore, Figure 4.7 displays that aromatics and resins exhibit a clear trend linked with aging, namely aromatics are significantly decreased while resins are markedly increased, whereas asphaltenes are (in general) unchanged or slightly increased and saturates remain about constant, as already noticed from Figure 4.6. All the binders tested show these tendencies, which are in agreement with literature (Lu and Isacsson, 2002; Lu and Isacsson, 2000; Stangl et al., 2006). However, in some cases, resins appear to be overestimated while asphaltenes are visibly underestimated, as happens for instance for B1 after PAV (Figures 4.7 (c) and 4.7 (d)). These results confirm what was qualitatively observed from Figure 4.6, namely the aging process seems to lead to the formation of compounds that have intermediate characteristics between resins and asphaltenes for both conventional bitumens and bio-binders, making the separation between such fractions poorer especially after long-term aging, similarly to previous findings in literature (Stangl et al., 2006). It cannot be excluded that the procedure followed to separate the different fractions might also have a certain influence on this aspect. In fact, it is well-known that the SARA fractions are defined as solubility classes rather than chemical component classes, and slight variations in the separation procedure or in the solvents may create differences in the fractions (Lu et al., 2017). Nevertheless, the results obtained in terms of sum of resins and asphaltenes (both fractions characterized by a strong polarity) seem to be reliable, and a remarkable increase is found after short- and long-term aging for the sum of these two fractions for all binders (Figure 4.7 (e)).

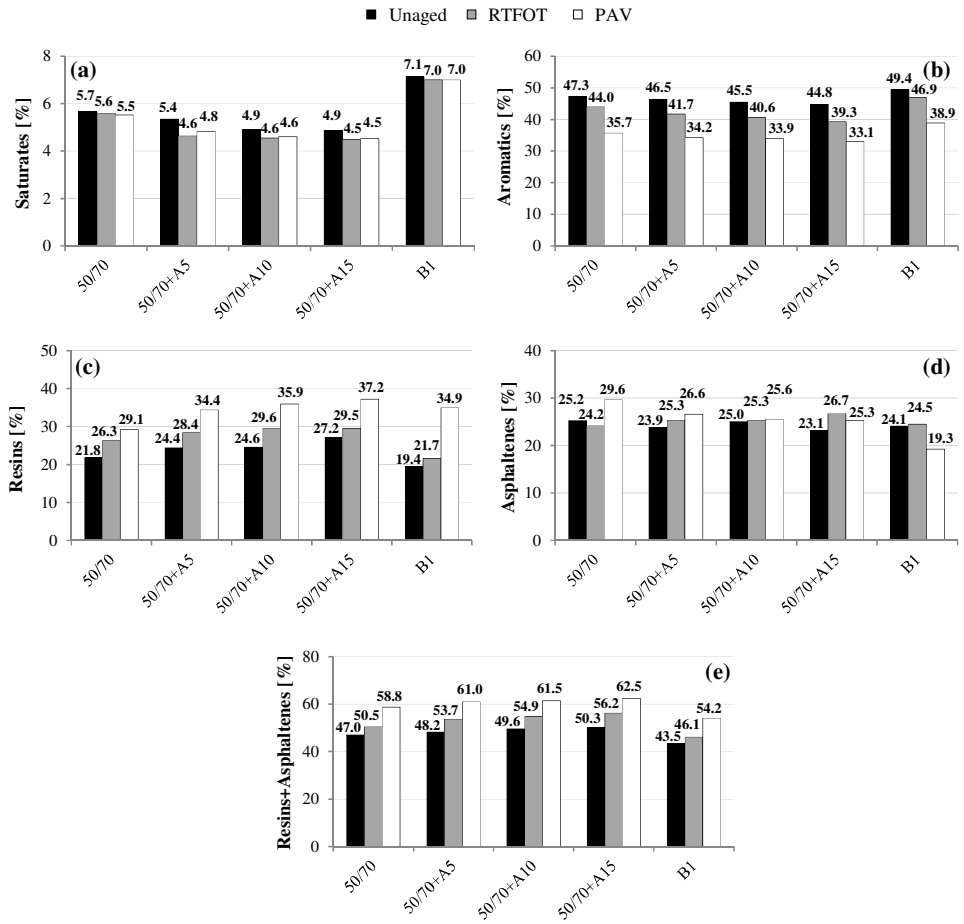


**Figure 4.7** SARA fractions: (a) saturates, (b) aromatics, (c) resins, (d) asphaltenes, (e) sum of resins and asphaltenes

### *4.3.4 Rheology*

As an example, the raw rheological results for 50/70+A15 at different aging levels are shown in Figure 4.8 (a) in the Black diagram. A good overall alignment of the experimental data can be observed from the figure, even though some imprecision emerges when the phase angle approaches 90° (i.e. at high temperatures) and also for lower phase angle values when the long-term aging condition is considered. Since the bio-binders with lower bio-oil amount (≤ 10%) and the conventional bitumens tend to exhibit an even better alignment of the experimental points in the Black diagram as compared to 50/70+A15, all the binders can be considered thermo-rheologically simple, which means that the time-

temperature superposition principle (TTSP) is valid and the master curves can be developed in all cases (Airey, 2002).
Moreover, for all the binders, aging causes an increase of the complex modulus and a decrease of the phase angle (see Figure 4.8 (a) as an example), which indicates that the binder is characterized by higher stiffness and elasticity after aging.
Figure 4.8 (b) displays that, regardless of the aging level, 1S2P1D model fits quite well the experimental data for 50/70+A15, except for some inaccuracy at low reduced frequencies (i.e. high temperatures). Since this is also true for all other binders, the model master curves can be reasonably considered to compare the binders' rheological behaviour. Specifically, Figure 4.9 shows that the softening effect of the bio-oil, already pointed out in Figure 4.3, results in a reduction of $|G^*|$ at all aging levels. Moreover, the comparison between 50/70+A10 and B1 shows that their $|G^*|$ values are comparable over a wide range of reduced frequencies in unaged conditions (Figure 4.9 (a)). A certain difference between 50/70+A10 and B1 emerges as the aging degree increases (Figures 4.9 (b) and 4.9 (c)), suggesting the possibility of a different aging susceptibility.

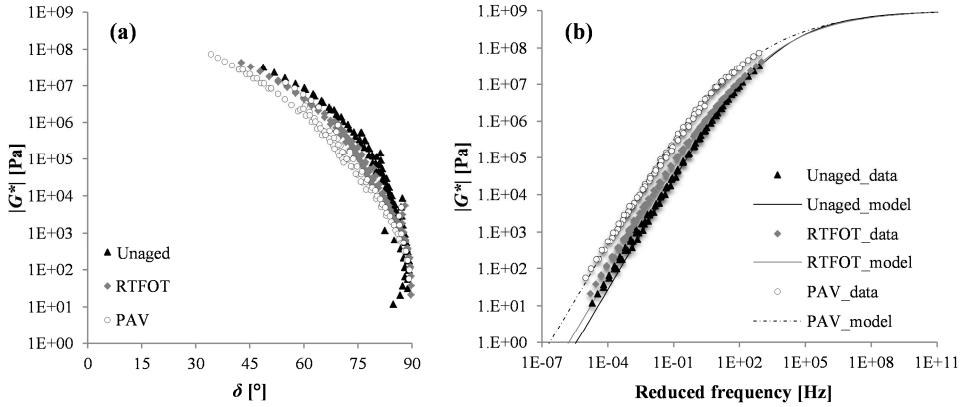


**Figure 4.8** Rheological results for 50/70+A15: (a) Black diagram, (b) master curve of complex modulus at 20°C

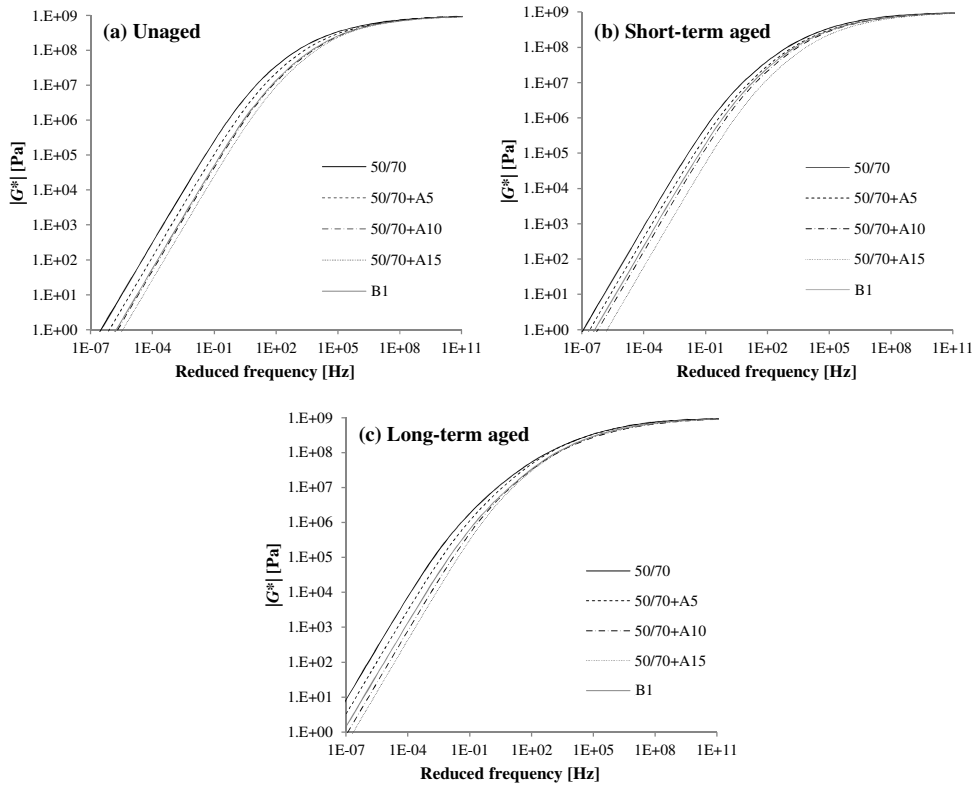


**Figure 4.9** Master curve of complex modulus at 20°C for (a) unaged binders, (b) short-term aged binders, (c) long-term aged binders

Table 4.1 summarizes the 1S2P1D and WLF parameters deriving from the rheological modelling. It can be noted that, when the same aging level is considered, $\alpha$ and $\tau_0$ decrease as the binder penetration grade increases, and this is valid for both bio-binders and conventional bitumens. As the binder grade becomes softer, a certain decreasing trend is observed also for $\beta$, even though it is less evident with respect to the trends of $\alpha$ and $\tau_0$. Such tendencies are in agreement with literature (Olard and Di Benedetto, 2003; Perez-Martinez et al., 2016; Yusoff et al., 2013).

Moreover, Table 4.1 indicates that $\alpha$, $\beta$ and $\tau_0$ increase with aging for all binders, in agreement with the results by Perez-Martinez et al. (2016), who studied the binders recovered from asphalt mixtures aged at different levels in several laboratories.

In terms of WLF parameters, the variation of $C_1$ and $C_2$ due to binder type and/or aging is not completely clear, similarly to previous findings by Alavi et al. (2013) on asphalt mixtures.

**Table 4.1** 1S2P1D and WLF parameters

| Binder | Aging level | $G_g$ [Pa] | $h$ | $k$ | $\alpha$ | $\beta$ | $\tau_0$ (20°C) | $C_1$ | $C_2$ |
|---|---|---|---|---|---|---|---|---|---|
| 50/70 | Unaged | 1.00E+09 | 0.56 | 0.22 | 2.4 | 55 | 8.90E-06 | 25 | 262 |
| | RTFOT | 1.00E+09 | 0.56 | 0.23 | 2.7 | 112 | 1.19E-05 | 21 | 219 |
| | PAV | 1.00E+09 | 0.56 | 0.24 | 3.9 | 387 | 3.42E-05 | 21 | 208 |
| 50/70+A5 | Unaged | 1.00E+09 | 0.56 | 0.22 | 2.2 | 54 | 3.59E-06 | 23 | 248 |
| | RTFOT | 1.00E+09 | 0.56 | 0.22 | 2.5 | 118 | 5.50E-06 | 23 | 231 |
| | PAV | 1.00E+09 | 0.56 | 0.23 | 3.1 | 296 | 1.75E-05 | 31 | 319 |
| 50/70+A10 | Unaged | 1.00E+09 | 0.56 | 0.25 | 2.0 | 55 | 1.41E-06 | 17 | 188 |
| | RTFOT | 1.00E+09 | 0.56 | 0.22 | 2.3 | 89 | 2.90E-06 | 18 | 204 |
| | PAV | 1.00E+09 | 0.56 | 0.22 | 3.4 | 165 | 7.83E-06 | 23 | 274 |
| 50/70+A15 | Unaged | 1.00E+09 | 0.56 | 0.22 | 1.7 | 54 | 7.97E-07 | 23 | 286 |
| | RTFOT | 1.00E+09 | 0.56 | 0.22 | 2.2 | 83 | 1.13E-06 | 20 | 237 |
| | PAV | 1.00E+09 | 0.56 | 0.22 | 2.0 | 110 | 6.34E-06 | 32 | 400 |
| B1 | Unaged | 1.00E+09 | 0.56 | 0.22 | 2.0 | 60 | 1.49E-06 | 19 | 204 |
| | RTFOT | 1.00E+09 | 0.56 | 0.22 | 2.4 | 89 | 4.18E-06 | 22 | 233 |
| | PAV | 1.00E+09 | 0.56 | 0.23 | 3.0 | 279 | 7.99E-06 | 26 | 256 |

### *4.3.5 Rutting and fatigue Superpave parameters*

The rheological data were further used to calculate the rutting and fatigue Superpave parameters (Kennedy et al., 1994), as shown in Figures 4.10 and 4.11.

The rutting parameter $|G^*|/\sin\delta$ was determined at 10 rad/s (i.e. 1.59 Hz) at four typical high service temperatures: 50, 60, 70, 80 °C (Figure 4.10). The permanent deformation resistance is considered satisfactory when $|G^*|/\sin\delta$ is higher than a reference threshold value, which is 1 kPa when the binder is unaged and 2.2 kPa when the binder is short-term aged (Kennedy et al., 1994). From Figure 4.10, it can be observed that the upper continuous Performance Grade (PG), i.e. the highest temperature at which both requirements are met, is slightly lower than 60°C for 50/70+A15, higher than 60°C for 50/70+A10 and B1, considerably higher than 60°C for 50/70+A5 and slightly higher than 70°C for 50/70. This means that the rutting parameter decreases with increasing bio-oil content, which is not surprising because the binder becomes softer when adding the bio-oil. Moreover, these results demonstrate that the mechanical behaviour of 50/70+A10 and B1 (which have comparable penetration grade) at high service temperatures is very similar, as the value of $|G^*|/\sin\delta$ is almost identical for the two binders at all temperatures and aging levels considered.

The fatigue parameter $|G^*|\sin\delta$ was determined at 10 rad/s (1.59 Hz) at three typical intermediate service temperatures: 10, 20, 30 °C (Figure 4.11). The fatigue performance is considered satisfactory when $|G^*|\sin\delta$ is lower than 5000 kPa after long-term aging (Kennedy et al., 1994). As can be seen from Figure 4.11, this requirement is not met for any

binder at 10°C, whereas it is met for all binders at 20°C, except for 50/70. Since the bio-oil provides a softening effect, the fatigue resistance improves as the bio-oil percentage increases. The behaviour of 50/70+A10 and B1 can be considered comparable also in terms of fatigue performance at intermediate temperatures, although B1 shows slightly higher values of $|G^*|\sin\delta$ probably due to its greater consistency (Figure 4.3 (a)) and stiffness (Figure 4.9).

These results are in good agreement with the findings by Gaudenzi et al. (2020), who investigated the healing properties of the binders 50/70, 50/70+A10 and B1 in unaged and long-term aged (RTFOT plus PAV) conditions, by performing healing tests at relatively high strain levels (beyond the LVE limit). The bio-binder 50/70+A10 showed an overall fatigue behaviour comparable to that of the conventional bitumen with similar penetration grade (B1) and a greater self-healing capability with respect to both conventional bitumens, especially in aged conditions.

Thus, it is expected that, at high and intermediate service temperatures, the mechanical behaviour of bio-binders and conventional bitumens having similar penetration grade will be at least comparable. Therefore, bio-binders might represent a sustainable alternative to traditional bituminous binders, without any performance penalisation. However, it is worth pointing out that the low-temperature behaviour should also be investigated for a thorough performance characterization.

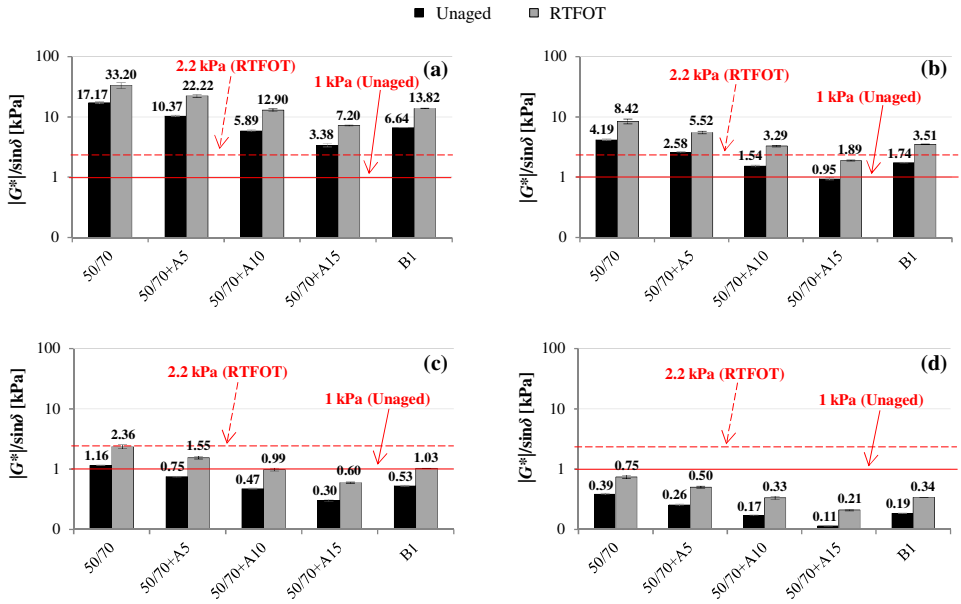


**Figure 4.10** Rutting parameter at (a) 50°C, (b) 60°C, (c) 70°C, (d) 80°C

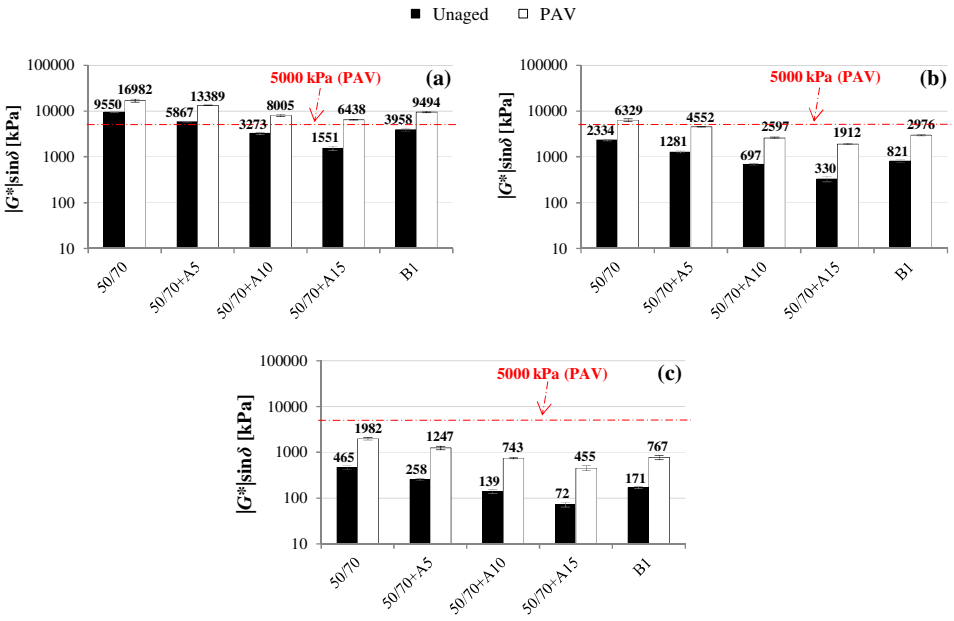


**Figure 4.11** Fatigue parameter at (a) 10°C, (b) 20°C, (c) 30°C

### *4.3.6 Correlation between chemical and rheological changes induced by aging*

Possible correlations between chemical and rheological changes induced by aging were also sought. The objective was to identify, among those studied, the chemical and rheological parameters most strictly related to the binders' oxidation, to be used as aging indicators (or aging indices, *AI*) for comparing the aging susceptibility of the binders tested.

The aging index of a certain property is defined as the ratio between this property for the aged binder and the same property for the unaged binder. Given this definition, values of *AI* close to 1 indicate a limited variation of the considered property after aging and thus a low aging tendency. Several aging indices are used in literature, such as the retained penetration, the softening point increment, the viscosity *AI*, the rutting *AI*, etc. (Zhang et al., 2018b). However, they are based on different tests and represent different performances, thus normally showing inconsistent correlation with each other. On the contrary, a reliable aging index should be unambiguously related to the oxidative level of the binder, regardless of the testing conditions considered (Cai et al., 2019).

In this regard, from the chemistry point of view, it is well-known that the SARA fractions determined by Iatroscan analysis significantly depend on the procedure and solvents employed (Lu et al., 2017), whereas the absorbance spectrum obtained from FTIR analysis can be considered a sort of chemical footprint of the material (Smith, 2011). Moreover, it has been shown that, for the bio-binders studied, oxidative aging causes the formation of

additional compounds at 1700 $cm^{-1}$, 1030 $cm^{-1}$ and 1735 $cm^{-1}$ (Figure 4.5). Consequently, $I_{1700} + I_{1030} + I_{1735}$ was adopted as chemical *AI*.

As possible rheological aging indicators, $\alpha$, $\beta$ and $\tau_0$ parameters from 1S2P1D model were considered, as they all increase with aging (Table 4.2).

Figures 4.12 (a), 4.12 (b) and 4.12 (c) show that, in general, a good linear relationship exists between such rheological parameters and $I_{1700} + I_{1030} + I_{1735}$ for all binders. In particular, in each graph, three points are plotted for each binder: the black symbol corresponds to the unaged condition, the grey symbol to the short-term aged condition, the white symbol to the long-term aged condition. These results are in line with previous findings by Perez-Martinez et al. (2016). In addition, Figure 4.12 demonstrates that these relationships are material-dependent and a similar ranking of the binders is obtained in terms of $\alpha$, $\beta$ and $\tau_0$. Specifically, the slope of the relationship seems to increase with the binder consistency.

Moreover, as suggested by Rad et al. (2018), the norm of the complex modulus measured at high temperature and 10 rad/s was selected as another potential rheological indicator to track the binders' oxidative aging. Thus, the relationship between $I_{1700} + I_{1030} + I_{1735}$ and $|G^*|$ at 70°C and 10 rad/s was also taken into consideration (Figure 4.12 (d)). Even in this case, a good linear correlation exists for all binders, and the slope of this relationship tends to be greater with increasing binder consistency.

It should be noted that, if all the tested binders are examined together, no correlations are found between chemical and rheological parameters (Figures 4.12 (a), 4.12 (b), 4.12 (c), 4.12 (d)).

In order to find only one reference aging indicator also in terms of rheology, it should be considered that the effect of oxidative aging is generally more evident at very low frequencies/very high temperatures (Rad et al., 2018). Thus, since $\beta$ is - for definition - the parameter that controls the slope of the master curve of $|G^*|$ at low frequencies/high temperatures (Yusoff et al., 2013) and 70°C is normally one of the highest temperatures investigated with the DSR, $\beta$ and $|G^*|$ at 70°C and 10 rad/s seem to be the most reliable rheological aging indices (besides, for such parameters the highest $R^2$ values were observed, see Figure 4.12). In this sense, Figure 4.13 suggests that both parameters can be effectively used as they are highly correlated. Nevertheless, since $\beta$ determines the shape of the master curve of $|G^*|$ in a certain range of low reduced frequencies, whereas the other parameter is a single measurement point at high service temperatures (which correspond to intermediate reduced frequencies), $\beta$ may provide more complete information about the rheological changes induced by aging as compared to a single value of $|G^*|$.

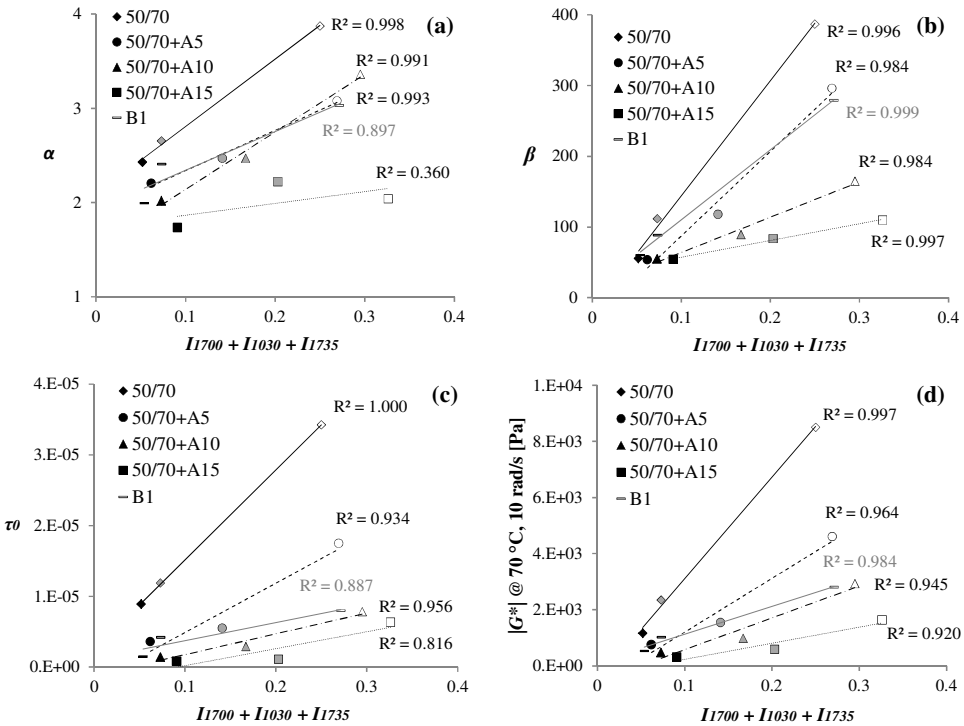


**Figure 4.12** Correlation between $I_{1700} + I_{1030} + I_{1735}$ and (a) $\alpha$, (b) $\beta$, (c) $\tau_0$, (d) $|G^*|$ at 70°C and 10 rad/s

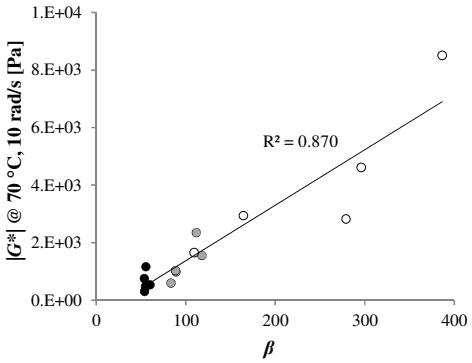


**Figure 4.13** Correlation between $|G^*|$ at 70°C and 10 rad/s and $\beta$

Based on the previous considerations, $I_{1700} + I_{1030} + I_{1735}$ and $\beta$ were found to be the chemical and rheological *AI* most suitable to analyse the oxidative aging susceptibility of the binders studied. In this regard, Figure 4.14 shows that, for all binders, there is an excellent linear relationship between $AI_\beta$ (the ratio between $\beta$ after and before aging) and $AI_{1700+1030+1735}$ (the ratio between $I_{1700} + I_{1030} + I_{1735}$ after and before aging), i.e. there is a

direct link between the chemical and the rheological changes induced by aging. Even in this case, no correlation is found if all the binders are considered together (Figure 4.14).
As for the comparison between the binders (Figure 4.14), it is worth noting that after short-term aging the values of $AI_\beta$ for the various binders do not differ significantly, probably because this aging condition is not severe enough to assess the actual aging resistance of the binders. Furthermore, the higher values of $AI_{1700+1030+1735}$ for 50/70+A5, 50/70+A10 and 50/70+A15 are due to the alteration of the shape of the absorbance spectrum around 1030 $cm^{-1}$ caused by the bio-oil (see Section 4.3.2). Conversely, the differences between the binders clearly emerge after long-term aging.
According to the values of $AI_\beta$, after long-term aging, the binders are ranked as follows (from the highest to the lowest aging tendency): 50/70, 50/70+A5, B1, 50/70+A10, 50/70+A15 (Figure 4.14). Therefore, it seems that a higher penetration grade results in a lower $AI_\beta$, and this is true also when considering separately the two conventional bitumens (50/70 and B1) and the bio-binders (characterized by increasing replacement percentage of 50/70). Moreover, from the comparison between 50/70+A10 and B1, having analogous penetration grade (Figure 4.3), it can be noted that the bio-binder exhibits lower aging susceptibility.
When comparing the binders in terms of $AI_{1700+1030+1735}$ after long-term aging, a similar ranking is observed, with the only difference that the highest $AI$ is exhibited by B1 in this case. Such result can be explained by considering that all binders are obtained from 50/70 as base bitumen, except B1 that has a different chemistry. In any case, the lower chemical changes experienced by 50/70+A10 with respect to B1 confirm that the bitumen replacement with the bio-oil does not negatively affect the aging tendency of the binder, but, on the contrary, it may even improve the aging resistance of the binder.
In conclusion, the results presented suggest that the bio-binders studied may represent a more sustainable and even more durable solution for road pavements as compared to traditional bitumens.

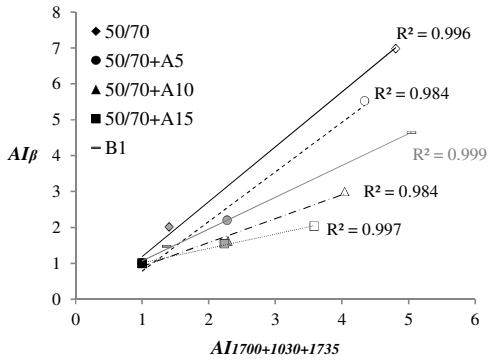


**Figure 4.14** Correlation between $AI_\beta$ and $AI_{1700+1030+1735}$

## 4.4 Summary of the findings

This part of the research project aimed at providing a comprehensive characterization of the short-term and long-term aging properties of bio-binders for road pavements obtained by partially replacing a 50/70 bitumen with a wood-based bio-oil at different percentages by weight (5, 10 and 15%). One conventional bitumen having similar penetration to that of one bio-binder was also included in the investigation for comparison purposes. The unaged, RTFOT-aged and PAV-aged binders were subjected to conventional, chemical and rheological tests as well as rheological modelling with 1S2P1D model.
The results and analyses presented lead to the following conclusions:

- as the bio-oil amount in the binder increases, the penetration is progressively increased whereas the softening point is progressively reduced. After aging, the ranking of the binders remains the same in terms of conventional properties;
- FTIR results indicate that, during aging, the formation of carbonyl compounds at 1700 $cm^{-1}$ is significantly reduced for the bio-binders as compared to conventional bitumens, but additional oxidized compounds related to esters are observed at 1735 $cm^{-1}$;
- the SARA analysis shows that the bio-oil addition to the base bitumen causes a reduction of saturates, aromatics and asphaltenes and an increment of resins at all aging conditions. For both conventional bitumens and bio-binders, the aging process apparently leads to the formation of compounds with intermediate characteristics between resins and asphaltenes, making the separation between such fractions poorer;
- a thermo-rheologically simple behaviour and a good fitting of 1S2P1D model to the rheological data are observed for all binders, regardless of bio-oil content and aging level. The softening effect of the bio-oil causes a reduction of the complex modulus at all aging conditions, as compared to the base bitumen;
- from the performance point of view, the permanent deformation resistance and fatigue resistance of the bio-binder with 10% bio-oil are comparable to those observed for the conventional bitumen with similar penetration grade, without any critical penalisation;
- for all binders tested, a linear material-dependent relationship exists between the chemical and rheological changes induced by aging;
- based on the variation of the chemical and rheological parameters most strictly related to the binders' oxidation, bio-binders may have similar or even higher aging resistance as compared to conventional bitumens with similar penetration grade.

In conclusion, it is expected that the bio-binders studied may have comparable or even better durability and long-term performance with respect to conventional bitumens. Therefore, they can be considered an effective sustainable alternative to traditional bituminous binders.
In the future, these results should be validated by studying also ultraviolet (UV) aging, which is another phenomenon occurring during the in-service life of asphalt pavements.

# 5. Adhesion between bio-binders and aggregates and moisture susceptibility of bio-binder/aggregate systems

## 5.1 Background and objectives

Performance and durability of asphalt pavements are significantly affected by the cohesion provided by the binder phase (bitumen or bitumen-filler mastic) and its interaction (adhesion) with the solid phase (aggregate) within bituminous mixtures. Generally, the solid skeleton provides compressive strength whereas tensile and flexural strength, necessary to withstand the loads, strongly depend on binder-aggregate interaction. Indeed, if a strong adhesion bond exists between aggregates and bitumen, mixture failure can occur within the binder (or because of aggregate breakdown), whereas a weak bond can lead to a failure at the binder-aggregate interface. The loss of adhesion at the interface is also responsible for major road distresses such as ravelling and potholes, which could lead to premature failure of the pavement (Kanitpong and Bahia, 2005; Roberts et al., 1996).

The interaction developed at the binder-aggregate interface is strictly related to the chemical properties of both materials. Bitumen tends to exhibit a higher chemical affinity with basic aggregates like calcareous ones as compared to acid aggregates such as siliceous ones (Tarrer and Wagh, 1991). In addition, the action of water can considerably weaken the bond between binder and aggregate leading to the phenomenon known as stripping (Kandhal, 1994; Taylor and Khosla, 1983), thus compromising the durability of the overall pavement. Based on this background, it is evident that the bond between binder and aggregates is a crucial aspect in pavement engineering.

Currently, the adhesive bond of binder-aggregate systems can be quantified according to chemical and thermodynamic theories based on surface free energy measurements (Bhasin et al., 2007; Bhasin et al., 2006; Tan and Guo, 2013). Nevertheless, routine empirical tests on bituminous mixtures, such as the boiling water test, the rolling bottle test or tests for measuring the strength retained after water immersion, are still commonly used for an indirect evaluation of the bitumen-aggregate affinity as well as the moisture damage potential of mixtures (EN 12697-11, 2012; EN 12697-12, 2018; Porot et al., 2016).

As a step forward with respect to such tests on mixtures, a pull-off test based on the use of a modified pneumatic adhesion tensile testing instrument (PATTI) has been optimized and effectively employed to directly assess the adhesive and cohesive properties of bituminous binder-aggregate systems in dry and wet conditions (Canestrari et al., 2010; Kanitpong and Bahia, 2003). The procedure, standardized as the binder bond strength (BBS) test by AASHTO T 361 (2016), can be satisfactorily applied to hot bitumens and mastics (Chaturabong and Bahia, 2018; Moraes et al., 2011) as well as cold bitumen emulsion composites (Graziani et al., 2018).

As anticipated in Section 2.3, the chemical and mechanical properties of certain bio-binders have been widely investigated so far. However, very few studies have been carried out on

the effects of bio-materials or bio-oils on the adhesive properties of bitumen (Bearsley and Haverkamp, 2007b; Gong et al., 2017). In this sense, the bond strength of bio-binder/aggregate systems as well as their stripping tendency are not yet well understood and further research is needed.
Within this context, this part of the research project aimed at evaluating the bond strength of bio-binder/aggregate systems through the BBS test. The bio-binders studied were the same investigated in the previous experimental phases (Sections 3 and 4). A full factorial experiment was performed in order to evaluate the effects of several parameters on the bond strength of bio-binder/aggregate systems. The set of investigated parameters includes bio-oil content, aggregate type and aging condition. In addition, the moisture damage was assessed by considering both dry and wet conditioned specimens. Prior to BBS tests, viscosity measurements of the binders were carried out to determine the appropriate temperatures for the preparation of BBS specimens.
The data presented in the following sections are published in Ingrassia et al. (2019c).

## 5.2 Materials and methods

### *5.2.1 Materials*

The experimental investigation was carried out on the same binders already studied in Sections 3 and 4, i.e. the base bitumen 50/70 and the bio-binders 50/70+A5, 50/70+A10 and 50/70+A15 containing respectively 5, 10 and 15 % by weight of wood-based bio-oil.
All the binders were studied at three aging levels: unaged, short-term aged by Rolling Thin Film Oven Test (RTFOT) (EN 12607-1, 2015) and long-term aged by applying both RTFOT and Pressure Aging Vessel (PAV) (EN 14769, 2013). The unaged and short-term aged conditions aimed at investigating the bond that develops between binder and aggregates in the early stages of mixture production and construction (i.e. mixing, hauling, laydown and compaction), whereas the long-term aged condition allowed to evaluate how the binder-aggregate bond changes when the binder is highly oxidative aged.
Two types of aggregate with different bitumen affinity were selected as solid substrate: limestone (calcareous) and porphyry (siliceous). Specifically, aggregate plates about 1 cm thick having rectangular shape were prepared by cutting quarry stone blocks.

### *5.2.2 Viscosity tests*

The dynamic viscosity of the unaged and aged binders was measured by means of a Brookfield rotational viscometer according to ASTM D4402 (2015) at six temperatures: 80, 90, 105, 120, 135 and 150 °C. At each temperature, the measurements were performed by applying five different shear rates (corresponding to fixed working rates of the viscometer: 10, 30, 50, 70 and 90 %), with the aim of assessing the shear rate dependency of the binders. In general, lower shear rates were applied at lower temperatures, as the higher viscosity of the binder implies a higher working rate of the viscometer, and spindles with different dimensions were employed depending on the expected viscosity. Two specimens

were tested for each binder. The viscosity data were then used to determine BBS application temperatures (i.e. the temperatures for preparing BBS specimens), based on the equiviscosity condition.

### *5.2.3 BBS tests*

The BBS tests were carried out with a modified PATTI consisting of a metal stub, a pneumatic piston, a reaction plate and a control module (Figure 5.1), based on AASHTO T 361 (2016). The pull-off stubs employed were made of brass (which exhibited good affinity with bitumen) and were characterized by an internal diameter (corresponding to the diameter of the binder-substrate contact area) of 12.5 mm, an external diameter of 12.7 mm and a 0.3 mm-thick edge (corresponding to the thickness of the binder specimen). Moreover, the edge presented 8 small cuts, which allowed the binder in excess to flow out during the stub application. This geometry was already adopted in previous studies (Canestrari et al., 2014; Canestrari et al., 2010; Graziani et al., 2018) and the results were found to be statistically reliable.

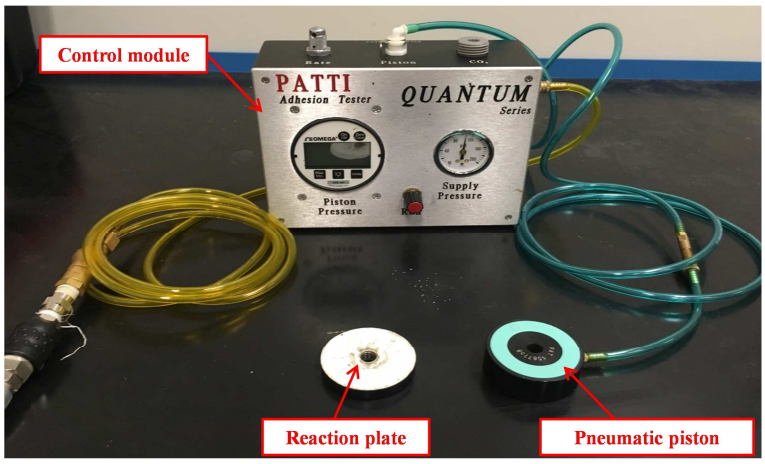


**Figure 5.1** Modified pneumatic adhesion tensile testing instrument (PATTI) employed

As for the preparation of BBS specimens, a small amount of binder (0.08 g) was placed on the pull-stub surface and then heated in the oven for 30 minutes at the application temperature determined from the viscosity data (see Section 5.3.1), allowing the binder to perfectly adhere to the pull-stub. Afterwards, the stub was immediately pressed onto the aggregate plate, previously cleaned and heated for 2 hours at the same application temperature of the binder. Figure 5.2 shows typical BBS specimens (before conditioning), consisting in the assembly of pull-stub, binder and aggregate plate.

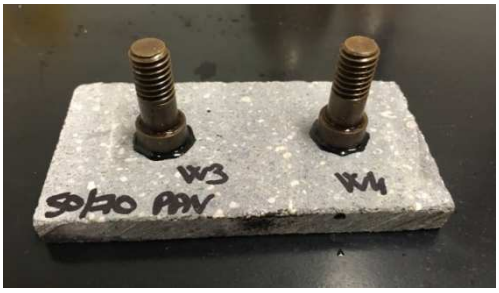


**Figure 5.2** BBS specimens, before conditioning (substrate: porphyry; binder: PAV-aged 50/70)

All the BBS specimens were first conditioned for one hour at ambient temperature, in order to allow the development of the adhesion between binder and substrate. Then, for the dry conditioning the specimens were left in a climatic chamber at 25°C for 24 hours, while for the wet conditioning the specimens were put in a water bath at 40°C for 24 hours. At the end of the 24 hours, the dry specimens were immediately subjected to the pull-off test, whereas the wet specimens were further conditioned for one hour in the climatic chamber at 25°C prior to testing. All the specimens were tested at ambient temperature (around 25°C).
During BBS tests, the piston and the reaction plate were screwed to the stub and an increasing pulling force was applied with a constant loading rate through the pneumatic system, as schematized in Figure 5.3. In such way, the binder specimen was subjected to a growing pulling force until reaching the failure. The failure pressure was recorded and then converted into the pull-off tensile strength (POTS) considering the actual contact area between binder and substrate. Moreover, the type of failure was identified by visually inspecting the coating level of the contact area after the test (see Section 5.3.2).

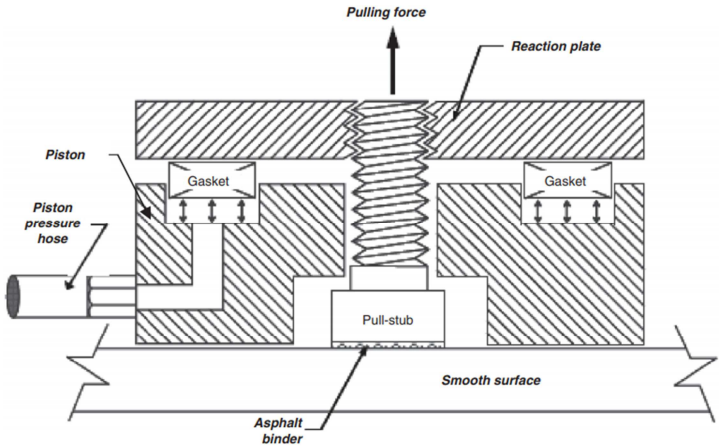


**Figure 5.3** Scheme of the BBS testing setup (Canestrari et al., 2014)

The BBS tests were performed on 48 binder-aggregate combinations by considering the following testing parameters:

- 2 aggregate substrates: limestone and porphyry;
- 4 binders with different bio-oil percentages: 0, 5, 10, 15 %;
- 3 aging levels of the binders: unaged, short-term aged, long-term aged;
- 2 types of conditioning: dry and wet.

For each combination 4 specimens were tested, allowing the calculation of the average POTS and the corresponding standard deviation value.

## 5.3 Results and discussion

### *5.3.1 Viscosity*

Figure 5.4 shows the results of the viscosity tests for the binder 50/70+A15, in unaged and aged (short-term and long-term) conditions. Six experimental points' series, each one corresponding to a specific testing temperature (80, 90, 105, 120, 135 or 150 °C), are plotted for each aging level as a function of the shear rate. Specifically, for each aging condition, the highest viscosity values are related to the lowest temperature investigated (80°C), whereas the lowest viscosity values refer to the highest temperature investigated (150°C). Note that at 150°C some data are missing, since shear rates higher than 200 $s^{-1}$ cannot be imposed with the equipment employed, and two different spindles were used (S28 for viscosities higher than 2000 mPa·s and S21 for viscosities lower than 2000 mPa·s). It can be observed that, regardless of the aging level, the viscosity is independent of the shear rate at all temperatures, suggesting a Newtonian behaviour for 50/70+A15. Analogous observations are valid also for the bio-binders containing lower bio-oil percentages (50/70+A5 and 50/70+A10) as well as for the control bitumen (50/70). Therefore, the viscosity value measured at a working rate of the viscometer equal to 50% can be reasonably considered for comparison purposes.

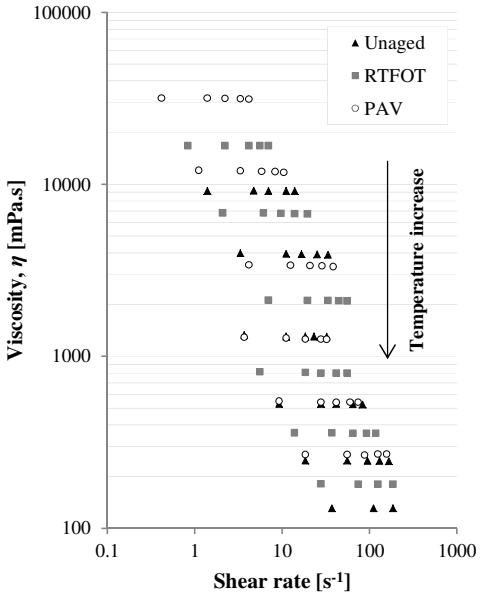


**Figure 5.4** Viscosity as a function of shear rate for 50/70+A15, at different aging levels

In Figure 5.5, for each binder the viscosity values obtained at 50% viscometer working rate are presented on the log(log$\eta$)-temperature diagram. In Section 3.4.5, it was already shown that, in unaged conditions, a viscosity reduction occurs with increasing bio-oil content (as in Figure 5.5 (a)), due to the softening effect provided by the bio-oil. Figures 5.5 (b) and 5.5 (c) confirm this effect also after short- and long-term aging, respectively. Comparing Figures 5.5 (a), 5.5 (b) and 5.5 (c), it can be also observed that the experimental points are progressively shifted towards higher values of log(log$\eta$) as the aging level of the binder increases, denoting the increase in viscosity due to aging.

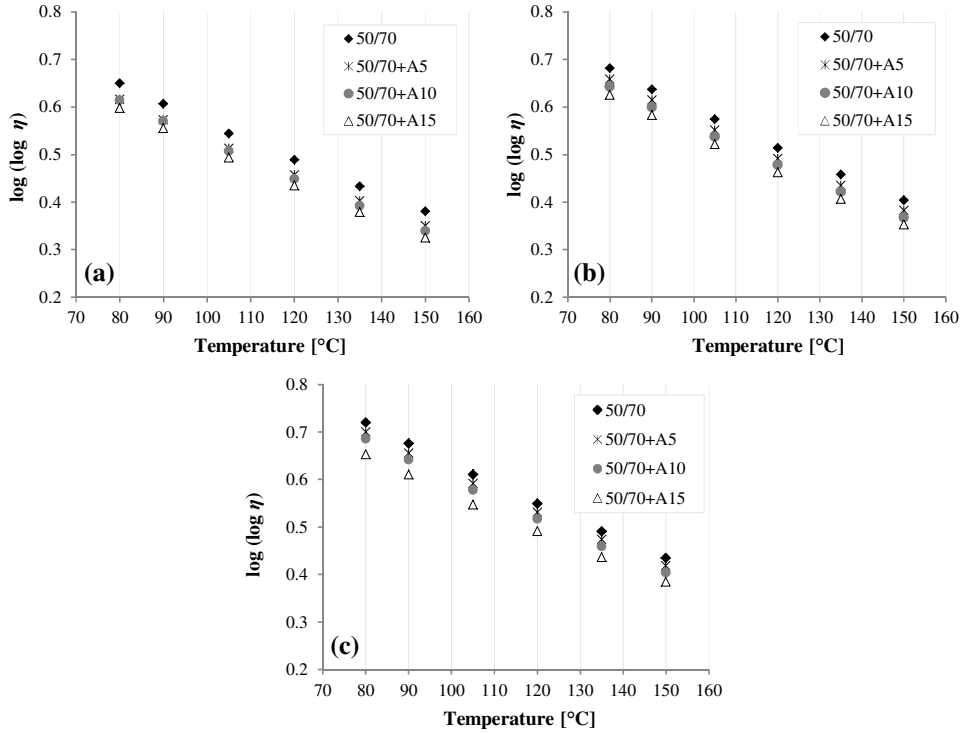


**Figure 5.5** Viscosity as a function of temperature for the binders tested, at different aging levels: (a) unaged, (b) RTFOT-aged, (c) PAV-aged

As can be noted from Figure 5.5, for each aging condition a linear regression can be adopted to identify the log(log$\eta$)-temperature relationship for all the binders:

$$\log(\log\eta) = RI + RS \cdot T \tag{5.1}$$

where $\eta$ is the viscosity (mPa·s), *RI* is the regression intercept, *RS* is the regression slope that reflects the temperature susceptibility and *T* is the temperature (°C). The results of the regression are given in Table 5.1, along with the correlation coefficients $R^2$. As can be observed, the value of *RI* tends to increase with the aging level and to decrease as the bio-oil content is increased, whereas *RS* does not exhibit any evident trend related to aging or bio-oil content. In addition, the high values of $R^2$ (very close to 1) indicate that BBS application temperatures ($T_{appl}$) can be effectively evaluated by considering Equation (5.1) and the regression parameters in Table 5.1.
In this regard, the viscosity value exhibited by the control bitumen 50/70 at 135°C (equal to 513.5 mPa·s) was considered as the reference to determine the BBS application temperatures for all binders. As can be seen from Table 5.1, the application temperatures range between 120°C for the least viscous binder (unaged 50/70+A15) and 150°C for the most viscous binder (long-term aged 50/70). In general, $T_{appl}$ is lower for higher bio-oil

amounts and increases with the aging level. It is worth pointing out that the same values of $T_{appl}$ were adopted for 50/70+A5 and 50/70+A10, as their viscosities did not differ considerably (see Figure 5.5). By considering the application temperatures in Table 5.1, it was possible to prepare the BBS specimens for all binders at comparable viscosity, similarly to the iso-stiffness condition recommended by Bahia et al. (2012).

**Table 5.1** Regression parameters and BBS application temperature

| Binder | Aging level | *RI* | *RS* | $R^2$ | $T_{appl}$ [°C] |
|---|---|---|---|---|---|
| 50/70 | Unaged | 0.9525 | -0.0038 | 0.9986 | 135 |
| | RTFOT | 0.9947 | -0.0040 | 0.9988 | 140 |
| | PAV | 1.0425 | -0.0041 | 0.9989 | 150 |
| 50/70+A5 | Unaged | 0.9148 | -0.0038 | 0.9988 | 125 |
| | RTFOT | 0.9698 | -0.0040 | 0.9987 | 135 |
| | PAV | 1.0181 | -0.0040 | 0.9988 | 145 |
| 50/70+A10 | Unaged | 0.9234 | -0.0039 | 0.9987 | 125 |
| | RTFOT | 0.9536 | -0.0039 | 0.9990 | 135 |
| | PAV | 1.0044 | -0.0040 | 0.9990 | 145 |
| 50/70+A15 | Unaged | 0.9063 | -0.0039 | 0.9990 | 120 |
| | RTFOT | 0.9338 | -0.0039 | 0.9990 | 130 |
| | PAV | 0.9548 | -0.0038 | 0.9984 | 135 |

### *5.3.2 BBS failure types*

Through the visual inspection of the aggregate surfaces and pull-stubs after the BBS test, three types of failure can be identified (Canestrari et al., 2010), as shown in Figure 5.6. The failure is considered purely cohesive when it occurs within the binder film, denoting that the binder-aggregate adhesion is stronger than the binder cohesion. In this case, the aggregate surface remains coated by bitumen after the test (Figure 5.6 (a)). A purely adhesive failure, instead, takes place at the interface between binder and aggregate and indicates that the cohesion within the binder is greater than the adhesion at the interface. When such failure occurs, the aggregate surface remains almost clean after the test (Figure 5.6 (b)). An intermediate failure, named hybrid failure and presenting the typical characteristics of both cohesive and adhesive mechanisms, is identified when the aggregate surface is partially coated by the binder and partially clean (Figure 5.6 (c)). Such failure may initially develop with a loss of adhesion at the weakest points of the interface; then, micro-cracks propagate within the binder film, resulting eventually in a cohesive failure. Thus, in this third case the failure mechanism is more complex.

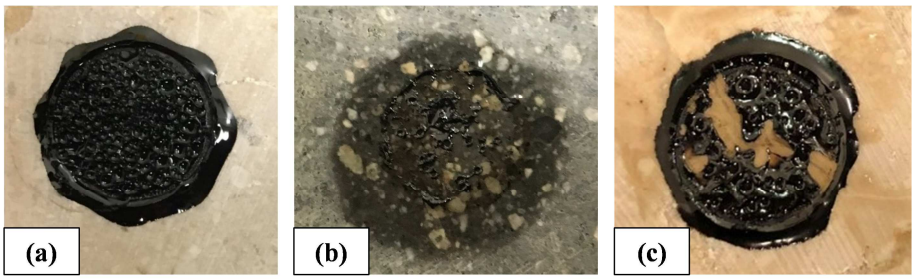


**Figure 5.6** BBS failure types: (a) cohesive failure, (b) adhesive failure, (c) hybrid failure

Table 5.2 presents the failure type observed for every binder-aggregate combination. Purely cohesive failures are coded as "C", purely adhesive failures as "A" and hybrid failures as "C/A". A C/A type was considered for the binder-aggregate combination also when part of the specimens of the combination showed cohesive failures whereas the rest exhibited adhesive failures.

**Table 5.2** Failure type for the binder-aggregate combinations studied

| Binder | Aging level | Conditioning | Failure type | |
|---|---|---|---|---|
| | | | Limestone | Porphyry |
| 50/70 | Unaged | Dry | C | C |
| | | Wet | C | A |
| | RTFOT | Dry | C | C |
| | | Wet | C | C/A |
| | PAV | Dry | C | C |
| | | Wet | C | A |
| 50/70+A5 | Unaged | Dry | C | C |
| | | Wet | C | C/A |
| | RTFOT | Dry | C | C |
| | | Wet | C | C/A |
| | PAV | Dry | C | C |
| | | Wet | C | C/A |
| 50/70+A10 | Unaged | Dry | C | C |
| | | Wet | C | C/A |
| | RTFOT | Dry | C | C |
| | | Wet | C | C/A |
| | PAV | Dry | C | C |
| | | Wet | C | C/A |
| 50/70+A15 | Unaged | Dry | C | C |
| | | Wet | C | C |
| | RTFOT | Dry | C | C |
| | | Wet | C | C |
| | PAV | Dry | C | C |
| | | Wet | C | C |

From the data reported in Table 5.2, it can be observed that all binders exhibit cohesive failures when limestone is considered as substrate, regardless of bio-oil content, aging level and type of conditioning. Conversely, in the case of porphyry, a cohesive failure is observed for all binders in dry conditions, whereas adhesive and hybrid failures are predominant in wet conditions, except for the 50/70+A15 binder that always shows cohesive failure. These results indicate that, even after the addition of the bio-oil, calcareous aggregates (such as limestone) have stronger affinity and adhesion with the binder as compared to siliceous aggregates (such as porphyry), especially in the presence of water.

The effect of the bio-oil on the failure type is quite evident when the systems with porphyry substrate are evaluated after wet conditioning. Indeed, the base bitumen 50/70 tends to exhibit purely adhesive failures, whereas the binder 50/70+A15, with the highest amount of bio-oil, shows purely cohesive failures at all aging conditions. When intermediate bio-oil contents are considered (i.e. 5 and 10 %), hybrid failures are observed. Therefore, a progressive transition from adhesive to cohesive failures is observed as the bio-oil percentage increases, meaning that the bio-oil might improve the bond at the interface between bitumen and substrate, especially in the case of aggregates with low affinity with bitumen and in the presence of water (see also Section 5.3.4).

A possible explanation of this phenomenon should be sought in the chemical peculiarities of the bio-oil and bio-binders investigated. The chemical analysis results presented in Sections 3.4.1 and 3.4.2 have shown that such bio-oil is characterized by a high content of resins and by the strong presence of ester functional groups. Therefore, its addition to bitumen leads to a noticeable increase in resins and, in general, in the polar fractions (sum of resins and asphaltenes). Moreover, the Fourier transform infrared spectroscopy (FTIR) analysis showed that the presence of esters in the bio-binders is identified by two peaks in the absorbance spectrum at 1735 and 1242 $cm^{-1}$, corresponding to the C=O and C-O stretch of esters. Esters are typically absent for conventional bitumens and become more prominent as the bio-oil percentage in the binder is increased. Then it was demonstrated that these observations remain valid also after short-term and long-term aging (Sections 4.3.2 and 4.3.3). In addition, it was found that the bio-oil addition provides, with respect to the control bitumen, a slight increase of the absorbance related to the C=O stretch of the carboxylic acids at 1700 $cm^{-1}$ in unaged conditions, but a significant reduction after short-term and long-term aging. Table 5.3 summarizes the above-mentioned results (taken from Sections 4.3.2 and 4.3.3), presenting the amount of resins and resins plus asphaltenes determined for the investigated binders through Iatroscan analysis (or TLC-FID) and three synthetic indices obtained from FTIR analysis. These indices quantify the absorption at 1700 $cm^{-1}$($I_{1700}$), 1735 $cm^{-1}$ ($I_{1735}$) and 1242 $cm^{-1}$ ($I_{1242}$).

**Table 5.3** Chemical characteristics of the binders studied

| Binder | Aging level | Iatroscan analysis | | FTIR analysis | | |
|---|---|---|---|---|---|---|
| | | Resins [%] | Res+Asph [%] | $I_{1700}$ | $I_{1735}$ | $I_{1242}$ |
| 50/70 | Unaged | 21.8 | 47.0 | 0.017 | 0.000 | 0.000 |
| | RTFOT | 26.3 | 50.5 | 0.037 | 0.000 | 0.000 |
| | PAV | 29.1 | 58.8 | 0.059 | 0.000 | 0.000 |
| 50/70+A5 | Unaged | 24.4 | 48.2 | 0.017 | 0.016 | 0.007 |
| | RTFOT | 28.4 | 53.7 | 0.025 | 0.016 | 0.006 |
| | PAV | 34.4 | 61.0 | 0.034 | 0.015 | 0.009 |
| 50/70+A10 | Unaged | 24.6 | 49.6 | 0.020 | 0.034 | 0.014 |
| | RTFOT | 29.6 | 54.9 | 0.022 | 0.037 | 0.015 |
| | PAV | 35.9 | 61.5 | 0.026 | 0.040 | 0.015 |
| 50/70+A15 | Unaged | 27.2 | 50.3 | 0.022 | 0.051 | 0.025 |
| | RTFOT | 29.5 | 56.2 | 0.024 | 0.059 | 0.024 |
| | PAV | 37.2 | 62.5 | 0.018 | 0.063 | 0.026 |

From Table 5.3, it is evident that the transition from adhesive to cohesive failures observed for porphyry substrates with increasing bio-oil content cannot be explained simply by the polar generic fractions obtained through Iatroscan analysis. Indeed, both the resins and the sum of resins and asphaltenes are increased by the bio-oil addition, but they are increased to an even higher extent by aging. For instance, the amount of resins (and resins plus asphaltenes) for 50/70 after long-term aging is greater than that for unaged 50/70+A15; however, the former exhibits a purely adhesive failure, whereas the latter a purely cohesive failure. Thus, it seems that the attention has to be focused on the nature and amount of the polar functional groups (determined through FTIR analysis), rather than on the amount of the polar fractions (determined through Iatroscan analysis).

In this regard, previous findings by Plancher et al. (1977) and Petersen and Plancher (1998) highlighted that the adhesion between bitumen and aggregate is mainly due to oxygen-containing compounds. Specifically, carboxylic acids are the compounds most strongly adsorbed by aggregates, but they are also the compounds that are most easily desorbed from the aggregate when affected by water. In addition, it was suggested that each aggregate has adsorption sites available for a limited number of binder molecules, and consequently different functional types compete with each other and are adsorbed selectively according to their relative concentration in the binder, as well as their affinity with the aggregate surface.

For the bio-binders examined, as the bio-oil amount is increased, carboxylic acids are reduced (especially after aging) while esters are increased, as shown by the values of $I_{1700}$, $I_{1735}$ and $I_{1242}$ in Table 5.3, and, as a consequence, esters might play a significant role in the adhesion mechanisms. In this sense, BBS results suggest that esters might be responsible for a good adhesion with aggregates in dry conditions and for a possible improved adhesion with siliceous aggregates in wet conditions as compared to carboxylic acids. However, these qualitative observations should be confirmed by further research.

It is worth underlining that the potential improvement of the adhesion between bitumen and aggregate due to the bio-oil seems consistent with previous findings reported by Bearsley and Haverkamp (2007b), who studied a bio-oil deriving from pinewood (named tall oil pitch), similar to the one examined in this research project. Specifically, they found that bituminous mixtures containing tall oil pitch exhibited higher tensile strength as compared to conventional mixtures both in dry and wet conditions as well as greater resistance to moisture damage, regardless of the type of aggregate employed in the mix. They also observed that tall oil pitch reduced the contact angle between bitumen and substrate in the presence of water, thus increasing the energy required for water to strip the bitumen from the substrate in terms of work of adhesion. However, a chemical characterization of the bio-binders explaining such results was not included in their investigation.
Finally, from Table 5.2, it should be noted that the aging level of the binder does not seem to affect the failure mechanism.

### *5.3.3 POTS values for dry specimens*

Figure 5.7 shows the POTS values obtained for all binder-aggregate systems tested in dry condition. In the plots, the error bars represent the standard deviation (n = 4). In dry conditions, a cohesive failure was observed for all binder-aggregate combinations, as already discussed in Section 5.3.2.
It can be noted that, as the aging level increases, a general increase in the POTS value emerges for all binder-aggregate combinations. The only exception is represented by 50/70+A15, which exhibits a slight POTS reduction in the transition from short-term to long-term aging. The increase of POTS values can be related to the hardening of the binder caused by aging.
Moreover, for dry specimens, a clear trend of POTS reduction with increasing bio-oil content is observed both on limestone and porphyry at all aging conditions (except for short-term aged binders on limestone substrate). These results can be explained by taking into account the softening effect provided by the bio-oil to bitumen.
In addition, from the comparison of limestone and porphyry substrates, comparable values of POTS are found for 10 out of 12 cases, with the only exceptions for the PAV-aged 50/70 and RTFOT-aged 50/70+A10.

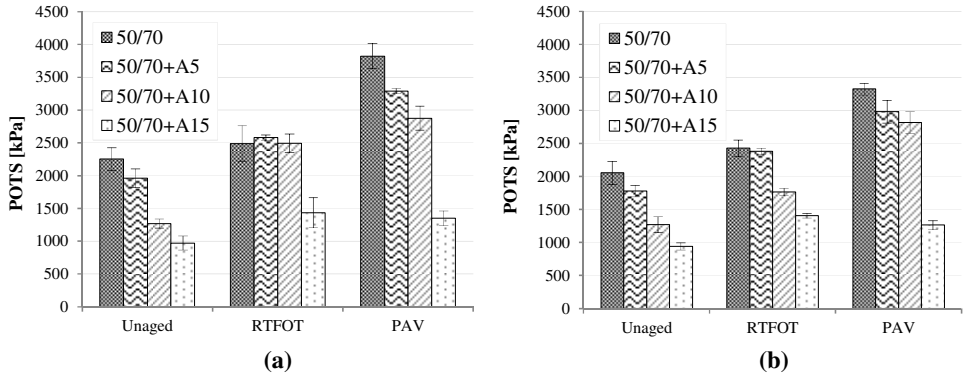


**Figure 5.7** POTS values for dry specimens: (a) limestone, (b) porphyry

The previous observations suggest that the strength of the system is mainly determined by the inner cohesion of the binder, regardless of the aggregate substrate. In this regard, Figure 5.8 demonstrates that there is a good correlation between the POTS obtained for dry specimens (average POTS values between systems with limestone and porphyry aggregate, Figures 5.7 (a) and 5.7 (b)) and the viscosity of the binders measured at 135°C (considered as a reference consistency measurement). This finding confirms how the viscosity of the binder plays a fundamental role in assessing the bond of the bitumen-aggregate interaction (Xiao and Amirkhanian, 2009).

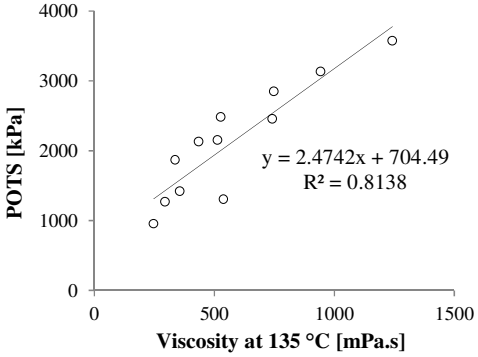


**Figure 5.8** POTS values for dry specimens vs. viscosity at 135°C

As regards the variability of the results, the POTS standard deviation ranges between 36 and 175 kPa for the binder-porphyry systems, whereas the binder-limestone systems show a slightly higher variability with a standard deviation ranging between 37 and 271 kPa. However, it should be emphasized that most of the tests (22 binder-aggregate combinations out of 24) show a standard deviation lower than 200 kPa, denoting a good test repeatability according to Canestrari et al. (2010). The good repeatability is also confirmed by the values of the coefficient of variation, determined as the percentage ratio between standard

deviation and average POTS, which is between 2 and 9 % for binder-porphyry systems and between 1 and 16 % for binder-limestone systems.

### *5.3.4 POTS values for wet specimens*

The POTS values obtained for the wet specimens on limestone and porphyry substrates are shown in Figures 5.9 (a) and 5.10 (a), respectively. In the plots, the error bars represent the standard deviation.
In order to quantify the effect of water, the Moisture Damage Index (MDI) was defined for each binder-aggregate system as the ratio between the POTS values obtained in wet and dry conditions:

$$MDI = \frac{POTS_{wet}}{POTS_{dry}} \tag{5.2}$$

Given this definition, a MDI equal to 1 means that water does not have any effect on the bond strength of the system, whereas a value less than 1 indicates a reduction of the strength due to water. MDI values calculated for limestone and porphyry substrates are presented in Figures 5.9 (b) and 5.10 (b), respectively.

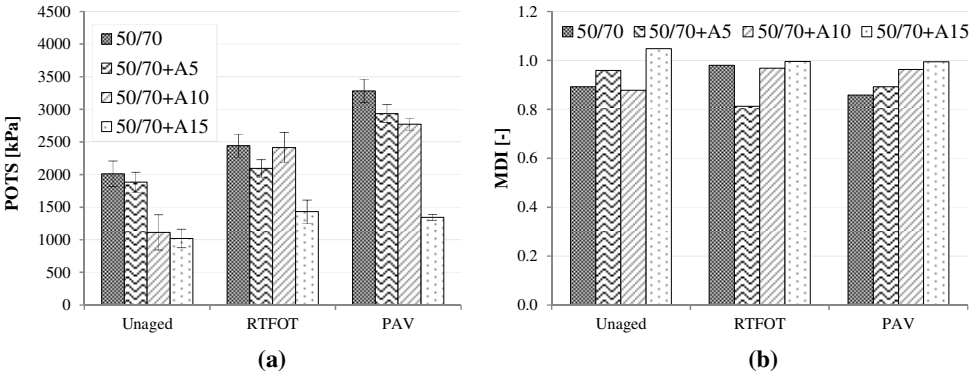


**Figure 5.9** Wet specimens with limestone: (a) POTS values with error bars, (b) Moisture Damage Index

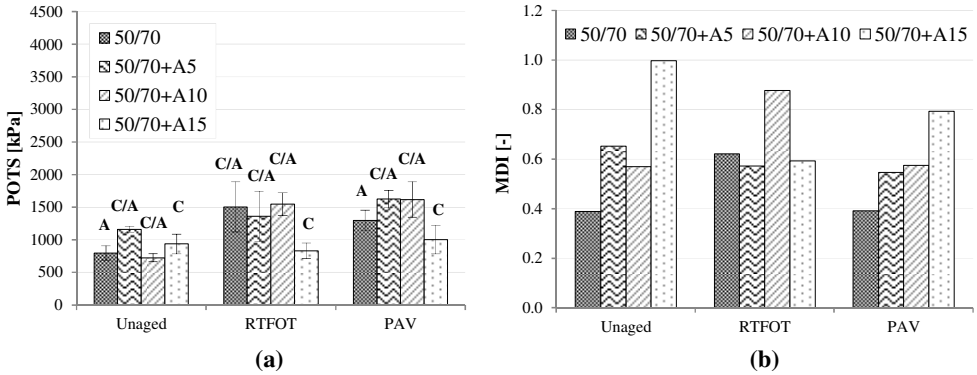


**Figure 5.10** Wet specimens with porphyry: (a) POTS values with error bars, (b) Moisture Damage Index

As can be seen from Figure 5.9 (a), for the limestone substrate in wet conditions, aging causes an increase in POTS whereas a higher bio-oil amount in the binder results in a lower POTS. These observations are analogous to those on the dry specimens (Section 5.3.3). Moreover, MDI is approximately between 0.8 and 1 for all binders and aging levels (it is even slightly higher than 1 for 50/70+A15), as shown in Figure 5.9 (b). This indicates that the POTS reduction caused by the water conditioning does not seem to exceed 20%. Since the systems continue to show only cohesive failures after water conditioning (see Section 5.3.2), the small reduction of the POTS is probably caused by an emulsification process, through which the water weakens the cohesive bonds within the binder film (Canestrari et al., 2010; Fromm, 1974). No clear effects of the aging condition on the MDI can be identified, while the increase in the bio-oil amount seems to lead, in general, to higher MDI values.

As for the results obtained on porphyry substrate for wet specimens (Figure 5.10 (a)), the POTS values should be interpreted by considering the combined effect of failure type (indicated in the figure) and binder consistency. Indeed, it can be noted that, despite being characterized by cohesive failure, because of its lower consistency, the binder 50/70+A15 tends to show comparable POTS values with respect to the base bitumen 50/70 that exhibits mainly adhesive failures instead. Given the different failure types, similar POTS values indicate that the adhesive bond between 50/70+A15 and substrate is greater than that between 50/70 and substrate. In addition, a general increase in the POTS can be observed as the aging level increases, especially when unaged and short-term aged binders are compared. However, this is less evident when comparing short-term aged and long-term aged binders. In terms of moisture damage, Figure 5.10 (b) shows that, when porphyry is considered as substrate, MDI significantly drops (reaching also the value of 0.4). It should be noted that the lowest MDI values are yielded by the base bitumen (50/70), which tends to exhibit adhesive failures (Section 5.3.2). Instead the binder 50/70+A15, which is always characterized by cohesive failures (see Section 5.3.2), tends to display the highest MDI values, especially in unaged and long-term aged conditions. Intermediate values of MDI are observed when hybrid failures occur, as in the case of 50/70+A5 and 50/70+A10. These outcomes indicate that the most significant reduction of the bond strength is associated to

adhesive failures, namely when water is able to weaken the adhesive bond at the interface between the binder and the aggregate, as in the case of the base bitumen 50/70. On the contrary, the lowest POTS reductions are related to cohesive failures (as for 50/70+A15), for which the emulsification action of water prevails. Such results suggest that, as the bio-oil content increases, the negative effects of water on POTS are reduced, probably thanks to the improved adhesion between binder and aggregate.
Finally, it should be pointed out that the moisture susceptibility observed also depends on the adopted protocol for the wet conditioning. Moreover, for a better understanding of the adhesive/cohesive properties of bio-binder/aggregate systems, the failure types and the POTS values observed for the bio-binders should be compared with those obtained for conventional bitumens having similar penetration grade (i.e. similar consistency).
In terms of variability of the results, for the wet specimens the POTS standard deviation ranges between 42 and 271 kPa for the binder-limestone systems and between 47 and 385 kPa for the binder-porphyry systems. Instead the coefficient of variation is between 3 and 24 % (only in one isolated case) for the systems with limestone and between 4 and 28 % for the systems with porphyry. Similarly to dry conditioning, a good test repeatability was achieved for the wet specimens, considering that in 18 out of 24 cases the standard deviation was lower than 200 kPa (Canestrari et al., 2010) and the coefficient of variation was lower than 15%. However, in the case of porphyry substrate, the wet specimens show a higher variability of the results with respect to the dry specimens. The slight increase in variability may be imputable to the different failure types occurring in wet conditions, as the highest standard deviation and coefficient of variation values are observed for hybrid failures, which are characterized by a complex failure mechanism (as explained in Section 5.3.2).

## 5.4 Summary of the findings

This part of the research project aimed at evaluating the bond strength between bio-binders and aggregate substrates. The bio-binders were obtained by partially replacing a conventional 50/70 bitumen with different percentages of a wood-based bio-oil (5, 10 and 15 %) and studied at different aging conditions (unaged, short-term aged and long-term aged). Limestone and porphyry aggregates were selected as solid substrates. All binder-aggregate systems were investigated by carrying out BBS tests, after both dry and wet conditioning. Viscosity measurements were also performed to assess the consistency of the binders.
Based on the results and discussion provided, the following conclusions can be drawn:

- all the bio-binders showed a Newtonian behaviour at the temperatures examined. The increase in the bio-oil amount resulted in a progressive viscosity reduction at all aging conditions;
- most binder-aggregate systems displayed purely cohesive failure under the different testing conditions, implying good affinity between the studied bio-binders and aggregates;

- all dry specimens were characterized by cohesive failures, and a direct relationship was observed between the POTS and the consistency (viscosity) of the binder, regardless of the type of aggregate;
- high moisture damage, shown by adhesive or hybrid failures associated to high POTS reduction, was found for the systems with porphyry. However, a progressive transition from adhesive to cohesive failures and a more moderate POTS reduction were observed with the increase in the bio-oil content, suggesting that the bio-oil might improve the bond strength between bitumen and siliceous aggregates in the presence of water;
- the strong presence of esters in the bio-oil is supposed to play a significant role in contributing to the adhesion between bio-binders and aggregates.

It is worth pointing out that the moisture sensitivity observed is dependent on the adopted wet conditioning protocol and, for a better understanding of the adhesive/cohesive properties of bio-binder/aggregate systems, conventional bitumens having similar penetration grade (i.e. similar consistency) to that of the bio-binders should also be tested for comparison.

Overall, these findings indicate that the use of the studied bio-oil as partial replacement of bitumen does not penalize the adhesive bond as well as the moisture sensitivity of binder-aggregate systems, but, on the contrary, it seems to even improve the adhesion in the presence of water when aggregates having a low affinity with bitumen are used. Therefore, the use of such bio-binders in road pavements could lead to significant benefits in terms of performance and durability.

# 6. “Circular propensity” of bio-binders

## 6.1 Background and objectives

The progress in hot recycling technologies is allowing the production of new hot asphalt mixtures containing extremely high percentages of reclaimed asphalt (RA) without negatively affecting the performance (Zaumanis and Mallick, 2015; Zaumanis et al., 2014a; Zaumanis et al., 2014b). RA, which derives from the milling of asphalt pavements at the end of their service life, is a very valuable material and, in hot recycling, the aged bitumen can be reactivated, at least partially (Lo Presti et al., 2020). The reuse of RA promotes the principles of sustainability and circular economy, by reducing the consumption of new non-renewable raw materials and the disposal of wastes, exactly as in the case of bio-binders.

The combined use of bio-binders and RA, both composed of used/end-of-life materials, may potentially result in sustainable asphalt mixtures with superior performance. Some bio-oils have been already studied as possible rejuvenators for RA (Behnood, 2019; Cavalli et al., 2018a; Gong et al., 2016; Kowalski et al., 2017). However, to date, there are still uncertainties on the most suitable rejuvenator addition location in the asphalt plant, and some ad-hoc modification to the plant may also be necessary (Behnood, 2019; Lu et al., 2019b; Zaumanis et al., 2019). A different employment for bio-oils in hot recycling might be to produce and store the bio-binder, by pre-blending bitumen and bio-oil. In this way, the issue of introducing the bio-based material in the production process could be easily overcome, provided that the stored bio-binder does not have problems in terms of storage stability. As shown in Section 3.4.3 and by previous findings by Abdullahi Ahmad et al. (2017), He et al. (2019) and Zhang et al. (2018a), this is generally true for bio-oil contents lower than 20–25 % and normal storage temperatures (except in the presence of modifiers like polymers or crumb rubber).

At the same time, as anticipated in Sections 2.2.1 and 2.5, to ensure a wide market acceptance of bio-binders, it is essential – in a long-term perspective – to verify also if asphalt mixtures containing bio-binders can be 100% recycled at the end of their service life, as normally happens for traditional mixtures. Nevertheless, to date, no study has focused on the recyclability of bio-asphalt mixtures.

Within this framework, this part of the research project had two main objectives: 1) to assess the effectiveness of bio-binders in the hot recycling of bitumen recovered from a typical RA, and 2) to evaluate, in a long-term perspective, the recyclability potential of bio-binders. For this purpose, two severely aged binders (one “RAP” binder recovered from reclaimed asphalt and one laboratory-produced “Bio-RAP” binder) and two fresh binders (one bio-binder and one bitumen) were blended to simulate four binders resulting from the hot recycling of asphalt. In order to investigate also their aging susceptibility, the blends were short-term and long-term aged in the laboratory. All binders were subjected to mechanical tests (including conventional tests as well as rheological testing and modelling) and chemical analysis (Fourier transform infrared spectroscopy).

The results provided in the following sections are published in Ingrassia et al. (2020b).

## 6.2 Materials and methods

### *6.2.1 Base binders and control bitumen*

In order to reproduce in the laboratory the binder resulting from the hot recycling of asphalt, two severely aged binders were considered. The first one, coded as "RAP", was recovered according to EN 12697-3 (2018) from a typical reclaimed asphalt, taken from a milled pavement at the end of its service life (more than 20 years). The second one, coded as "Bio-RAP", was artificially aged in the laboratory by subjecting the bio-binder A (described below) to one Rolling Thin Film Oven Test (RTFOT) (EN 12607-1, 2015) and two consecutive Pressure Aging Vessel (PAV) conditionings (EN 14769, 2013) (i.e. 40 hours PAV). Indeed, according to several studies (Bowers et al., 2014; Samieadel et al., 2018b; Zadshir et al., 2018), such procedure allows to prepare a reliable artificial RA in the laboratory. This approach was necessary for producing RA deriving from a bio-binder (bio-RA), because no asphalt pavement containing bio-binders had been in service for a sufficiently long period of time when this study was carried out. It is worth noting that the RAP binder was harder, stiffer and more elastic than the Bio-RAP binder (Table 6.1 and Figure 6.1). These differences were properly considered in the materials preparation.
Moreover, the study included two different fresh binders to be combined with RAP and Bio-RAP: a bio-binder "A" composed of 10% by weight of wood-based bio-oil, and a bitumen "B" having physical and mechanical properties similar to A (Table 6.1 and Figure 6.1), both characterized by a penetration of 120 dmm (basically, the same bio-binder and bitumen studied and compared in Section 4).
In addition, one bitumen, coded as "Control" and having intermediate mechanical properties between the aged binders (RAP and Bio-RAP) and the fresh ones (A and B) (Table 6.1 and Figure 6.1), was added to the investigation as a commonly used virgin bitumen, with the aim of comparing its mechanical behaviour and aging susceptibility with those of the recycled blends.

**Table 6.1** Penetration and softening point of the base binders and the Control bitumen

| Binder | Penetration [dmm] | Softening point [°C] |
|---|---|---|
| RAP | 19 | 65.8 |
| Bio-RAP | 27 | 61.6 |
| A | 120 | 45.3 |
| B | 120 | 45.0 |
| Control | 55 | 52.4 |

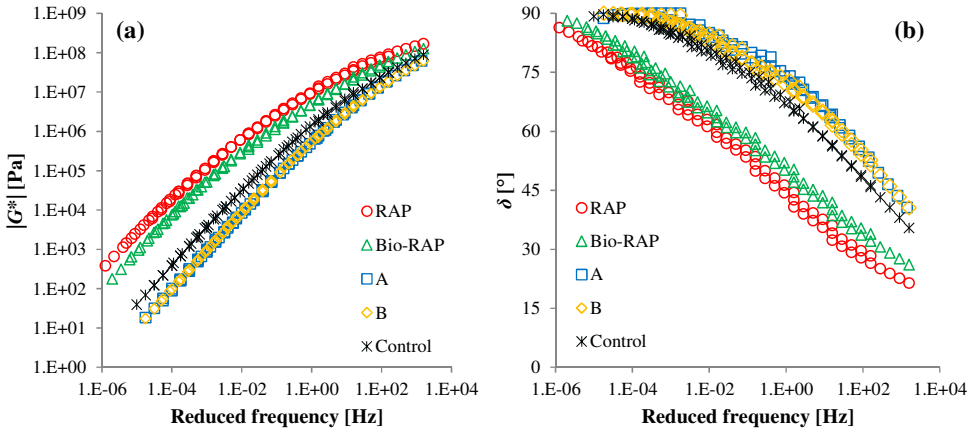


**Figure 6.1** Master curves of (a) complex modulus and (b) phase angle for the base binders and the Control bitumen, at a reference temperature of 20°C

### *6.2.2 Recycled blends*

The base binders (RAP, Bio-RAP, A and B) were combined according to appropriate proportions to prepare four blends (Table 6.2) having physical-mechanical properties similar to each other and comparable to the Control bitumen (see Section 6.3). After pre-heating the base binders at 160°C (similarly to the temperatures usually adopted for hot recycling), the blends were produced by means of a laboratory mixer (Figure 6.2), considering a mixing speed of 500 rpm for 10 min.

A brief description of the recycled blends is provided in Table 6.2. Among the blends produced, B+RAP can be considered a sort of reference, as it represents the binder of a typical hot recycled asphalt mixture. The blend A+bio-RAP allows to evaluate, in a long-term perspective, the actual bio-binders' recyclability potential, whereas the blend A+RAP is useful to assess the effectiveness of bio-binders in hot recycling of bitumen. Finally, the blend B+bio-RAP represents an intermediate situation, opposite to that of A+RAP.

**Table 6.2** Recycled blends produced

| Blend | Composition (by weight) | Description |
|---|---|---|
| A+RAP | 71% A + 29% RAP | Recycled binder formed by a severely aged bitumen blended with a fresh bio-binder |
| B+RAP | 71% B + 29% RAP | Recycled binder in which the aged and the fresh binders are composed of 100% bitumen |
| A+bio-RAP | 62% A + 38% Bio-RAP | Recycled binder in which the aged and the fresh binders are bio-based (both contain 10% by weight of wood bio-oil) |
| B+bio-RAP | 62% B + 38% Bio-RAP | Recycled binder formed by a severely aged bio-binder blended with a fresh bitumen |


**Figure 6.2** Laboratory mixer used to prepare the recycled blends

It is worth noting that the blends studied (Table 6.2) reproduce the binders of recycled asphalt mixtures with high reclaimed asphalt content. Indeed, the correspondence between the composition of the blends shown in Table 6.2 and the RA content in the recycled mixture can be evaluated through Equation (6.1) (Jiménez del Barco Carrión et al., 2017c).

$$RA\ in\ the\ recycled\ mixture\ (\%) = 100 \cdot \frac{RVB \cdot DB\ content}{RAb\ content \cdot DOB} \tag{6.1}$$

where *RVB* is the replaced virgin binder, i.e. the percentage of fresh binder in the recycled mixture that is replaced by the RA binder (29% for A+RAP and B+RAP, 38% for A+bio-RAP and B+bio-RAP); *DB content* is the designed binder content in the recycled mixture, given by fresh binder plus reactivated RA binder (fixed equal to a typical value of 5% in the calculation); *RAb content* is the binder content in the RA (fixed equal to a typical value of 4% in the calculation); *DOB* is the degree of blending between the RA binder and the fresh binder (assumed equal to 70%, i.e. partial blending, according to Jiménez del Barco Carrión et al. (2017), Shirodkar et al. (2011) and Stimilli et al. (2015)). Consequently, the blends A+RAP and B+RAP represent mixtures containing about 50% RA by weight, whereas the blends A+bio-RAP and B+bio-RAP are representative of mixtures containing about 70% RA by weight.

The four blends (Table 6.2) were short-term (RTFOT) and long-term (PAV) aged, in order to reproduce the binder properties immediately after laying of hot recycled asphalt and after 10-15 years of in-service life of hot recycled asphalt, respectively.

Therefore, nineteen binders were studied overall, including the four base binders, the four blends at three different aging levels as well as the Control bitumen at three aging levels.

### *6.2.3 Mechanical tests*

The mechanical properties of the binders were investigated through conventional and rheological tests.
The conventional properties, i.e. penetration and softening point, were assessed according to EN 1426 (2015) and EN 1427 (2015), respectively.
The rheological properties were studied through frequency sweep tests at different temperatures with a dynamic shear rheometer (DSR) in plate-plate configuration using 8 mm and 25 mm geometry, according to EN 14770 (2012). The testing conditions were the same adopted in the previous experimental phases (Sections 3 and 4), namely the norm of the complex modulus $|G^*|$ and the phase angle $\delta$ were determined at temperatures ranging from 0 to 80 °C with a step of 10°C, increasing the frequency from 1 to 100 rad/s (i.e. from 0.159 to 15.9 Hz) with a fixed logarithmic step. All tests were carried out at a low shear strain of 0.05%, in order to study the behaviour of the binders in the linear viscoelastic (LVE) domain. At least two specimens were tested for each binder.
The master curves of $|G^*|$ and $\delta$ were developed by shifting the experimental data in the frequency domain at 20°C, which was chosen as reference temperature ($T_{ref}$). The temperature-dependency of the shift factors was modelled according to the Williams-Landel-Ferry (WLF) law (Williams et al., 1955), as in Equation (3.8).
The complex modulus master curve was then modelled through the modified Christensen-Anderson-Marasteanu (CAM) model (Bahia et al., 2001), defined as in Equation (6.2) in the case of bituminous binders.

$$|G^*(f)| = \frac{G_g}{\left[1 + \left(\frac{f_c}{f}\right)^k\right]^{\frac{m_e}{k}}} \tag{6.2}$$

where $f$ is the reduced frequency, $G_g$ is the glassy modulus (i.e. the value of the complex modulus for $f \to \infty$), $f_c$ is the crossover frequency (i.e. the frequency at which the storage modulus $G_1$ and the loss modulus $G_2$ are approximately equal), $k$ and $m_e$ are dimensionless shape parameters. The distance between $G_g$ and $|G^*(f_c)|$ is the so-called rheological index $R$, whose expression is as in Equation (6.3) in the case of bituminous binders.

$$R = \frac{m_e}{k} \log 2 \tag{6.3}$$

In the modelling procedure, $G_g$ was fixed equal to $10^9$ Pa based on literature suggestions (Anderson et al., 1994), whereas the parameters $f_c$, $k$ and $m_e$ (and consequently $R$) were determined by minimizing the error between model and experimental data, with the aim of achieving the best fitting.
In addition, the rheological behaviour at typical high service temperatures (60, 70 and 80 °C) was further investigated in terms of permanent deformation resistance through multiple stress creep and recovery (MSCR) tests, performed with the DSR with the 25 mm plate-plate geometry (with 1 mm gap), according to EN 16659 (2015). At each testing temperature, two consecutive shear stress levels were considered, 0.1 and 3.2 kPa. The

single stress level involved the application of 10 creep and recovery cycles, each one consisting in 1 s of loading and 9 s of recovery (without any load). The non-recoverable creep compliance $J_{nr}$ and the percent strain recovery $\%R$ were determined for each binder, by testing at least two specimens. The non-recoverable creep compliance is the residual strain in the specimen after a creep and recovery cycle divided by the stress applied and is an indicator of the sensitivity to permanent deformation. The percent recovery is the recovered strain in the specimen during the recovery portion of a cycle, expressed in percent, and thus it is related to the elastic response of the binder. For a given specimen, $J_{nr\ 0.1}$ and $J_{nr\ 3.2}$ were calculated as the average of the values obtained for each of the 10 creep and recovery cycles at 0.1 kPa and 3.2 kPa, respectively. Analogously, for every specimen, $\%R_{\ 0.1}$ and $\%R_{\ 3.2}$ were calculated as the average of the values obtained for each of the 10 creep and recovery cycles at 0.1 kPa and 3.2 kPa, respectively.

### *6.2.4 Chemical analysis*

The chemical characteristics of the binders were investigated through Fourier transform infrared (FTIR) spectroscopy in transmission mode (Marsac et al., 2014). The specimens were prepared by dissolving the binder in chloroform ($CHCl_3$). This solution was spread on sodium chloride (NaCl) plates and then the solvent was evaporated, in order to have a very thin binder film to be analysed. The transmittance/absorbance was evaluated at ambient temperature for wavenumbers between 500 and 4000 $cm^{-1}$ with a resolution of 4 $cm^{-1}$, and each spectrum was obtained as the average of 16 consecutive scans on the specimen. For each binder, at least three specimens were tested and then the average spectrum was determined. The spectral analysis was carried out with an integration method consisting in the calculation of the areas under the most significant peaks by means of a tangential approach (Hofko et al., 2017). The FTIR tests were carried out at Università Politecnica delle Marche in the laboratories of the Department of Materials, Environmental Science and Urban Planning (SIMAU).

## 6.3 Results and analyses

### *6.3.1 Conventional properties*

The penetration and softening point data are summarized in Table 6.3. It can be observed that the conventional properties of the four recycled blends are very similar at all aging levels. In terms of penetration and softening point, the Control bitumen seems slightly harder than the recycled blends in unaged conditions, but this difference tends to become smaller as aging increases. In general, the results in Table 6.3 indicate that the recycled blends and the Control bitumen are characterized by similar grade, which makes their comparison reasonable. The effect of aging emerges, as expected, as a penetration decrease and softening point increase due to the binder hardening.

Nevertheless, it is worth noting that a more reliable comparison between the binders in terms of mechanical behaviour as well as aging susceptibility can be made by considering the results of the rheological and chemical tests, presented in the following sections.

Table 6.3 Penetration and softening point of the recycled blends and the Control bitumen

| Aging level | Binder | Penetration [dmm] | Softening point [°C] |
|---|---|---|---|
| Unaged | A+RAP | 64 | 50.1 |
| | B+RAP | 65 | 50.2 |
| | A+bio-RAP | 60 | 50.4 |
| | B+bio-RAP | 61 | 50.2 |
| | Control | 55 | 52.4 |
| RTFOT | A+RAP | 47 | 55.7 |
| | B+RAP | 43 | 54.8 |
| | A+bio-RAP | 45 | 54.7 |
| | B+bio-RAP | 47 | 55.4 |
| | Control | 35 | 55.7 |
| PAV | A+RAP | 25 | 61.6 |
| | B+RAP | 25 | 62.5 |
| | A+bio-RAP | 24 | 62.2 |
| | B+bio-RAP | 28 | 62.9 |
| | Control | 25 | 63.0 |

### *6.3.2 Master curves*

Figures 6.3, 6.4 and 6.5 show the master curves of complex modulus $|G^*|$ and phase angle $\delta$ (experimental data) for the recycled blends and the Control bitumen in unaged, short-term aged and long-term aged conditions, respectively. In general, the rheological behaviour of the binders is comparable at all aging levels. From the comparison between Figures 6.3, 6.4 and 6.5, it can be observed that for all binders the effect of aging results in increased complex modulus and decreased phase angle, meaning that the stiffness and the elasticity of the binders increase with aging (as expected). It is also important to notice that the Control bitumen seems the binder that undergoes the most significant rheological changes due to the aging process ($|G^*|$ increase and $\delta$ reduction). This finding is in contrast with what emerged from the conventional tests, suggesting that the latter may not be sufficiently reliable to examine the mechanical behaviour and aging susceptibility of bituminous binders. It should be noted also that all binders are thermo-rheologically simple (including the ones that contain the bio-oil), as perfectly continuous $|G^*|$ and $\delta$ master curves can be obtained by using the same shift factors (Yusoff et al., 2011).

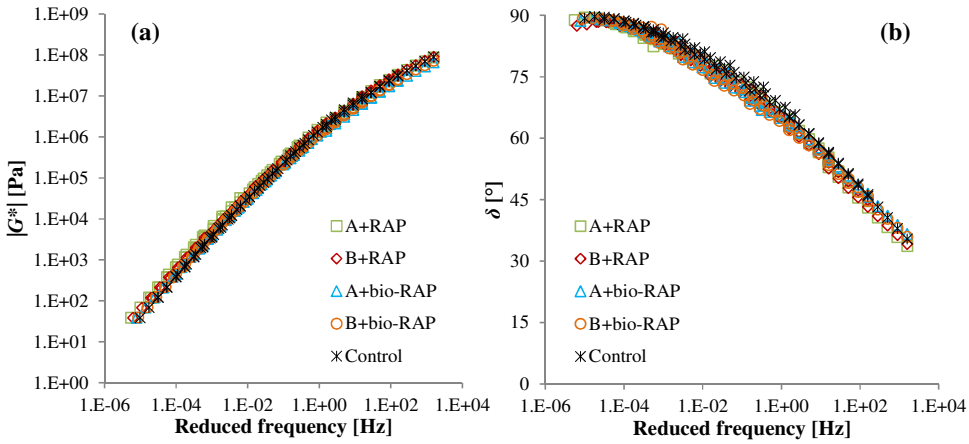


**Figure 6.3** Master curves of (a) complex modulus and (b) phase angle for the unaged recycled blends and Control bitumen, at a reference temperature of 20°C

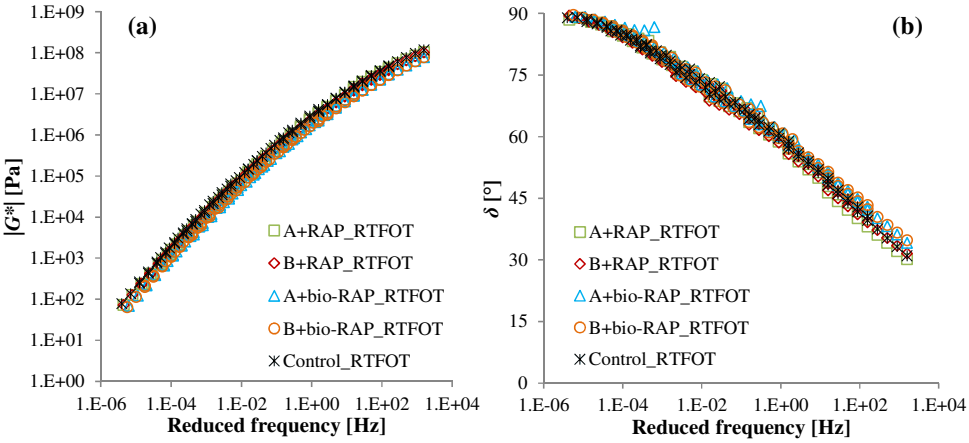


**Figure 6.4** Master curves of (a) complex modulus and (b) phase angle for the short-term aged recycled blends and Control bitumen, at a reference temperature of 20°C

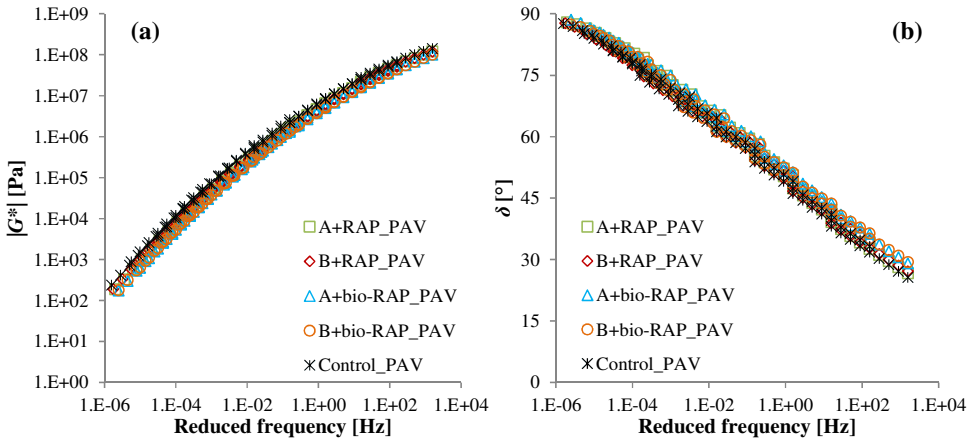


**Figure 6.5** Master curves of (a) complex modulus and (b) phase angle for the long-term aged recycled blends and Control bitumen, at a reference temperature of 20°C

In order to better compare the rheological behaviour of the binders, the parameters deriving from the modelling of the complex modulus master curves can be considered. As an example of the model fitting to the experimental data, Figure 6.6 shows the $|G^*|$ master curve for A+bio-RAP at different aging levels. The figure depicts more clearly the increase of $|G^*|$ due to aging.

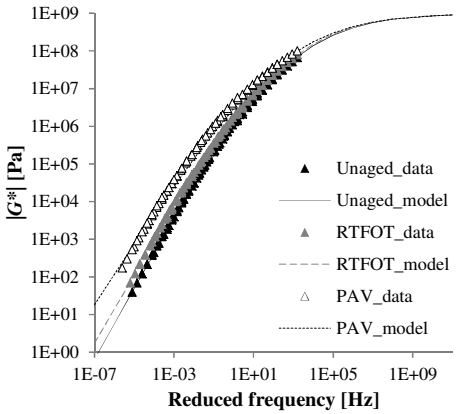


**Figure 6.6** Complex modulus master curve at 20°C for A+bio-RAP at different aging levels (experimental data and modified CAM model)

Table 6.4 summarizes the modified CAM and WLF parameters obtained from the modelling. In terms of modified CAM parameters, aging causes a general reduction of $f_c$ (which does not emerge, however, after RTFOT) and $m_e$ as well as a slight decrease of $k$. Consequently, $R$ decreases with aging as well. Based on the physical meaning of these parameters (Bahia et al., 2001), the reduction of the crossover frequency $f_c$ indicates greater

elastic component in the binder behaviour, while the decrement of the rheological index $R$ denotes a more rapid transition from the elastic to the viscous behaviour (in fact, a hypothetical $R$ value equal to zero would indicate a sudden transition between perfectly elastic and purely viscous behaviour). As for the WLF parameters, greater $C_1$ and $C_2$ values are observed for higher aging levels, suggesting a reduced molecular mobility. All these aging-related trends are in line with previous findings by Mazzoni et al. (2018), who studied the influence of different rejuvenators on the aging of hot recycled asphalt binders. It is worth noting that the variation of the parameters due to aging is more evident in the case of the Control bitumen, denoting a possible greater aging susceptibility (in accordance with the observations made from the comparison between Figures 6.3, 6.4 and 6.5), once again in contrast with the outcomes of the conventional tests.
Since the RAP binder is stiffer and more elastic than the Bio-RAP binder (Figure 6.1), it exhibits lower $f_c$, $m_e$ and $R$ as well as higher $C_1$ and $C_2$ than Bio-RAP. Conversely, the parameters are almost the same for the bio-binder A and the conventional bitumen B, as their rheological behaviour is basically identical (Figure 6.1). When the same aging level is considered, in general, all the recycled blends and the Control bitumen exhibit comparable modified CAM and WLF parameters, confirming the similarity of the master curves noticed from Figures 6.3, 6.4 and 6.5. More in detail, for the blends containing Bio-RAP as aged binder, $R$ tends to be higher, while $C_1$ and $C_2$ tend to be lower, as compared to the other blends and the Control bitumen. Finally, $f_c$ seems to be mainly affected by the long-term aging rather than by the material type.

**Table 6.4** Modified CAM and WLF parameters

| Binder | $f_c$ [Hz] | $k$ | $m_e$ | $R$ | $C_1$ | $C_2$ |
|---|---|---|---|---|---|---|
| RAP | 200 | 0.21 | 0.75 | 1.08 | 39 | 382 |
| Bio-RAP | 300 | 0.21 | 0.79 | 1.14 | 31 | 307 |
| A | 400 | 0.22 | 1.06 | 1.48 | 16 | 181 |
| B | 400 | 0.21 | 1.06 | 1.51 | 15 | 171 |
| A+RAP | 350 | 0.22 | 0.95 | 1.33 | 22 | 228 |
| A+RAP_RTFOT | 350 | 0.21 | 0.89 | 1.28 | 24 | 248 |
| A+RAP_PAV | 250 | 0.20 | 0.80 | 1.20 | 32 | 323 |
| B+RAP | 350 | 0.22 | 0.95 | 1.30 | 21 | 220 |
| B+RAP_RTFOT | 350 | 0.21 | 0.89 | 1.25 | 24 | 248 |
| B+RAP_PAV | 250 | 0.20 | 0.80 | 1.20 | 35 | 348 |
| A+bio-RAP | 350 | 0.20 | 0.96 | 1.44 | 20 | 215 |
| A+bio-RAP_RTFOT | 350 | 0.20 | 0.92 | 1.38 | 22 | 239 |
| A+bio-RAP_PAV | 250 | 0.19 | 0.82 | 1.30 | 30 | 303 |
| B+bio-RAP | 350 | 0.21 | 0.96 | 1.41 | 19 | 206 |
| B+bio-RAP_RTFOT | 350 | 0.20 | 0.90 | 1.35 | 23 | 242 |
| B+bio-RAP_PAV | 250 | 0.19 | 0.82 | 1.30 | 30 | 303 |
| Control | 350 | 0.22 | 0.97 | 1.33 | 19 | 203 |
| Control_RTFOT | 350 | 0.21 | 0.89 | 1.20 | 25 | 257 |
| Control_PAV | 250 | 0.21 | 0.78 | 1.11 | 35 | 344 |

### *6.3.3 Fatigue parameter*

In order to evaluate the fatigue behaviour of the binders, the rheological data were elaborated to determine the Superpave fatigue parameter $|G^*|\sin\delta$ (Kennedy et al., 1994). The parameter was calculated at the reference frequency of 10 rad/s (1.59 Hz) and at 20°C, which was selected as a representative intermediate service temperature (Figure 6.7). It should be recalled that a maximum limiting value of 5000 kPa is set for $|G^*|\sin\delta$ after PAV aging.

From Figure 6.7 (a), it can be observed that the fresh binders A and B exhibit almost identical values of $|G^*|\sin\delta$, which are relatively low due to their high penetration grade (see Table 6.1). Moreover, as expected, the RAP binder shows a higher $|G^*|\sin\delta$ value as compared to the Bio-RAP binder.

As for the comparison between the recycled blends, Figure 6.7 (b) shows that, at all aging levels, the blends containing Bio-RAP as aged binder are characterized by lower values of $|G^*|\sin\delta$ with respect to the blends containing RAP. Instead, the effect of the fresh binder type (A or B) is not very evident. Moreover, the Control bitumen exhibits higher $|G^*|\sin\delta$ values than the recycled blends, especially after aging, suggesting a possible faster aging rate (it is the only binder that does not meet the limit of 5000 kPa after PAV). These observations are generally in line with the results of rheological testing and modelling presented in Section 6.3.2.

The meaning of these results in terms of performance is discussed more in depth after the analysis of the aging susceptibility of the binders in Section 6.3.6.

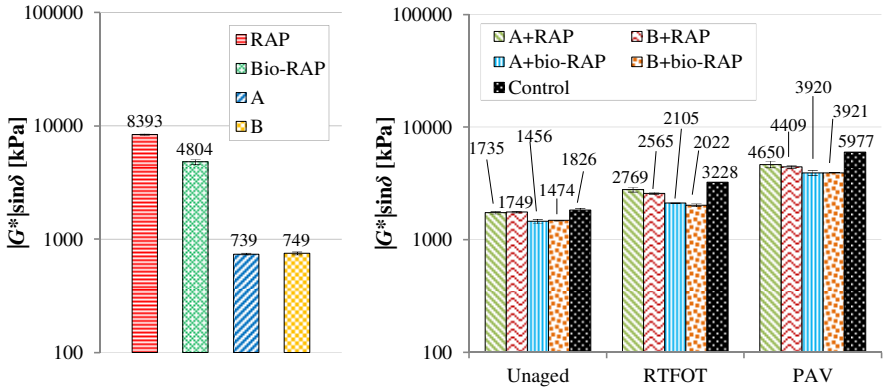


**Figure 6.7** Fatigue parameter at 20°C and 10 rad/s for (a) base binders, (b) recycled blends and Control bitumen at different aging levels

### *6.3.4 Non-recoverable creep compliance and percent strain recovery*

The values of the non-recoverable creep compliance ($J_{nr}$) obtained at 70°C and 3.2 kPa are shown in Figure 6.8, whereas Figure 6.9 displays the values of the percent strain recovery (*%R*) calculated at the same temperature and stress level.

Firstly, it can be noted that – as expected – aging causes a reduction of $J_{nr}$ and a simultaneous increase of *%R*. In fact, as already discussed in Section 6.3.2, the binder becomes stiffer and more elastic with aging, thus exhibiting lower deformability and higher recovery capability. In general, lower $J_{nr}$ and higher *%R* indicate a greater resistance against permanent deformations.

As for the base binders (Figures 6.8 (a) and 6.9 (a)), the bio-binder A and the bitumen B are characterized by identical values of $J_{nr}$ and *%R* (equal to zero), further confirming that their mechanical behaviour is very similar (Table 6.1 and Figure 6.1). Instead, the RAP binder exhibits lower $J_{nr}$ and higher *%R* as compared to the Bio-RAP binder, in line with what observed in terms of conventional properties and master curves (Table 6.1 and Figure 6.1).

Figures 6.8 (b) and 6.9 (b) show that all the recycled blends and the Control bitumen have comparable $J_{nr}$ and *%R* values in unaged conditions. Some differences between the binders emerge with aging, once more suggesting that the binders may have dissimilar aging susceptibility. Specifically, after aging, the blends containing Bio-RAP tend to exhibit the highest $J_{nr}$ values together with the lowest *%R*, while the Control bitumen, on the contrary, is characterized by the lowest $J_{nr}$ values and the highest *%R*. The effect of the fresh binder type in the blend can be mainly observed in the percent strain recovery after PAV (Figure 6.9 (b)). In fact, the blends containing A (A+RAP, A+bio-RAP) present smaller *%R* values than the corresponding blends containing B (B+RAP, B+bio-RAP). All these observations are consistent with the results presented in Sections 6.3.2 and 6.3.3.

Analogous observations are valid also at the other temperatures (60 and 80 °C) and stress levels (0.1 kPa) investigated.

The implications of these outcomes in terms of performance are further discussed in Section 6.3.6, after the in-depth analysis of the aging susceptibility of the binders.

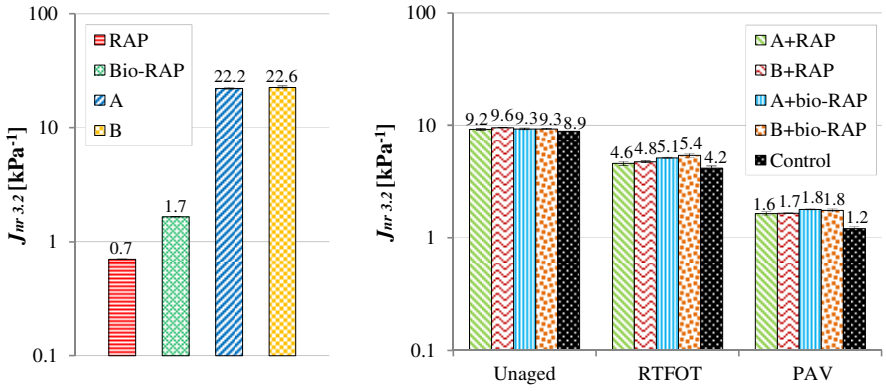


**Figure 6.8** Non-recoverable creep compliance at 70°C and 3.2 kPa for (a) base binders, (b) recycled blends and Control bitumen at different aging levels

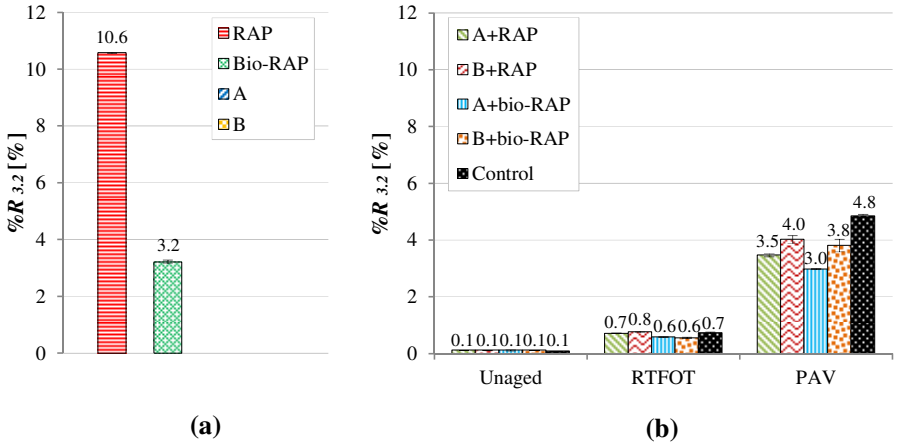


**Figure 6.9** Percent strain recovery at 70°C and 3.2 kPa for (a) base binders, (b) recycled blends and Control bitumen at different aging levels

### *6.3.5 FTIR spectra*

The absorbance spectra of the base binders are shown in Figure 6.10, where the main peaks are highlighted. From the spectra of binders A and Bio-RAP, it can be observed that the bio-oil modification is identified by the peak at 1735 cm$^{-1}$, which is absent in the spectrum of conventional bitumen (e.g. binders B and RAP) and corresponds to the C=O stretch of the bio-oil's esters, as already discussed in Sections 3.4.1 and 4.3.2. Moreover, for all the binders, the effect of aging emerges as the formation of new bonds at about 1700 and 1030

$cm^{-1}$ (see the comparison between bio-based binders A and Bio-RAP and between conventional bitumens B and RAP), corresponding respectively to the C=O stretch of carbonyl functional groups and the S=O stretch of sulfoxides. As anticipated in Section 4.3.2, the C=O and S=O bonds formed during aging at these wavenumbers are responsible for significant physical and rheological changes undergone by bituminous binders (Petersen and Glaser, 2011; Petersen, 2009). However, the previous investigation on the aging properties of the bio-binders highlighted that, for the bio-binders in question, aging can imply also the formation of new compounds that show absorption at 1735 $cm^{-1}$ (Section 4.3.2).

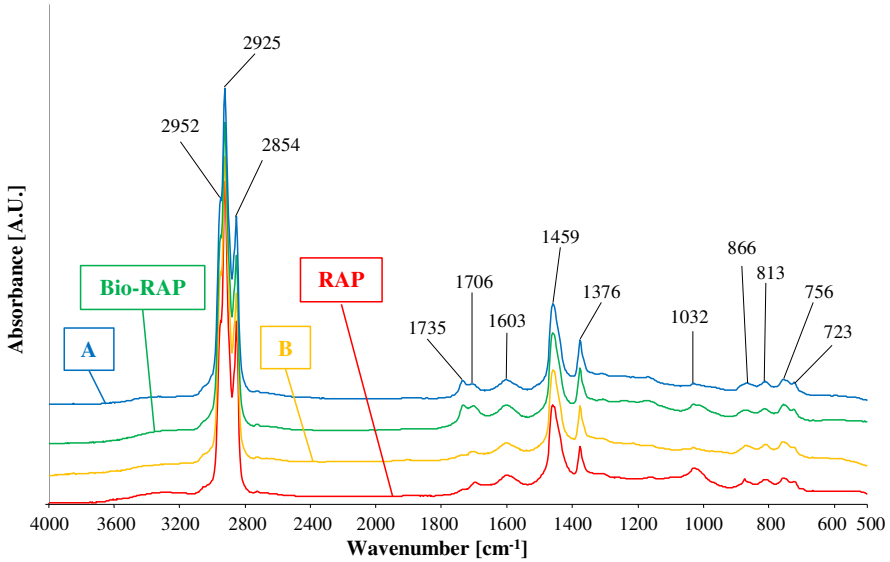


**Figure 6.10** FTIR spectra of the base binders

No additional peaks were observed in the spectra of the recycled blends, indicating that in all cases only a physical blending occurred between the binders, without any chemical reaction (not even in the presence of the bio-binder). Therefore, in the quantitative analysis, the area between 1679 and 1753 $cm^{-1}$ ($A_{CO}$) and the area between 972 and 1063 $cm^{-1}$ ($A_{SO}$) were calculated to assess the effect of aging. It should be pointed out that both peaks at 1700 and 1735 $cm^{-1}$ were included in the calculation of $A_{CO}$ because of the peculiar shape of the bio-binder spectrum in this wavenumber range (Figure 6.10), which did not allow to consider these peaks as completely distinct and independent from each other. In order to minimise the influence of specimen thickness (or infrared radiation path length), these areas were normalised as in Equations (6.4) and (6.5), where $A_{ref}$ is the reference area between 1330 and 1518 $cm^{-1}$ including the peaks at 1376 and 1459 $cm^{-1}$, which correspond to the $CH_3$ and $CH_2$ bend of the aliphatic groups (that are supposed not to be affected by oxidation) (Marsac et al., 2014).

$$I_{CO} = \frac{A_{CO}}{A_{ref}} \tag{6.4}$$

$$I_{SO} = \frac{A_{SO}}{A_{ref}} \tag{6.5}$$

The indices $I_{CO}$ and $I_{SO}$ calculated for the recycled blends and the Control bitumen are shown in Figures 6.11 (a) and 6.11 (b), respectively, whereas their sum is shown in Figure 6.11 (c). It should be noted that, in Figure 6.11, each graph presents a different scale on the y-axis to emphasize the differences between the binders.

As can be seen from Figure 6.11 (a), the index $I_{CO}$ increases with aging for all binders, and such increment seems to be almost linear. Moreover, it can be noted that the blends containing the bio-oil exhibit higher $I_{CO}$ values due to the peak at 1735 $cm^{-1}$. Indeed, the highest values are shown by A+bio-RAP, followed by A+RAP and B+bio-RAP, whereas B+RAP and the Control bitumen exhibit significantly lower $I_{CO}$ values.

Conversely, the index $I_{SO}$ is almost unchanged after RTFOT, while it markedly increases after long-term aging (PAV) (Figure 6.11 (b)). In general, higher $I_{SO}$ values are observed in the presence of RAP (A+RAP and B+RAP), as this binder was recovered from the reclaimed asphalt deriving from a pavement which was in service for more than 20 years (see Section 6.2.1). Furthermore, since the Control bitumen is entirely virgin (unlike the recycled blends), it exhibits the lowest $I_{SO}$ values, especially in unaged and short-term aged conditions.

Finally, the sum of $I_{CO}$ and $I_{SO}$ seems to be a reliable chemical aging indicator, as it increases with aging for all binders (Figure 6.11 (c)). Specifically, this increment is relatively small after RTFOT, whereas it becomes larger after PAV, which seems consistent with the severity of the mechanical changes typically undergone by bituminous binders after short-term and long-term aging. A similar FTIR index was effectively used to compare the aging susceptibility of bio-binders and conventional bitumens in Section 4.

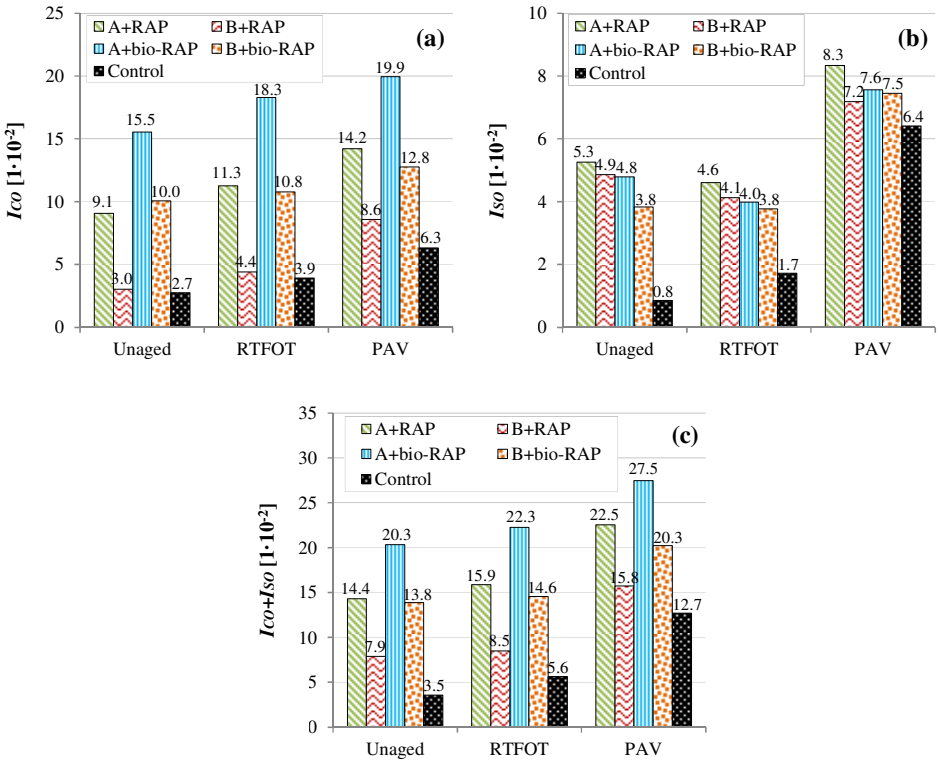


**Figure 6.11** FTIR indices: (a) $I_{CO}$, (b) $I_{SO}$, (c) $I_{CO}$+$I_{SO}$

### *6.3.6 Aging susceptibility*

In order to compare the aging susceptibility of the binders, one chemical and one mechanical parameter strictly related to the oxidation of the binders were considered.
As already discussed in Section 4.3.6, the FTIR spectrum is a sort of chemical fingerprint of the material (Smith, 2011). In Section 6.3.5, it has been shown that, for the binders studied, aging causes the formation of additional compounds at 1700, 1735 and 1030 cm$^{-1}$, quantified through the sum of the indices $I_{CO}$ and $I_{SO}$.
Therefore, the chemical aging index $AI_{FTIR}$, defined as the ratio between $I_{CO}$+$I_{SO}$ for the aged binder and $I_{CO}$+$I_{SO}$ for the unaged binder (Equation (6.6)), was considered.

$$AI_{FTIR} = \frac{(I_{CO} + I_{SO})_{aged}}{(I_{CO} + I_{SO})_{unaged}} \tag{6.6}$$

From the mechanical point of view, it has been shown that the modified CAM parameters $m_e$ and $R$ and the WLF parameters $C_1$ and $C_2$ exhibit a clear trend with aging, but their variation due to aging is relatively small as compared to that of the fatigue parameter

$|G^*|\sin\delta$, the non-recoverable creep compliance $J_{nr}$ and the percent strain recovery $\%R$ (Sections 6.3.2, 6.3.3 and 6.3.4). Moreover, it is worth pointing out that $|G^*|\sin\delta$, $J_{nr}$ and $\%R$ are determined directly from rheological tests, whereas the modified CAM and WLF parameters are the results of a modelling procedure that might be affected by a certain degree of inaccuracy. In addition, as already mentioned in Section 4.3.6, the effect of oxidative aging can be more easily quantified at very low frequencies/very high temperatures (Rad et al., 2018). Therefore, based on these considerations, $J_{nr}$ was considered as the most appropriate mechanical parameter to be used in the analysis of the aging susceptibility of the binders studied. Specifically, the values of $J_{nr}$ determined at the highest stress level (3.2 kPa) and 70°C were considered. This temperature was chosen among those investigated (60, 70 and 80 °C) because the recycled blends and the Control bitumen should have an upper performance grade (PG) close to 70°C.
Since the non-recoverable creep compliance decreases with aging, the mechanical aging index $AI_{MSCR}$ was defined as the ratio between $J_{nr}$ of the unaged binder and $J_{nr}$ of the aged binder (Equation (6.7)), in order to have $AI$ values higher than 1 (as in the case of $AI_{FTIR}$).

$$AI_{MSCR} = \frac{(J_{nr}@70°C, 3.2\ kPa)_{unaged}}{(J_{nr}@70°C, 3.2\ kPa)_{aged}} \tag{6.7}$$

The values of $AI_{FTIR}$ and $AI_{MSCR}$ obtained are shown in Figures 6.12 (a) and 6.12 (b), respectively. Firstly, it can be observed that, after short-term aging, no big differences emerge between the binders (except for $AI_{FTIR}$ for the Control bitumen), probably because this aging condition is not severe enough to assess the aging susceptibility of the binders or all the studied binders are highly aging-resistant in RTFOT. On the contrary, after long-term aging, there is a clear distinction between the binders, which are ranked as follows (from the highest to the lowest aging susceptibility): Control bitumen, B+RAP, A+RAP, B+bio-RAP, A+bio-RAP. It should be noted that this ranking is observed both in terms of $AI_{FTIR}$ and $AI_{MSCR}$ after PAV.
These findings indicate that the aging susceptibility of the recycled blends is significantly lower than that of the Control bitumen, analogously to previous results by Mazzoni et al. (2018). As a possible explanation of this phenomenon, it should be considered that the recycled blends already contain a certain amount of severely aged binder, and the aging rate tends to be faster when the binder is virgin whereas it progressively slows down as aging develops (Luo et al., 2018). Moreover, the blends containing Bio-RAP as aged binder (A+bio-RAP and B+bio-RAP) have lower aging susceptibility than the blends containing RAP (A+RAP and B+RAP). At the same time, the blends containing the bio-binder A as fresh binder (A+RAP and A+bio-RAP) tend to exhibit lower aging susceptibility than the blends containing the conventional bitumen B (B+RAP, B+bio-RAP). These results are fully in agreement with the results presented in Section 4, which highlighted that the bio-binders investigated are less affected by aging as compared to conventional bitumens with similar penetration grade.

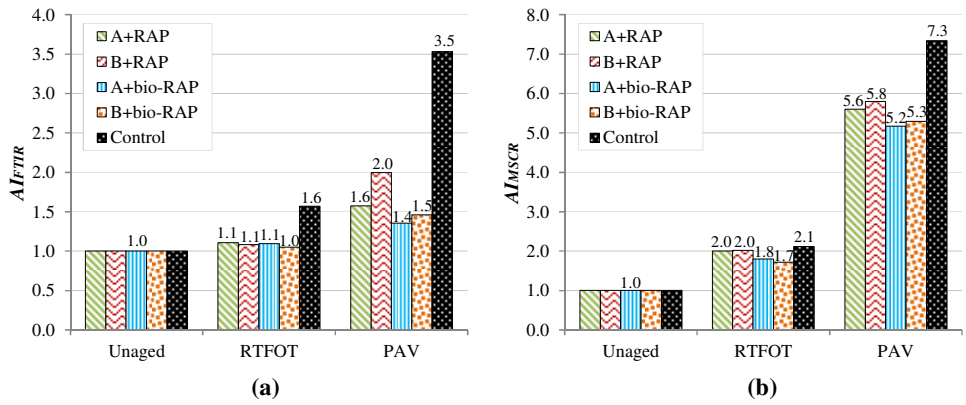


**Figure 6.12** Aging index based on (a) FTIR results, (b) MSCR results

Based on these outcomes and on the results provided in Sections 6.3.3 and 6.3.4, the hot recycling of bio-RA may lead to asphalt mixtures less susceptible to cracking as compared to the recycling of conventional RA, as well as the use of bio-binders in the hot recycling of conventional RA may be beneficial in terms of cracking, thanks to a lower aging rate of the binder. On the other hand, the reduced aging undergone by the blends with the bio-binder might imply a higher rutting tendency for the resulting asphalt mixture. Nevertheless, it should be emphasized that rutting is usually a concern when the binder is unaged or short-term aged, and under these circumstances the behaviour of all the recycled blends studied is broadly the same. Moreover, the results obtained suggest that mixtures containing reclaimed asphalt may be characterized by a lower aging rate as compared to virgin asphalt mixtures (with possible consequences in terms of mechanical behaviour).
In Figure 6.13, three pairs of values ($AI_{FTIR}$, $AI_{MSCR}$) are plotted for every binder. The pair at (1,1) is the origin of the graph, as it represents the unaged condition ("zero" condition) for all binders, intermediate ($AI_{FTIR}$, $AI_{MSCR}$) values represent the short-term aged condition, whereas the highest ($AI_{FTIR}$, $AI_{MSCR}$) values correspond to the long-term aged condition. The figure demonstrates that, if the binders are examined separately, there is an excellent linear relationship between $AI_{MSCR}$ and $AI_{FTIR}$ ($R^2$ very close to 1), indicating that the chemical and mechanical parameters considered as aging indicators ($I_{CO}$+$I_{SO}$ and $J_{nr}$) are effectively correlated with the binder oxidation.

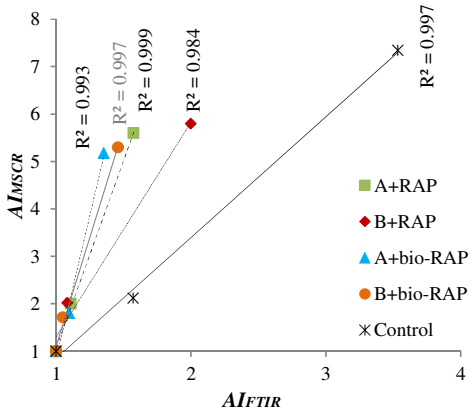


**Figure 6.13** Correlation between $AI_{MSCR}$ and $AI_{FTIR}$

## 6.4 Summary of the findings

The objectives of this part of the project were 1) to assess the effectiveness of bio-binders in the hot recycling of bitumen from typical reclaimed asphalt (RA), and 2) to evaluate the recyclability potential of bio-binders. Two severely aged binders (one "RAP" binder recovered from reclaimed asphalt and one laboratory-produced "Bio-RAP" binder) and two fresh binders (one bio-binder and one bitumen) were properly blended to simulate four binders resulting from the hot recycling of asphalt. The blends were then short-term (RTFOT) and long-term (PAV) aged in order to investigate their aging susceptibility. The mechanical behaviour and the aging susceptibility of the recycled blends were also compared to those of a common virgin bitumen ("Control"). The experimental investigation included mechanical tests (conventional tests as well as rheological testing and modelling) and chemical analysis (Fourier transform infrared spectroscopy).
The main conclusions can be summarized as follows:

- FTIR analysis highlights that, for all the binders tested (with and without the bio-binder), oxidative aging can be tracked from the chemical point of view by considering the formation of C=O bonds at 1700 and 1735 $cm^{-1}$ plus S=O bonds at 1030 $cm^{-1}$;
- from the mechanical point of view, the aging susceptibility of the binders studied can be assessed through the evolution of the non-recoverable creep compliance, which is linearly correlated with the chemical oxidation for each binder;
- the recycled blends containing the bio-binder undergo lower aging than the corresponding blends containing the conventional bitumen;
- the hot recycling of reclaimed bio-asphalt (bio-RA) may lead to mixtures less susceptible to cracking as compared to the recycling of conventional RA, as well as the use of bio-binders in the hot recycling of conventional RA may be beneficial in terms of cracking, thanks to a lower aging rate of the binder;

- the reduced aging undergone by the blends with the bio-binder might imply a higher rutting tendency for the resulting asphalt mixture. However, the behaviour of all the recycled blends studied is generally comparable in unaged and short-term aged conditions, i.e. when rutting is usually a concern;
- the recycled blends show significantly lower aging susceptibility than the Control bitumen (virgin), probably because they already contain a certain percentage of severely aged binder.

Overall, these results suggest that the bio-binders studied can be considered effective in the hot recycling of RA and 100% recyclable, and their use in asphalt pavements can lead to significant technical as well as environmental benefits. However, to get the full picture, the results of this investigation should be integrated also with the study of other aspects, such as low-temperature performance and water sensitivity.

# 7. Mechanical behaviour of bio-asphalt mixtures

## 7.1 Background and objectives

Fatigue cracking is a major distress for asphalt pavements and causes the worsening of the pavement bearing capacity, often leading to the pavement failure. It consists in the progressive degradation of the asphalt mixture properties due to cyclic stresses/strains caused by traffic loadings whose value is actually lower than the mixture strength. Asphalt pavements can be affected by two main fatigue failure mechanisms, bottom-up cracking and top-down cracking. Bottom-up cracking is the bending-induced cracking that initiates at the bottom of the asphalt layers due to critical tensile stress/strain conditions and propagates upwards. Top-down cracking, instead, consists in the formation of cracks on the pavement surface due to the combination of tensile and shear stresses/strains which then propagate downwards. The predominance of one mechanism over the other depends on several factors, including the pavement structure and the characteristics of the wearing layer (Hu and Walubita, 2009).

Fatigue cracking is a complex phenomenon in which two degradation phases occur. The first phase, called initiation, consists in the development of a diffused micro-crack network, which results in a decrease in the macroscopic stiffness of the material. In the second phase, called propagation, the micro-cracks coalesce and form a macro-crack which then propagates within the material (Di Benedetto et al., 2004). The complexity of fatigue characterization of bituminous mixtures is amplified by the fact that fatigue behaviour is very sensitive to the boundary and loading conditions and fatigue failure has an intrinsic stochastic nature (Di Benedetto et al., 2004; Lundström et al., 2004a). Moreover, other phenomena, often referred to as biasing effects, can occur during fatigue testing of bituminous mixes, including non-linearity, self-heating (or hysteretic heating) and thixotropy. All these phenomena cause the reduction of the material stiffness during the test and therefore they can be misinterpreted as damage effects related to fatigue (Babadopulos et al., 2017; Di Benedetto et al., 2011; Lundström et al., 2004b; Mangiafico et al., 2015).

The fatigue properties of bio-binders have been investigated by several authors so far (Cao et al., 2019; Lei et al., 2017; Wang et al., 2018). At the mixture level, the attention has been mainly focused on the effect of bio-oils on the fatigue performance with respect to the mixture with the base bitumen (Yang et al., 2014) or on the fatigue behaviour of recycled mixtures in which the bio-oil was used as a rejuvenator (Blanc et al., 2019; Kowalski et al., 2017; Mogawer et al., 2016). However, there is still limited data regarding the comparison between bio-asphalt mixtures and corresponding traditional asphalt mixtures (i.e. prepared with a bitumen having physical and rheological properties similar to the bio-binder) in terms of fatigue behaviour.

The tests carried out at the binder level in the previous experimental phases highlighted that the bio-binders may have a better fatigue behaviour as compared to conventional bitumens with similar physical and rheological properties, especially in aged conditions thanks to a

greater aging resistance (Section 4). Analogous results were obtained from the study of recycled blends, from which it emerged that blends containing the bio-binder undergo lower aging than corresponding blends containing the conventional bitumen, suggesting the possibility of obtaining recycled mixtures less prone to cracking (Section 6). However, these results need to be confirmed at the mixture level.
Within this general background, this part of the research project aimed at characterizing the mechanical behaviour (in particular, the fatigue behaviour) of a selected bio-asphalt mixture and the corresponding traditional asphalt mixture, investigating also the effect of aging. The mixtures were mixed and compacted in the laboratory considering the same mix design as well as the same mixing and compaction conditions. The only difference between the two mixtures was the binder type. The mixtures were subjected to complex modulus tests and cyclic fatigue tests, and the results were analysed according to the viscoelastic continuum damage (VECD) theory. This part of the experimental activities was possible thanks to a training period spent in Prof. Y. Richard Kim's research group at North Carolina State University (Raleigh, USA).

## 7.2 Fundamentals of VECD theory

Despite the complexity of fatigue cracking and fatigue testing, several empirical fatigue tests exist, such as indirect tension tests, two-/ three-/ four-point bending tests, Texas overlay tests, etc. (EN 12697-24, 2018; Tex-248-F, 2019). These tests are still widely used because of their simplicity, but provide index parameters which represent the fatigue behaviour of the asphalt mixture only under the specific boundary and loading conditions considered. On the contrary, mechanics-based models provide a sound theoretical framework to analyse and interpret the fatigue behaviour of asphalt mixtures, allowing to determine fundamental fatigue properties of the material that are independent of the testing conditions.
The physical evolution laws governing crack initiation and propagation are different, and therefore the two phases are usually modelled with different theories.
Fracture mechanics is the branch of mechanics that studies the evolution of flaws and cracks in solids and thus is usually considered to model the crack propagation phase. The traditional approach of fracture mechanics assumes that flaws or micro-cracks already exist in the material, meaning that this theory, on the other hand, does not allow a rigorous description of the crack initiation phase. The propagation of fatigue cracks is traditionally considered a continuous process, which can be described through the Paris law (Luo et al., 2016; Luo et al., 2013), even though some authors postulate that the crack growth in asphalt materials is a discontinuous process linked with the exceeding of a damage energy threshold (Roque et al., 2002; Zhang et al., 2001).
In this research project, instead, the fatigue test results were analysed according to the VECD theory, which is considered one of the most solid theories to study the fatigue cracking of asphalt mixtures. The VECD theory is based on three main theoretical pillars: continuum damage mechanics, the elastic-viscoelastic correspondence principle and the time-temperature superposition principle with growing damage. Continuum damage mechanics assumes the material as a continuous and homogeneous body and studies

damage growth through internal state variables, which allow to take into account the micro-structural degradation of the material (e.g. formation of multiple micro-cracks) at a global level (i.e. considering properties that are measurable at a macro-scale). Consequently, this theory allows to properly model the crack initiation phase, but does not allow a rigorous description of the crack propagation phase. The elastic-viscoelastic correspondence principle allows to separate the viscous effects from the damage-related effects. In fact, by replacing physical strains with pseudo-strains, the viscoelastic problem can be reduced to the corresponding elastic problem, removing the time-dependence (Schapery, 1984). The time-temperature superposition principle with growing damage allows to take into account the combined effect of time (rate) of loading and temperature even beyond the linearity range of the material behaviour (Chehab et al., 2002).
Within this framework, the material integrity is quantified through the pseudo-stiffness $C$, which is defined as the ratio between the applied stress ($\sigma$) and the pseudo-strain ($\varepsilon^R$). The internal state variable is the damage parameter $S$, which can be defined considering Schapery's work potential theory (Schapery, 1984), based on thermodynamic principles:

$$\frac{dS}{dt} = \left(-\frac{\partial W^R}{\partial S}\right)^{\alpha} \tag{7.1}$$

where $W^R$ is the pseudo-strain energy density function and $\alpha$ is the damage growth rate, which is correlated with the slope of the relaxation modulus versus time in log-log scale. The relationship between $C$ and $S$ is the so-called *damage characteristic curve* and represents the core of the VECD theory. The $C$ vs. $S$ curve describes the reduction of material integrity as damage increases and is a fundamental property of the material, as it does not depend on mode of loading (i.e. stress- or strain-controlled, cyclic or monotonic load), temperature, frequency and stress-strain level (Daniel and Kim, 2002). The relationship between $C$ and $S$ can be expressed with a power function law, as follows:

$$C = 1 - C_{11} \cdot S^{C_{12}} \tag{7.2}$$

where $C_{11}$ e $C_{12}$ are the model coefficients.
In the case of cyclic loads, the VECD model can be considerably simplified from the computational point of view and in this case it is usually referred to as *simplified viscoelastic continuum damage* (S-VECD) *model* (Underwood et al., 2010). Therefore, the damage characteristic curve of a given asphalt mixture can be obtained by performing cyclic tension tests, always combined with complex modulus tests.
However, the damage characteristic curve only describes how damage grows in the material, and thus a failure criterion is necessary to define the material failure. In this regard, Wang and Kim (2019) have recently proposed a pseudo-strain energy-based fatigue failure criterion for asphalt mixtures, known as the $D^R$ failure criterion. $D^R$ is defined as the slope of the linear relationship between the sum (1-$C$) to failure and the number of loading cycles to failure ($N_f$), as follows:

$$D^R = \frac{\int_0^{N_f}(1-C)dN}{N_f} = \frac{sum(1-C)}{N_f} \quad (7.3)$$

The definition of this criterion is based on experimental observations which highlighted that the average reduction of the pseudo-stiffness until failure is independent of mode of loading, temperature and load level (i.e. material-specific). From a physical point of view, $D^R$ represents the material toughness, i.e. the ability to absorb energy without fracturing.
This theoretical background can be used to reliably compare the fatigue behaviour of traditional and innovative asphalt mixtures.

# 7.3 Materials and methods

## *7.3.1 Materials*

The mixtures were designed based on the Italian motorway technical specifications for dense-graded wearing layers. The aggregate gradation considered for the tested mixtures is shown in Figure 7.1. This gradation curve was obtained by combining 18% of basalt 8/14, 40% of basalt 4/8, 35% of limestone 0/2 and 7% of limestone filler. The nominal maximum aggregate size (NMAS) of the mixes was equal to 12.5 mm.

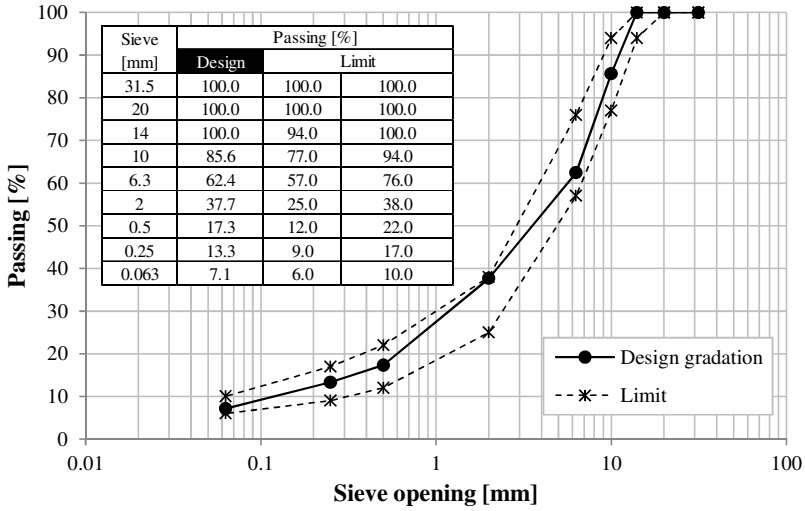


**Figure 7.1** Aggregate gradation of the mixtures studied

A binder content equal to 5.8% by aggregate weight was adopted. The bio-asphalt mixture, hereinafter coded as "Bio", was produced with a bio-binder composed of 90% of bitumen 50/70 and 10% of wood-based bio-oil, whereas the traditional asphalt mixture, hereinafter coded as "B120", was produced with a conventional bitumen (the same bio-binder and

bitumen studied and compared in the previous experimental phases, see Sections 4 and 6). As already shown in Section 6.2.1, the two binders were characterized by similar physical properties (penetration around 120 dmm and softening point around 45°C) and rheological behaviour.
Both mixes were produced at 150°C and then the loose mix was subjected to the short-term aging procedure prescribed by the standard AASHTO R 30 (2015), consisting in 4 hours at 135°C in the oven. Afterwards, gyratory compactor specimens with 150 mm diameter and 180 mm height were prepared at a compaction temperature of 135°C. The short-term aged condition was assumed as the "zero" condition in the experimental investigation, because it corresponds to the actual state of the mixture at the beginning of its service life.
Four test specimens with 38 mm diameter and 110 mm height were obtained from each gyratory compactor specimen according to the standard AASHTO PP 99 (2019), as shown in Figure 7.2. Test specimens with such geometry are considered representative in the case of dense-graded mixtures with NMAS up to 19 mm (AASHTO PP 99, 2019).

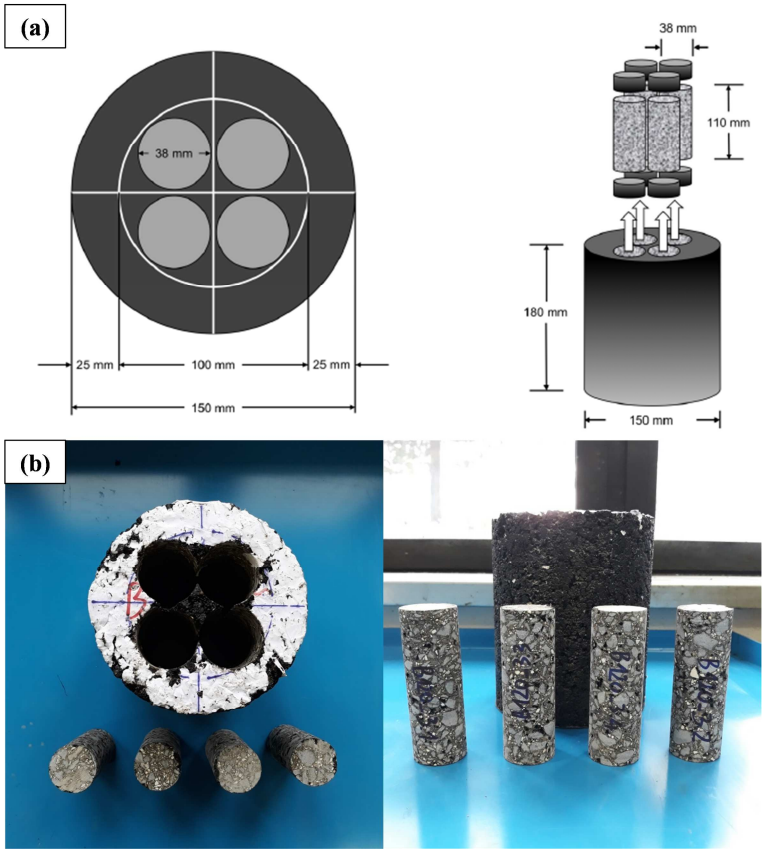


**Figure 7.2** Test specimens obtained from the gyratory compactor specimen: (a) schemes, (b) pictures

To simulate long-term aging, the test specimens were conditioned in the oven for 5 days (120 hours) at 85°C, as prescribed by the standard AASHTO R 30 (2015), a procedure that should simulate five to ten years of aging in the field. The long-term aged bio-asphalt mixture and the long-term aged traditional asphalt mixture are coded in the following as "Bio_LT" and "B120_LT", respectively. Figure 7.3 shows a comparison between one short-term aged specimen and one long-term aged specimen.
The target air void content for the test specimens was 4.0% (calculated by measuring the bulk density of the specimen with the dry method according to EN 12697-6 (2020)). Testing was carried out only on specimens characterized by the target air void content ±0.5%.

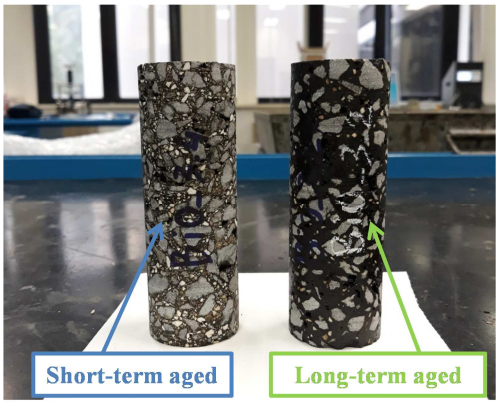


**Figure 7.3** Comparison between one short-term aged specimen and one long-term aged specimen

## *7.3.2 Complex modulus tests*

The mechanical behaviour of the mixtures in the linear viscoelastic (LVE) range was investigated through complex modulus tests (i.e. oscillatory tests with sinusoidal loading) carried out according to the standard AASHTO TP 132 (2019).
For the measurement of axial deformations during the tests, three vertical LVDTs were mounted on the middle part of the specimen 120° apart from each other. For this purpose, three pairs of mounting studs were glued to the specimen at a gauge length of 70 mm.
The norm of the complex modulus $|E^*|$ and the phase angle $\delta$ were determined respectively as the ratio between axial stress amplitude and axial strain amplitude and the phase difference between stress and strain. All the mixtures were tested at 4, 20 and 35 °C, starting from the lowest temperature and then moving to higher temperatures to avoid any permanent deformation in the specimen. Five testing frequencies were considered for each temperature, i.e. 10, 5, 1, 0.5 and 0.1 Hz. Before starting the test, the specimen was conditioned for at least 90 min. The test consisted in subjecting the specimen to a sinusoidal cyclic axial compression load whose amplitude was defined in order to keep the axial strain between 50 and 75 microstrain. Three specimens were tested for each mixture.

All the tests were carried out using a universal testing machine with 30 kN capacity (UTM-30), as shown in Figure 7.4.

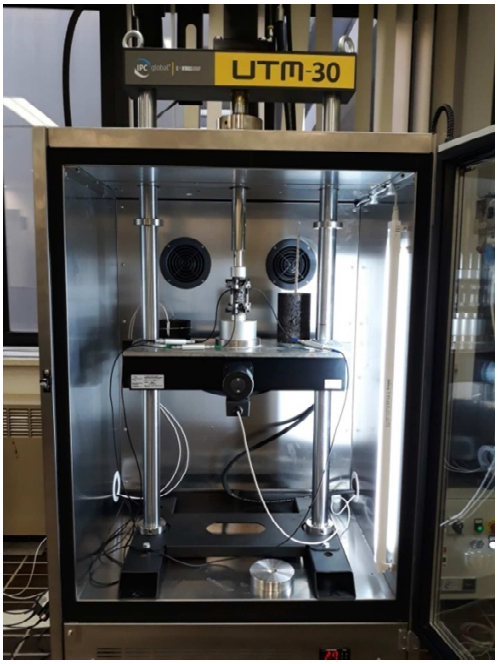


**Figure 7.4** Testing setup for complex modulus tests (UTM-30)

### *7.3.3 Cyclic fatigue tests*

The fatigue behaviour of the mixtures was studied through cyclic fatigue tests, carried out according to AASHTO TP 133 (2019) and based on the S-VECD theory. All the tests were performed using an Asphalt Mixture Performance Tester (AMPT) (Figure 7.5), after verifying the correspondence between the complex modulus results obtained with the UTM-30 and the complex modulus results obtained with the AMPT.
Three pairs of mounting studs were glued to the specimen at a gauge length of 70 mm in order to position three vertical LVDTs on the middle part of the specimen 120° apart from each other. Specific end plates were also glued to the specimen.
The testing temperature was selected as the average temperature of the PG of the binder minus 3°C. Since the expected PG for the bio-binder and the bitumen B120 is PG58-28, all the tests (on short-term aged as well as long-term aged mixtures) were carried out at 12°C.
Preliminarily to the fatigue test, a complex modulus fingerprint test was performed, consisting in measuring the complex modulus of the specimen in tension-compression at 10 Hz in the strain range between 50 and 75 microstrain. The fingerprint test was used to evaluate the specimen-to-specimen variability and to estimate the strain amplitude to be considered in the fatigue test. Prior to the fingerprint test, the specimen was conditioned at

the testing temperature for a minimum of 90 min, whereas after the fingerprint test a rest period of at least 5 min was considered.
In the fatigue test, the specimen was subjected to a sinusoidal cyclic axial tensile load (f = 10 Hz) until failure. According to AASHTO TP 133 (2019), the number of cycles to failure $N_f$ corresponds to the peak in the phase angle (that precedes the phase angle drop). The tests were considered valid only if the failure surface was entirely included in the LVDTs measurement area ("middle failure", Figure 7.6) and $N_f$ was between 2000 and 80000 cycles, as prescribed by AASHTO TP 133 (2019). Specifically, the standard AASHTO TP 133 (2019) provides guidelines that allow to select the proper strain level to achieve test durations between 5000 and 40000 cycles, based on the specimen stiffness. It is worth pointing out that, for the materials tested in this experimental investigation, it was necessary to consider lower strain levels than those suggested in the standard in order to achieve test durations longer than 2000 cycles. In addition, it was decided to study the material behaviour also for tests with duration between 40000 and 80000 cycles (i.e. lower strain level), with the aim of investigating a wider range of strain levels. The previous considerations led to the adoption of target peak-to-peak on-specimen strain amplitudes between 180 and 320 microstrain. Three valid tests were achieved for each mixture, considering different strain amplitudes within the above-mentioned range.
It should be emphasized that, thanks to the solid background provided by the VECD theory, three valid tests are sufficient to predict with good accuracy the number of cycles to failure for every temperature, strain amplitude and loading frequency.
The results of complex modulus tests and cyclic fatigue tests were analysed with FlexMAT™ Cracking spreadsheet (v. 1.1.2), kindly provided by Prof. Y. Richard Kim's research group.

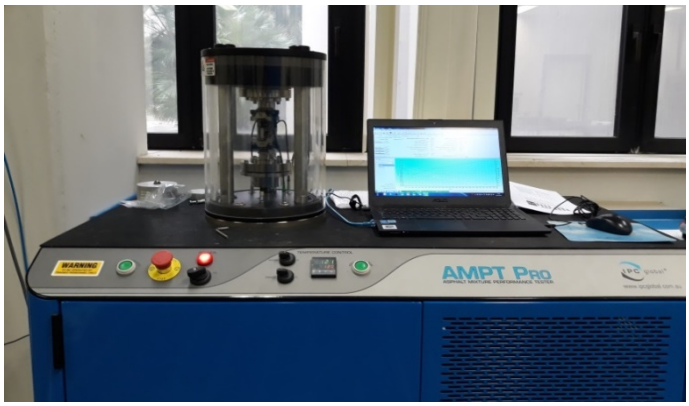


**Figure 7.5** Testing setup for cyclic fatigue tests (AMPT)

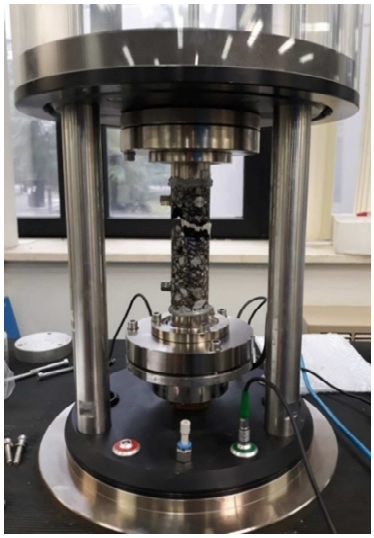

**Figure 7.6** Example of specimen middle failure

## 7.4 Results and analyses

### *7.4.1 Complex modulus*

The raw results of the complex modulus tests are shown in Figure 7.7 (a) and Figure 7.7 (b). In Figure 7.7 (a), the data are represented in the Black diagram, i.e. norm of complex modulus $|E^*|$ vs. phase angle $\delta$, whereas in Figure 7.7 (b) the data are represented in the Cole-Cole diagram, i.e. loss modulus *E2* ($E2 = |E^*| \cdot \sin\delta$) vs. storage modulus *E1* ($E1 = |E^*| \cdot \cos\delta$). Note that the y-axis in the Black diagram is in logarithmic scale, whereas both axes in the Cole-Cole diagram are in linear scale.

As for the comparison between the short-term aged materials, the results indicate that the bio-asphalt mixture is slightly stiffer than the B120 mixture, as denoted by higher $|E^*|$ values and lower $\delta$ values (Figure 7.7 (a)), resulting in higher *E1* values (Figure 7.7 (b)). This difference could be due to a certain over-aging of the bio-asphalt mixture during mixing, short-term aging and compaction phases.

After long-term aging, instead, the viscoelastic behaviour of the two mixtures is very similar. A small difference can be observed from Figure 7.7 (b) only at 4°C, at which the bio-asphalt mixture seems slightly stiffer (higher *E1* and *E2* moduli). Based on these preliminary observations, the effect of the long-term aging procedure considered, which leads to an increase of $|E^*|$ and a reduction of $\delta$, seems more pronounced for B120.

The fact that, in the Black diagram, the experimental data are aligned along the same curve (Figure 7.7 (a)) indicates that the time-temperature superposition principle (TTSP) is valid for all mixtures, including the bio-asphalt mixture. This finding was expected, as the bio-binder and the bitumen B120 have a thermo-rheologically simple behaviour (see Sections 4.3.4 and 6.2.1).

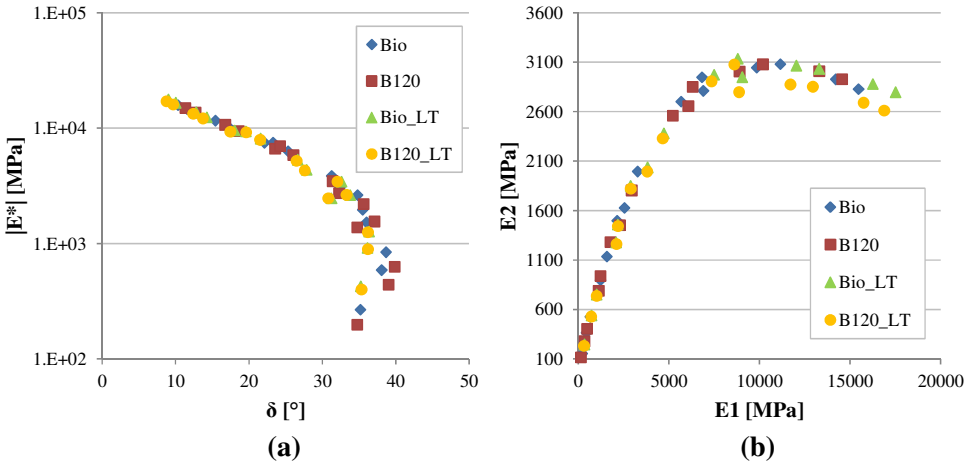


**Figure 7.7** Results of complex modulus tests: (a) Black diagram, (b) Cole-Cole diagram

To obtain the complex modulus master curve, the following sigmoidal function was considered:

$$\log|E^*| = k + \frac{\log(\max E^*) - k}{1 + \exp(\delta + \gamma \log(f_r))} \tag{7.4}$$

Where max$E^*$ is the maximum complex modulus, whose value was determined based on the volumetric properties of the mixtures ($2.29 \cdot 10^7$ kPa) according to the Hirsch model (Christensen et al., 2003); $k$, $\delta$ and $\gamma$ are fitting coefficients ($k$ is equal to the logarithm of the minimum complex modulus, $\delta$ is a translation factor, $\gamma$ is a shape parameter); $f_r$ is the reduced frequency, calculated as:

$$f_r = f \cdot a_T \tag{7.5}$$

Where $f$ is the frequency and $a_T$ is the shift factor at temperature $T$, determined as in Equation (7.6):

$$\log(a_T) = \alpha_1 T^2 + \alpha_2 T + \alpha_3 \tag{7.6}$$

In which $\alpha_1$, $\alpha_2$ and $\alpha_3$ are fitting coefficients that depend on the reference temperature. Specifically, the coefficients $k$, $\delta$, $\gamma$, $\alpha_1$, $\alpha_2$ and $\alpha_3$ were optimized simultaneously by minimizing the error between the measured storage modulus ($E1$) values and the $E1$ values predicted with Equation (7.4), as the storage modulus is a perfectly sigmoidal function ($E2 \rightarrow 0$ when $f \rightarrow 0$ and $f \rightarrow \infty$).
The complex modulus master curve at a reference temperature of 21.1°C is shown in a log-log graph in Figure 7.8 (a) and in a semi-log graph in Figure 7.8 (b). The same shift factors

were used to obtain also the phase angle master curves at 21.1°C, which are shown in Figure 7.8 (c).
Analogously to what observed from the Black and Cole-Cole diagrams (Figure 7.7), it can be noted that in short-term aged conditions the bio-asphalt mixture exhibits higher $|E^*|$ values and lower $\delta$ values. As expected, the effect of aging results in increased complex modulus and reduced phase angle, i.e. higher stiffness and elasticity of the material. As already observed from Figure 7.7, the mechanical behaviour of the bio-asphalt mixture and the B120 mixture is almost identical after long-term aging, except for a very small difference at 4°C (at which the bio-asphalt mixture presents slightly higher $|E^*|$ values than B120).
In addition Figure 7.8 (d), showing the shift factors values, indicates that the temperature-dependency is similar for the two mixtures before and after long-term aging, as demonstrated by the very similar slope of the fitting functions. The long-term aged materials are characterized by a more marked temperature susceptibility with respect to the short-term aged ones (as expected).

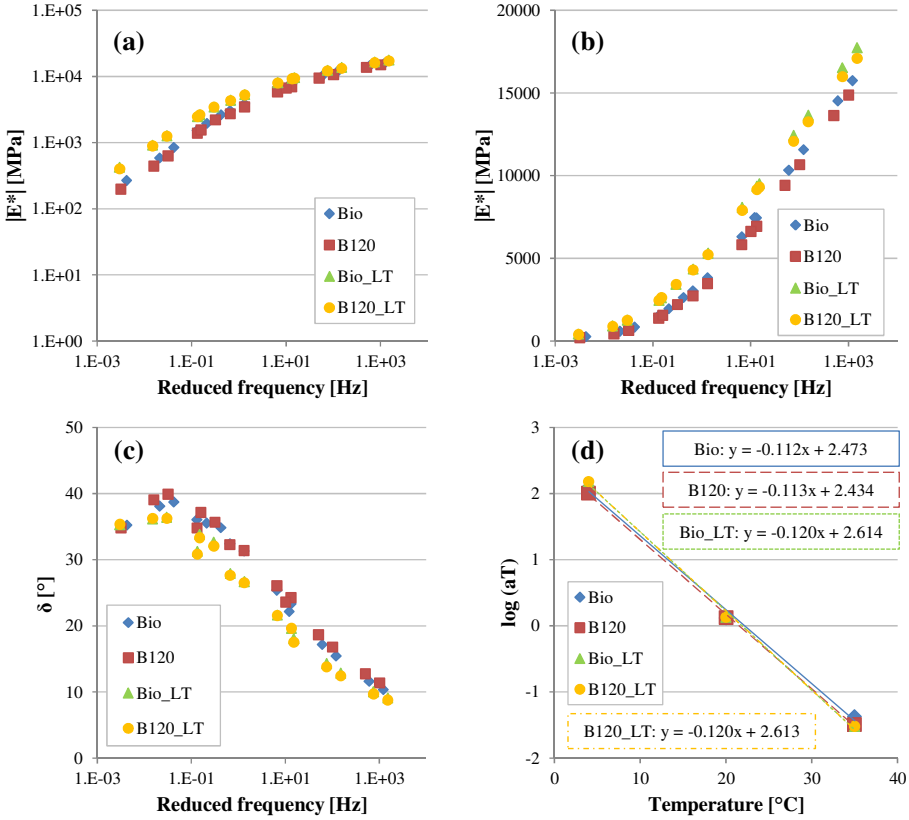


**Figure 7.8** Analysis of complex modulus test results: (a) complex modulus master curve (log-log graph), (b) complex modulus master curve (semi-log graph), (c) phase angle master curve, (d) shift factors

The aging susceptibility of the bio-asphalt mixture and the B120 mixture was further assessed by considering the sigmoidal functions of the storage modulus *E1* in the range of reduced frequencies investigated in the laboratory (approximately $10^{-3} \div 10^{3}$ Hz), as shown in Figure 7.9. This choice is motivated by the fact that the model fitting is more accurate in terms of *E1* and in the range of reduced frequencies actually tested. Specifically, the area below the log($f_r$)-log(*E1*) curve was determined through the trapezoidal method, an approach similar to that proposed by Cavalli et al. (2018b) to assess the effect of aging on the mechanical properties of binders from reclaimed asphalt treated with bio-based rejuvenators. The results, summarized in Table 7.1, confirm that the Bio mixture is slightly stiffer than the B120 mixture in short-term aged conditions, whereas their master curves are basically overlapped after long-term aging. The difference between the area below the master curve before and after long-term aging is greater for B120, further suggesting that the bio-asphalt mixture has a reduced long-term aging susceptibility as compared to the corresponding traditional asphalt mixture.

The analysis of the parameters of the sigmoidal function (summarized in Table 7.2) confirms that the long-term aging susceptibility is more marked for the traditional asphalt mixture. In fact, the translation factor $\delta$ and the shape parameter $\gamma$ decrease with aging for both mixes. However, the reduction is greater in the case of B120, especially in terms of $\delta$, denoting that the translation towards lower reduced frequencies due to aging is greater for the traditional asphalt mix. On the contrary, no clear trend is observed in terms of $k$, probably because the estimate of the minimum complex modulus is partly influenced by the fact that the highest testing temperature was 35°C (as recommended by AASHTO TP 132 (2019)).

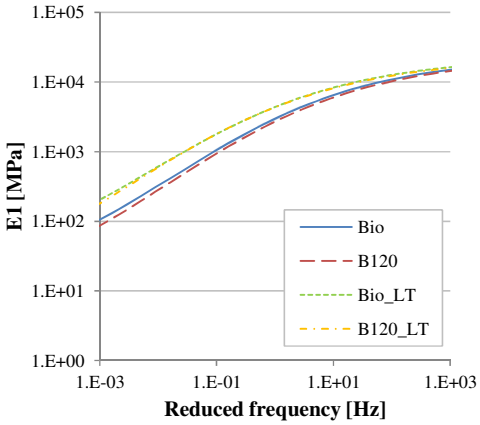


**Figure 7.9** Storage modulus master curve (sigmoidal function)

**Table 7.1** Area below the storage modulus master curve (log($f_r$)-log(*E1*))

| Mixture | ST aged | LT aged | Difference |
|---|---|---|---|
| Bio | 19.98 | 20.94 | 0.96 |
| B120 | 19.72 | 20.92 | 1.20 |

**Table 7.2** Parameters of the sigmoidal function

| Mixture | Max*E1* [kPa] | *k* | *δ* | *γ* |
|---|---|---|---|---|
| Bio | 2.29E+07 | 3.93 | -1.05 | -0.61 |
| B120 | 2.29E+07 | 3.71 | -1.07 | -0.59 |
| Bio_LT | 2.29E+07 | 4.09 | -1.27 | -0.60 |
| B120_LT | 2.29E+07 | 3.64 | -1.42 | -0.56 |

The results obtained suggest that the bio-asphalt mixture is probably more susceptible than the conventional mixture to the oxidation effects caused by high temperatures (the mixing and compaction temperatures were equal respectively to 150°C and 135°C), whereas the aging susceptibility of the bio-asphalt mixture is lower in the case of lower temperatures (the long-term aging temperature was 85°C), which are closer to the actual temperatures experienced by the pavement in the field. It is possible that the bio-binder chemical composition is more affected by the effects of high temperatures with respect to the conventional bitumen. In fact, it is known that aging kinetics and the formation of sulfoxides and carbonyls during aging are strongly material- and temperature-dependent. Specifically, temperatures above 100°C can disrupt polar molecular associations and lead to the thermal decomposition of sulfoxides in asphalt binders, significantly changing the kinetics of the oxidation reaction as well as the reaction products (Petersen and Glaser, 2011; Petersen, 2009; Rad et al., 2017). In addition, the aging behaviour of the bio-asphalt mixture could be affected somehow also by the chemical interaction between bio-binder and aggregates.
However, it is worth pointing out that the previous experimental phases at the binder level did not indicate a significant over-aging and /or mass loss of the bio-binder after short-term aging with RTFOT (Section 4). Conversely, the findings concerning the long-term aged mixtures are in agreement with the results obtained at the binder level, which indicated that bio-binders may have higher aging resistance with respect to conventional bitumens with similar physical and rheological properties (see Sections 4.3.6 and 6.3.6). For a better understanding of the aging-related mechanisms of the bio-asphalt mixture, these aspects should be deepened in the future with a more chemistry-oriented approach.

### *7.4.2 Fatigue behaviour*

As an example, Figure 7.10 shows the typical evolution of complex modulus and phase angle during the cyclic fatigue test. The phase angle increases during the test, reaches a peak (which defines the number of cycles to failure $N_f$ according to AASHTO TP 133 (2019)) and then drops. As for the complex modulus, after a quasi-linear reduction, it exhibits a sharp decrease when the phase angle approaches its maximum value.
The damage characteristic curves obtained for each specimen are shown in Figure 7.11 (a). It can be observed that, for each mixture, the experimental data corresponding to different specimens overlap, as expected.
From the power function fit shown in Figure 7.11 (b), it can be noted that, in short-term aged conditions, for a given *S* value (i.e. damage level) the Bio mixture is characterized by

higher *C* values as compared to the B120 mixture. This is probably due to the fact that the bio-asphalt mixture exhibits greater stiffness with respect to the B120 mixture, as discussed in Section 7.4.1. In addition, the fact that the Bio mixture presents a higher *C* value at failure than the B120 mixture indicates that the bio-asphalt mixture is less tolerant to damage after short-term aging.

For the B120 mixture, the effect of aging emerges as a slight upward shift of the damage characteristic curve along with an increase in the *C* value at failure. These effects are in agreement with the results available in literature concerning the effect of aging on the fatigue behaviour of asphalt mixtures (Babadopulos et al., 2018; Saleh et al., 2020). In the case of the Bio mixture, the upward shift of the curve is much more evident. However, contrary to what could be expected, the value of *C* at failure decreases with respect to the short-term aged condition.

When the Bio mixture and the B120 mixtures are compared after long-term aging, it can be observed that the bio-asphalt mix exhibits significantly higher *C* value for the same *S* value as well as lower *C* value at failure, even though the stiffness of the two long-term aged mixtures is almost identical, as shown in Section 7.4.1.

The relationships between the sum of (1-*C*) to failure and the number of cycles to failure, whose slope is $D^R$ (Equation (7.3)), are shown in Figure 7.12. In short-term aged conditions, the Bio mixture is characterized by a lower $D^R$ value as compared to the B120 mixture, meaning that the toughness (i.e. the ability to absorb energy without fracturing) of the bio-asphalt mixture is worse than that of the corresponding traditional asphalt mixture. This finding is consistent with what observed in terms of stiffness and *C* vs. *S* curve, denoting that after short-term aging the B120 mixture may have a better fatigue resistance with respect to the Bio mixture.

Previous studies (Saleh et al., 2020; Zhang et al., 2019) have shown that aging usually determines a $D^R$ reduction, corresponding to the worsening of the material toughness. This effect is observed for the B120 mix, whereas for the bio-asphalt mix the $D^R$ value is basically unchanged after long-term aging. As a consequence, the $D^R$ value exhibited by B120_LT is slightly higher than that of Bio_LT.

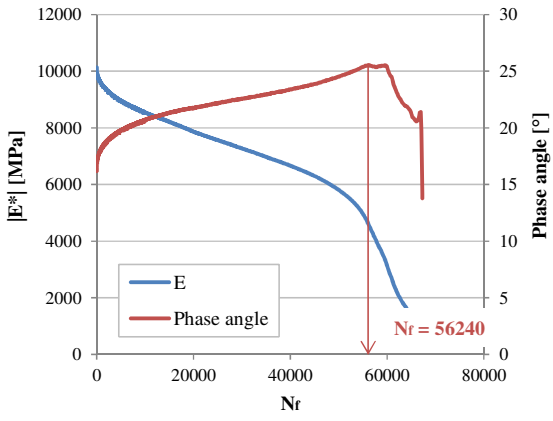


**Figure 7.10** Typical evolution of complex modulus and phase angle during the cyclic fatigue test

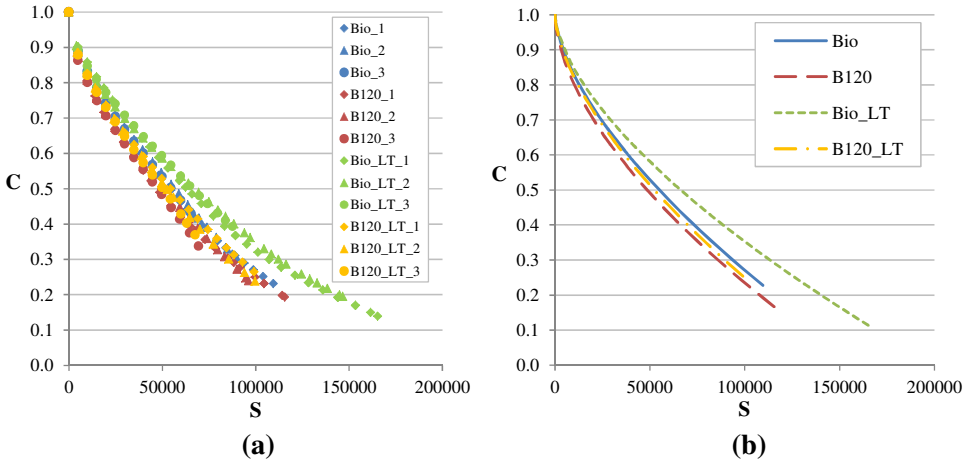


**Figure 7.11** Damage characteristic curves: (a) experimental data, (b) power function fit

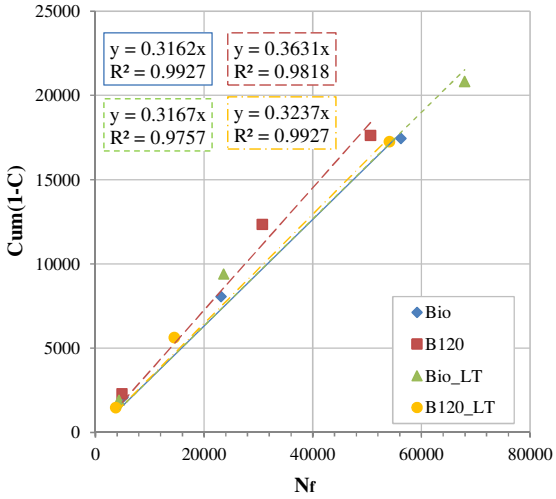


**Figure 7.12** $D^R$ failure criterion

However, the fatigue performance of the mixture cannot be assessed solely based on the damage characteristic curve or $D^R$ value, because both the modulus and the toughness contribute to the mixture fatigue performance within the pavement. In fact, under the same loading conditions, a material with a higher modulus value shows a lower strain value with respect to a material with a lower modulus value. If the toughness is similar for the two materials, the lower strain value in the material with the higher modulus value would result in a longer fatigue life. At the same time, when two materials with similar stiffness and different toughness are subjected to the same strain level, the tougher material would have a longer fatigue life as compared to the less tough material (Wang et al., 2020).

Therefore, in order to take into account both these aspects, Wang et al. (2020) have recently proposed the so-called *apparent damage capacity index* ($S_{app}$), whose expression is as follows:

$$S_{app} = 1000^{\left(\frac{\alpha}{2}-1\right)} \cdot \frac{a_T^{1/(\alpha+1)} \cdot \left(\frac{D^R}{C_{11}}\right)^{1/C_{12}}}{|E^*|^{\alpha/4}} \quad (7.7)$$

where $\alpha$ is the damage growth rate (Equation (7.1)), $a_T$ is the time-temperature shift factor between the testing temperature of the cyclic fatigue test and the reference temperature considered to develop the complex modulus master curve, $|E^*|$ is the complex modulus at the testing temperature for a frequency of 10 Hz (in kPa), $C_{11}$ and $C_{12}$ are the coefficients of the damage characteristic curve (Equation (7.2)), $D^R$ is the slope of the linear relationship between the sum (1-$C$) to failure and the number of cycles to failure (Equation (7.3)).

As can be noted from Equation (7.7), the $S_{app}$ index accounts for the resistance to deformation (through $a_T$ and $|E^*|$), the damage characteristics (through $\alpha$, $C_{11}$ and $C_{12}$) and the failure criterion (through $D^R$) of the asphalt mixture. The $S_{app}$ value is normally between 0 and 50, and higher $S_{app}$ values correspond to a better mixture fatigue resistance. Previous studies demonstrated that the $S_{app}$ index decreases with aging, which is consistent with the typical worsening of the fatigue performance observed for aged materials (Saleh et al., 2020; Wang et al., 2020).

The $S_{app}$ values calculated for the mixtures studied are shown in Figure 7.13. In short-term aged conditions, the B120 mixture exhibits a higher value of $S_{app}$ (i.e. better cracking performance) as compared to the Bio mixture. As expected, aging causes a reduction of $S_{app}$ for both mixtures. However, this reduction is very small for the bio-asphalt mixture, whereas it is more evident in the case of the traditional asphalt mixture. As a result, after long-term aging, the $S_{app}$ value of the Bio mix is higher than that of the B120 mix, meaning that the bio-asphalt mixture may exhibit better fatigue cracking performance in the long term.

The results of the cyclic fatigue tests (in terms of $C$ vs. $S$ curve, $D^R$ and $S_{app}$) also denote that the long-term aging susceptibility is greater for the B120 mixture as compared to the Bio mixture, in line with the complex modulus test results (Section 7.4.1) and the behaviour of the binders (Sections 4.3.6 and 6.3.6).

It is worth pointing out that the $S_{app}$ values obtained for all the mixtures studied are relatively small. This means that the fatigue performance of the mixes should be improved by changing the mix design (e.g. in terms of binder content, aggregate gradation, etc.). Nevertheless, it should be recalled that the main objective of this part of the PhD project was the comparison between a bio-asphalt mix and a traditional asphalt mix that were identical except for the binder type, not the definition of the optimum mix design.

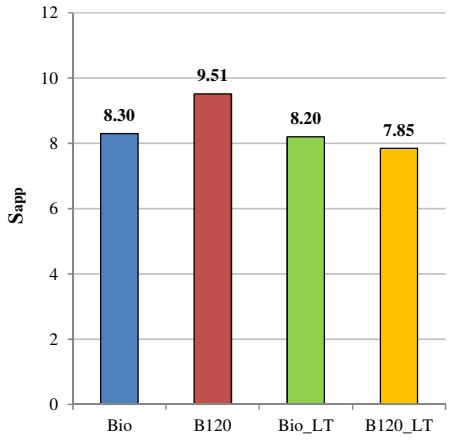


**Figure 7.13** $S_{app}$ values

To further analyse the fatigue results, the classical Wöhler representation, in which the target strain amplitude ($\varepsilon$) is plotted as a function of the number of cycles to failure ($N_f$), can be considered. Figure 7.14 shows that, in short-term aged conditions, the B120 mixture is characterized by longer fatigue life as compared to the Bio mixture. This finding is consistent with the results obtained in terms of damage characteristic curve, $D^R$ and $S_{app}$. For both mixtures, aging causes a worsening of the fatigue performance, which is more marked for B120. As a consequence, after long-term aging, the bio-asphalt mixture exhibits significantly longer fatigue life with respect to the traditional asphalt mixture. Moreover, it should be noted that, for low strain levels, the long-term aged bio-asphalt mixture may even be characterized by longer fatigue life than in short-term aged conditions.

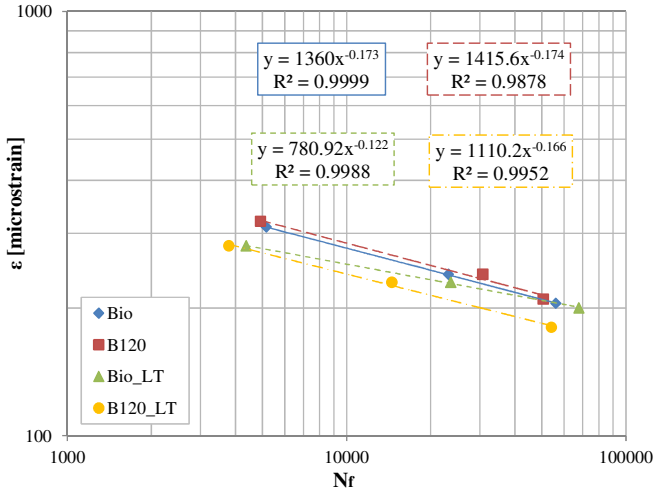


**Figure 7.14** Wöhler's fatigue curves

In a recent study, Saleh et al. (2020) have proposed a different definition of the specimen failure during the cyclic fatigue test as compared to the one provided by AASHTO TP 133 (2019). From an extensive experimental investigation, they observed that the maximum phase angle often occurs after micro-cracks coalesce into a macro-crack on the specimen. Since failure is actually defined as the onset of macro-cracking, they defined $N_f$ as the number of cycles at which the product of modulus and cycle number ($|E^*| \cdot N$) reaches a maximum during the test. This criterion, in fact, leads to lower $N_f$ values as compared to the phase angle drop criterion (Figure 7.15), and this difference can be significant especially for tests longer than 30000 cycles (which is the case of several tests carried out in this experimental investigation). Therefore, the fatigue results were analysed also with this approach.

The damage characteristic curves determined in this way are shown in Figure 7.16. It can be immediately observed that, according to the $|E^*| \cdot N$ criterion, the specimen failure occurs much earlier, i.e. for lower values of $S$ and higher values of $C$ than in the case of the phase angle criterion (Figure 7.11). Nevertheless, all the comments made on Figure 7.11 about the materials behaviour are still valid.

Moreover, even the $D^R$ value changes when the $|E^*| \cdot N$ criterion is considered, as $N_f$ appears in both the numerator and the denominator in $D^R$ expression (Equation (7.3)). The results in Figure 7.17 show that this criterion leads to lower $D^R$ values for all mixtures as compared to the phase angle criterion (Figure 7.12). In this case the fitting of the experimental data with a linear regression is even better than in Figure 7.12 (higher coefficients of correlation $R^2$). Moreover, based on the $|E^*| \cdot N$ criterion, the $D^R$ value decreases with aging for both mixtures, following the aging-related trend reported in literature. The $D^R$ reduction is relatively small for the Bio mixture, whereas it is more apparent for the B120 mixture. As for the comparison between the two mixes, the traditional asphalt mixture is characterized by higher values of $D^R$ before and after long-term aging, in agreement with the results obtained with the phase angle criterion (Figure 7.12).

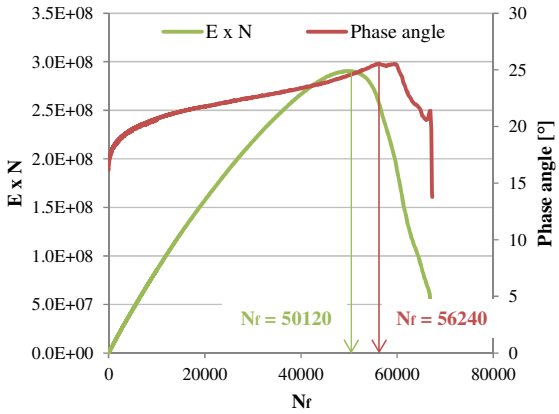


**Figure 7.15** Number of cycles to failure determined with the phase angle criterion and the $|E^*| \cdot N$ criterion

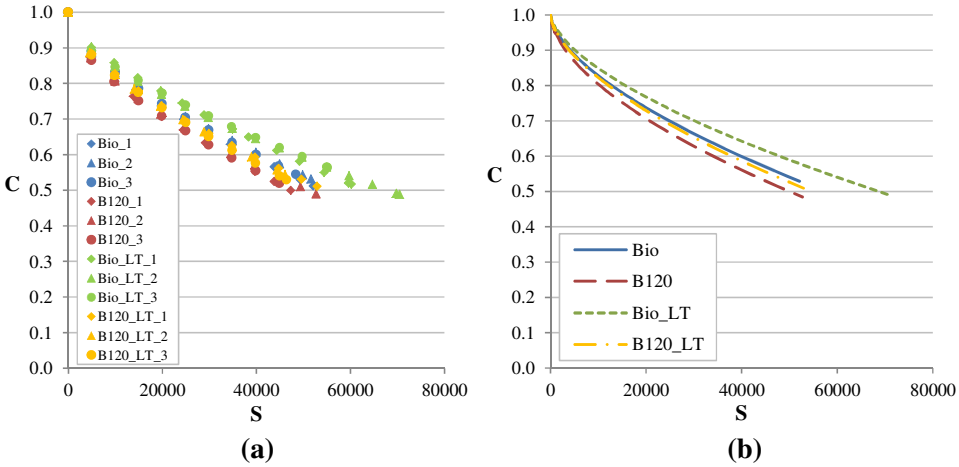


**Figure 7.16** Damage characteristic curves based on the $|E^*| \cdot N$ criterion: (a) experimental data, (b) power function fit

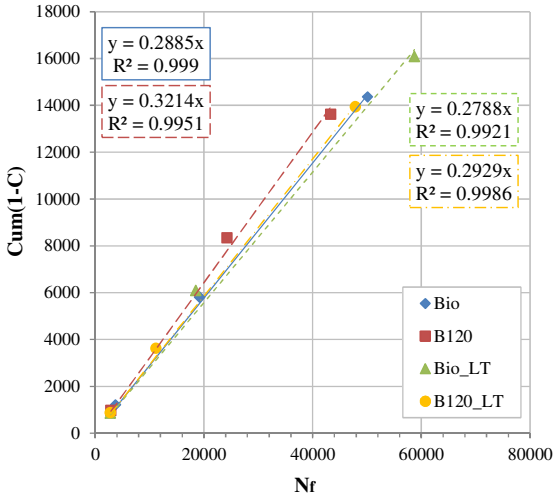


**Figure 7.17** $D^R$ values based on the $|E^*| \cdot N$ criterion

The resulting $S_{app}$ values are shown in Figure 7.18, from which it can be observed that, for all mixtures, the $|E^*| \cdot N$ criterion leads to lower $S_{app}$ values with respect to those obtained with the phase angle criterion (Figure 7.13). Even with this approach, the B120 mixture exhibits a higher $S_{app}$ value than the Bio mixture in short-term aged conditions, but the difference between the two mixes is smaller. The $S_{app}$ reduction due to aging is more marked for B120 than for Bio, as in Figure 7.13. However, as compared to Figure 7.13, this reduction is greater for the Bio mix and smaller for the B120 mix. Consequently, the two mixtures show a comparable $S_{app}$ value after long-term aging.

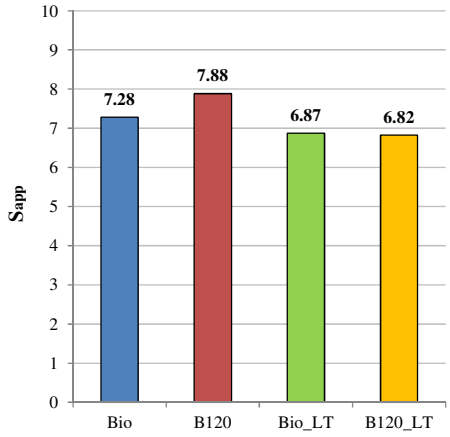


**Figure 7.18** $S_{app}$ values based on the $|E^*| \cdot N$ criterion

The representation of the results in the Wöhler's diagram (Figure 7.19) leads to considerations similar to those made considering the phase angle criterion (Figure 7.14). In short-term aged conditions the fatigue life of the B120 mix is slightly longer than that of the Bio mix, whereas after long-term aging the bio-asphalt mixture shows significantly longer fatigue life with respect to the traditional asphalt mixture.

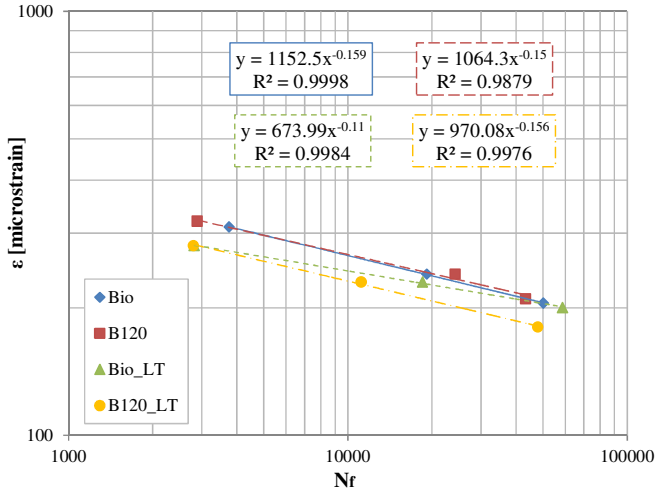


**Figure 7.19** Wöhler's fatigue curves based on the $|E^*| \cdot N$ criterion

In summary, after short-term aging, the B120 mixture exhibits better fatigue performance as compared to the Bio mixture, which may be a consequence of the possible over-aging of the bio-asphalt mixture during mixing and compaction phases. The effect of long-term aging on the fatigue behaviour is more pronounced for the B120 mixture. As a result, the

bio-asphalt mixture may be characterized by better fatigue performance with respect to the traditional asphalt mixture in the long term. The $|E^*| \cdot N$ criterion for the definition of the specimen failure mainly leads to $D^R$ aging-related trends more in line with the results available in literature.

## 7.5 Summary of the findings

The final part of the research project aimed at comparing a selected bio-asphalt mixture (coded as "Bio") and the corresponding traditional asphalt mixture (coded as "B120") in terms of viscoelastic properties and fatigue behaviour. The mixtures were mixed and compacted in the laboratory considering the same mix design as well as the same mixing and compaction conditions. The only difference between the two mixtures was the binder type. The effect of long-term aging was assessed by oven aging the test specimens. The mixtures were subjected to complex modulus tests and cyclic fatigue tests, and the results were analysed according to the S-VECD theory.
The main findings are the following:

- in short-term aged conditions, the Bio mixture is slightly stiffer than the B120 mixture (i.e. higher complex modulus and lower phase angle). This difference may be due to a certain over-aging of the bio-asphalt mixture during mixing, short-term aging and compaction phases caused by the effects of high temperatures;
- after long-term aging, however, the viscoelastic behaviour of the two mixtures is very similar and their complex modulus and phase angle master curves are substantially overlapped. This outcome indicates that the effect of the adopted long-term aging protocol on the viscoelastic properties is more pronounced for the B120 mixture than for the Bio mixture;
- the shift factors values indicate that the temperature-dependency is similar for the two mixtures before and after long-term aging;
- the analysis of the cyclic fatigue test results shows that, in short-term aged conditions, the B120 mixture exhibits better fatigue performance with respect to the Bio mixture (as denoted by a higher $S_{app}$ value), thanks to a lower stiffness (lower $C$ vs. $S$ curve) and a greater toughness (higher $D^R$ value);
- for the Bio mixture, the effect of long-term aging emerges as an upward shift of the $C$ vs. $S$ curve and un unchanged $D^R$ value, resulting in a slightly lower $S_{app}$ value (corresponding to a slight worsening of the fatigue performance). Aging causes also an unexpected decrease of the $C$ value at failure, which would suggest improved damage tolerance;
- for the B120 mixture, instead, the effect of long-term aging results in a less evident upward shift of the $C$ vs. $S$ curve along with a higher $C$ value at failure, as expected. The reduction of $D^R$ and $S_{app}$ due to aging is more evident than in the case of the Bio mix. Consequently, after long-term aging, the B120 mixture exhibits lower $S_{app}$ than the Bio mixture;
- the representation of the fatigue results as classical Wöhler's fatigue curves confirms that in short-term aged conditions the fatigue behaviour of the B120 mix is better than that of the Bio mix, whereas this trend is inverted after long-term

aging. Even from the Wöhler's diagram, the effect of long-term aging seems more evident for the B120 mixture;

- the previous observations remain generally valid also when, for the definition of the specimen failure, the maximum ($|E^*| \cdot N$) criterion is considered instead of the maximum phase angle criterion (the one indicated by the reference standard AASHTO TP 133 (2019)). However, the $|E^*| \cdot N$ criterion leads to shorter $C$ vs. $S$ curves and, most importantly, to $D^R$ aging-related trends that are more in line with the results available in literature.

Overall, these findings suggest that bio-asphalt mixes may be stiffer and thus more prone to fatigue cracking than traditional mixtures after short-term aging (which is not generally considered a critical condition for cracking). However, the long-term aging susceptibility of bio-asphalt mixtures appears less severe than that of asphalt mixtures, with potential fatigue performance benefits in the long term.

Nevertheless, given the numerous variables involved in laboratory fatigue testing, this investigation cannot be considered fully exhaustive. Therefore, before drawing final conclusions, additional tests should be carried out to expand the amount of data available.

# 8. Conclusions

Sustainability and circular economy are two key principles in today's world, as a sustainable and circular-economy-based production would allow to meet the needs of the present without compromising the ability of future generations to meet their own needs, by minimizing resources and energy consumption, wastes and emissions. The construction sector is responsible for significant environmental impact, as it implies the consumption of natural resources (mostly non-renewable), causes emissions and produces wastes, and therefore should undergo important changes in a relatively short time, such as the adoption of new construction technologies and innovative materials, aimed at promoting sustainability and circular economy without penalizing the performance. In this regard, one of the main current trends in pavement engineering is to use bio-binders, i.e. binders in which petroleum-based bitumen is partially replaced with renewable bio-oils, which typically derive from residues or by-products like waste wood, non-edible vegetable biomass, waste cooking oil or animal manure (all deriving from bio-materials not subjected to depletion).

The literature analysis highlights that the use of bio-binders in road pavements can lead to significant environmental (and economic) benefits, such as the reduction of carbon footprint, the reduction of petroleum-based products, the recycling of industrial by-products and residues, the decrease of materials to be disposed in landfills. However, a series of concerns/drawbacks has not allowed a wide use of bio-materials in road pavements up to now, including the limited knowledge of the long-term performance, durability and recyclability of bituminous binders and mixtures containing bio-materials, the possible over-aging of bio-binders, the lack of data about the HSE (health, safety, environment) impact and life cycle assessment of these materials.

Within this context, the materials investigated in this PhD project (which was co-funded by the Swedish petrochemical company Nynas AB) were bio-binders obtained by partially replacing a conventional 50/70 penetration grade bitumen (base bitumen) with a wood-based bio-oil. The bio-oil studied is a residue generated in the processing of a by-product from wood pulp and paper industries, and it is available in large quantities in Northern Europe (especially in Scandinavia) as well as in Northern America. The research project aimed at filling some of the gaps emerged from the literature review, especially in terms of performance and durability. Specifically, the project mainly focused on the laboratory characterization of the bio-binders properties, including chemistry, morphology, rheology, aging susceptibility, adhesion with aggregates, moisture susceptibility and recycling aspects. A preliminary performance-based characterization of the resulting bio-asphalt mixtures was also included in the project.

The first part of the project focused on the chemical, morphological and rheological characterization of the bio-binders, considering different bitumen replacement percentages, i.e. 0, 5, 10 and 15 %. The chemical analyses highlighted that the bio-oil is rich in ester functional groups and resin fractions, and bitumen and bio-oil undergo a mere physical blending when mixed together (without any chemical reaction). The morphological analysis showed that the bio-binders are perfectly homogeneous, and thus no issues in terms of blending energy and storage stability are expected. From the mechanical point of view, the

bio-oil provides a softening effect, reducing the softening point, the viscosity and the complex modulus while increasing the penetration grade and the phase angle. A Newtonian behaviour, an unchanged temperature susceptibility and a thermo-rheological simple behaviour were observed up to 15% bitumen replacement. In addition, parallel activities demonstrated that the bio-binders do not have a negative impact on HSE and can be carbon neutral in terms of carbon footprint. Overall, these findings indicate that the bio-oil examined is suitable to be used in partial replacement of bitumen for road pavements and the resulting bio-binders (soft) could be used, for instance, in cold climates or as fresh binders in the recycling of reclaimed asphalt.

In the second part of the project, focused on the aging properties of the bio-binders, the base bitumen and the bio-binders containing 5, 10 and 15 % bio-oil were short- and long-term aged in the laboratory with RTFOT and PAV equipment. The bio-binder with 10% bio-oil was compared with a conventional bitumen with similar penetration grade. The results of the chemical and rheological tests carried out indicated that the aging susceptibility of the binder decreases as the bio-oil content increases, and the bio-binders studied may have similar or even higher aging resistance as compared to conventional bitumens with similar penetration grade. The aging resistance improvement can be attributed to the chemical peculiarities of the bio-oil. Moreover, from the performance point of view, the permanent deformation resistance and fatigue resistance of the bio-binder with 10% bio-oil were found to be comparable to those observed for the conventional bitumen having similar penetration grade, without any penalisation. Therefore, it is expected that the bio-binders studied may have comparable or even better durability and long-term performance with respect to traditional bitumens.

The investigation on the adhesion between bio-binders and aggregates and the moisture susceptibility of bio-binder/aggregate systems was carried out through BBS tests on the base bitumen and the bio-binders with 5, 10 and 15 % bio-oil, considering three aging conditions (unaged, RTFOT-aged, PAV-aged), two aggregate substrates with different bitumen affinity (limestone and porphyry) and two types of conditioning (dry and wet). Most binder-aggregate systems exhibited a purely cohesive failure, indicating good affinity between bio-binders and aggregates. For the porphyry substrate, a progressive transition from adhesive to cohesive failures and a less detrimental effect of water on the bond strength were observed as the bio-oil content increased, suggesting that the bio-oil may improve the bond strength between bitumen and siliceous aggregates in the presence of water. This effect is mainly ascribable to the strong presence of esters in the bio-oil. Therefore, the partial replacement of bitumen with the bio-oil in question could lead to binders with enhanced moisture damage resistance (and thus durability).

The fourth part of the project aimed at assessing the effectiveness of bio-binders in the hot recycling of bitumen from reclaimed asphalt and evaluating the recyclability potential of bio-binders. Four blends simulating the binders resulting from hot recycling of asphalt were prepared by combining two severely aged binders (one bitumen recovered from reclaimed asphalt and one laboratory-aged bio-binder) and two fresh binders (the bio-binder with 10% bio-oil and the corresponding conventional bitumen). The blends were also short- and long-term aged to reproduce the binder properties immediately after laying of hot recycled asphalt and after 10-15 years of in-service life of hot recycled asphalt, respectively. The mechanical and chemical tests carried out indicated that the blends containing the bio-binder undergo lower aging than the corresponding blends containing the conventional

bitumen. Consequently, the use of bio-binders in the hot recycling of reclaimed asphalt as well as the hot recycling of reclaimed bio-asphalt may lead to mixtures less susceptible to cracking, thanks to the lower aging rate of the binder. Overall, these findings suggest that the bio-binders studied are effective in the hot recycling of typical reclaimed asphalt and 100% recyclable.

The final part of the research project aimed at comparing a selected bio-asphalt mixture (prepared with the bio-binder containing 10% bio-oil) and the corresponding traditional asphalt mixture in terms of viscoelastic properties and fatigue behaviour. The two mixtures were laboratory-mixed and laboratory-compacted, and the only difference between them was the binder type. The effect of long-term aging was assessed by oven aging the test specimens. All mixtures were subjected to complex modulus tests and cyclic fatigue tests, and the results were analysed according to the VECD theory. It was found that, in short-term aged conditions, the bio-asphalt mixture may be slightly stiffer and thus more prone to fatigue cracking than the control mixture due to a possible over-aging during mixing, short-term aging and compaction caused by the effects of high temperatures. Nevertheless, the long-term aging susceptibility of the bio-asphalt mix appeared to be less severe as compared to the control mix, with potential fatigue performance benefits in the long term. However, before drawing final conclusions on the fatigue behaviour of the bio-asphalt mix, additional tests should be performed to expand the amount of data available.

The results obtained are very promising and suggest that the use of these bio-binders can be beneficial not only from the environmental point of view, but also in terms of performance and durability. The investigation of the low-temperature performance and the UV aging of the bio-binders would probably complete the picture at the binder level (which is already well defined). At the mixture level, instead, in order to fully understand the mechanical behaviour of the bio-asphalt mixtures, other aspects should be studied, including the rutting performance and the moisture susceptibility. Recycled mixtures prepared with the bio-binder as fresh binder should also be studied. Based on the materials properties, predictions of the pavement performance could be performed through specific softwares to compare scenarios with bio-asphalt mixes and traditional asphalt mixes. In addition, the monitoring and analysis of the full-scale field trials already existing in Sweden could provide extremely valuable data on the long-term performance and durability of asphalt pavements constructed with bio-asphalt mixtures. The construction of new trial sections (for instance in Italy) is also recommended, with the final goal of understanding whether bio-based products can truly be alternative to the traditional bituminous ones. Finally, the HSE impact and the life cycle assessment of the bio-binders are aspects that must be deepened in the future.

The approach adopted to characterize these specific bio-binders can be used again in the future to investigate also other similar materials. Some of the results presented (e.g. the link between the mechanical properties of the bio-binders and their composition) can be already considered a step towards the generalization of the results of this PhD project.

# References

AASHTO PP 99, 2019. Standard practice for preparation of small cylindrical performance test specimens using the Superpave gyratory compactor (SGC) or field cores.

AASHTO R 30, 2015. Standard practice for mixture conditioning of hot mix asphalt (HMA).

AASHTO T 361, 2016. Standard method of test for determining asphalt binder bond strength by means of the binder bond strength (BBS) test.

AASHTO TP 132, 2019. Standard method of test for determining the dynamic modulus for asphalt mixtures using small specimens in the Asphalt Mixture Performance Tester (AMPT).

AASHTO TP 133, 2019. Standard method of test for determining the damage characteristic curve and failure criterion using small specimens in the Asphalt Mixture Performance Tester (AMPT) cyclic fatigue test.

Abdullahi Ahmad, K., Ezree Abdullah, M., Abdul Hassan, N., Usman, N., Ambak, K., 2017. Investigating the feasibility of using jatropha curcas oil (JCO) as bio based rejuvenator in reclaimed asphalt pavement (RAP). MATEC Web of Conferences 103, 09013.

Abiola, O.S., Kupolati, W.K., Sadiku, E.R., Ndambuki, J.M., 2014. Utilisation of natural fibre as modifier in bituminous mixes: A review. Construction and Building Materials, 54, 305-312.

Ahmad, K.A., Abdullah, M.E., Hassan, N.A., Usman, N., Mohd Hassan, M.R., Bilema, M.A.M., Saeed, S.M., Batari, A., 2018. Effect of bio based rejuvenator on mix design, energy consumption and GHG emission of high RAP mixture. IOP Conference Series: Earth and Environmental Science, 140 (1), 012086.

Airey, G.D., Grenfell, G.R.A., Apeagyei, A., Subhy, A., Lo Presti, D., 2016. Time dependent viscoelastic rheological response of pure, modified and synthetic bituminous binders. Mechanics of Time-Dependent Materials, 20, 455-480.

Airey, G.D., 2002. Use of Black diagrams to identify inconsistencies in rheological data. Road Materials and Pavement Design, 3 (4), 403-424.

Alavi, M.Z., Hajj, E.Y., Morian, N.E., 2013. Approach for quantifying the effect of binder oxidative aging on the viscoelastic properties of asphalt mixtures. Transportation Research Record, 2373 (1), 109-120.

Andersson-Sköld, Y., Andersson, K., Lind, B., Claesson, A., Larsson, L., Suer, P., Jacobson, T., 2007. Coal tar-containing asphalt: Resource or hazardous waste? Journal of Industrial Ecology, 11 (4), 99-116.

ASTM D2493, 2016. Standard practice for viscosity-temperature chart for asphalt binders.

ASTM D4402, 2015. Standard test method for viscosity determination of asphalt at elevated temperatures using a rotational viscometer.

Anderson, D.A., Christensen, D.W., Bahia, H.U., Dongre, R., Sharma, M.G., Antle, C.E., Button, J., 1994. Binder characterization and evaluation, volume 3: physical characterization. SHRP Report A-369, Strategic Highway Research Program, National Research Council, Washington DC, USA.

Angelone, S., Cauhapé Casaux, M., Borghi, M., Martinez, F.O., 2016. Green pavements: reuse of plastic waste in asphalt mixtures. Materials and Structures, 49, 1655-1665.

Azahar, W.N.A.W., Bujang, M., Jaya, R.P., Hainin, M.R., Mohamed, A., Ngadi, N., Jayanti, D.S., 2016. The potential of waste cooking oil as bio-asphalt for alternative binder – an overview. Jurnal Teknologi, 78 (4), 111-116.

Babadopulos, L.F.A.L., Soares, J.B., Ferreira, J.L.S., do Nascimento, L.A.H., 2018. Fatigue cracking simulation of aged asphalt pavements using a viscoelastic continuum damage model. Road Materials and Pavement Design, 19 (3), 546-560.

Babadopulos, L.F.A.L., Sauzéat, C., Di Benedetto, H., 2017. Softening and local self-heating of bituminous mixtures during cyclic loading. Road Materials and Pavement Design, 18, 164-177.

Bahia, H.U., Moraes, R., Velasquez, R., 2012. The effect of bitumen stiffness on the adhesive strength measured by Bitumen Bond Strength test. 5th Eurasphalt & Eurobitume Congress, Istanbul, Turkey.

Bahia, H.U., Hanson, D.I., Zeng, M., Zhai, H., Khatri, M.A., Anderson, R.M., 2001. Characterization of modified asphalt binders in Superpave mix design. NCHRP Report 459, Transportation Research Board, Washington DC, USA.

Bal, C., Ağiş, E.R., Büyükşekerci, M., Gündüzöz, M., Tutkun, L., Yilmaz, O.H., 2018. Occupational exposure to asphalt fume can cause oxidative DNA damage among road paving workers. American Journal of Industrial Medicine, 61 (6), 471-476.

Balaguera, A., Carvajal, G.I., Albertí, J., Fullana-i-Palmer, P., 2018. Life cycle assessment of road construction alternative materials: A literature review. Resources, Conservation and Recycling, 132, 37-48.

Ball, G.F.A., Herrington, P.A., Patrick, J.E., 1993. Tall oil pitch as bitumen extender. New Zealand Journal of Forestry Science, 23 (2), 236-242.

Batista, K.B., Padilha, R.P.L., Castro, T.O., Silva, C.F.S.C., Araújo, M.F.A.S., Leite, L.F.M., Pasa, V.M.D., Lins, V.F.C., 2018. High-temperature, low-temperature and weathering aging performance of lignin modified asphalt binders. Industrial Crops and Products, 111, 107-116.

Bearsley, S.R., Haverkamp, R.G., 2007a. Age hardening potential of tall oil pitch modified bitumen. Road Materials and Pavement Design, 8 (3), 467-481.

Bearsley, S.R., Haverkamp, R.G., 2007b. Adhesive properties of tall oil pitch modified bitumen. Road Materials and Pavement Design, 8 (3), 449-465.

Behnood, A., 2019. Application of rejuvenators to improve the rheological and mechanical properties of asphalt binders and mixtures: A review. Journal of Cleaner Production, 231, 171-182.

Bhasin, A., Little, D.N., Vasconcelos, K.L., Masad, E., 2007. Surface free energy to identify moisture sensitivity of materials for asphalt mixes. Transportation Research Record, 2001, 37-45.

Bhasin, A., Masad, E., Little, D.N., Lytton, R., 2006. Limits on adhesive bond energy for improved resistance of hot-mix asphalt to moisture damage. Transportation Research Record, 1970, 3-13.

Binet, S., Pfohl-Leszkowicz, A., Brandt, H., Lafontaine, M., Castegnaro, M., 2002. Bitumen fumes: Review of work on the potential risk to workers and the present knowledge on its origin. Science of the Total Environment, 300 (1-3), 37-49.

Blanc, J., Hornych, P., Sotoodeh-Nia, Z., Williams, C., Porot, L., Pouget, S., Boysen, R., Planche, J.P., Lo Presti, D., Jimenez, A., Chailleux, E., 2019a. Full-scale validation of bio-recycled asphalt mixtures for road pavements. Journal of Cleaner Production, 227, 1068-1078.

Blanc, J., Chailleux, E., Hornych, P., Williams, R.C., Lo Presti, D., Jimenez del Barco Carrion, A., Porot, L., Planche, J.-P., Pouget, S., 2019b. Bio materials with reclaimed asphalt: from lab mixes properties to non-damaged full scale monitoring and mechanical simulation. Road Materials and Pavement Design, 20 (sup1), S95-S111.

Boffetta, P., Jourenkova, N., Gustavsson, P., 1997. Cancer risk from occupational and environmental exposure to polycyclic aromatic hydrocarbons. Cancer Causes and Control, 8 (3), 444-472.

Bowers, B.F., Huang, B., Shu, X., 2014. Refining laboratory procedure for artificial RAP: A comparative study. Construction and Building Materials, 52, 385-390.

Brundtland, G.H., 1987. Our common future. Report of the World Commission on Environment and Development, Oxford University Press, Oxford.

Cai, X., Zhang, J., Xu, G., Gong, M., Chen, X., Yang, J., 2019. Internal aging indexes to characterize the aging behavior of two bio-rejuvenated asphalts. Journal of Cleaner Production, 220, 1231-1238.

Canestrari, F., Ferrotti, G., Cardone, F., Stimilli, A., 2014. Innovative testing protocol for evaluation of binder-reclaimed aggregate bond strength. Transportation Research Record, 2444, 63-70.

Canestrari, F., Cardone, F., Graziani, A., Santagata, F.A., Bahia, H.U., 2010. Adhesive and cohesive properties of asphalt-aggregate systems subjected to moisture damage. Road Materials and Pavement Design, 11 (sup 1), 11-32.

Cao, W., Wang, Y., Wang, C., 2019. Fatigue characterization of bio-modified asphalt binders under various laboratory aging conditions. Construction and Building Materials, 208, 686-696.

Cardone, F., Ferrotti, G., Frigio, F., Canestrari, F., 2014. Influence of polymer modification on asphalt binder dynamic and steady flow viscosities. Construction and Building Materials, 71, 435-443.

Cashman, S.A., Moran, K.M., Gaglione, A.G., 2015. Greenhouse gas and energy life cycle assessment of pine chemicals derived from crude tall oil and their substitutes. Journal of Industrial Ecology, 20 (5), 1108–1121.

Cavalli, M.C., Zaumanis, M., Mazza, E., Partl, M.N., Poulikakos, L.D., 2018a. Aging effect on rheology and cracking behaviour of reclaimed binder with bio-based rejuvenators. Journal of Cleaner Production, 189, 88-97.

Cavalli, M.C., Zaumanis, M., Mazza, E., Partl, M.N., Poulikakos, L.D., 2018b. Effect of ageing on the mechanical and chemical properties of binder from RAP treated with bio-based rejuvenators. Composites Part B, 141, 174-181.

Çelik, A., Yildirim, S., Ekinci, S.Y., Taşdelen, B., 2013. Bio-monitoring for the genotoxic assessment in road construction workers as determined by the buccal micronucleus cytome assay. Ecotoxicology and Environmental Safety, 92, 265-270.

CEN/TR 16970, 2016. Sustainability of construction works - Guidance for the implementation of EN 15804.

Chailleux, E., Audo, M., Bujoli, B., Queffelec, C., Legrand, J., Lepine, O., 2012. Alternative binder from microalgae – Algoroute Project. Transportation Research Circular E-C165, 7-14.

Chaturabong, P., Bahia, H.U., 2018. Effect of moisture on the cohesion of asphalt mastics and bonding with surface of aggregates. Road Materials and Pavement Design, 19 (3), 741-753.

Chauhan, S.K., Sharma, S., Shukla, A., Gangopadhyay, S., 2010. Recent trends of the emission characteristics from the road construction industry. Environmental Science and Pollution Research, 17 (9), 1493-1501.

Chehab, G. R., Kim, Y. R., Schapery, R. A., Witczak, M. W., Bonaquist, R., 2002. Time-temperature superposition principle for asphalt concrete with growing damage in tension state. Journal of the Association of Asphalt Paving Technologists, 71, 559-593.

Christensen, D.W., Pellinen, T., Bonaquist, R.F., 2003. Hirsch model for estimating the modulus of asphalt concrete. Journal of the Association of Asphalt Paving Technologists, 72, 97-121.

Cooper III, S.B., Mohammad, L.N., Elseifi, M., 2013. Evaluation of asphalt mixtures containing renewable binder technologies. International Journal of Pavement Research and Technology, 6 (5), 570-575.

Daniel, J. S., Kim, Y. R., 2002. Development of a simplified fatigue test and analysis procedure using a viscoelastic damage model. Journal of the Association of Asphalt Paving Technologists, 71, 619-650.

Di Benedetto, H., Nguyen, Q.T., Sauzéat, C., 2011. Nonlinearity, heating, fatigue and thixotropy during cyclic loading of asphalt mixtures. Road Materials and Pavement Design, 12 (1), 129-158.

Di Benedetto, H., de La Roche, C., Baaj, H., Pronk, A., Lundström, R., 2004. Fatigue of bituminous mixtures. Materials and Structures, 37, 202-216.

Eberhardsteiner, L., Füssl, J., Hofko, B., Handle, F., Hospodka, M., Blab, R., Grothe, H., 2015. Influence of asphaltene content on mechanical bitumen behaviour: experimental investigation and micromechanichal modeling. Materials and Structures, 48 (10), 3099-3112.

EN 12591, 2009. Bitumen and bituminous binders – Specifications for paving grade bitumens.

EN 12595, 2015. Bitumen and bituminous binders – Determination of kinematic viscosity.

EN 12607-1, 2015. Bitumen and bituminous binders – Determination of the resistance to hardening under influence of heat and air - Part 1: RTFOT method.

EN 12697-3, 2018. Bituminous mixtures – Test methods – Part 3: Bitumen recovery: Rotary evaporator.

EN 12697-6, 2020. Bituminous mixtures – Test methods – Part 6: Determination of bulk density of bituminous specimens.

EN 12697-11, 2012. Bituminous mixtures - Test methods for hot mix asphalt - Part 11: Determination of the affinity between aggregate and bitumen.

EN 12697-12, 2018. Bituminous mixtures - Test methods - Part 12: Determination of the water sensitivity of bituminous specimens.

EN 12697-24, 2018. Bituminous mixtures - Test methods - Part 24: Resistance to fatigue.

EN 1426, 2015. Bitumen and bituminous binders – Determination of needle penetration.

EN 1427, 2015. Bitumen and bituminous binders – Determination of the softening point – Ring and Ball method.

EN 14769, 2013. Bitumen and bituminous binders – Accelerated long-term ageing conditioning by a Pressure Ageing Vessel (PAV).

EN 14770, 2012. Bitumen and bituminous binders – Determination of complex shear modulus and phase angle – Dynamic Shear Rheometer (DSR).

EN 15804, 2012. Sustainability of construction works — Environmental product declarations — Core rules for the product category of construction products.

EN 16659, 2015. Bitumen and bituminous binders – Multiple Stress Creep and Recovery Test (MSCRT).

Eurobitume, 2012. Life cycle inventory: bitumen. European Bitumen Association, Brussels, Belgium.

Farina, A., Zanetti, M.C., Sanatagata, E., Blengini, G.A., 2017. Life cycle assessment applied to bituminous mixtures containing recycled materials: Crumb rubber and reclaimed asphalt pavement. Resources, Conservation and Recycling, 117, 204-212.

Fernandes, S., Peralta, J., Oliveira, J.R.M., Williams, R.C., Silva, H.M.R.D., 2017. Improving asphalt mixture performance by partially replacing bitumen with waste motor oil and elastomer modifiers. Applied Sciences, 7 (8), 794.

Ferrotti, G., Ragni, D., Lu, X., Canestrari, F., 2017. Effect of warm mix asphalt chemical additives on the mechanical performance of asphalt binders. Materials and Structures, 50, 226.

Fini, E.H., Al-Qadi, I.L., You, Z., Zada, B., Mills-Beale, J., 2012. Partial replacement of asphalt binder with bio-binder: characterisation and modification. International Journal of Pavement Engineering, 13 (6), 515-522.

Fini, E.H., Kalberer, E.W., Shahbazi, A., Basti, M., You, Z., Ozer, H., Aurangzeb, Q., 2011. Chemical characterization of biobinder from swine manure: Sustainable modifier for asphalt binder. Journal of Materials in Civil Engineering, 23 (11), 1506-1513.

Frigio, F., Canestrari, F., 2018. Characterisation of warm recycled porous asphalt mixtures prepared with different WMA additives. European Journal of Environmental and Civil Engineering, 22 (1), 82-98.

Fromm, H.J., 1974. The mechanisms of asphalt stripping from aggregate surface. Journal of the Association of Asphalt Paving Technologists, 43, 191-223.

Garcia, A., Schlangen, E., Van de Ven, M., Sierra-Beltran, G., 2010. Preparation of capsules containing rejuvenators for their use in asphalt concrete. Journal of Hazardous Materials, 184 (1-3), 603–611.

Gaudenzi, E., Cardone, F., Lu, X., Canestrari, F., 2020. Analysis of fatigue and healing properties of conventional bitumen and bio-binder for road pavements. Materials, 13, 420.

Geissdoerfer, M., Savaget, P., Bocken, N.M.P., Hultink, E.J., 2017. The circular economy – a new sustainability paradigm? Journal of Cleaner Production, 143, 757-768.

Ghisellini, P., Ji, X., Liu, G., Ulgiati, S., 2018. Evaluating the transition towards cleaner production in the construction and demolition sector of China: A review. Journal of Cleaner Production, 195, 418-434.

Giani, M.I., Dotelli, G., Brandini, N., Zampori, L., 2015. Comparative life cycle assessment of asphalt pavements using reclaimed asphalt, warm mix technology and cold in-place recycling. Resources, Conservation and Recycling, 104, 224-238.

Gjessing, E., Lygren, E., Berglind, L., Gulbrandsen, T., Skanne, R., 1984. Effect of highway runoff on lake water quality. Science of the Total Environment, 33 (1-4), 245-257.

Godenzoni, C., Graziani, A., Bocci, E., Bocci, M., 2018. The evolution of the mechanical behaviour of cold recycled mixtures stabilised with cement and bitumen: field and laboratory study. Road Materials and Pavement Design, 19 (4), 856-877.

Gondim, L.M., Soares, S.A., Barroso, S.H.A., 2016. Petroleum plant sap as an asphalt modifier for pavement applications. International Journal of Engineering & Technology IJCEE-IJENS, 16, 6.

Gong, M., Zhu, H., Pauli, T., Yang, J., Wei, J., Yao, Z., 2017. Evaluation of bio-binder modified asphalt's adhesion behavior using sessile drop device and atomic force microscopy. Construction and Building Materials, 145, 42-51.

Gong, M., Yang, J., Zhang, J., Zhu, H., Tong, T., 2016. Physical-chemical properties of aged asphalt rejuvenated by bio-oil derived from biodiesel residue. Construction and Building Materials, 105, 35-45.

Graziani, A., Virgili, A., Cardone, F., 2018. Testing the bond strength between cold bitumen emulsion composites and aggregate substrate. Materials and Structures, 51, 14.

Grilli, A., Bocci, E., Bocci, M., 2016. Hot recycling of reclaimed asphalt using a bio-based additive. RILEM Bookseries, 11, 953-964.

He, M., Tu, C., Cao, D.W., Chen, Y.J., 2019. Comparative analysis of bio-binder properties derived from different sources. International Journal of Pavement Engineering, 20 (7), 792-800.

Heikkilä, P.R., Väänänen, V., Hämeilä, M., Linnainmaa, K., 2003. Mutagenicity of bitumen and asphalt fumes. Toxicology in Vitro, 17 (4), 403-412.

Hendrickson, C., Horvath, A., 2000. Resource use and environmental emissions of U.S. construction sectors. Journal of Construction Engineering and Management, 126 (1), 38-44.

Hofko, B., Porot, L., Falchetto Cannone, A., Poulikakos, L., Huber, L., Lu, X., Mollenhauer, K., Grothe, H., 2018. FTIR spectral analysis of bituminous binders: reproducibility and impact of ageing temperature, Materials and Structures, 51, 45.

Hofko, B., Alavi, M.Z., Grothe, H., Jones, D., Harvey, J., 2017. Repeatability and sensitivity of FTIR ATR spectral analysis methods for bituminous binders. Materials and Structures, 50, 187.

Hu, X., Walubita, L.F., 2009. Modelling tensile strain response in asphalt pavements: Bottom-up and/or top-down fatigue crack initiation. Road Materials and Pavement Design, 10 (1), 125-154.

Hunter, R.N., Self, A., Read, J., 2015. The Shell Bitumen Handbook, sixth edition, Thomas Telford Ltd.

Ingrassia, L.P., Lu, X., Ferrotti, G., Canestrari, F., 2020a. Chemical, morphological and rheological characterization of bitumen partially replaced with wood bio-oil: Towards more sustainable materials in road pavements. Journal of Traffic and Transportation Engineering (English Edition), 7 (2), 192-204.

Ingrassia, L.P., Lu, X., Ferrotti, G., Conti, C., Canestrari, F., 2020b. Investigating the "circular propensity" of road bio-binders: Effectiveness in hot recycling of reclaimed asphalt and recyclability potential. Journal of Cleaner Production, 255, 120193.

Ingrassia, L.P., Lu, X., Ferrotti, G., Canestrari, F., 2019a. Renewable materials in bituminous binders and mixtures: Speculative pretext or reliable opportunity? Resources, Conservation and Recycling, 144, 209-222.

Ingrassia, L.P., Lu, X., Ferrotti, G., Canestrari, F., 2019b. Chemical and rheological investigation on the short- and long-term aging properties of bio-binders for road pavements. Construction and Building Materials, 217, 518-529.

Ingrassia, L.P., Cardone, F., Canestrari, F., Lu, X., 2019c. Experimental investigation on the bond strength between sustainable road bio-binders and aggregate substrates. Materials and Structures, 52 (4), 80.

IP 469/01, 2006. Determination of saturated, aromatic and polar compounds in petroleum products by thin layer chromatography and flame ionization detection.

Jiménez del Barco Carrión, A., Carvajal-Muñoz, J.S., Lo Presti, D., Airey, G., 2019. Intrinsic adhesive and cohesive assessment of the moisture sensitivity of bio-rejuvenated recycled asphalt binders. Road Materials and Pavement Design, 20 (sup1), S347-S364.

Jimenez del Barco-Carrion, A., Lo Presti, D., Pouget, S., Airey, G.D., Chailleux, E., 2017a. Linear viscoelastic properties of high reclaimed asphalt content mixes with biobinders. Road Materials and Pavement Design, 18, 1-11.

Jimenez del Barco-Carrion, A., Perez-Martinez, M., Themeli, A., Lo Presti, D., Marsac, P., Pouget, S., Hammoum, F., Chailleux, E., Airey, G.D., 2017b. Evaluation of bio-materials' rejuvenating effect on binders for high-reclaimed asphalt content mixtures. Materiales de Construccion, 67 (327).

Jiménez del Barco Carrión, A., Lo Presti, D., Pouget, S., Chailleux, E., Airey, G.D., 2017c. Toward non-petroleum-derived asphalt mixes: Using biobinders for high-modulus asphalt mixes with high reclaimed asphalt content. Transportation Research Board 96th Annual Meeting, Washington DC, 8-12 January 2017.

Jullien, A., Monéron, P., Quaranta, G., Gaillard, D., 2006. Air emissions from pavement layers composed of varying rates of reclaimed asphalt. Resources, Conservation and Recycling, 47 (4), 356-374.

Kandhal, P.S., 1994. Field and laboratory investigation of stripping in asphalt pavements: state of the art report. Transportation Research Record, 1454, 36-47.

Kanitpong, K., Bahia, H.U., 2005. Relating adhesion and cohesion of asphalts to the effect of moisture on laboratory performance of asphalt mixtures. Transportation Research Record, 1901, 33-43.

Kanitpong, K., Bahia, H.U., 2003. Role of adhesion and thin film tackiness of asphalt binders in moisture damage of HMA. Journal of the Association of Asphalt Paving Technologists, 72, 502-528.

Kennedy, T.W., Huber, G.A., Harrigan, E.T., Cominsky, R.J., Hughes, C.S., Von Quintus, H., Moulthrop, J.S., 1994. Superior performing asphalt pavements (Superpave): the product

of the SHRP Asphalt Research Program. SHRP Report A-410, Strategic Highway Research Program, National Research Council, Washington DC, USA.

Kluttz, R., 2012. Considerations for use of alternative binders in asphalt pavements – Material characteristics. Transportation Research Circular E-C165, 2-6.

Kocher, B., Wessolek, G., Stoffregen, H., 2005. Water and heavy metal transport in roadside soils. Pedosphere, 15 (6), 746-753.

Kowalski, K.J., Król, J.B., Bańkowski, W., Radziszewski, P., Sarnowski, M., 2017. Thermal and fatigue evaluation of asphalt mixtures containing RAP treated with a bio-agent. Applied Sciences (Switzerland), 7 (3), 216.

Kowalski, K.J., Krol, J., Radziszewski, P., Casado, R., Blanco, V., Perez, D., Viñas, V.M., Brijsse, Y., Frosch, M., Le, D.M., Wayman, M., 2016. Eco-friendly materials for a new concept of asphalt pavement. Transportation Research Procedia, 14, 3582-3591.

Krol, J.B., Kowalski, K.J., Niczke, L., Radziszewski, P., 2016. Effect of bitumen fluxing using a bio-origin additive. Construction and Building Materials, 114, 194-203.

Kucukvar, M., Tatari, O., 2013. Towards a triple bottom-line sustainability assessment of the U.S. construction industry. International Journal of Life Cycle Assessment, 18 (5), 958-972.

Lamontagne, J., Dumas, P., Mouillet, V., Kister, J., 2001. Comparison by Fourier transform infrared (FTIR) spectroscopy of different ageing techniques: application to road bitumens, Fuel 80 (4), 483-488.

Lei, Z., Bahia, H.U., Yi-qiu, T., Ling, C., 2017. Effect of refined waste and bio-based oil modifiers on rheological properties of asphalt binders. Construction and Building Materials, 148, 504-511.

Lindberg, H.K., Väänänen, V., Järventaus, H., Suhonen, S., Nygren, J., Hämeilä, M., Valtonen, J., Heikkilä, P., Norppa, H., 2008. Genotoxic effects of fumes from asphalt modified with waste plastic and tall oil pitch. Mutation Research - Genetic Toxicology and Environmental Mutagenesis, 653 (1-2), 82-90.

Lo Presti, D., Vasconcelos, K., Orešković, M., Pires, G.M., Bressi, S., 2020. On the degree of binder activity of reclaimed asphalt and degree of blending with recycling agents. Road Materials and Pavement Design, 21 (8), 2071-2090.

Lu, G., Liu, P., Wang, Y., Faßbender, S., Wang, D., Oeser, M., 2019a. Development of a sustainable pervious pavement material using recycled ceramic aggregate and bio-based polyurethane binder, Journal of Cleaner Production, 220, 1052-1060.

Lu, D.X., Saleh, M., Nguyen, N.H.T., 2019b. Effect of rejuvenator and mixing methods on behaviour of warm mix asphalt containing high RAP content. Construction and Building Materials, 197, 792-802.

Lu, X., Robertus, C., Ostlund, J.-A., 2020. Bituminous binders extended with a renewable plant-based oil: towards a carbon neutral bitumen. Proceedings of the 2020 LJMU Annual

International Conference on Highways and Airport Pavement Engineering, Asphalt Technology, and Infrastructure, Liverpool, UK.

Lu, X., Sjövall, P., Soenen, H., 2017. Structural and chemical analysis of bitumen using time-of-flight secondary ion mass spectrometry (TOF-SIMS), Fuel, 199, 206-218.

Lu, X., Isacsson, U., 2002. Effect of ageing on bitumen chemistry and rheology. Construction and Building Materials, 16, 15-22.

Lu, X., Isacsson, U., 2000. Artificial aging of polymer modified bitumens. Journal of Applied Polymer Science, 76, 1811-1824.

Lundström, R., Di Benedetto, H., Isacsson, U., 2004a. Influence of asphalt mixture stiffness on fatigue failure. Journal of Materials in Civil Engineering, 16, 516-525.

Lundström, R., Ekblad, J., Isacsson, U., 2004b. Influence of hysteretic heating on asphalt fatigue characterization. Journal of Testing and Evaluation, 32 (6), 484-493.

Luo, X., Gu, F., Zhang, Y., Lytton, R.L., Birgisson, B., 2018. Kinetics-based aging evaluation of in-service recycled asphalt pavement. Journal of Cleaner Production, 200, 934-944.

Luo, X., Zhang, Y., Lytton, R.L., 2016. Implementation of pseudo J-integral based Paris' law for fatigue cracking in asphalt mixtures and pavements. Materials and Structures, 49 (9), 3713-3732.

Luo, X., Luo, R., Lytton, R.L., 2013. Modified Paris's law to predict entire crack growth in asphalt mixtures. Transportation Research Record, 2373, 54-62.

Lygren, E., Gjessing, E., Berglind, L., 1984. Pollution transport from a highway. Science of the Total Environment, 33 (1-4), 147-159.

Mangiafico, S., Di Benedetto, H., Sauzéat, C., Olard, F., Pouget, S., Planque, L. 2016. Effect of colloidal structure of bituminous binder blends on linear viscoelastic behaviour of mixtures containing Reclaimed Asphalt Pavement. Materials and Design, 111, 126-139.

Mangiafico, S., Sauzéat, C., Di Benedetto, H., Pouget, S., Olard, F., Planque, L., 2015. Quantification of biasing effects during fatigue tests on asphalt mixes: Non-linearity, self-heating and thixotropy. Road Materials and Pavement Design, 16 (sup 2), 143-180.

Marsac, P., Piérard, N., Porot, L., Van den bergh, W., Grenfell, J., Mouillet, V., Pouget, S., Besamusca, J., Farcas, F., Gabet, T., Hugener, M., 2014. Potential and limits of FTIR methods for reclaimed asphalt characterisation. Materials and Structures, 47, 1273-1286.

Mazzoni, G., Bocci, E., Canestrari, F., 2018. Influence of rejuvenators on bitumen ageing in hot recycled asphalt mixtures. Journal of Traffic and Transportation Engineering (English Edition), 5 (3), 157-168.

McCready, N.S., Williams, R.C., 2008. Utilization of biofuel coproducts as performance enhancers in asphalt binder. Transportation Research Record, 2051, 8-14.

Michalica, P., Kazatchkov, I.B., Stastna, J., Zanzotto, L., 2008. Relationship between chemical and rheological properties of two asphalts of different origins. Fuel, 87, 3247-3253.

Mogawer, W.S., Fini, E.H., Austerman, A.J., Booshehrian, A., Zada, B., 2016. Performance characteristics of high reclaimed asphalt pavement containing bio-modifier. Road Materials and Pavement Design, 17 (3), 753-767-

Moraes, R., Velasquez, R., Bahia, H.U., 2011. Measuring the effect of moisture on asphalt-aggregate bond with the bitumen bond strength test. Transportation Research Record, 2209, 70-81.

Norambuena-Contreras, J., Yalcin, E., Garcia, A., Al-Mansoori, T., Yilmaz, M., Hudson-Griffith, R., 2018. Effect of mixing and ageing on the mechanical and self-healing properties of asphalt mixtures containing polymeric capsules. Construction and Building Materials, 175, 254-266.

Oda, S., Leomar Fernandes Jr., J., Ildefonso, J.S., 2012. Analysis of use of natural fibers and asphalt rubber binder in discontinuous asphalt mixtures. Construction and Building Materials, 26 (1), 13-20.

Olard, F., Di Benedetto, H., 2003. General "2S2P1D" model and relation between the linear viscoelastic behaviours of bituminous binders and mixes. Road Materials and Pavement Design, 4 (2), 185-224.

Oldham, D.J., Fini, E.H., Chailleux, E., 2015. Application of a bio-binder as a rejuvenator for wet processed asphalt shingles in pavement construction. Construction and Building Materials, 86, 75-84.

Pan, T., 2012. A first-principles based chemophysical environment for studying lignins as an asphalt antioxidant. Construction and Building Materials, 36, 654-664.

Peralta, J., Williams, R.C., Silva, H.M.R.D., Machado, A.V.A., 2014. Recombination of asphalt with bio-asphalt: binder formulation and asphalt mixes application. Journal of the Association of Asphalt Paving Technologists, 83, 1-36.

Peralta, J., Williams, R.C., Silva, H.M.R.D., Machado, A.V., 2013. Combining Asphalt Rubber (AR) and fast-pyrolysis bio-oil to create a binder for flexible pavements. WASTES: solutions, treatments and opportunities (2nd International Conference), 11-13 September.

Peralta, J., Williams, R.C., Rover, M., Silva, H.M.R.D., 2012a. Development of rubber-modified fractionated bio-oil for use as noncrude petroleum binder in flexible pavements. Transportation Research Circular E-C165, 23-36.

Peralta, J., Raouf, M.A., Tang, S., Williams, R.C., 2012b. Bio-renewable asphalt modifiers and asphalt substitutes. Sustainable Bioenergy and Bioproducts, Green Energy and Technology, 89-115.

Perez-Martinez, M., Marsac, P., Gabet, T., Chailleux, E., 2016. Prediction of the mechanical properties of aged asphalt mixes from FTIR measurements. RILEM Bookseries, 11, 399-409.

Petersen, J.C., Glaser, R., 2011. Asphalt oxidation mechanisms and the role of oxidation products on age hardening revisited. Road Materials and Pavement Design, 12 (4), 795-819.

Petersen, J.C., 2009. A review of the fundamentals of asphalt oxidation, Transportation Research Circular E-C140.

Petersen, J.C., Plancher, H., 1998. Model studies and interpretative review of the competitive adsorption and water displacement of petroleum asphalt chemical functionalities on mineral aggregate surfaces. Petroleum Science and Technology, 16 (1-2), 89-131.

Plancher, H., Dorrence, S.M., Petersen, J.C., 1977. Identification of chemical types in asphalts strongly adsorbed at the asphalt-aggregate interface and their relative displacement by water. Journal of the Association of Asphalt Paving Technologists, 46, 151-175.

Podolsky, J.H., Buss, A., Williams, R.C., Cochran, E., 2016. Comparative performance of bio-derived/chemical additives in warm mix asphalt at low temperature. Materials and Structures, 49, 563-575.

Porot, L., Besamusca, J., Soenen, H., Apeagyei, A., Grenfell, J., Sybilski, D., 2016. Bitumen/aggregate affinity - rilem round robin test on rolling bottle test. RILEM Bookseries, 11, 153-164.

Pouget, S., Loup, F., 2013. Thermo-mechanical behaviour of mixtures containing bio-binders. Road Materials and Pavement Design, 14 (suppl 1), 212-226.

Poulikakos, L.D., Papadaskalopoulou, C., Hofko, B., Gschösser, F., Cannone Falchetto, A., Bueno, M., Arraigada, M., Sousa, J., Ruiz, R., Petit, C., Loizidou, M., Partl, M.N., 2017. Harvesting the unexplored potential of European waste materials for road construction. Resources, Conservation and Recycling, 116, 32-44.

Purinton, R.J., Manning, T.S., 1996. New role of HSE in chemical product development. International Conference on Health, Safety and Environment in Oil and Gas Exploration and Production, 1, 485-494.

Rad, F. Y., Elwardany, M.D., Castorena, C., Kim, Y.R., 2018. Evaluation of chemical and rheological aging indices to track oxidative aging of asphalt mixtures. Transportation Research Record, 2672 (28), 349-358.

Rad, F.Y., Elwardany, M.D., Castorena, C., Kim, Y.R., 2017. Investigation of proper long-term laboratory aging temperature for performance testing of asphalt concrete. Construction and Building Materials, 147, 616-629.

Ramalingam, S., Murugasan, R., Nagabhushana, M.N., 2017. Laboratory performance evaluation of environmentally sustainable sisal fibre reinforced bituminous mixes. Construction and Building Materials, 148, 22-29.

Raouf, M.A., Williams, R.C., 2010a. Temperature and shear susceptibility of a nonpetroleum binder as a pavement material. Transportation Research Record, 2180, 9-18.

Raouf, M.A., Williams, R.C., 2010b. General rheological properties of fractionated switchgrass bio-oil as a pavement material. Road Materials and Pavement Design, 11, 325-353.

Roberts, F.L., Kandhal, P.S., Brown, E.R., Lee, D-Y., Kennedy, T.W., 1996. Hot mix asphalt materials, mixture design, and construction, 2nd edition. National Center for Asphalt Technology, Lanham MD.

Roque, R., Birgisson, B., Sangpetngam, B., Zhang, Z., 2002. Hot mix asphalt fracture mechanics: A fundamental crack growth law for asphalt mixtures. Journal of the Association of Asphalt Paving Technologists, 71, 816-827.

Rubio, M.C., Martínez, G., Baena, L., Moreno, F., 2012. Warm Mix Asphalt: An overview. Journal of Cleaner Production, 24, 76-84.

Saleh, N.F., Keshavarzi, B., Rad, F.Y., Mocelin, D., Elwardany, M., Castorena, C., Underwood, B.S., Kim, Y.R., 2020. Effects of aging on asphalt mixture and pavement performance. Construction and Building Materials, 258, 120309.

Samieadel, A., Schimmel, K., Fini, E.H., 2018a. Comparative life cycle assessment (LCA) of bio-modified binder and conventional asphalt binder. Clean Technologies and Environmental Policy, 20, 191–200.

Samieadel, A., Oldham, D.J., Fini, E.H., 2018b. Investigating molecular conformation and packing of oxidized asphaltene molecules in presence of paraffin wax. Fuel, 220, 503-512.

Santos, J., Flintsch, G., Ferreira, A., 2017. Environmental and economic assessment of pavement construction and management practices for enhancing pavement sustainability. Resources, Conservation and Recycling, 116, 15-31.

Sayegh, G., 1967. Viscoelastic properties of bituminous mixtures. In: The Second International Conference on Structural design of Asphalt Pavement, Rackham Lecture Hall, University of Michigan, Ann Arbor, USA, 743–755.

Schapery, R., 1984. Correspondence principles and a generalized J-integral for large deformation and fracture analysis of viscoelastic media. International Journal of Fracture, 25 (3), 195-223.

Seidel, J.C., Haddock, J.E., 2012. Soy Fatty Acids as a sustainable modifier for asphalt binders. Transportation Research Circular E-C165, 15-22.

Shanbara, H.K., Ruddock, F., Atherton, W., 2018. A laboratory study of high-performance cold mix asphalt mixtures reinforced with natural and synthetic fibres. Construction and Building Materials, 172, 166-175.

Shirodkar, P., Mehta, Y., Nolan, A., Sonpal, K., Norton, A., Tomlinson, C., Dubois, E., Sullivan, P. Sauber, R., 2011. A study to determine the degree of partial blending of reclaimed asphalt pavement (RAP) binder for high RAP hot mix asphalt. Construction and Building Materials, 25, 150-155.

Singh-Ackbarali, D., Maharaj, R., Mohamed, N., Ramjattan-Harry, V., 2017. Potential of used frying oil in paving material: solution to environmental pollution problem. Environmental Science and Pollution Research, 24, 12220-12226.

Smith, B.C., 2011. Fundamentals of Fourier transform infrared spectroscopy, CRC Press, Boca Raton FL.

Soenen, H., Redelius, P., 2014. The effect of aromatic interactions on the elasticity of bituminous binders. Rheological Acta, 53, 741-754.

Somé, S.C., Pavoine, A., Chailleux, E., 2016. Evaluation of the potential use of waste sunflower and rapeseed oils-modified natural bitumen as binders for asphalt pavement design. International Journal of Pavement Research and Technology, 9, 368-375.

Stangl, K., Jäger, A., Lackner, R., 2006. Microstructure-based identification of bitumen performance. Road Materials and Pavement Design, 7 (sup 1), 111-142.

Stimilli, A., Virgili, A., Canestrari, F., 2017. Warm recycling of flexible pavements: Effectiveness of Warm Mix Asphalt additives on modified bitumen and mixture performance. Journal of Cleaner Production, 156, 911-922.

Stimilli, A., Virgili, A., Giuliani, F., Canestrari, F., 2016. In plant production of hot recycled mixtures with high reclaimed asphalt pavement content: a performance evaluation. RILEM Bookseries, 11, 927-939.

Stimilli, A., Virgili, A., Canestrari, F., 2015. New method to estimate the "re-activated" binder amount in recycled hot-mix asphalt. Road Materials and Pavement Design, 16, 442-459.

Stimilli, A., Ferrotti, G., Graziani, A., Canestrari, F., 2013. Performance evaluation of a cold-recycled mixture containing high percentage of reclaimed asphalt. Road Materials and Pavement Design, 14 (sup1), 149-161.

Su, J.-F., Qiu, J., Schlangen, E., Wang, Y.-Y., 2015. Investigation the possibility of a new approach of using microcapsules containing waste cooking oil: in situ rejuvenation for aged bitumen. Construction and Building Materials, 74, 83-92.

Sun, Z., Yi, J., Huang, Y., Feng, D., Guo, C., 2016. Properties of asphalt binder modified by bio-oil derived from waste cooking oil. Construction and Building Materials, 102, 496-504.

Tan, Y., Guo, M., 2013. Using surface free energy method to study the cohesion and adhesion of asphalt mastic. Construction and Building Materials, 47, 254-260.

Tarrer, A.R., Wagh, V., 1991. The effect of the physical and chemical characteristics of the aggregate on bonding. SHRP-A/UIR-91-507. Strategic Highway Research Program, National Research Council, Washington DC.

Taylor, M.A, Khosla, N.P., 1983. Stripping of asphalt pavements: state of the art. Transportation Research Record, 911, 150-158.

Tex-248-F, 2019. Test procedure for overlay test.

Thives, L.P., Ghisi, E., 2017. Asphalt mixtures emission and energy consumption: A review. Renewable and Sustainable Energy Reviews, 72, 473-484.

Underwood, B. S., Kim, Y. R., Guddati, M. N., 2010. Improved calculation method of damage parameter in viscoelastic continuum damage model. International Journal of Pavement Engineering, 11 (6), 459-476.

Väänänen, V., Elovaara, E., Nykyri, E., Santonen, T., Heikkilä, P., 2006. Road pavers' occupational exposure to asphalt containing waste plastic and tall oil pitch. Journal of Environmental Monitoring, 8 (1), 89-99.

Väänänen, V., Hämeilä, M., Kalliokoski, P., Nykyri, E., Heikkilä, P., 2005. Dermal exposure to polycyclic aromatic hydrocarbons among road pavers. Annals of Occupational Hygiene, 49 (2), 167-178.

Väänänen, V., Hämeilä, M., Kontsas, H., Peltonen, K., Heikkilä, P., 2003. Air concentrations and urinary metabolites of polycyclic aromatic hydrocarbons among paving and remixing workers. Journal of Environmental Monitoring, 5 (5), 739-746.

Vahčič, M., Milačič, R., Mladenovič, A., Murko, S., Zuliani, T., Zupančič, M., Ščančar, J., 2008. Leachability of Cr(VI) and other metals from asphalt composites with addition of filter dust. Waste Management, 28 (12), 2667-2674.

Van Bohemen, H.D., Van De Laak, W.H.J., 2003. The influence of road infrastructure and traffic on soil, water, and air quality. Environmental Management, 31 (1), 50-68.

Vassilev, S.V., Baxter, D., Andersen, L.K., Vassileva, C.G., 2010. An overview of the chemical composition of biomass. Fuel, 89, 913-933.

Wang, Y.D., Underwood, B.S., Kim, Y.R., 2020. Development of a fatigue index parameter, Sapp, for asphalt mixes using viscoelastic continuum damage theory. International Journal of Pavement Engineering, DOI: 10.1080/10298436.2020.1751844.

Wang, Y. D., Kim, Y. R., 2019. Development of a pseudo strain energy-based fatigue failure criterion for asphalt mixtures. International Journal of Pavement Engineering, 20 (10), 1182-1192.

Wang, C., Xue, L., Xie, W., You, Z., Yang, X., 2018. Laboratory investigation on chemical and rheological properties of bio-asphalt binders incorporating waste cooking oil. Construction and Building Materials, 167, 348-358.

Wen, H., Bhusal, S., Wen, B., 2012. Laboratory evaluation of waste cooking oil-based bioasphalt as a sustainable binder for Hot-Mix Asphalt. Transportation Research Circular E-C165, 49-60.

Williams, M.L., Landel, R.F., Ferry, J.D., 1955. The temperature dependence of relaxation mechanisms in amorphous polymers and other glass-forming liquids. Journal of the American Chemical Society, 77 (14), 3701–3707.

Xi, J., Zhu, Y., Yu, X., Wang, R., 2015. Study of blending mechanism of bio-binder and petroleum asphalt. International Conference on Chemical, Material and Food Engineering (CMFE-2015).

Xiao, F., Amirkhanian, S.N., 2009. Laboratory investigation of moisture damage in rubberised asphalt mixtures containing reclaimed asphalt pavement. International Journal of Pavement Engineering, 10 (5), 319-328.

Xie, S., Li, Q., Karki, P., Zhou, F., Yuan, J.S., 2017. Lignin as renewable and superior asphalt binder modifier. ACS Sustainable Chemistry and Engineering, 5 (4), 2817-2823.

Xu, G., Wang, H., Zhu, H., 2017. Rheological properties and anti-aging performance of asphalt binder modified with wood lignin. Construction and Building Materials, 151, 801-808.

Yang, X., Mills-Beale, J., You, Z., 2017. Chemical characterization and oxidative aging of bio-asphalt and its compatibility with petroleum asphalt. Journal of Cleaner Production, 142, 1837-1847.

Yang, X., You, Z., Mills-Beale, J., 2015. Asphalt binders blended with a high percentage of biobinders: aging mechanism using FTIR and rheology. Journal of Materials in Civil Engineering, 27 (4), 04014157.

Yang, X., You, Z., 2015. High temperature performance evaluation of bio-oil modified asphalt binders using the DSR and MSCR tests. Construction and Building Materials, 76, 380-387.

Yang, X., You, Z., Dai, Q., Mills-Beale, J., 2014. Mechanical performance of asphalt mixtures modified by bio-oils derived from waste wood resources. Construction and Building Materials, 51, 424-431.

You, Z., Mills-Beale, J., Yang, X., Dai, Q., 2012. Alternative Materials for Sustainable Transportation. Report RC-1591. Michigan Technological University1400 Townsend Drive Houghton, Michigan 49931.

Yusoff, N.I.M., Mounier, D., Marc-Stéphane, G., Hainin, M.R., Airey, G.D., Di Benedetto, H., 2013. Modelling the rheological properties of bituminous binders using the 2S2P1D model. Construction and Building Materials, 38, 395-406.

Yusoff, N.I.M., Shaw, M.T., Airey, G.D., 2011. Modelling the linear viscoelastic rheological properties of bituminous binders. Construction and Building Materials, 25 (5), 2171-2189.

Zadshir, M., Oldham, D.J., Hosseinnezhad, S., Fini, E.H., 2018. Investigating bio-rejuvenation mechanisms in asphalt binder via laboratory experiments and molecular dynamics simulation. Construction and Building Materials, 190, 392-402.

Zargar, M., Ahmadinia, E., Asli, H., Karim, M.R., 2012. Investigation of the possibility of using waste cooking oil as a rejuvenating agent for aged bitumen. Journal of Hazardous Materials, 233-234, 254-258.

Zaumanis, M., Boesiger, L., Kunz, B., Cavalli, M.C., Poulikakos, L., 2019. Determining optimum rejuvenator addition location in asphalt production plant. Construction and Building Materials, 198, 368-378.

Zaumanis, M., Mallick, R.B., 2015. Review of very high-content reclaimed asphalt use in plant-produced pavements: State of the art. International Journal of Pavement Engineering, 16 (1), 39-55.

Zaumanis, M., Mallick, R.B., Frank, R., 2014a. 100% recycled hot mix asphalt: A review and analysis. Resources, Conservation and Recycling, 92, 230-245.

Zaumanis, M., Mallick, R.B., Poulikakos, L., Frank, R., 2014b. Influence of six rejuvenators on the performance properties of reclaimed asphalt pavement (RAP) binder and 100% recycled asphalt mixtures. Construction and Building Materials, 71, 538-550.

Zhang, R., Sias, J.E., Dave, E.V., Rahbar-Rastegar, R., 2019. Impact of aging on the viscoelastic properties and cracking behavior of asphalt mixtures. Transportation Research Record, 2673 (6), 406-415.

Zhang, R., Wang, H., Jiang, X., You, Z., Yang, X., Ye, M., 2018a. Thermal storage stability of bio-oil modified asphalt. Journal of Materials in Civil Engineering, 30 (4), 04018054.

Zhang, H., Chen, Z., Xu, G., Shi, C., 2018b. Evaluation of aging behaviors of asphalt binders through different rheological indices. Fuel, 221, 78-88.

Zhang, R., Wang, H., Gao, J., You, Z., Yang, X., 2017. High temperature performance of SBS modified bio-asphalt. Construction and Building Materials, 144, 99-105.

Zhang, H., Yu, J., Feng, Z., Xue, L., Wu, S., 2012. Effect of aging on the morphology of bitumen by atomic force microscopy. Journal of Microscopy, 246 (1), 11-19.

Zhang, Z., Roque, R., Birgisson, B., 2001. Evaluation of laboratory-measured crack growth rate for asphalt mixtures. Transportation Research Record, 1767, 67–75.

Zhou, X., Moghaddam, T.B., Chen, M., Wu, S., Adhikari, S., Xu, S., Yang, C., 2020a. Life cycle assessment of biochar modified bioasphalt derived from biomass. ACS Sustainable Chemistry and Engineering, 8 (38), 14568-14575.

Zhou, X., Moghaddam, T.B., Chen, M., Wu, S., Adhikari, S., 2020b. Biochar removes volatile organic compounds generated from asphalt. Science of the Total Environment, 745, 141096.

Zhou, F., Karki, P., Xie, S., Yuan, J.S., Sun, L., Lee, R., Barborak, R., 2018. Toward the development of performance-related specification for bio-rejuvenators. Construction and Building Materials, 174, 443-455.

Zhu, H., Xu, G., Gong, M., Yang, J., 2017. Recycling long-term-aged asphalts using bio-binder/plasticizer-based rejuvenator. Construction and Building Materials, 147, 117-129.

Zofka, A., Yut, I., 2012. Investigation of rheology and aging properties of asphalt binder modified with waste coffee grounds. Transportation Research Circular E-C165, 61-72.

# Publications, conferences presentations and awards

## Publications

Canestrari, F., Ingrassia, L.P., Ferrotti, G., Lu, X., 2017. State of the art of tribological tests for bituminous binders. Construction and Building Materials, 157, 718-728.

Ingrassia, L.P., Lu, X., Canestrari, F., Ferrotti, G., 2018. Tribological characterization of bituminous binders with Warm Mix Asphalt additives. Construction and Building Materials, 172, 309-318.

Ingrassia, L.P., Lu, X., Ferrotti, G., Canestrari, F., 2019. Renewable materials in bituminous binders and mixtures: Speculative pretext or reliable opportunity? Resources, Conservation and Recycling, 144, 209-222.

Ingrassia, L.P., Lu, X., Ferrotti, G., Canestrari, F., 2019. Chemical and rheological investigation on the short- and long-term aging properties of bio-binders for road pavements. Construction and Building Materials, 217, 518-529.

Ingrassia, L.P., Cardone, F., Canestrari, F., Lu, X., 2019. Experimental investigation on the bond strength between sustainable road bio-binders and aggregate substrates. Materials and Structures, 52 (4), 80.

Ingrassia, L.P., Lu, X., Marasteanu, M. O., Canestrari, F., 2019. Tribological characterization of graphene nano-platelet (GNP) bituminous binders. Airfield and Highway Pavements 2019: Innovation and Sustainability in Highway and Airfield Pavement Technology – Selected Papers from the International Airfield and Highway Pavements Conference 2019, 96-105.

Ingrassia, L.P., Lu, X., Ferrotti, G., Canestrari, F., 2020. Chemical, morphological and rheological characterization of bitumen partially replaced with wood bio-oil: Towards more sustainable materials in road pavements. Journal of Traffic and Transportation Engineering (English Edition), 7 (2), 192-204.

Ingrassia, L.P., Lu, X., Ferrotti, G., Conti, C., Canestrari, F., 2020. Investigating the "circular propensity" of road bio-binders: Effectiveness in hot recycling of reclaimed asphalt and recyclability potential. Journal of Cleaner Production, 255, 120193.

Yan, T., Ingrassia, L.P., Kumar, R., Turos, M., Canestrari, F., Lu, X., Marasteanu, M., 2020. Evaluation of graphite nanoplatelets influence on the lubrication properties of asphalt binders. Materials, 13 (3), 772.

Ingrassia, L.P., Virgili, A., Canestrari, F., 2020. Effect of geocomposite reinforcement on the performance of thin asphalt pavements: Accelerated pavement testing and laboratory analysis. Case Studies in Construction Materials, 12, e00342.

Ingrassia, L.P., Spinelli, P., Paoloni, G., Canestrari, F., 2020. Top-down cracking in Italian motorway pavements: A case study. Case Studies in Construction Materials, 13, e00442.

Canestrari, F., Ingrassia, L.P., 2020. A review of top-down cracking in asphalt pavements: Causes, models, experimental tools and future challenges. Journal of Traffic and Transportation Engineering (English Edition), 7 (5), 541-572.

Ingrassia, L.P., Cardone, F., Ferrotti, G., Canestrari, F., 2021. Monitoring the evolution of the structural properties of warm recycled pavements with Falling Weight Deflectometer and laboratory tests. Road Materials and Pavement Design, DOI: 10.1080/14680629.2021.1906302.

Canestrari, F., Ingrassia, L.P., Virgili, A., 2021. A semi-empirical model for top-down cracking depth evolution in thick asphalt pavements with open-graded friction courses. Submitted to the Journal of Traffic and Transportation Engineering (English Edition).

Ingrassia, L.P., Canestrari, F., 2021. VECD analysis to investigate the performance of long-term aged bio-asphalt mixtures compared to conventional asphalt mixtures. Submitted to Road Materials and Pavement Design.

## Conferences presentations

Oral presentation “Tribological characterization of bituminous binders with Warm Mix Asphalt additives” during the International SIIV Arena at the 1st International Winter School “Advances in Sustainable Asphalt Pavements” organized by Università Politecnica delle Marche and Società Italiana Infrastrutture Viarie, Moena (Italy), December 17$^{th}$-20$^{th}$, 2017.

Oral presentation “Tribological characterization of graphene nano-platelet (GNP) bituminous binders” at the “International Airfield and Highway Pavements Conference 2019” organized by the American Society of Civil Engineers (ASCE), Chicago (USA), July 20$^{th}$-24$^{th}$, 2019.

Oral presentation “Advanced experimental characterization of bituminous binders extended with renewable materials in asphalt pavements” during the International SIIV Arena at the Winter School “Fundamentals for Innovative Research in Sustainable Transportation” organized by Università Politecnica delle Marche and Società Italiana Infrastrutture Viarie, Moena (Italy), December 15$^{th}$-18$^{th}$, 2019.

# Awards

"Best innovative idea" award obtained for the oral presentation "Tribological characterization of bituminous binders with Warm Mix Asphalt additives" during the International SIIV Arena at the 1st International Winter School "Advances in Sustainable Asphalt Pavements" organized by Università Politecnica delle Marche and Società Italiana Infrastrutture Viarie, Moena (Italy), December 17$^{th}$-20$^{th}$, 2017.